UNIVERSITY OF SOUTHAMPTON

Faculty of Medicine
Clinical and Experimental Sciences

Putative IgD binding proteins of *Neisseria* species

by

Muhammad Ahmed (Student ID 29065127)

ORCID ID 0000-0003-3234-2788

Thesis for the degree of Doctor of Philosophy

February 2020

Academic Thesis: Declaration of Authorship

Name: Muhammad Ahmed

Title of thesis: Putative IgD binding proteins of *Neisseria* species

I declare that this thesis and the work presented in it was carried out in accordance with the Regulations of the University of Southampton. The work is original and carried out by me, except where indicated by special reference in the text. No part of this thesis has been submitted for any other degree or academic award.

Signed:Date:

Abstract

Neisseria lactamica is a commensal bacterium of the upper respiratory tract. It is closely related to *Neisseria meningitidis*; an opportunistic pathogen that asymptomatically colonises the upper respiratory tract, but under certain circumstances, causes invasive disease. In this thesis, it is demonstrated that outer membrane vesicles extracted from *Neisseria lactamica*, *N. cinerea, N. flavescens* and *N. polysaccharea* induce proliferation of peripheral blood-derived B cells. Furthermore, this proliferative response is specific to B cells expressing IgDλ cell surface receptors. Pre-treatment of B cells with $F(ab')_2$ polyclonal goat anti-human IgD and λ light chain antibodies reduced the proliferation in response to *N. lactamica*, *N. cinerea, N. flavescens and N. polysaccharea*. It is also shown here that this phenotype is not shared among all *Neisseria* since the outer membrane vesicles extracted from *N. elongata, N. subflava, N. mucosa, N. macacae, N. gonorrhoea* and *N. meningitidis* are unable to induce a proliferative response in B cells.

Two genes of *N. lactamica* with homology to *Moraxella catarrhalis* IgD binding protein were identified. Both genes were experimentally knocked out, generating two single knockout strains (ΔNLY_37260 and ΔNLY_36660) and one double knockout strain (ΔNLY_36660 ΔNLY_37260). The double knockout strain does not induce proliferation of B cells expressing IgDλ, while single knockout strains are still mitogenic for IgDλ+ B cells, albeit at reduced levels, suggesting *N. lactamica* contains two IgD binding proteins, with redundancy between them.

Additionally, homologues of *Moraxella catarrhalis* IgD binding protein MID have been identified in *N. cinerea, N. flavescens* and *N. polysaccharea* and experimentally knocked out. Unlike wild-type strains, all knockout strains lacking the gene for putative IgDbp lack the ability to induce proliferation in IgDλ+ B cells. These knockout strains may be used as tools to further explore the putative IgDλ binding protein present in commensal *Neisseria* spp.

In summary, this work shows that *N. lactamica* induces an IgDλ+ B cell proliferative response likely due to the presence of an IgDλ binding protein, a characteristic shared by *N. cinerea, N. flavescens and N. polysaccharea*. This response may play an important role in evasion of the adaptive immune system of the upper respiratory tract, analogous to the activation of intestinal B cells and subsequent production of sIgA.

Contents

List of Figures

List of Tables

Acknowledgements

Completing my doctoral degree was the biggest challenge that I have ever attempted and to have survived the myriad of hurdles is my greatest achievement to date. This thesis is the summary of my hard work over the 3 years of life and hard work and support of many amazing people.

I would like to thank my supervisors Rob Read and Andrew Vaughan for their supervision and guidance over the last couple of years. I would like to extend my sincere gratitude to Dr Jay Laver for guiding me throughout the molecular biology projects. I would also like to thank everyone whom I have shared LC 76 office (both past and present). Especially thanks go to Alison, Rachel and Victoria for being a reliable source of knowledge and comforting words. Last but not least thanks to Emma, Adam and everyone in LC 70 (both past and present) for making my time at the University of Southampton more positive and enjoyable.

List of Abbreviations

Ab	Antibody
α-IgD	Ant-IgD
α -IgM	Ant-IgM
α-λ	Ant-λ
α-k	Ant-k
A488	Alexa Fluor™ 488 Carboxylic Acid, 2,3,5,6-Tetrafluorophenyl Ester, 5-isomer
BALT	Bronchus associated lymphoid tissue
BCR	B cell receptor
B-reg	Regulatory B cell
BSA	Bovine serum albumin
BTK	Bruton's tyrosine kinase
CFSE	5(6)-carboxyfluorescein diacetate N-succinimidyl ester
CLP	Common lymphoid progenitor
CSR	Class switch recombination
CXCR4	CXC chemokine receptor 4
dOMV	deoxycholate-extracted outer membrane vesicle
DM	Double mutant
Fc	Fragment crystallisable
FCS	Foetal calf serum
FO	Follicular
GALT	Gut-associated lymphoid tissue
GC	Germinal centre
GI	Gastrointestinal
HM	Hypermethylated
HSC	Haematopoietic stem cells
IBD	Inflammatory bowel disease
IFN	Interferon
Ig	Immunoglobulin
Igbp	Bacterial immunoglobulin binding proteins
IgDbp	Immunoglobulin D binding protein
IgDbr	Immunoglobulin D binding region
IL	Interleukin
IMD	Invasive meningococcal disease
LCL	Lymphoblastoid cell line
LOS	Lipooligosaccharide

LRT	Lower respiratory tract
LPS	Lipopolysaccharide
LRT	Lower respiratory tract
MALT	Mucosa-associated lymphoid tissue
MAMP	Microbe associated molecular pattern
MBP	Mannose-binding protein
Mcat	*Moraxella catarrhalis*
MC.7	Modified Catlin media 7
MFI	Mean fluorescence intensity
MHC	Major Histocompatibility Complex
MID	Moraxella IgD binding protein
MM	Meningococcal meningitis
MPC	Multipotent progenitor cells
MNC	Mononuclear cell
MZ	Marginal zone
NALT	Nasopharyngeal-associated lymphoid tissue
Nbac	*Neisseria bacilliformis*
Ncin	*Neisseria cinerea*
Nelong	*Neisseria elongata*
Nflav	*Neisseria flavescens*
Ngon	*Neisseria gonorrhoeae*
Nlac	*Neisseria lactamica*
Nmac	*Neisseria macacae*
Nmen	*Neisseria meningitidis*
Nmuc	*Neisseria mucosa*
NTHi	Non-typeable *Haemophilus influenzae*
Npol	*Neisseria polysaccharea*
Nsub	*Neisseria subflava*
ns	Not significant
OMV	Outer membrane vesicle
ORF	Open reading frame
PBMC	Peripheral blood mononuclear cell
PBS	Phosphate-buffered saline
PE	Phycoerythrin
PRR	Pattern recognition receptor
PWM	Pokeweed mitogen
SBA	Serum bactericidal activity
SDS-PAGE	Sodium dodecyl sulphate-polyacrylamide gel electrophoresis

SHM	Somatic hypermutation
SQRT-PCR	Semi-quantitative Reverse Transcription Polymerase Chain Reaction
TD	Thymus-dependent
TI-1	Thymus-independent type 1
TI-2	Thymus-independent type 2
TLR	Toll-like receptor
T-reg	Regulatory T cell
TSB	Tryptone soya broth
URT	Upper respiratory tract
WT	Wild-type

1. Introduction

1.1 Background

From birth, mucosal surfaces such as the gastrointestinal (GI) and respiratory tracts are colonised by a diverse range of microorganisms, which reside in the mucosae for long periods without causing disease (Littman and Pamer, 2011). These are primarily commensal bacteria that play a vital role in regulating metabolic function and maintaining immune homeostasis. In immunocompetent hosts, the interaction between commensal bacteria and host cells is stable without priming of any major adaptive immune response. Furthermore, the colonisation of human mucosal surfaces by commensal bacteria is believed to protect against potential pathogenic bacteria by presenting competition for nutrients, environmental niche and cognate receptors (Turnbaugh *et al.*, 2007; Zhang and He, 2015; Bosch *et al.*, 2016; Blacher *et al.*, 2017). The specific mechanisms that underlie tolerance of commensal bacteria by the host are not determined, and their indirect impact on immune responses to pathobionts has not been explored. The overarching objective of my studentship has been to study one facet of the relationship between the human nasopharyngeal commensal *Neisseria*, and cells of the human immune system.

1.2 Mucosal immunity distinguishes between pathogenic and commensal bacteria

The cells of the immune system such as macrophages, neutrophils, dendritic cells and epithelial cells express pattern recognition receptors (PRRs) which recognise microbe-associated molecular patterns (MAMPs) (Wissinger, Goulding and Hussell, 2009). According to the “infectious non-self” theory, an immune response occurs when an infectious foreign agent expressing MAMPs crosses the innate barriers of the host (Murphy *et al.*, 2012). PRRs include Toll-like receptors (TLRs), such as TLR4 and TLR2 which recognise bacterial lipopolysaccharides (LPS) and peptidoglycans respectively (Table 1) (Armant and Fenton, 2002; Chamaillard *et al.*, 2003). Recognition by PRRs results in activation of the nuclear factor-kappa B (NF-kB) signalling pathway and induction of cytokine production along with other innate immune responses (Tlaskalova-Hogenova *et al.*, 2005).

Table 1 MAMPs and corresponding PRRs.

Taken from (Tlaskalova-Hogenova *et al.*, 2002; Wilson, McNab and Henderson, 2002).

Microbe associated molecular patterns (MAMPs) and corresponding pattern recognition receptors (PRRs)	
MAMPs	**PRRs**
Peptidoglycan	CD14, TLR2
Lipopolysaccharide	CD14, TLR4, LBP
Lipoproteins	TLR2
CpG (bacterial DNA)	TLR9
Mannose	CD14, TLR2, MBP
Phosphorycholine	Serum C-reactive protein
Mannose-rich glycans	MBP, MMR
Flagellin	TLR5
Lipoteichoic acid	TLR6
Heat shock proteins	TLR4, TLR2

TLR= Toll-like receptors; MBP= Mannose-binding protein; LBP= Lipopolysaccharide binding protein; MMR= Macrophage mannose receptor

The immune system responds to potential pathogens by recognizing their MAMPs, however, it appears that recognition of commensal MAMPs does not lead to such immune responses, suggesting the commensal flora are tolerated by the immune system and not routinely cleared. It would appear that the immune system has evolved mechanisms that allow it to distinguish between the pathogenic and commensal bacteria or alternatively the commensal bacteria have evolved specific ligands in order to allow a mutualistic relationship between the host and the commensals. This has been shown in mice where *Bacteroides fragilis* uses its symbiotic factor polysaccharide A (PSA) to activate Foxp3+ regulatory T cells via interaction with TLR2 expressed in intestinal dendritic cells, promoting immune tolerance (Round *et al.*, 2011; Chu and Mazmanian, 2013; Jiang *et al.*, 2017).

Other general mechanisms whereby commensal bacteria engage a tolerant response by the immune system have been postulated. Both commensal and pathogenic bacteria have similar MAMPs. However, compared to pathogens, commensal bacteria may express a reduced quantity of MAMPs (such as flagellin) thus allowing the pathogen to circumvent the host immune response (Chu and Mazmanian, 2013). Furthermore, it is possible that commensal bacteria produce proteins which are able to inhibit the synthesis or action of host cytokines and cause immunosuppressive effects. There is growing evidence that commensal bacteria modulate inflammatory mechanisms through released proteinases as described for Arg-1 gingipain proteinase of *Porphyromonas gingivalis* that cleaves and inactivates cytokines IL-1 and IL-6 (Tlaskalova-Hogenova *et al.*, 2005; Glowczyk *et al.*, 2017)

Additionally, our immune system may utilize further cues to differentiate between commensal and pathogenic bacteria. For example, pathogenic but not commensal bacteria induce cell damage causing inflammation which may be used as a supplementary signal in addition to MAMP recognition (danger theory) (Matzinger, 2002;2007).

Since “danger theory” includes the assumption that every immune response is due to damage, it fails to explain observed immune responses in the absence of accompanying damage (Bingaman *et al.*, 2000; Pradeu and Cooper, 2012). Furthermore, studies have shown that commensal bacteria which do not elicit “danger” signals are still not ignored; indeed an interaction between the commensals and host is important for the development of the immune system (Macpherson *et al.*, 2000). It has been shown that oral administration of CpG oligonucleotides and gut flora DNA (i.e. MAMPs without the presence of bacteria) restored the protective immune response to subsequent infection with *E. cuniculi* in antibiotic-treated mice (Hall *et al.*, 2008). However, immune responses

are complex and multifactorial and therefore our immune system may utilize different mechanisms for differentiation between commensal and pathogenic bacteria.

Commensal bacteria can produce immunosuppressive molecules, allowing them to evade the adaptive immune system (Wilson, McNab and Henderson, 2002; Tlaskalova-Hogenova *et al.*, 2005). For example, the suppressive sequences, TTAGGG and TCAAGCTTGA, found in the DNA of all *Lactobacillus* spp. have been shown to block the production of TNF-α, IL-6 and IL-12 by dendritic cells (Bouladoux *et al.*, 2012). The use of suppressive motifs by *Lactobacillus* spp. to inhibit activation of dendritic cells suggests that the immune system and the commensals have both evolved mechanisms to allow a mutualistic relationship between the host and the commensals.

In humans, the immune system is strictly regulated to maintain tolerance of the flora in order to maintain normal health (Smith, McCoy and Macpherson, 2007). This is evident in the case of inflammatory bowel diseases (IBD) such as Crohn's disease and ulcerative colitis. IBD is a chronic condition triggered upon the breakdown of tolerance of the intestinal flora resulting in intestinal inflammation. In IBD patients there is an increased bacterial adherence to the mucosal surfaces, indicating a decreased ability to limit the contact between the intestinal flora and epithelium resulting in an immune response directed at the intestinal flora. This suggests the importance of homeostasis between the host and the normal flora (Duchmann *et al.*, 1995; Swidsinski *et al.*, 2005).

The general subject of this thesis pertains to the interaction between *Neisseria* spp. with B cells and potential downstream effects on host responses.

1.3 B cell immunity

The main function of B cells is to make antibodies against antigens, develop into memory B cells and perform the role of antigen-presenting cells (APC) (Hoffman, Lakkis and Chalasani, 2016).

1.3.1 Maturation

B cells develop from haematopoietic stem cells (HSC) found in the bone marrow. A B cell goes through several antigen-independent developmental stages within the bone marrow before becoming a fully mature naive B cell. After several stages of signalling the HSC gives rise to the Pro-B cell (Figure 1) (Gathings, Lawton and Cooper, 1977).

B cells recognise antigens via the help of membrane-bound immunoglobulins (mIgs), and early B cell development primarily constitutes the steps that lead to the expression of mIgs (Avalos and Ploegh, 2014). During B cell maturation Pro-B cells undergo through heavy

chain V-D-J rearrangement resulting in Pre-B cells. Pre-B cells undergo κ light chain gene rearrangement resulting in immature IgMκ light chain surface Ig. In the case of failed k light chain gene rearrangement, Pre-B cells undergo λ light chain gene rearrangement resulting in immature IgMλ light chain surface Ig (Figure 2). Successful IgM+ immature B cells are tested for reactivity to self-antigens before leaving the bone marrow. Immature B cells with strong reactivity to self-antigens do not survive the central tolerance checkpoint, whereas immature B cells that lack strong reactivity towards self-antigens survive the central tolerance checkpoint. Non-autoreactive B cells leave the bone marrow and migrate to secondary lymphoid tissues such as the spleen, lymph nodes etc, where they are referred to as transitional B cells. At this stage, the transitional B cells start to express IgD as the second BCR (Agrawal *et al.*, 2013; Vale *et al.*, 2015).

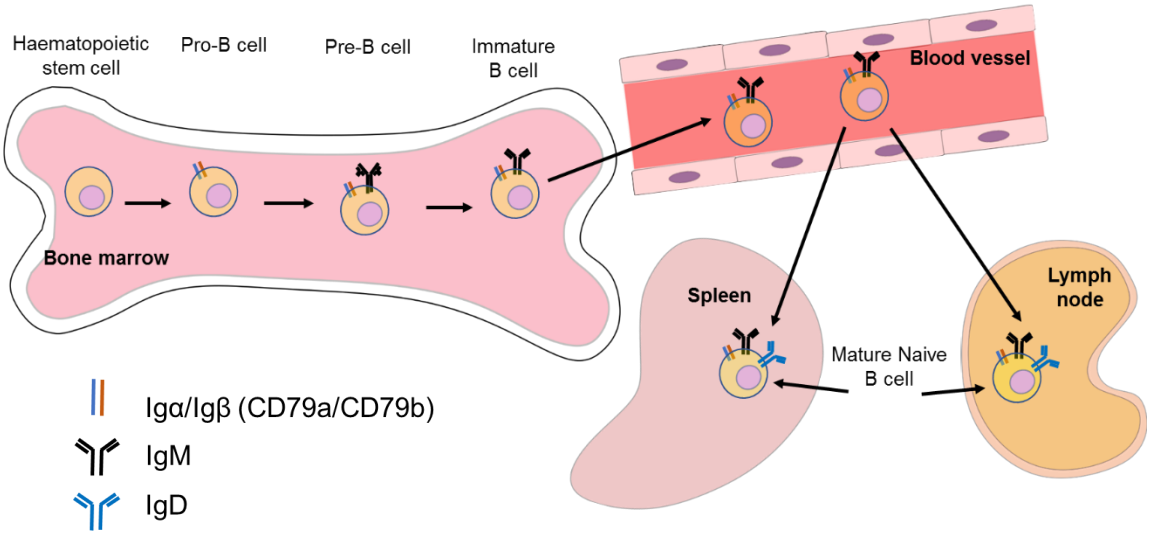

Figure 1 Diagram showing the various stages and sites of B cell development.

HSC in the Bone marrow gives rise to Pro-B cells. These Pro-B cells undergo heavy chain Ig gene rearrangement resulting in Pre-B cells expressing surface μ heavy chain and two surrogate light chains. Pre- B cells goes through light chain Ig gene rearrangement resulting in immature B cells expressing only IgMλ or IgMκ. Next, IgMλ and IgMκ+ cells go through negative selection to remove any autoreactive B cells. Following successful negative selection, the B cells then migrate to the spleen and lymph nodes where they start to express IgD as a BCR.
Adapted from (Schroeder and Cavacini, 2010; Vaughan, Roghanian and Cragg, 2011; Schelonka and Maheshwari, 2013).

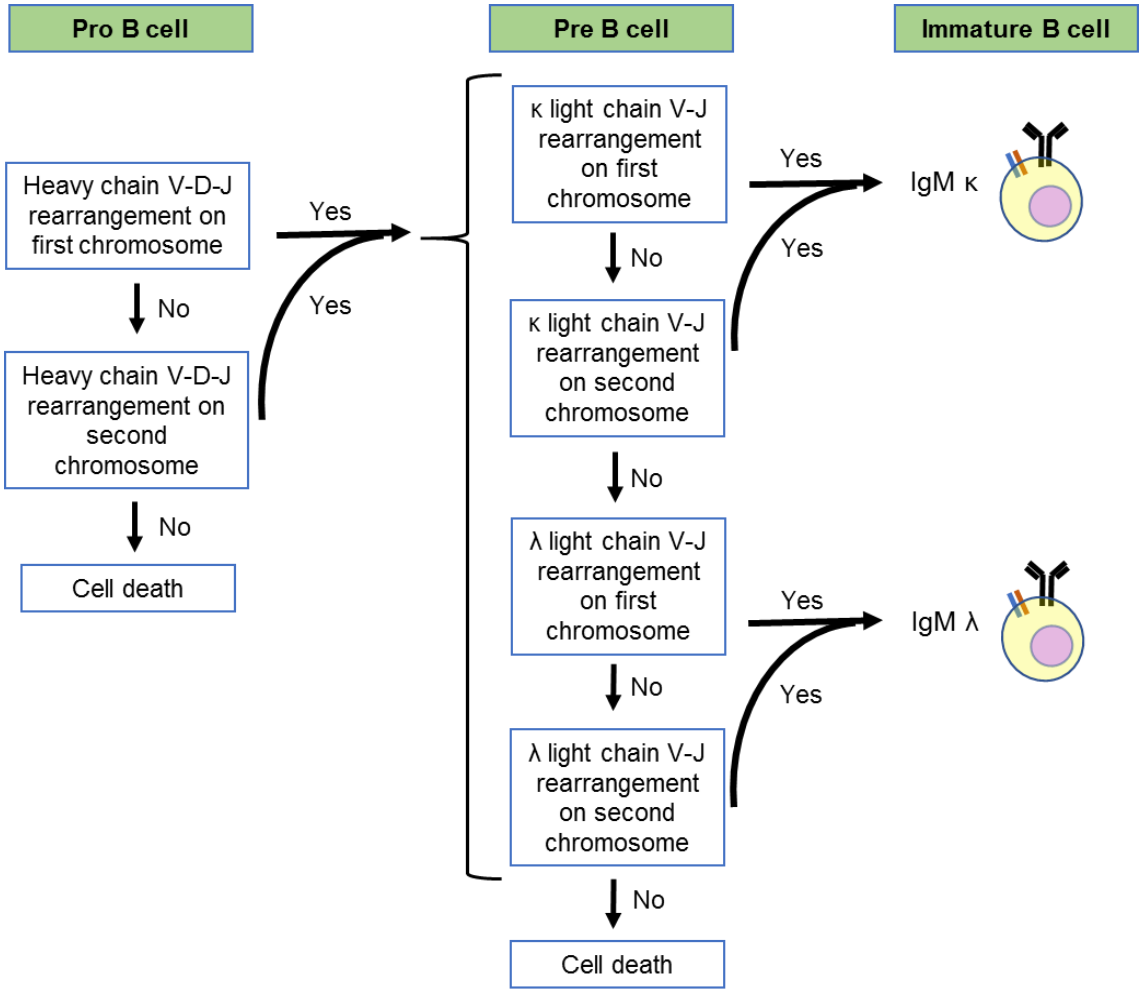

Figure 2 B cell rearrangement of Ig genes.

During B cell maturation, the B cell goes through Variable (V), Diversity (D) and Joining (J) Ig gene rearrangement. In pro-B cells the heavy chain of D-J followed by V-DJ rearranges on chromosome 1 resulting in a pre-B cell. In case of unsuccessful rearrangement, the V-D-J rearrangement is repeated on chromosome 2 to rescue the cell from cell death. Unsuccessful VDJ rearrangement on both chromosomes results in cell death. The pre-B cell goes through k light chain VJ gene rearrangement resulting in the immature B cell expressing k light chain IgM surface antibody. Unsuccessful k light chain gene rearrangement on chromosome one and two is followed by λ light chain VJ gene rearrangement to rescue the cell and result in the immature B cell expressing λ light chain IgM surface antibody. Unproductive λ light chain gene rearrangement on chromosome 1 and 2 results in death of the cell by apoptosis.
Adapted from (Chen and Alt, 1993; Murphy *et al.*, 2012).

1.3.2 Differentiation

Once B cell maturation is completed the mature naive B cell migrates to secondary lymphoid tissue, such as the spleen, lymph nodes etc. (Figure 1) (Agrawal *et al.*, 2013).

When the B cell encounters an antigen in the secondary lymphoid tissue, after 4-6 days the activated B cell can go through one of two fates. In some cases, the B cells proliferate and differentiate immediately into short-lived plasma cells without the help of a CD4 T cell. TI B cell activation results in short-lived plasma cells (Figure 3) (Bortnick and Allman, 2013; Tak Mak, 2014). However, since these B cells have not been through somatic hypermutation or isotype switching, they lack memory B cells. Furthermore, the antibodies produced by these plasma cells are low-affinity IgM and IgD.

In other cases, the B cell encounters the CD4 T cell. Engagement with CD40 ligand by CD40 and the stimulatory cytokines secreted by the CD4 T cells helps the B cells to convert the primary follicle into the secondary follicle. By day 9-12 the secondary follicle becomes a germinal centre (GC) composed of the dark and light zone. Within GC somatic hypermutation and isotype class switch recombination occurs resulting in long-lived memory B cells and plasma cells. Long-lived plasma cells are capable of secreting IgG, IgA and IgE isotype Immunoglobulin (Ig). Long-lived memory B cells migrate to bone marrow (Paramithiotis and Cooper, 1997; Becker *et al.*, 2018), spleen and lymph nodes whereas long-lived plasma cells migrate to bone marrow where they reside and secrete high-affinity Abs (Schroeder and Cavacini, 2010; Schelonka and Maheshwari, 2013; Tak Mak, 2014; Shinnakasu and Kurosaki, 2017) (Figure 3).

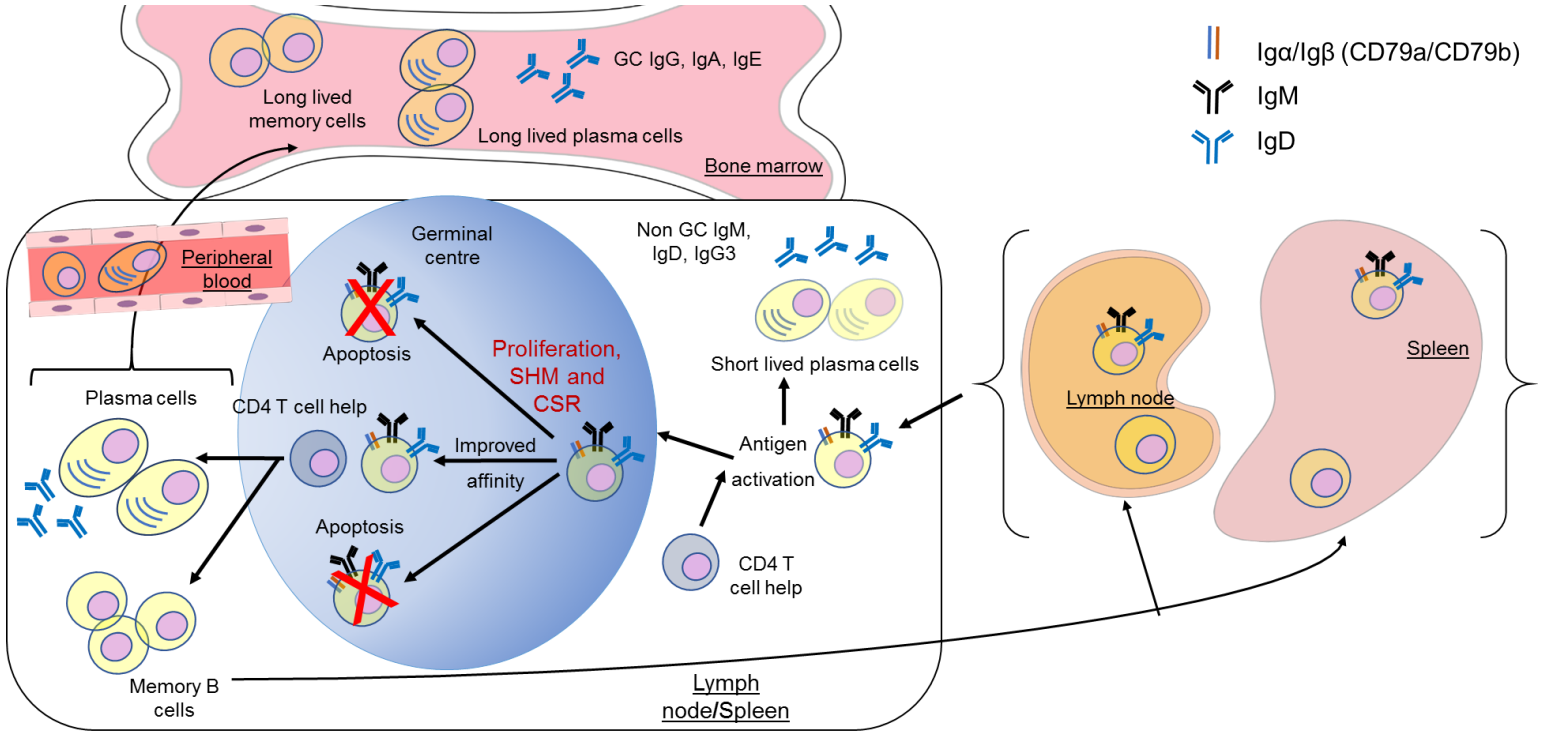

Figure 3 B cell activation and differentiation into memory B cells and plasma cells.

Upon encountering of antigen in the lymph node or spleen the B cells either proliferate and differentiate into short-lived plasma cells or in case of help from the CD4 T cell they proliferate and form germinal centres. Within the germinal centre (GC), activated B cells will proliferate and go through somatic hypermutation (SHM) and class switch recombination (CSR). B cells with decreased affinity for the antigen results in apoptosis, whereas B cells with improved affinity develops into long-lived plasma cells and memory B cells. Long-lived plasma cells migrate to Bone marrow where they reside and secrete Abs, whereas long-lived memory B cells migrate to Bone marrow, lymph node and spleen where they reside for a long time and provide an accelerated secondary immune response.

1.3.3 Immunoglobulins (Ig)

Immunoglobulin is composed of two identical heavy chains and two identical light chains. All four chains contain a variable (V) region at the amino terminus and a constant (C) region at the carboxyl terminus. The heavy and light chains are held together by many non-covalent interactions and disulphide bonds forming a flexible Y shaped structure. The V regions of the heavy and light chains join in each arm of the Ig resulting in two antigen-binding sites. These are called the fragment antigen-binding (Fab) fragments. The lower shaft of the Y shaped Ig is composed of C regions of two heavy chains. This region is referred to as Fc (fragment crystallisable) and it binds to the Fc receptors on effector cells, whereas the V domain of Ig confers antigenic specificity (Figure 4), (Chen and Cerutti, 2011; Murphy *et al.*, 2012; Hoffman, Lakkis and Chalasani, 2016).

There are two classes of human light chains, lambda and kappa, found in all immunoglobulin isotypes. The human light chain consists of ~107 amino acid residues amino terminus (variable region (V)) and ~107 amino acid carboxyl terminus (constant region (C)). The proportion of lambda and kappa light chain differs from species to species. The average serum Ig with kappa to lambda ratio in mice is 20:1, in cattle, it is 1:20 and in humans, it is 2:1 (Murphy *et al.*, 2012; Townsend *et al.*, 2016).

Immunoglobulins can be distinguished by the type of heavy chain they possess, resulting in five classes of immunoglobulin isotypes named IgA, IgG, IgM, IgD, and IgE existing in humans (Table 2) (Rowe and Fahey, 1965; Chen and Cerutti, 2011). These Isotypes differ in terms of size, complement fixation and Fc receptor binding. These deviations in heavy chains, allow each isotype to function either in a different type of immune response or at a different stage of response (Solomon and Weiss, 1995).

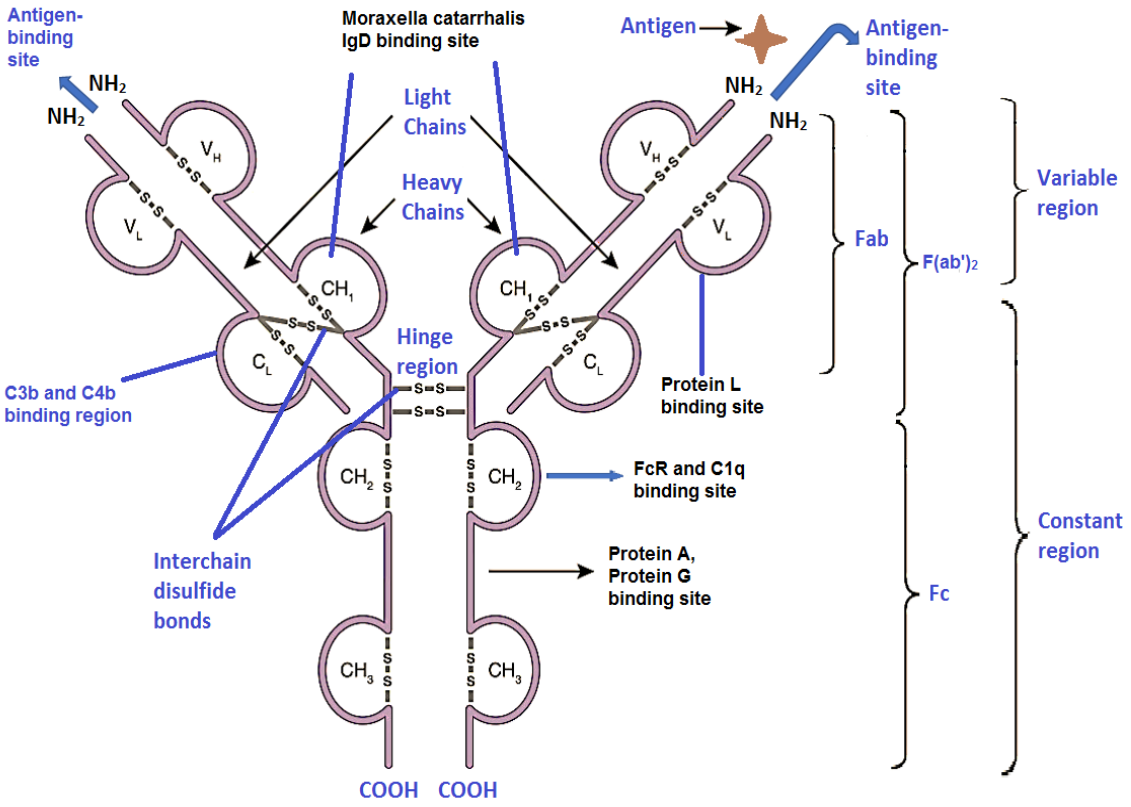

Figure 4 Structure of Immunoglobulin with labelled bacterial Ig binding protein binding sites.

Immunoglobulin is composed of two identical heavy and light chains. The amino terminus of the heavy chain and one light chain are joined together by disulphide bonds. The Ig recognises a unique antigen via the Fab fragment. The two heavy chains are also joined together by disulphide bonds at the hinge region forming an immunoglobulin molecule with two antigen binding sites.

Adapted from (Hoffman, Lakkis and Chalasani, 2016).

Table 2 Immunoglobulin isotypes: structure and major function

(Corthesy, 2007; Schroeder and Cavacini, 2010; Vidarsson, Dekkers and Rispens, 2014)

	IgM	**IgD**	**IgG**	**IgA**	**IgE**
Structure	Monomeric, Pentameric	Monomeric	Monomeric	Dimeric	Monomeric
Sub-classes	None	None	IgG1, IgG2, IgG3, IgG4	IgA1, IgA2	None
Function	Produced in the primary response against a foreign antigen. Fixes complement	Found on the surface of B cells and in serum. May play a key role in host-commensal homeostasis	Main Ab in the secondary immune response. Plays a role in opsonization, toxin neutralization and complement fixation	Secretory IgA coats the bacteria and prevents their adherence to the mucosal surfaces and complement fixation	Partakes in allergy and antiparasitic activity

1.3.3.1 The function of Immunoglobulin D

While the function of IgA, IgG, IgM and IgE is well known (Table 2), the role of IgD has remained unclear since its discovery in 1965 (Rowe and Fahey, 1965; Chen and Cerutti, 2011). Initially, IgD was assumed to be a recently evolved isotype since it was only identified in primates and very few mammals, including dogs, rats, mice, rabbits but undetectable in swine, birds, sheep, cattle and frogs. However, IgD was subsequently discovered in various animals where it was previously thought to be absent i.e. pig, sheep and cattle. Recently IgD has been detected in cartilaginous and bony fishes. The discovery of IgD in cartilaginous fish is striking since these fish are evolutionarily ancient and populated the earth around 500 million years ago. This indicates that IgD is an ancestral immunoglobulin isotype with a conserved function (Ohta and Flajnik, 2006; Chen and Cerutti, 2010;2011).

In humans, IgD is found in two forms. It is either expressed as surface B cell receptor or as secreted IgD (sIgD). The concentration of circulating IgD can range from15-300 μg/ml and has a half-life of ~2.8 days. However, IgD concentration can increase in a number of diseases i.e. IgD myeloma, Hodgkin's disease, autoimmune disorders, tuberculosis, chronic obstructive pulmonary disease (COPD) and hyper IgD syndrome (Sechet *et al.*, 2003). Soluble IgD can react with specific bacterial proteins, i.e. IgD binding protein of *Moraxella catarrhalis*, via the constant region independent of the variable region. This binding results in activation of B cells (Schroeder and Cavacini, 2010).

B cells recognise antigens via antigen recognising B cell receptors (BCR). The BCR is composed of a membrane-bound Ig linked with the Igα/Igβ (CD79a/CD79b) (Reth, 1992). IgD and IgM are usually co-expressed on the surface of mature naive IgM+IgD+ B cells as a transmembrane antigen receptor (Finkelman *et al.*, 1976; Ruddick and Leslie, 1977; Geisberger, Lamers and Achatz, 2006), thus accounting for ~75% of the total B cell population (Jendholm *et al.*, 2008). IgM is secreted in two forms, a monomeric and a pentameric form, whereas cell surface IgM is expressed exclusively in the monomeric form. In order to express IgD, B cells utilise two methods; class switch recombination and alternative RNA splicing (Stavnezer and Amemiya, 2004). In humans, IgD has a long hinge (H) region compared to other immunoglobulin isotypes, which allows it to acquire a flexible T shape instead of the Y shape of other isotypes (Sun *et al.*, 2005). The hinge region of only IgD and IgA1 isotype contains carbohydrate.

Soluble IgD has been shown to bind to circulating basophils and mast cells. IgD binding to basophils results in cross-linking of IgD, this stimulates the basophils to produce proinflammatory cytokines i.e. IL-1β and TNF-α, chemokines i.e. IL-8 and CXC chemokine ligand 10 (CXCL10) and immunoactivating cytokines i.e. B cell activating factor (BAFF),

IL-4, IL-13 and a proliferation-inducing ligand (APRIL) (Sechet *et al.*, 2003; Chen *et al.*, 2009).

IgM is the first BCR to be expressed by pre-B cells (Figure 1) whereas IgD develops at a later stage during B cell development and therefore is mostly expressed by the mature naive B cells (Chen and Cerutti, 2011). Early studies involving the analysis of BCR transgenic mice expressing hen egg lysozyme (HEL)-reactive IgM, IgD or both IgD and IgM simultaneously have revealed that IgM and IgD receptors display no major differences in HEL-mediated induction of B-cell tolerance and activation, including CD80 and CD86 up-regulation and antibody secretion (Brink, Goodnow and Basten, 1995; Lutz *et al.*, 1998). However, other studies argue against a complete functional redundancy of IgM and IgD BCR (Roes and Rajewsky, 1993). Although IgD and IgM BCR use the same signalling route, they cause different cellular effects i.e. interleukin secretion, tolerance induction or apoptosis. It has been shown that the employment of IgM-BCR results in the deletion of immature B cells, whereas IgD-BCR engagement lacks this impact (Kim and Reth, 1995b). Cross-linking of B cell lines expressing only IgD or IgM BCR with either antigen or class-specific antibody results in activation and phosphorylation of protein tyrosine kinase (PTK). Phosphorylation via IgM-BCR reaches its maximum after one minute and declines within one hour, whereas, phosphorylation via IgD-BCR reaches its maximum after one hour and starts to decline after 4 hours (Kim and Reth, 1995a). This difference in activation signal could be due to IgM-BCR but not IgD-BCR having a negative feedback loop. Thus, this lack of negative feedback loop in IgD-BCR could be the cause of this prolonged phosphorylation (Kim and Reth, 1995b).

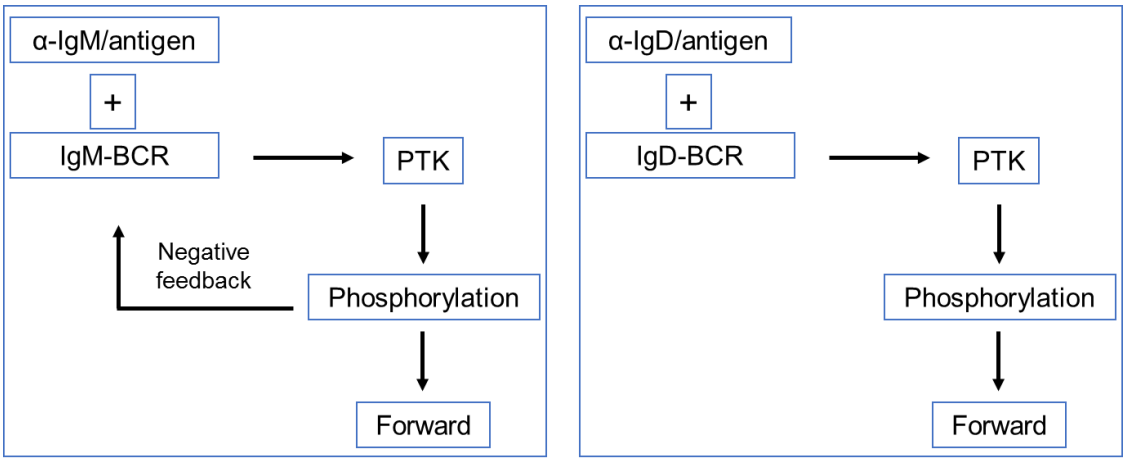

Figure 5 Diagram explaining a probable reason for the difference in PTK phosphorylation.

Cross-linkage of IgD or IgM-BCR with antigen or class specific antibody results in phosphorylation of protein tyrosine kinase. IgM-BCR cross linkage results in a negative feedback signal which could silence the cell surface receptor by modifying the signalling part of the receptor. IgD-BCR cross linkage does not result in negative feedback signal and proceeds with the reaction.
Adapted from (Kim and Reth, 1995b;a)

It is known that a considerable number of IgD cells are found in lacrimal, nasal, salivary and mammary glands. Additionally, high levels of IgD have reported in palatine tonsils compared to spleen and lymph nodes (Surjan, Brandtzaeg and Berdal, 1978; Brandtzaeg *et al.*, 1979; Sorensen and Larsen, 1988; Litwin, Zehr and Insel, 1990). This has led to the hypothesis that IgD is involved in the local immune response. The secreted IgD or IgM in response to IgDbp perhaps coats the bacteria thereby shielding its MAMPs, which reduces the cellular activation and prevents the stimulation of an adaptive immune response. This is beneficial to the host as this would prevent induction of local inflammatory cytokine production which could otherwise cause damage to the host tissue. However, this secreted IgD is also beneficial for the bacterium. As mentioned earlier coating the bacteria with immunoglobulin would shield its PAMPs from being detected by the PRRs and therefore would prevent a continuous adaptive immune response, allowing prolonged colonization of the nasopharynx and preventing complete clearance of the bacterium.

The functional importance of IgD is also suggested by the fact that a small subset of B cells found in the tonsils, lachrymal glands, nasal cavities and salivary glands undergo class switching from IgM to IgD, indicating a functional advantage of IgD over IgM (Chen *et al.*, 2009; Chen and Cerutti, 2010).

Through imaging studies IgD is known to be found in close proximity to various other B cell surface receptors such as CD19 and CXC chemokine receptor 4 (CXCR4) (Maity *et al.*, 2015), suggesting it may engage in cross-talk with these receptors leading to downstream signalling. CXCR4 belongs to the superfamily of G protein-coupled receptors. The CXCR4 activation instigates a series of signals incorporating actin cytoskeleton remodelling, phosphatidylinositol-3-kinase (PI3K) and spleen tyrosine kinase (Syk) dependent IgD-BCR signals, leading to induction of Ca2+ influx, Akt, Foxo1 and Erk pathway activation (Busillo and Benovic, 2007; Becker *et al.*, 2017).

The functional importance of IgD has been shown in a recent study exploring the relationship between the CXCR4 signal and IgD-BCR. Their investigation revealed that the B cells from IgD-deficient but not IgM-deficient mice displayed abrogation of CXCL12-mediated CXCR4 signalling and B-cell migration (Becker *et al.*, 2017). The fact that CXCR4 function is hindered in the absence of IgD-BCR suggests that IgD plays an important role in maintaining homeostasis of the B cells.

1.3.4 Waldeyer's ring

The adenoids (nasopharyngeal tonsils), palatine tonsils, tubal tonsils and lingual tonsils collectively form a ring, known as Waldeyer's ring (Figure 6). It is a collection of lymphoid tissue forming tonsils located at the back of the mouth (Brandtzaeg, 2011; Murphy *et al.*, 2012). The strategic placement of these components in the Waldeyer's ring allows it to perform local immune functions against exposure to airborne and dietary antigens (Brandtzaeg, 2003).

The function of the components of the Waldeyer's ring is very similar to that of the nasopharynx associated lymphoid tissue (NALT) found in rodents (Kuper *et al.*, 1992). Besides rodents, tissues equivalent to human Waldeyer's ring have been discovered in goat, sheep, horses, monkeys, cattle and pigs (Kuper *et al.*, 1992; Casteleyn *et al.*, 2011).

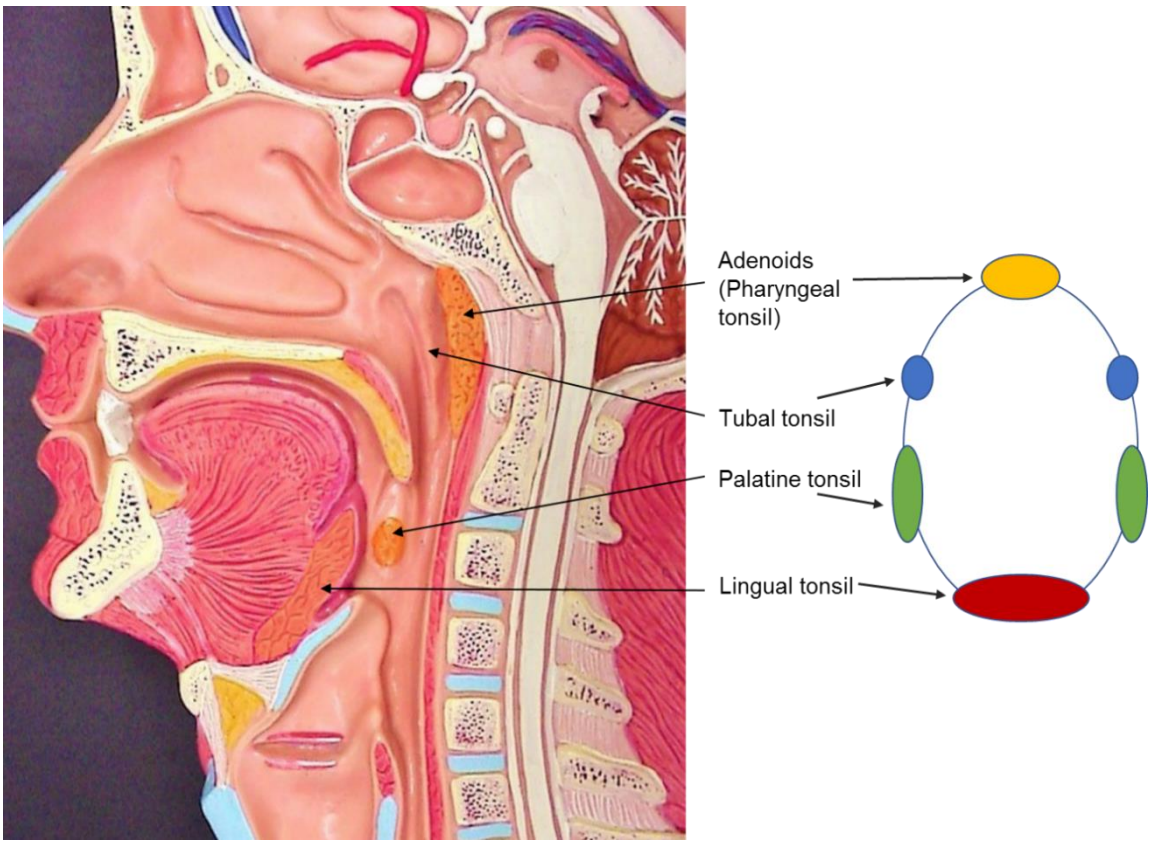

Figure 6 Diagram representing the lymphoid organs of Waldeyer's ring.

Waldeyer's ring is situated in the mucosal epithelia of both the nasopharynx and oropharynx. The ring is composed of the adenoids (nasopharyngeal tonsils), palatine tonsils, tubal tonsils, and lingual tonsils.
Adapted from (Perry and Whyte, 1998).

Despite the presence of an abundant commensal flora in the URT, little is known about how this flora interacts with the host to maintain the commensal relationship and far fewer investigations have been conducted to explore this than for the gut flora. As a breakdown in the host-commensal relationship in the URT can lead to serious systemic infection, such as *Neisseria meningitidis*, therefore it is important to understand how homeostasis is maintained in this location. As in the intestinal epithelium, an abundance of IgA is secreted by the lymphoid tissues of Waldeyer's ring, but it is not known whether this response is analogous to the IgA produced in response to the commensal flora in the intestine and whether it is produced via a T-independent mechanism. Interestingly, 2-5 % of the tonsillar B cell population expresses IgD+IgM-CD38+ cell markers. These cells are exclusive to tonsils and are not produced by any other MALT (Johansen *et al.*, 2005). These IgD+IgM- B cells are mostly resident in the respiratory mucosal environments and can be found in the lymphoid tissues, tonsils, nasal cavities, lachrymal gland and salivary gland (Vladutiu, 2000; Chen and Cerutti, 2010). They differentiate into antibody-secreting cells, producing soluble IgD (Chen *et al.*, 2009; Loh, Vale and McLean-Tooke, 2013). In normal serum, IgD concentration is only 0.2% of total Ig molarity, which is higher than trace amounts of IgE but much lower than IgG (80%), IgA (15%) and IgM (5%) (Loh, Vale and McLean-Tooke, 2013). However, large numbers of local IgD secreting plasma cells have been observed in human bronchus-associated lymphoid tissue and tonsils (Forsgren and Grubb, 1979). In tonsils, the IgD+IgM−ve B cell subgroup accounts for up to 20-25% of plasma cells and about 1.5-5% of total CD19+ B cells (Chen *et al.*, 2009). This compartmentalisation suggests that IgD might play an important role in the humoral immunity of the URT.

IgD is often viewed as a predominantly mucosal Ig isotype because of the preferential localization of IgD producing B cells in MALTs, but the presence of IgD, as well as IgD producing B cells in the circulation in addition to MALTs, indicates that IgD can potentially exert its immunological functions both systemically and in mucosal compartments. However, at the time of writing, the exact function of the respiratory tract IgD is unknown.

A number of URT colonisers can interact with IgD via the production of IgD binding proteins, including *Moraxella catarrhalis* (Forsgren *et al.*, 2001) and *Haemophilus influenzae*. It has been shown that heat-killed *M. catarrhalis* is mitogenic for B lymphocytes. It induces B cell proliferation via interaction with IgD BCR and class I major histocompatibility complex antigens on the surface of B lymphocytes (Forsgren *et al.*, 1988). Similar experiments with *H. influenzae* indicate that the mitogenic response of human lymphocytes to *H. influenzae* can be abolished by anti-IgD antibodies (Janson *et al.*, 1991). Furthermore, it has been shown that *N. lactamica* exhibits the same activity, the first commensal to exhibit this (Vaughan *et al.*, 2010). This may suggest that the ability of

URT bacterial colonisers to interact with IgD may play a role in the host-commensal relationship, rather than mediating virulence as previously suggested (Janson *et al.*, 1991). The presence of URT bacterial species that specifically interact with IgD via their antigens (Janson *et al.*, 1991; Forsgren *et al.*, 2001; Vaughan *et al.*, 2010) and the unique production of sIgD in this location (Chen *et al.*, 2009), suggests that targeting IgM-IgD+ cells and/or the production of soluble IgD may play a very important role in maintaining URT immune homeostasis.

The activation of B cells and the subsequent secretion of immunoglobulins can be caused by thymus-dependent (TD) and thymus independent (TI) antigens.

1.4 Thymus dependent and independent B cell antigens

Antibodies are key molecules in adaptive immune responses but also modulate and augment innate defence. All antibody generated at mucosal surfaces derives from B cells, which are mostly, in turn, under the influence of the host's T cell repertoire. Thus, thymus-dependent (TD) antigens are dependent upon CD4 helper T cells to enable them to induce proliferation and differentiation of B cells into antibody-secreting plasma cells. The CD4 T cells bind to peptide-loaded MHC class II on the surface of the B cells via the T cell receptor (TCR). T cells also express CD40 ligand on the surface which binds to CD40 present on the surface of the B cells. This triggers the T cell to secrete cytokines. The interaction of B and T cells in conjunction with the secreted cytokines leads to an increased B cell proliferation, somatic hypermutation and immunoglobulin class switching (Noelle *et al.*, 1983; Murphy *et al.*, 2012; Vazquez, Catalan-Dibene and Zlotnik, 2015).

In comparison to thymus-dependent antigens, thymus-independent (TI) antigens, which include bacterial antigens, are able to induce B cell proliferation without the help of CD4 T cells (Noelle *et al.*, 1983; Mond, Lees and Snapper, 1995; Mond *et al.*, 1995).

There are two classes of TI antigen, which activate B cells by using 2 distinctive mechanisms, TI-1 and TI-2. TI-1 antigens comprise molecules that cause the B cells to proliferate and differentiate irrespective of antigen specificity. This type of activation is called polyclonal activation. Lipopolysaccharide (LPS), lipooligosaccharide (LOS) and bacterial DNA containing CpG motifs are all examples of MAMPs that are TI-1 antigens because they activate TLRs expressed on the surface of B cells. LPS and LOS binds to TLR4 and CpG DNA binds to TLR9 (Table 1). These TI-1 antigens induce B cells to undergo mitosis by activation of TLRs expressed by B cells (Mond *et al.*, 1995; Murphy *et al.*, 2012).

Human B cells do not express TLR4 and hence do not respond to LPS, but they do express TLR9 and can be activated by microbial CpG DNA. TLR signals can replace the T

helper signals and co-binding of bacteria to both BCR and TLR on a cell can activate that cell more quickly than a late signal from T helper cell (Owen *et al.*, 2013).

TI-2 antigens comprise molecules with highly recurring structures, e.g. cell wall, capsular polysaccharides. They can cross-link a large fraction of the BCR Ig on the surface of the B cells, which allows them to induce the TI activation signal. TI-1 antigens can activate both mature and immature B cells due to the unconventional nature of the mitogen. In contrast, TD and TI-2 antigens can activate only mature B cells. Unlike the polyclonal response to TI-1 antigens, the TI-2 responses are confined to cells with a cognate BCR recognising the TI-2 antigen (*Table 3*) (Mond, Lees and Snapper, 1995; Mond *et al.*, 1995; Vos *et al.*, 2000).

Table 3 Characteristics of Thymus-dependent and Thymus-independent antigens.

Adapted from (Tak Mak, 2014).

Characteristics	Thymus dependent	Thymus Independent-1 antigen	Thymus Independent-2 antigen
Requires direct interaction with CD4 T cell for B cell activation	Yes	No	No
Requires cytokines secreted by CD4 T cells (indirect T cell help)	Yes	No	Yes
Response time	Slow	Fast	Fast
Antibody isotypes secreted by B cell in response	IgG, IgA, IgE, and IgM	IgM	IgM
Generation of memory B cells	Yes	No	No
Activates Immature B cells	No	Yes	No
Polyclonal B cell activation	No	Yes	No

Two B cell subsets that are particularly influenced by bacterial mitogens are B1 B cells and MZ B cells (Figure 7). Data from murine studies suggest that CD5+ B1 cells arise from B1 progenitor cells in foetal liver and primarily reside in the peritoneal and pleural cavity fluid. Their placement in the peritoneal and pleural cavity allows them to protect the lungs and gut against microbial invasion. They are self-renewing cells and do not require continuous input from bone marrow. The Ig secreted by the B1 B cells bind to a wide range of antigens with low-affinity and mainly belong to the IgM isotype (Fagarasan and Honjo, 2000; Garraud et al., 2012; Murphy et al., 2012; Owen et al., 2013). However, in humans, CD5 is expressed on pre-naive, transitional and activated follicular B cell populations (Lee *et al.*, 2009).

The role of B1 B cells in humans has been controversial. Investigators have used the phenotypic profile of murine B1 B cells i.e. spontaneous Ab secretion (mostly IgM) to identify human B1 B cells (Griffin, Holodick and Rothstein, 2011). Using this feature the presence of B1 B cell population in humans has been profiled as CD20+CD27+CD43+ (Griffin, Holodick and Rothstein, 2011; Griffin and Rothstein, 2012; Rothstein *et al.*, 2013). It has been shown that CD20+CD27+CD43+ cells are phenotypically similar to memory B cells, while developmentally close to plasmablasts (Covens *et al.*, 2013; Inui *et al.*, 2015). Furthermore, CD20+CD27+CD43- cells can be differentiated into plasmablasts and plasma cells (Covens *et al.*, 2013). This suggests that the proposed B1 B cells represent an intermediate between memory B cells and plasmablasts. Therefore, the presence of B1 B cells in humans remains questionable.

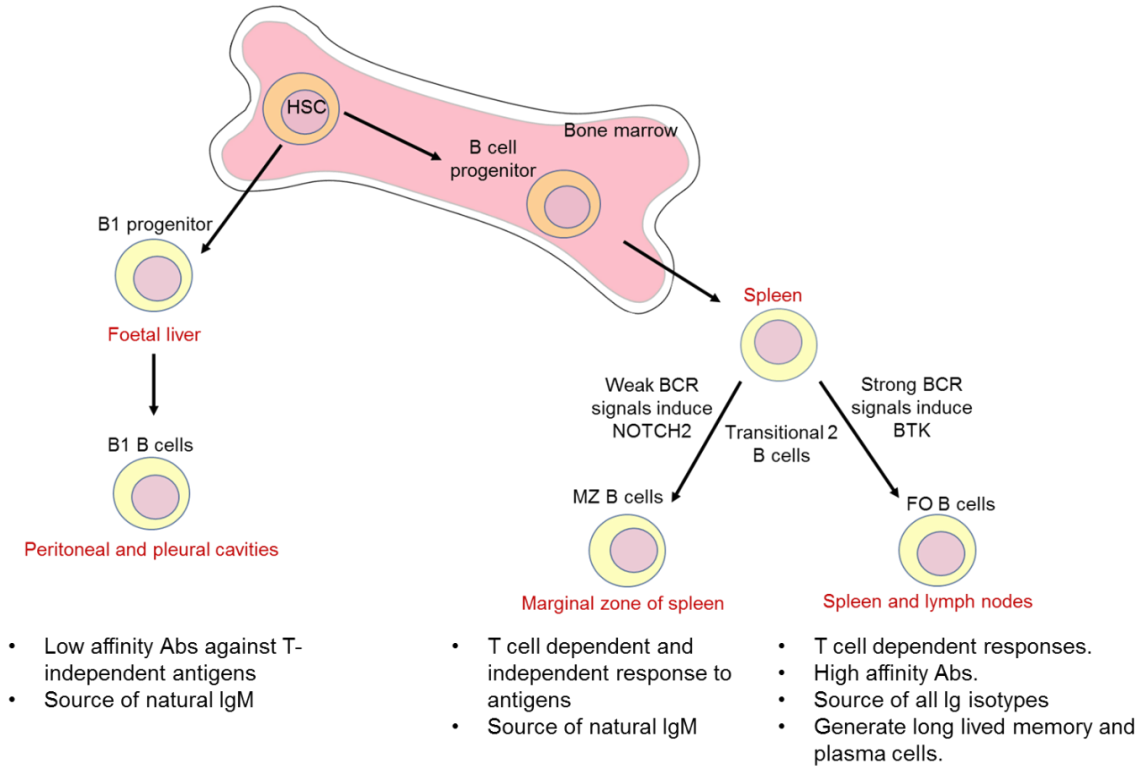

Figure 7 Diagram showing the sites and function of different B cell subsets.

Immature B cells migrate from bone marrow to spleen as transitional B cells. Within spleen transitional B cells either become MZ B cells or Follicular B cells depending on the strength of signal received through the BCR. Another class of B cell is B1 B cells (found in mice) which arise from B1 progenitor cells in foetal liver and reside in the peritoneal and pleural cavities.

Adapted from (Hoffman, Lakkis and Chalasani, 2016).

MZ B cells are non-circulating mature B cells that reside in the marginal sinus of the white pulp in the spleen of rodents (Weill, Weller and Reynaud, 2009). MZ B cells express similar BCR selection to that of B1 B cells. Both MZ and B1 B cells display a rapid response to antigens, likely independent of T cells (Martin, Oliver and Kearney, 2001; Balazs *et al.*, 2002). MZ B cells are regarded as innate resembling cells that in the absence of BCR ligation can be stimulated to differentiate into short-lived plasma cells (Allman and Pillai, 2008). They are also believed to be the cells largely responsible for TI-2 responses. This explains why Infants and young children ≤ 2 years of age lack effective Ig responses to TI-2 antigens, as the MZ B Cell compartment does not mature until after the age of 2 years (Murphy *et al.*, 2012).

Follicular B2 cells originate from bone marrow precursors and reside mainly in the B cell follicles of the secondary lymphoid organs, including spleen and lymph nodes. B2 B cells are non-self-renewing cells and require continuous replenishment from bone marrow. They are a mature B cell subset that recirculates in the blood and participates mainly in T cell-dependent immune responses aimed at foreign antigens resulting in Ig producing memory B cells specific to the antigen (Pillai and Cariappa, 2009). Although B2 cells may participate less in TI responses, some follicular B cells that reside in bone marrow sinusoids can partake in the thymus-independent immune response to bloodborne pathogens (Cariappa *et al.*, 2005; Hoffman, Lakkis and Chalasani, 2016).

In summary, antigens responsible for inducing TI-1 B cell responses are found in various microbial species and generally activate B cells via PRR such as TLR (Ahmad-Nejad *et al.*, 2002). Antigens responsible for inducing TI-2 responses are polyvalent with highly repetitive epitopes such as polysaccharides (Vos *et al.*, 2000). A third class responsible for polyclonal activation of B cells includes the family of the bacterial immunoglobulin binding proteins, which bind to and stimulate the BCR via a non-cognate mechanism, functioning as superantigens e.g. staphylococcal enterotoxin B (SEB) (Goodyear and Silverman, 2005).

1.4.1 T cell-independent IgA production prevents translocation of the intestinal commensal flora and dampens T cell-mediated adaptive immunity

Secretory IgA (sIgA) is the most abundant Ig found across the mucous membranes of mammals. It is secreted in response to commensal bacteria penetrating the Peyer's patches where they are taken up by dendritic cells and presented to B cells found in the mesenteric lymph node. These antigen-loaded DCs induce the secretion of IgA by B cells

via a TI mechanism (Pollard and Sharon, 1970; Macpherson *et al.*, 2000; Jiang *et al.*, 2004; Macpherson, Geuking and McCoy, 2005). SIgA coats the colonising bacteria and prevents them from adhering to the intestinal epithelium thus preventing the bacteria from inducing chronic stimulation of germinal centre reactions (Shroff, Meslin and Cebra, 1995; Mantis, Rol and Corthésy, 2011). Further evidence for the involvement of sIgA in maintaining homeostasis of the gut comes from a cholera toxin study where mice lacking sIgA were more susceptible to infection by cholera toxin compared to normal mice (Uren *et al.*, 2005).

It has been purported that sIgA production is a bacteria-mediated strategy of evading the adaptive immune system. Evidence for the involvement of flora in the production of sIgA comes from a study of germ-free animals where the inoculation of *Morganella morganii* resulted in limited levels of intestinal sIgA compare to high levels of sIgA in conventional animals (Shroff, Meslin and Cebra, 1995). It is hypothesised that the constant coating of commensal bacteria by SIgA may cause a different form of recognition by epithelial cells and dendritic cells as compared to pathogens. Thus, an appropriate level of SIgA can attenuate chronic stimulation of germinal centre reactions in GALT in response to gut bacteria to ensure undue overgrowth of gut bacteria (Suzuki *et al.*, 2004; Corthésy, 2013). Moreover, since sIgA is only induced by viable bacteria (Jiang *et al.*, 2004) and this strategy is not used by all commensals suggests that it is a bacterial-mediated strategy rather than a host-mediated response (Pollard and Sharon, 1970).

Murine studies have shown that sIgA production is partly due to T cell-independent activation of B1 B cells, suggesting that the commensal bacteria are stimulating the production of sIgA via a T cell-independent mechanism (Shroff, Meslin and Cebra, 1995; Macpherson *et al.*, 2000; Macpherson, Martinic and Harris, 2002; Jiang *et al.*, 2004; Macpherson, Geuking and McCoy, 2005). Furthermore, overgrowth of commensal flora in IgA deficient mice suggests that the T independent activation of B1 B cells and the subsequent secretion of sIgA may play a role in controlling the size of the colonising flora. SIgA coats the bacteria and activates complement by binding to mannose-binding lectin (MBL) and promotes complement-dependent lysis or opsonization of the sIgA coated bacteria (Roos *et al.*, 2001) and prevents it from inducing an adaptive immune response. Thus, maintaining homeostasis of the gut commensal flora and host immune system (Macpherson *et al.*, 2000).

As discussed above, sIgA provides a defence against harmful gut microbiota by limiting bacterial association with the epithelium and preventing bacterial penetration of host tissue. However, it is possible that the B cell mitogens present in the commensal flora are responsible for mediating the T-independent IgA response in the intestine which prevents overgrowth of flora and maintains homeostasis in the gut (Hooper and Gordon, 2001). In a

similar way, bacterial activation of B cells by the commensal flora of URT using IgD binding protein could be a strategy to evade a prolonged adaptive immune response.

1.4.2 Mechanisms of T cell-independent B cell proliferation in response to mitogens

Certain B cell subgroups i.e. mice B1 B cells do not require a signal from the CD4+ T cells to be activated as a result, these cells are activated more quickly than T dependent B cells (Martin, Oliver and Kearney, 2001). T cell-independent B cell activation has also been observed in humans (Vaughan *et al.*, 2010). However, as discussed above, the role of a B1 B cell population in humans is not prominent so a T cell-independent B cell response is perhaps more likely due to TI antigens rather than the B cell having TI property (Mond, Lees and Snapper, 1995; Mond *et al.*, 1995).

Although it is still not understood how the commensal flora induces T-independent IgA production in the intestine, there are a number of mechanisms by which bacterial antigens induce T-independent responses that could explain the response (Vos *et al.*, 2000).

Mitogens are antigens that are capable of inducing proliferation in T cells and/or B cells. Various mitogens are plant-derived proteins called lectins, e.g. pokeweed mitogen. Lectin are carbohydrate-binding proteins that has proliferative effects on various cell types. When a mitogen binds to a receptor on the cell membrane it triggers a signal transduction pathway that eventually produces mitogen-activated protein kinase (MAPK) which facilitates mitosis (Bekeredjian-Ding *et al.*, 2012; Owen *et al.*, 2013).

Besides plant-derived mitogens, there are also non-lectin mitogens. These non-lectin mitogens are bacterial antigens that are capable of activating B cells. For protein antigens that bind to the BCR in a cognate fashion, activation of B cells is dependent upon the stimulation from $CD4^+$ T cells. Conversely, bacterial lipopolysaccharide (LPS), lipooligosaccharide (LOS) and certain polymeric proteins are mitogens that can activate B lymphocytes independent of $CD4^+$ T cells via binding to the B cell receptor and TLR (Owen *et al.*, 2013).

1.4.3 Bacterial immunoglobulin binding proteins

Bacterial immunoglobulin binding proteins (Igbp) bind to complementary regions of the immunoglobulin molecule, including conserved residues within the variable domains, the constant regions of the heavy chain and to the constant region of the light chain (Figure 4), crosslinking the receptor and inducing polyclonal activation (Banck and Forsgren, 1978; Forsgren and Grubb, 1979). They are considered to be virulence factors and are mostly expressed by pathogenic bacteria. Various Igbp helps the bacterium to evade the

host's immune response due to protection against the action of complement and a decrease in phagocytosis (Kirjavainen *et al.*, 2008; Kobayashi and DeLeo, 2013). During the last four decades, numerous bacterial Igbps have been discovered. Many Gram-positive bacteria are known to generate immunoglobulin-binding proteins including streptococcal protein G and staphylococcal protein A (Forsgren and Sjoquist, 1966).

Protein A and protein G have a specific affinity for the Fc region of IgG (Figure 4), however low-level non-specific binding of these proteins to $F(ab')_2$ region of other human immunoglobulin isotypes have been reported (Erntell *et al.*, 1988). Protein A also has a specific binding affinity to conserved residues within the variable region of VH3 family antibodies (Roben, Salem and Silverman, 1995; Graille *et al.*, 2000). An IgA binding protein called Arp has been identified in *Streptococcus pyogenes* (Frithz, Hedén and Lindahl, 1989; Janson *et al.*, 1991). There are few examples of IgE, IgM, and IgD binding proteins. *Clostridium perfringens* expresses 'protein P' with high specificity for IgM but also binds to IgA and IgG (Ruan *et al.*, 1990). Another Gram-positive bacterium *Peptostreptococcus magnus* has been shown to express an immunoglobulin binding protein called 'Protein L', which binds to Kappa light chain expressed on IgA, IgG and IgM (Figure 4), (Myhre and Erntell, 1985). Amongst Gram-negative bacteria, *Taylorella equigenitalis* and *Haemophilus somnus* produce IgG binding protein (Forsgren and Grubb, 1979; Corbeil, Bastida-Corcuera and Beveridge, 1997). *Escherichia coli* has been shown to possess trimeric autotransporter Ig binding proteins (Eibs) which binds to the Fc region of IgG (Sandt *et al.*, 1997; Lu *et al.*, 2006; Leo and Goldman, 2009; Leo *et al.*, 2011).

Moraxella catarrhalis (Mcat) IgD binding protein (IgDbp) MID has been isolated and characterised by (Forsgren *et al.*, 2001). MID binds specifically to the C-terminus heavy chain domain of IgD. The binding of MID to the IgD expressed on B cells causes activation and proliferation of B cells which results in the production of non-specific IgGs (Forsgren *et al.*, 2001; Gjorloff Wingren *et al.*, 2002; Forsgren *et al.*, 2003).

1.4.4 Trimeric Autotransporter adhesins

In this thesis, I will show that *N. lactamica* expresses a trimeric autotransporter adhesin with polyclonal B cell activation activity. In general, gram-negative bacteria possess an outer membrane which restricts the diffusion of molecules to and from the extracellular environment. Various bacterial proteins execute their function outside the cytoplasm and therefore need to be expressed on the surface membrane or secreted to the extracellular space. Bacteria exploit various highly specialized protein secretion systems to translocate their proteins (Leo, Grin and Linke, 2012). These range from type I to type VIII secretion systems. Type V secretion systems are the autotransporters.

Autotransporters constitute a diverse superfamily of bacterial outer membrane proteins. A subgroup of this family is type Vc trimeric autotransporter adhesins (TAAs) also known as oligomeric coiled-coil adhesins (OCAs). These TAAs are embedded in the outer membrane and primarily acts as adhesins. They bind to various molecules such as cell surface receptors and components of the extracellular matrix e.g. collagen and fibrinoectin. TAA often provide protection for the bacterium from the host immune responses by binding to modulators of antibody-mediated and innate pathways of complement, e.g. Factor H, antibodies, or C4b binding protein (Kirjavainen *et al.*, 2008). Some well-studied TAAs are referenced in the list in Table 4.

Based on electron microscopy, all TAAs share a similar trimeric surface structure, consisting of N-terminal head, a stalk and a C-terminal anchor domain (Figure 8)(Hoiczyk *et al.*, 2000; Leo *et al.*, 2011). The N-terminus head domain facilitates adhesion to extracellular matrix proteins. A highly conserved sequence referred to as the neck domain connects the head to the stalk domain. The stalk domains are fibrous and play a structural role by keeping the head domain away from the bacterial cell surface and towards its eukaryotic host cells. The C-terminus anchor domain is responsible for translocation through the outer membrane and is highly conserved between all TAAs, whereas stalk and head domains can be found in different orientations (Koretke *et al.*, 2006; Linke *et al.*, 2006b; Fialho and Mil-Homens, 2011). In simple TAAs, e.g. YadA, the fibre consists of only one head and one stalk, whereas in complex TAAs, multiple head and stalk regions alternate along the fibre (Bassler *et al.*, 2015).

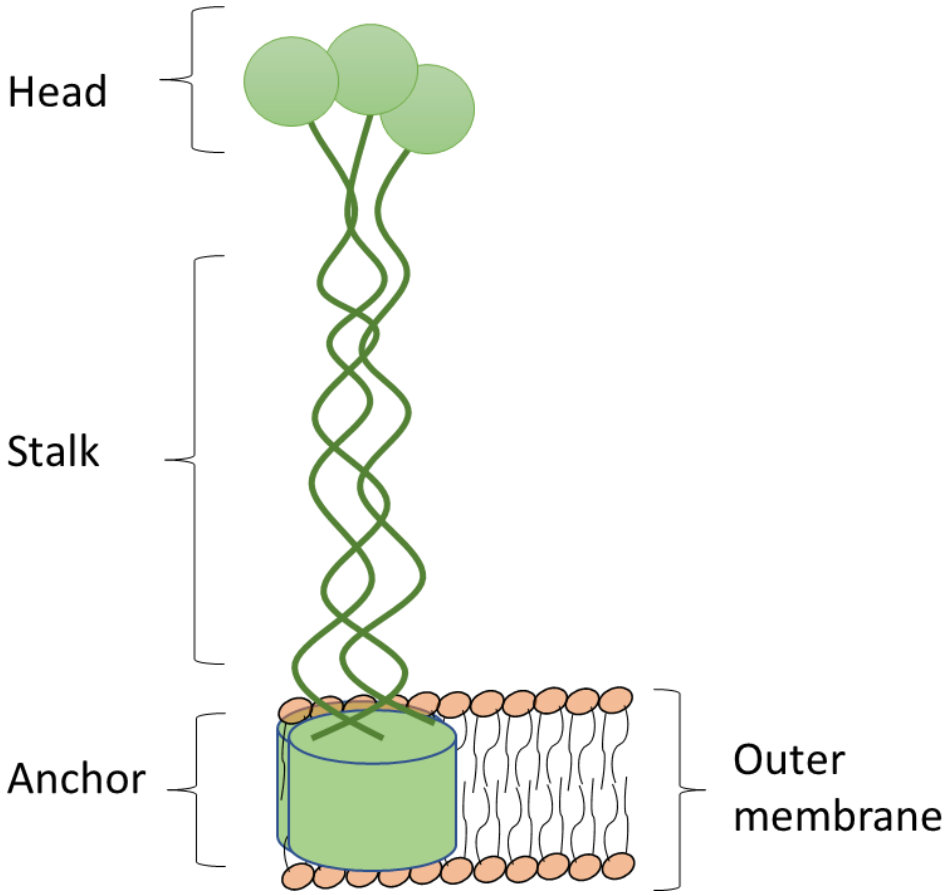

Figure 8 Diagram demonstrating the typical structure of the trimeric autotransporter adhesin

All TAAs share a similar trimeric surface structure, consisting of N-terminal head, a stalk, and a C-terminal anchor domain. The passenger domain is responsible for specific adhesion and other activities of the protein. Its globular head domain(s), where ligands often bind, are projected away from the bacterial surface by an extended triple α-helical coiled coil stalk attached to the β-barrel anchor. The membrane-anchored C-terminal domain forms a β-barrel pore which allows the translocation of a passenger domain into the extracellular space via the type V protein secretion pathway.
Adapted from (Linke *et al.*, 2006a; Hallström *et al.*, 2008; Szczesny and Lupas, 2008; Lyskowski, Leo and Goldman, 2011).

Table 4 List of Trimeric autotransporter adhesins

Protein	Organism(S)	Functions	Reference
Ata	*Acinetobacter baumanii*	Adhesion to human primary endothelial and epithelial cells	(Bentancor *et al.*, 2012)
AhsA	*Mannheimia haemolytica*	Collagen binding	(Daigneault and Lo, 2009)
BadA	*Bartonella henselae*	Collagen binding, binding to epithelial cells, phagocytosis resistance and proangiogenic factor	(Riess *et al.*, 2004)
BimA	*Burkholderia pseudomallei*	Actin binding, polymerisation and actin-based motility	(Stevens *et al.*, 2005)
Cha	*Haemophilus sp.*	Binding to epithelial cells	(Sheets *et al.*, 2008)
DsrA	*Haemophilus ducreyi*	Serum resistance, keratinocyte binding, ECM binding	(Elkins, Morrow and Olsen, 2000)
EibA, EibE	*Escherichia coli*	IgG binding, serum resistance	(Sandt and Hill, 2000)
EibC, EibD, EibF	*Escherichia coli*	IgA and IgG binding, serum resistance	(Sandt and Hill, 2000)
EibG	*Escherichia coli*	IgA and IgG binding, chain-like adhesion to mammalian cells	(Merkel *et al.*, 2010)
EmaA	*Aggregatibacter actinomycetemcomitans*	Collagen binding	(Tang *et al.*, 2008)
HadA	*Haemophilus influenza*	Autoagglutination, ECM binding, epithelial cell binding and invasion	(Serruto *et al.*, 2009)
Hia, Hsf	*Haemophilus influenza*	Epithelial cell binding	(St Geme, Cutter and Barenkamp, 1996; St Geme and Cutter, 2000)
MID	*Moraxella catarrhalis*	IgD binding, adhesion to lung and middle ear epithelial cells, biofilm formation	(Forsgren *et al.*, 2001)
NadA	*Neisseria meningitidis*	Adhesion to and invasion of epithelial cells	(Comanducci *et al.*, 2002)
NhhA	*Neisseria meningitidis*	ECM binding, binding to epithelial cells, serum and phagocytosis resistance	(Scarselli *et al.*, 2006)
SadA	*Escherichia coli*	Autoagglutination, binding to epithelial cells	(Raghunathan *et al.*, 2011)
UpaG	*Escherichia coli*	ECM binding, biofilm formation, autoagglutination	(Valle *et al.*, 2008)
UspA1, UspA2	*Moraxella catarrhalis*	ECM and epithelial cell binding, serum resistance, biofilm formation	(Lafontaine *et al.*, 2000)
VompA, VompB, VompC, VompD	*Bartonella quintana*	Collagen binding, autoagglutination	(Zhang *et al.*, 2004)
YadA	*Yersinia pestis, Y. enterocolitica, Y. pseudotuberculosis*	ECM binding, serum and phagocytosis resistance, autoagglutination, binding to epithelial cells and neutrophils	(Bolin, Norlander and Wolf-Watz, 1982)
YadB, YadC	*Yersinia pestis*	Epithelial cell invasion	(Murphy *et al.*, 2007)

1.4.5 IgD binding trimeric autotransporter protein

YadA, the Yersinia adhesin A of *Yersinia enterocolitica* is the prototype of all TAAs (Hoiczyk *et al.*, 2000). However, *Haemophilus influenzae* adhesin Hia (St Geme and Cutter, 2000) and *Moraxella catarrhalis* IgD binding protein (MID) are particularly relevant to this thesis.

Moraxella catarrhalis contains a 200 kDa outer membrane protein composed of 2139 amino acids, known as *Moraxella catarrhalis* Immunoglobulin D binding protein (MID) (Figure 9). MID is a trimeric autotransporter that binds to both soluble and membrane-bound IgD on B cells. MID targets IgD expressed on the surface of the B cells resulting in the activation of human B cells (Jendholm *et al.*, 2008). MID is a TI Ag and therefore induces T cell-independent B cell proliferation resulting in the production of non-specific IgGs (Gjorloff Wingren *et al.*, 2002). MID is also a hemagglutinin and adhesin that binds to type II alveolar epithelial cells(Forsgren *et al.*, 2003). The adhesive part of MID is found within MID amino acid (aa) 764-913 located upstream of the IgD-binding site (Hallström *et al.*, 2008).

Recombinantly expressed MID translocates to the outer membrane of *E*. *coli*. MID has been shown to bind two purified IgD myeloma proteins, four IgD myeloma sera, and finally one IgD standard serum. Furthermore, MID does not bind IgG, IgM, IgA, or IgE myeloma proteins. Flow cytometry experiments have shown that fluorescein isothiocyanate (FITC)-conjugated MID specifically binds to the IgD BCR on human $CD19^{+}$ B cells.

MID shows no similarity with other Ig-binding proteins including protein D from *H. influenzae*. However, MID in parts has homology (48%) with USPA1 and 2 (Forsgren *et al.*, 2001)

It has been claimed that *Haemophilus influenzae* also contains an IgD binding protein called protein D. Purified protein D is highly conserved surface lipoprotein with a molecular mass of approximately 42 kDa (Ruan *et al.*, 1990; Forsgren, Riesbeck and Janson, 2008). OMVs derived from two strains of *H. influenzae*; Non-typable *Haemophilus influenzae* (NTHi) KR404 and KR403 have been shown to induce proliferation in B cell. This proliferative response is abrogated upon pre-treatment with anti-IgD Ab. Furthermore, OMVs from both strains have been shown to bind to B cells. However, pre-treatment of B cells with anti-IgD Ab only inhibited the binding of NTHi KR404 OMVs, and this was not fully the case for NTHi KR403. This suggests that another molecule on the surface of B lymphocyte might contribute to the binding of OMV derived from KR403 (Deknuydt, Nordstrom and Riesbeck, 2014).

In a different study it has been shown that myeloma proteins bind strongly to type b MinnA strain but failed to bind to *E. coli* expressing recombinant protein D suggests that protein D is not sufficient for IgD binding to type b strains (Sasaki and Munson, 1993).

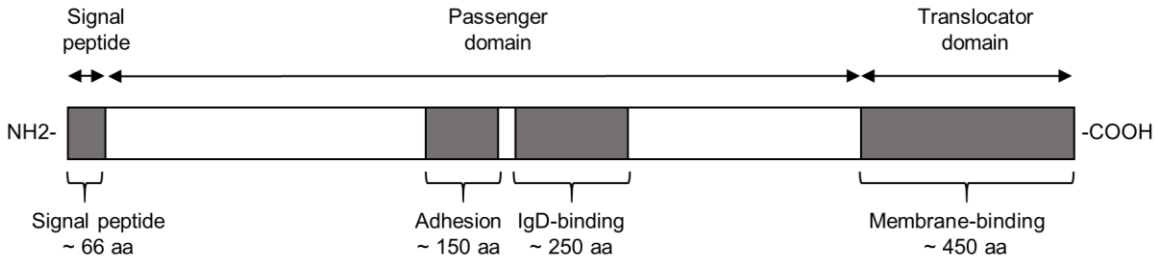

Figure 9 Diagram showing the known domains of the IgD binding protein MID.

Moraxella catarrhalis contains an IgD binding trimeric autotransporter protein called MID. MID is composed of 2139 amino acids. The IgD binding region of MID protein is within the passenger domain between amino acids 962-1200.
Adapted from (Riesbeck and Nordstrom, 2006; Hallström *et al.*, 2008).

1.5 Upper respiratory tract microbiome

The respiratory tract is partitioned into the URT and LRT. The LRT comprises a section of the larynx below the vocal cord, the trachea, lungs (bronchi, bronchiole and alveoli, whereas the URT consists of the nasopharynx, oropharynx, nasal cavity, paranasal sinuses and the section of the larynx above the vocal cord (Man, de Steenhuijsen Piters and Bogaert, 2017)

Human URT is colonised by a variety of bacterial species (Table 5), most of which are non-pathogenic in an immunocompetent host and do not prime any major inflammatory response in the epithelial cells but rather contributes to the development and enhancement of host immune function (Belkaid and Hand, 2014). The URT microbiome plays a vital part in administering the normal function of the URT framework, preventing the intrusion and colonisation of exogenous pathogens (Zhang and He, 2015). Despite this, the oro- and nasopharynx is colonised by a high percentage of potential pathogens (pathobionts) which under certain circumstances can result in life-threatening infections such as pneumonia, meningitis and many other diseases (Tlaskalova-Hogenova *et al.*, 2004).

Mucosal surfaces are exposed to a vast burden of antigens, including potential antigens from the air, food, and the residing commensal flora. Therefore, these surfaces are protected by a broad system of lymphoid tissues collectively known as the Mucosa Associated Lymphoid Tissue (MALT). MALT is estimated to contain more than 50% of the lymphocytes of the immune system (Murphy *et al.*, 2012). MALT is found in various locations throughout the body along the mucosal surfaces and is composed of Gut Associated Lymphoid Tissue (GALT) lining the intestinal tract, Bronchus Associated Lymphoid Tissue (BALT) lining the respiratory tract and Nasopharynx Associated Lymphoid Tissue (NALT). Peyer's patches, appendix, tonsils and adenoids are all part of GALT and are responsible for collecting antigen from the epithelial surfaces of the GI tract (Cesta, 2006; Murphy *et al.*, 2012).

Table 5 Bacteria colonising the URT of humans.

Taken from (Robinson, 2004; Stearns *et al.*, 2015; Man, de Steenhuijsen Piters and Bogaert, 2017)

Species
Staphylococcus spp.
Streptococcus spp.
Haemophilus influenzae
Moraxella catarrhalis
Neisseria spp.
Escherichia coli
Mycoplasma pneumoniae
Propionibacterium spp.
Corynebacterium spp.
Propionibacterium spp.
Rothia spp.
Veillonella spp.
Prevotella spp.
Leptotrichia spp.
Tropheryma whipplei
Pseudomonas aeruginosa
Klebsiella spp.
Lactobacillus spp.
Micrococcus spp.

1.5.1 *Moraxella catarrhalis*

Moraxella catarrhalis (Mcat) formerly called *Neisseria catarrhalis* is a gram-negative, aerobic diplococcus is a commensal bacterium that colonizes the nasopharynx of 66% of healthy infants during their first year of development and 4% of the general adult population (Verduin *et al.*, 2002; Mollenkvist *et al.*, 2003). However, *M. catarrhalis* has increasingly gained a reputation as a respiratory pathogen due to its frequent presence in lower respiratory tract infections, particularly in adults with chronic obstructive pulmonary disease (COPD) (Murphy *et al.*, 2005). *M. catarrhalis* is the third most commonly isolated bacterium in cases of otitis media in children after *Haemophilus influenzae* and *Streptococcus pneumoniae* (Sillanpää *et al.,* 2016). It has also been associated with sinusitis, acute laryngitis, and in rare cases, septicaemia (Hol *et al.*, 1996; Sheikhi *et al.*, 2015).

1.5.2 *Neisseria* species

Human *Neisseria* consists of Gram-negative, oxidase-positive, catalase-positive and diplococci bacteria (except *N. elongata* and *N. bacilliformis*). The bacteria belonging to this genus are aerobic, non-sporing, non-motile and ferment sugars with the production of acid but no gas (Parija, 2014).

10 species in the Neisseria genus colonise humans, most of these species are commensals of the mouth and upper respiratory tract except for *N. meningitidis* (Nmen), an opportunistic pathogen of the URT, and *N. gonorrhoeae*, an obligate pathogen of the genitourinary tract and rectum (Table 6, Figure 10) (Smith *et al.*, 1999; Bennett *et al.*, 2014).

The two *Neisseria* spp. that are most relevant to this thesis are *N. lactamica* and *N. meningitidis*.

Table 6 *Neisseria* species found in humans

Species
Neisseria meningitidis (Nmen)
Neisseria gonorrhoeae (Ngon)
Neisseria lactamica (Nlac)
Neisseria cinerea (Ncin)
Neisseria flavescens (Nflav)
Neisseria mucosa (Nmuc)
Neisseria polysaccharea (Npol)
Neisseria subflava (Nsub)
Neisseria elongata (Nelong)
Neisseria bacilliformis (Nbac)

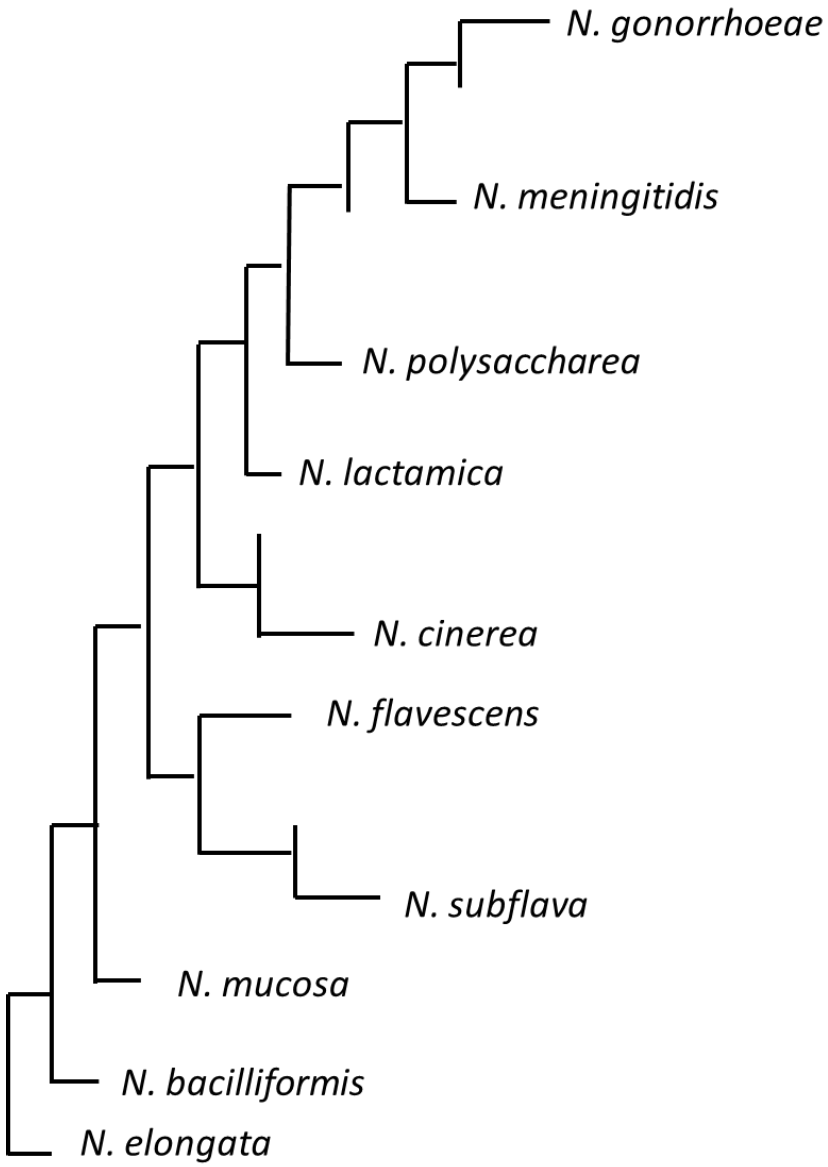

Figure 10 Diagram representing the evolutionary relationship among human colonising *Neisseria* spp.

Neisseria species groups have been identified based on the analysis of the concatenated sequences from 246 genes from genus *Neisseria*.

Adapted from (Bennett *et al.*, 2012)

1.5.2.1 *Neisseria meningitidis*

Neisseria meningitidis, also known as meningococcus, is a fastidious bacterium. Nmen is an opportunistic pathogen of the human URT. Nmen is only found in human hosts and therefore it must coincide with the immune system in a state of homeostasis. It is carried asymptomatically by 10% of the adult population but under certain circumstances causes inflammation of the meninges (meningococcal meningitis), and septicaemia (Bernardini *et al.*, 2004; Lo, Tang and Exley, 2009; Aspholm *et al.*, 2010). Nmen spreads from contact with URT secretions of Nmen carriers, through coughing, sneezing and kissing (Yazdankhah and Caugant, 2004). Carriage rates of Nmen among university students increase rapidly in the first week of term and continues to increase throughout the term (Neal *et al.*, 2000). Furthermore, university students have been shown to be at the greatest risk of invasive meningococcal disease compared to other people of the same age group. Carriage rates of meningococci can rise to 80% in overcrowded places i.e. during the Hajj (al-Gahtani *et al.*, 1995) and military recruits (Caugant *et al.*, 1992).

Its outer membrane can be enclosed by a polysaccharide capsule. The meningococci express diverse capsule polysaccharides, which are the basis for serogroup classification. So far 12 serogroups are recognised using the serologic method based on capsular polysaccharides. Out of 12 serogroups of Nmen 6 serogroups (A, B, C, W, X, Y) cause human invasive meningococcal disease (IMD), and the serogroups A, B, C and W have been most frequently associated with epidemics. The majority of IMD cases occur in infancy and early childhood (3 months - 2 years) (Rosenstein *et al.*, 2001; Halperin *et al.*, 2012).

Nmen strains that cause IMD are predominantly encapsulated (Uria *et al.*, 2008). The capsule enhances its ability to cause disease by helping the bacteria to resist phagocytosis and complement-mediated lysis (Halperin *et al.*, 2012). Nmen uses factor H binding protein to inhibit the alternative pathway of complement (Lewis, Carter and Ram, 2012). Additionally, the polysaccharide capsule evades both alternative and classical complement pathways by preventing the deposition of C3b on the bacterium (Tan *et al.*, 2007; Hallstrom and Riesbeck, 2010; Hyams *et al.*, 2010).

1.5.2.2 *Neisseria lactamica*

Neisseria lactamica is a lactose fermenting harmless commensal bacterium of the URT. It chiefly resides in the nasopharyngeal epithelium of infants and children. It is closely related to *N. meningitidis* and shares many mutual antigens to *N. meningitidis* but lacks a polysaccharide capsule and porA antigen (Gold *et al.*, 1978; Gorringe *et al.*, 2005; Parija, 2014). Comparisons of the genome of *N. lactamica* with *N. meningitidis* has shown that

they share around 1190 CDSs, corresponding to ~ 60% of the genome (Bennett *et al.*, 2010). Furthermore, analysis by sodium dodecyl sulphate polyacrylamide gel electrophoresis (SDS-PAGE) and immunoblotting of *N. lactamica* and *N. meningitidis* has shown that these two species share multiple LOS epitopes (Kim, Mandrell and Griffiss, 1989). However, unlike *N. meningitidis, N. lactamica* never causes invasive disease in the context of immunocompetent hosts (Schifman and Ryan, 1983; Denning and Gill, 1991; Fowler *et al.*, 2006). Rare cases of *N. lactamica*-associated invasive disease have been reported in the context of immunocompromised patients (Brown, Ragge and Speller, 1987; Denning and Gill, 1991; Wang *et al.*, 2006; Zavascki *et al.*, 2006; Everts *et al.*, 2010). However, the identification of *N. lactamica* in these studies was done by biochemical tests and not confirmed by whole genome sequencing, MALDI-TOF or PCR based identification. Therefore, the specificity of these results is questionable (Jesumirhewe *et al.*, 2016).

Interest in *N. lactamica* stemmed from epidemiological studies which observed an inverse relationship between carriage of *N. lactamica* and *N. meningitidis.* In contrast to *N. meningitidis* in which carriage is low during infancy and rises to high levels in adolescents and young adults, carriage of *N. lactamica* is high in young children but declines with age (Gold *et al.*, 1978; Cartwright *et al.*, 1987). It has been theorized that the inverse relationship between *N. lactamica* and *N. meningitidis* colonisation was due to the development of SBA to *N. lactamica* antigens that are cross-reactive to MenB antigens (Goldschneider, Gotschlich and Artenstein, 1969a;b; Kremastinou *et al.*, 1999; Troncoso *et al.*, 2002). It has been demonstrated in a longitudinal study of healthy infants and children that those who naturally acquired *N. lactamica* colonisation also developed a fourfold or greater rise in cross-reactive SBA titre to a meningococcal panel (Gold *et al.*, 1978). Cross-reactive immunity has been shown in mice where immunization by *N. lactamica* OMV-based vaccine protected the mice against lethal challenge with serogroup B and C meningococcal isolates, however, this effect was not due to the induction of cross-reactive SBA (Oliver *et al.*, 2002). A different study investigating anti-meningococcal IgG and IgM Abs in response to *N. lactamica* found no evidence of the association between carriage of *N. lactamica* and bactericidal Abs against meningococci (Kremastinou *et al.*, 1999). Furthermore, experimental data from the mouse studies have shown that *N. lactamica* vaccines comprising outer membrane vesicles or whole killed bacterial cells elicit protection in mice against disseminated meningococcal disease without detectable serum bactericidal activity (Li *et al.*, 2006). Based on this it has been hypothesised that *N. lactamica* colonization may prevent *N. meningitidis* colonisation and the subsequent development of IMD.

In order to confirm the hypothesis that *N. lactamica* colonisation can reduce meningococcal colonisation an experimental human challenge in university students was

carried out which demonstrated that, nasal inoculation of *N. lactamica* caused a significant decrease in the meningococcal carriage (Deasy *et al.*, 2015). This effect was either due to microbial competition or cross-reactive immune responses that operate only in individuals actively carrying the commensal *N. lactamica*.

Additionally, in a recent *N. lactamica* human challenge study it was demonstrated that the colonisation with *N. lactamica* is an immunising event which results in a significant increase in *N. lactamica* specific IgG (blood) and IgA (saliva) (Evans *et al.*, 2011). Furthermore, they demonstrated a significant increase in cross-reactive opsonophagocytic antibody against a meningococcal panel in *N. lactamica* colonised subjects, however a significant rise in cross-reactive SBA titres was not demonstrated.

Collectively, these findings imply that either *N. lactamica* is providing protection against *N. meningitidis* by presenting additional competition for meningococci or *N. lactamica* could be priming an immune response that cross-reacts with *N. meningitidis* by inducing secretion of cross-reactive antibodies resulting in natural immunity against meningococci.

In contrast to *N. meningitidis,* which rapidly induces adaptive immunity upon colonisation of the nasopharyngeal epithelium (Davenport *et al.*, 2003), Vaughan et al quantified *N. lactamica* specific T-cell memory and B-cell memory responses in the URT of children and found that *N. lactamica*-specific memory remained low in young children during the peak period of nasopharyngeal colonisation (Vaughan *et al.*, 2009). This suggests that *N. lactamica* may interact differently with the host during colonisation than *N. meningitidis* allowing it to evade the adaptive immune system.

Based on a previous investigation (Vaughan *et al.*, 2010) I postulate that the B cell proliferative response to *N. lactamica* is due to the interaction between a putative IgD binding protein present on *N. lactamica* dOMV and IgD expressed on B cells. This interaction seems to be biased towards the λ light chain-expressing B cells (Vaughan *et al.,* unpublished data). *Moraxella catarrhalis* also exhibits similar activity*,* it induces a potent mitogenic effect on human B lymphocytes and efficiently binds serum IgD. In contrast, *E. coli*, *N. meningitidis*, and *N. gonorrhoeae,* which bind serum IgD weakly are weakly mitogenic (Banck and Forsgren, 1978; Forsgren and Grubb, 1979). *M. catarrhalis* IgD binding protein (MID) has been identified (Forsgren *et al.*, 2001; Gjorloff Wingren *et al.*, 2002; Hallström *et al.*, 2008) and the BLAST search of *N. lactamica* revealed two homologous genes, NLY_36660 and NLY_37260, suggesting the presence of two putative IgD binding proteins in *N. lactamica*.

1.6 Aims and objectives

Previous investigations have found that despite being closely related and sharing a similar ecological niche, *N. meningitidis* and *N. lactamica* appear to interact very differently with the host immune system during commensal colonisation. Unlike *N. meningitidis,* which induces a pro-inflammatory effector T cell response (Davenport *et al.*, 2003) that may be attenuated by Treg, *N. lactamica* appears not to prime an adaptive T cell response (Vaughan *et al.*, 2009). This project will use *N. lactamica* and *N. meningitidis* as a model to investigate bacterial factors relevant to nasopharyngeal colonisation and look into how commensal bacterial species of the human upper respiratory tract interact with the host immune system in order to promote long-term colonisation and avoid being cleared by the immune system. Understanding this may provide knowledge that may be applied to improve the design of current vaccines in order to prevent colonisation by pathogenic bacteria.

Based on a previous investigation (Vaughan *et al.*, 2010) we suspect that the B cell proliferative response to *N. lactamica* is due to the interaction between putative IgD binding protein present on *N. lactamica* OMV and IgD expressed on B cells. I purport that the ability of a number of URT bacterial species to specifically interact with IgD expressing B cells may represent an important strategy by which these organisms interact with the host immune system during colonisation. Furthermore, the discovery of this activity in a commensal species, suggests that any functional role may be in commensal colonisation and not pathogenesis.

In this work, possible candidates for the gene encoding the IgD binding protein were knocked out from mitogenic *Neisseria* strains generating ΔIgDbp strains. These strains were then used as tools for further studying the putative IgD binding protein.

This study aimed to identify and subsequently purify the putative IgD binding protein in *N. lactamica* as well as explore the potential functional consequences that targeting IgD has on the interaction between *N. lactamica* and the host immune system during colonisation. I also surveyed the commensal species in the genus *Neisseria* to determine whether the ability to interact with and activate B cells expressing IgDλ is a conserved property within related commensal species that inhabit the URT.

1.6.1 Hypotheses

- B cell activation in response to *N. lactamica* Y92-1009 is due to the presence of an IgDλ binding protein/proteins present in *N. lactamica*.
- The ability to induce proliferation in B cells is a conserved property among *Neisseria* spp.
- Knockout strains lacking the putative IgD binding protein gene will not be able to induce proliferation in B cells.

2. Materials and Methods

2.1 Bacterial Strains and growth conditions

Neisseria lactamica Y92-1009 (Evans *et al.*, 2011) and *N. meningitidis* H44/76 (Piet *et al.*, 2011) stocks were stored at -80°C. *N. gonorrhoeae* MS11 strain was kindly provided by Dr Victoria Humbert, Clinical and Experimental Sciences, Southampton. CCUG 346T *N. cinerea*, CCUG 50858T *N. bacilliformis,* CCUG 2043T *N. elongata ss elongata*, CCUG 17913T *N. flavescens*, CCUG 41451T *N. macacae*, CCUG 26878T *N. mucosa ss Heidelbergensis*, CCUG 18031T *N. polysaccharea* and CCUG 23930T *N. subflava* strains were obtained from Culture Collection, University of Göteborg (CCUG), Sweden.

All strains were grown on TSB+ plates (1.5% agar containing 3% Tryptone Soya Broth (TSB) and 0.2% yeast extract) overnight at 37°C 5% CO_2. Bacterial stocks were prepared in Modified Catlin 7 (MC.7) media by growing the bacteria to log phase, centrifuging and re-suspending the pellet in a 1:1 suspension of Phosphate Buffer Saline (PBS) and glycerol. Glycerol stocks were maintained at -80°C. Glycerol stocks were revived on TSB+ plates overnight at 37°C 5% CO_2 and grown in MC.7 media to log phase in 50 ml tubes at 37°C in Galaxy® 170R incubator (New Brunswick) shaking at 340 rpm on a KS 130 basic shaker (IKA).

2.2 Modified Catlin media

Modified Catlin 7 Media is a modification of MC.6 medium recipe prepared using the same method as *Mukjopadhyay et al*. The following ingredients were used to formulate the MC.7 media: 100mM NaCl, 20mM K_2HPO_4, 18mM NH_4Cl, 5.7mM K_2SO_4, 55mM D-(+)-glucose, 2mM $MgCl_2 \bullet 6H_2O$, 0.2mM $CaCl_2 \bullet 2H_2O$, 0.08% (W/V) Yeast extract, 25mM HEPES, 0.03mM Ethylenediamine-N, N′-diacetic acid (EDDA), 0.6mM L-Cysteine●HCl and 26.5mM L-glutamic acid. The final pH of the medium was adjusted to pH 7 (Mukhopadhyay *et al.*, 2005).

2.3 Primers

Primers (*Sigma-Aldrich,* Gillingham, UK) were designed to amplify sections of plasmid or extend overlapping regions. Primers were designed making sure the difference between the melting temperatures (Tm) of primer pairs did not exceed 5°C. Where possible primer length was kept between 20-40 nucleotides and a GC content of 40-60%.

Table 7 List of primers used in the transformation of NEICINOT_03770 ORF present in *N. cinerea*.

DNA uptake sequence is highlighted magenta; Nucleotide added to cause a frameshift is shown in red; *N. cinerea* chromosomal DNA sequence is highlighted yellow; Antibiotic sequence is highlighted grey; Plasmid sequence is highlighted blue.

No.	Oligonucleotide	Sequence
1	NEICINOT_03770_5 PRIMEEND_FOR	GATCCTCTAGAGTCATGAATAAAGTATTCCGAGTGATTTGGAAGCC
2	NEICINOT_03770_5 PRIMEEND_REV	CAGTTGCCGAATATGTATGCCGTCTGCATTAATCG
3	NEICINOT_03770_3 PRIMEEND_FOR	GTCGGCAAATAATGCCGTCTGAAGTTGAATGCGGGTTGGAACACTGC
4	NEICINOT_03770_3 PRIMEEND_REV	GCATGCCTGCAGGTCTTACCAGAGGTAGCCGACGCCGACAC
5	PUC19_03770FOR	CGGCTACCTCTGGTAAGACCTGCAGGCATGCAAGCTTGG
6	PUC19_03770REV	GAATACTTTATTCATGACTCTAGAGGATCCCCGGGTACC
7	NEICINOTSpec03770_FOR	ATTAATGCAGACGGCATACATATTCGGCAACTGTCGGAATATCTG
8	NEICINOTSpec03770_REV	CAACCCGCATTCAACTTCAGACGGCATTATTTGCCGACAACTTTGG
9	5PrimeEND-03770-ORF_FOR	TGCAATACGCTACAAGCC
10	3PrimeEND-03770-ORF_REV	GAGCAAGGGTGAATGTGC

Table 8 List of primers used in the transformation of DYC64_RS10620 ORF present in *N. flavescens*.

DNA uptake sequence is highlighted magenta; Nucleotide added to cause a frameshift is shown in red; *N. flavescens* chromosomal DNA sequence is highlighted yellow; Antibiotic sequence is highlighted grey; Plasmid sequence is highlighted blue.

No.	Oligonucleotide	Sequence
1	FLAV_12978_5PRIMEEND_FOR	GATCCTCTAGAGTCATGAATAAAGTATTCCAGAG
2	FLAV_12978_5PRIMEEND_REV	GACAGTTGCCGAATATCATTTGTGTATCCGTTAG
3	FLAV_12978_3PRIMEEND_FOR	CTAATGCCGTCTGAAGTAAACACACATAATAGCG
4	FLAV_12978_3PRIMEEND_REV	GCCTGCAGGTCTTACCAGAGGTAGCCG
5	PUC19_FLAV_12978FOR	GCTACCTCTGGTAAGACCTGCAGGCATGCAAGCTTGG
6	PUC19_FLAV_12978REV	GAATACTTTATTCATGACTCTAGAGGATCCCCGGGTACC
7	FLAV_12978_kanFOR	CGGATACACAAATGATATTCGGCAACTGTCG
8	FLAV_12978_kanREV	CATTATGTGTGTTTACTTCAGACGGCATTAGAATAATTCATCCAACAGG
9	FLAV_12978_testFOR	ATTGGCTATCTCAAACATAT
10	FLAV_12978_testREV	AAGTTGAAAAACCTCCGTAT

Table 9 List of primers used in the transformation of NEIPOLOT_RS07545 ORF present in *N. polysaccharea*.

DNA uptake sequence is highlighted magenta; Nucleotide added to cause a frameshift is shown in red; *N. polysaccharea* chromosomal DNA sequence is highlighted yellow; Antibiotic sequence is highlighted grey; Plasmid sequence is highlighted blue.

No.	Oligonucleotide	Sequence
1	Polysac_11136_5PRIMEEND_FOR	GATCCTCTAGAGTCATGAACAAAATTTTCCGTAGTC
2	Polysac_11136_5PRIMEEND_REV	CAGTTGCCGAATATATCCACCTTGCGGTATC
3	Polysac_11136_3PRIMEEND_FOR	GTCGGCAAATAATGCCGTCTGAAGACGGTACTGCCGACAAAG
4	Polysac_11136_3PRIMEEND_REV	GCATGCCTGCAGGTCTTACCACTGATAACCGACAG
5	PUC19_11136FOR	CGGTTATCAGTGGTAAGACCTGCAGGCATGCAAGCTTGG
6	PUC19_11136REV	GGAAAATTTTGTTCATGACTCTAGAGGATCCCCGGGTACC
7	Polysac_spec11136FOR	GATACCGCAAGGTGGATATATTCGGCAACTGTCGGAATATCTG
8	Polysac_spec11136REV	GTCGGCAGTACCGTCTTCAGACGGCATTATTTGCCGACAACTTTGG
9	Polysac_11136_testFOR	CGGCGTATTGAAAACAGAG
10	Polysac_11136_testREV	ACAGGCGGGAAAGTCTT

Table 10 List of primers used in the transformation of NEICINOT_03770 present in *N. cinerea*.

DNA uptake sequence is highlighted magenta; *N. cinerea* chromosomal DNA sequence is highlighted yellow; Antibiotic sequence is highlighted grey; Plasmid sequence is highlighted blue.

No.	Oligonucleotide	Sequence
1	NEICINOT_03770_5PRIMEEND_FOR	GATCCTCTAGAGTCTTACCTCTGGTAATCTGTTTAG
2	NEICINOT_03770_5PRIMEEND_REV	CAGTTGCCGAATATGATATAACCCTTTAAAATGTG
3	NEICINOT_03770_3PRIMEEND_FOR	GTCGGCAAATAATGCCGTCTGAAACCAAGTTGAAAAACCTCCG
4	NEICINOT_03770_3PRIMEEND_REV	GCATGCCTGCAGGTCATACATTGCAGGGCAGTTCG
5	PUC19_03770FOR	CTGCCCTGCAATGTATGACCTGCAGGCATGCAAGCTTGG
6	PUC19_03770REV	GATTACCAGAGGTAAGACTCTAGAGGATCCCCGGGTACC
7	NEICINOTSpec03770_FOR	CATTTTAAAGGGTTATATCATATTCGGCAACTGTCGGAATATCTG
8	NEICINOTSpec03770_REV	GTTTTTCAACTTGGTTTCAGACGGCATTATTTGCCGACAACTTTGG
9	5PrimeEND-03770-ORF_FOR	CAGCGACAACGGCAAACTG
10	3PrimeEND-03770-ORF_REV	GGGAATTGTATGCGGGATCAAG

Table 11 List of primers used in the transformation of NEICINOT_04577 ORF present in *N. cinerea*.

DNA uptake sequence is highlighted magenta; *N. cinerea* chromosomal DNA sequence is highlighted yellow; Antibiotic sequence is highlighted grey; Plasmid sequence is highlighted blue.

No.	Oligonucleotide	Sequence
1	NEICINOT_04577_5PRIMEEND_FOR	GATCCTCTAGAGTCAATATAAGCCATCTGCTTTTTAG
2	NEICINOT_04577_5PRIMEEND_REV	CAGTTGCCGAATATAGATAGTTCCCTTATCTTAG
3	NEICINOT_04577_3PRIMEEND_FOR	GTCGGCAAATAATGCCGTCTGAATGAAGTTTGGTTGTATCTAAGTATAAG
4	NEICINOT_04577_3PRIMEEND_REV	GCCTGCAGGTCCAACAACATCTAAAGCATGGGAC
5	PUC19_04577FOR	CTTTAGATGTTGTTGGACCTGCAGGCATGCAAGCTTGG
6	PUC19_04577REV	CAGATGGCTTATATTGACTCTAGAGGATCCCCGGGTACC
7	NEICINOTSpec04577_FOR	GATAAGGGAACTATCTATATTCGGCAACTGTCGGAATATCTG
8	NEICINOTSpec04577_REV	CAACCAAACTTCATTCAGACGGCATTATTTGCCGACAACTTTGG
9	5PrimeEND-04577-ORF_FOR	GAGTCTCTCCGTCCGCAC
10	3PrimeEND-04577-ORF_REV	CCGCACGGTTCTTCTACC

Table 12 List of primers used in the transformation of NEIFLAOT_01884 ORF present in *N. flavescens*.

DNA uptake sequence is highlighted magenta; *N. flavescens* chromosomal DNA sequence is highlighted yellow; Antibiotic sequence is highlighted grey; Plasmid sequence is highlighted blue.

No.	Oligonucleotide	Sequence
1	NEIFLAOT_01884_5PRIMEEND_FOR	GATCCTCTAGAGTCGAGTATGAACTTGTGGCAGAG
2	NEIFLAOT_01884_5PRIMEEND_REV	CAGTTGCCGAATATTTTGTTTTCTCTTTCGGTTTG
3	NEIFLAOT_01884_3PRIMEEND_FOR	GTCGGCAAATAATGCCGTCTGAAGGGGTTTTTCCCTATCGG
4	NEIFLAOT_01884_3PRIMEEND_REV	GCATGCCTGCAGGTCGATAGGATTCTTTTGGCATTGGTTC
5	PUC19_01884FOR	CAAAAGAATCCTATCGACCTGCAGGCATGCAAGCTTGG
6	PUC19_01884REV	CACAAGTTCATACTCGACTCTAGAGGATCCCCGGGTACC
7	NEIFLAOTSpec01884_FOR	GAAAGAGAAAACAAAATATTCGGCAACTGTCGGAATATCTG
8	NEIFLAOTSpec01884_REV	GATAGGGAAAAACCCCTTCAGACGGCATTATTTGCCGACAACTTTGG
9	5PrimeEND-01884-ORF_FOR	GTTGTCCGCGTTTTCCGTATC
10	3PrimeEND-01884-ORF_REV	GCTGCCCAATGATTTTCCACC

Table 13 List of primers used in Reverse transcription polymerase chain reaction (RT-PCR)

No.	Oligonucleotide	Sequence
1	RTNlac36660_5PrimeFOR	GAACCATCTTGACCATAGCTAGAACG
2	RTNlac36660_5PrimeREV	GTGAAAGTATTGGCGAAAGCCTTTG
3	RTNlac36660_3PrimeFOR	TTACCACTGATAACCGACAGATGCG
4	RTNlac36660_3PrimeREV	GCATTGAATGTCGGCAGTAAGAAGG
5	RTNlac37260_5PrimeFOR	CTCAACGCCTGGGTAGTCGTATC
6	RTNlac37260_5PrimeREV	CCGTGTTTTACTTTGAATTTGGCG
7	RTNlac37260_3PrimeFOR	GAAAGACGTATCCAAAACGTCGCG
8	RTNlac37260_3PrimeREV	TTACCAGATATAGCCCACGCCG
9	RTNcin03770_5PrimeFOR	GATCTATCACCAGTCGCATTAGCTC
10	RTNcin03770_5PrimeREV	GTATTCCGAGTGATTTGGAGCCAG
11	RTNcin03770_3PrimeFOR	CACCGGTTTTGGCTTTAGTATTGAC
12	RTNcin03770_3PrimeREV	GTGAATTTCAACAGCCTGTCTCTC
13	RTNcin04577_5PrimeFOR	CTCGGTTTCCGATTAACGTATCAC
14	RTNcin04577_5PrimeREV	CTTCCGTGTTGTATGGAGCCATAC
15	RTNcin04577_3PrimeFOR	TTACCACTGATAGCCGACAGATGTG
16	RTNcin04577_3PrimeREV	CCAACTAAGATTACAGGCGTAGCAC
17	RTNmennhhA_5PrimeFOR	GCATCATTTGGAATAGTGCCCTC
18	RTNmennhhA_5PrimeREV	CCAACACTGGTCAGATCTGTGAG
19	RTNmennhhA_3PrimeFOR	CAAGAAGGACAACAAACCCGTC
20	RTNmennhhA_3PrimeREV	TTACCACTGATAACCGACAGATGC
21	RTNsub948_5PrimeFOR	GGTGCTTTGAGCGAGATCGATACTG
22	RTNsub948_5PrimeREV	GTACAGACAAATCCCGCATCAATAAC
23	RTNsub948_3PrimeFOR	CTTGTTGCTTAGCGTATATTCGCACC
24	RTNsub948_3PrimeREV	CAGTATCGATCTCGCTCAAAGCAC
25	RTNelongata5PrimeFOR	CCACCAATGGCAATTGAAGAATCGC
26	RTNelongata5PrimeREV	CATTGAGAATGGCTCTGCTCAATGG
27	RTNelongata_3PrimeFOR	CTGATAACCTACTGCTGCCGTAG
28	RTNelongata_3PrimeREV	GCAACAAGATTACCAATGTTGCTG
29	SecA_FOR	TACCTGCGCGACAATATGG
30	SecA_REV	ACGATTTCGCCGTCTTG
31	gyrB_FOR	CGGCATCCACCCGAAAGAAG
32	gyrB_REV	TGCGGTTCATGTATTGCACGA

2.4 Transformation of DH5α cells

Chemically competent *E. coli* DH5α cells were thawed on ice and 50 µl cells were transferred to a pre-chilled Eppendorf tube and incubated on ice for 10 minutes. Next 100 ng of chilled plasmid prep was added to the cells and gently mixed by pipetting up and down. The mixture was then incubated on ice for 30 minutes. After 30 minutes the cells were heat-shocked at 42°C for 30 seconds followed by a further 2 minutes incubation on ice. Next 950ml of room temperature SOC media was added to the Eppendorf tubes containing the cells and the tubes were incubated for 1 hour at 37°C. Following the incubation, 100 µl of the sample was plated onto agar plates with appropriate antibiotics for selection and the plates were incubated overnight at 37°C in Galaxy® 170R incubator (New Brunswick), with shaking at 320 rpm on a KS 130 basic shaker (IKA).

2.5 Transformation of *N. lactamica*, *N. cinerea*, *N. flavescens* and *N. polysaccharea*

N. lactamica, *N. cinerea*, *N. flavescens* or *N. polysaccharea* were grown on TSB+ plates (1.5% agar containing 3% Tryptone Soya Broth (TSB) and 0.2% yeast extract) overnight at 37°C 5% CO_2. Five bacterial colonies from the agar plate were inoculated into 10ml of TSB and incubated at 37°C 5% CO_2 Shaking at 320 rpm to log phase. The bacterial culture was then diluted 100-fold in TSB and 10 µl aliquots were pipetted onto TSB+ plates. Next, the plates were incubated for 6 hours at 30 °C 5% CO_2. Following the incubation, 1 µg of hypermethylated (HM) insert DNA was pipetted onto the colonies and the plates were incubated for a further 9 hours at 30°C 5% CO_2. The colonies were collected and resuspended in 1 ml of TSB. After applying the relevant dilutions, 100 µl was plated onto TSB+ agar with the relevant antibiotic for selection.

For all *Neisseria* spp. transformation, cytosine residues in the insert DNA were replaced with hypermethylated cytosine residues as this has been shown by Laver *et al.* (Awaiting publication) to inhibit the digestion of insert DNA by restriction enzymes.

2.6 Plasmid extraction

Escherichia coli DH5α were grown overnight in the relevant media and next day the plasmid DNA was extracted using a miniprep purification kit (Thermo Scientific) following the manufacturer's protocol. DNA concentrations were estimated using a NanoDrop ND-1000 spectrophotometer (Thermo Scientific).

2.7 Genomic DNA extraction

Bacteria were grown overnight in the relevant media and next day the genomic DNA was extracted using GeneJET genomic DNA extraction kit (Thermo Scientific) according to the manufacturer's instructions. DNA concentrations were estimated using a NanoDrop for downstream application.

2.8 DNA Gel Electrophoresis

Separation of DNA fragments was performed by agarose gel electrophoresis. The gel was prepared using 0.7% agarose electrophoresis gel (Sigma-Aldrich) boiled/dissolved in 1x Tris acetate EDTA (TAE) buffer (40 mM Tris (pH 7.6), 20 mM acetic acid, 1 mM EDTA) and 0.005% Midori green. 1 kb or 100bp DNA Ladder (NEB) was run in parallel to the samples. The sample was mixed with 5x DNA binding loading buffer and loaded into wells and the gel was run at 95V for 50 minutes before visualising the DNA bands by exposure to UV light using a UVP BioDoc-It™ Transilluminator system or Gel Doc™ XR+ Imager (Bio-Rad).

2.9 PCR amplification of DNA

Polymerase Chain reaction (PCR) was used to amplify DNA fragments. Template DNA (20ng per reaction) was mixed with 1x Q5 buffer, deoxynucleoside triphosphates (dNTPs) 800 µM, 0.5 µM of relevant primers and Q5 DNA polymerase in RNAse-free H_2O. Where necessary Dimethyl Sulfoxide (DMSO) was added to reduce non-specific DNA binding and to disrupt the secondary structure formation in DNA template. Next, the DNA of interest was amplified by PCR using the Veriti™ 96-Well Thermal Cycle (Thermo Scientific).

For hypermethylated (HM) PCR, the dNTP mix contained methyl Deoxycytidine triphosphate instead of Deoxycytidine triphosphate (dCTP) lacking methyl groups, the 1x Q5 buffer was replaced with 1x GC buffer and instead of Q5 DNA polymerase Phusion polymerase was used (All reagents from NEB).

Table 14 Overview of PCR steps

PCR step	PCR cycles	Temperature	Time
Initial denaturation		95°C	3 min
Denaturation	20-25 Cycles	98°C	20 s
Annealing		50-72 °C (Dependent on primers)	30 s
Extension		72 °C	30 s/kb or 1 min/kb (Hypermethylated PCR)
Hold		4 °C	Indefinitely

2.10 PCR purification

All PCR products were purified using the GeneJET PCR purification kit (Thermo Scientific) following the manufacturer's protocol. Subsequently, the DNA concentrations were estimated using a NanoDrop ND-1000 spectrophotometer (Thermo Scientific).

2.11 Gibson Isothermal assembly

Gibson assembly developed by Dr Daniel Gibson is a cloning method that joins multiple DNA fragments in a single isothermal reaction. This reaction is based on 3 different enzymatic reactions. The exonuclease nicks 5' ends leaving 3´ overhangs that facilitate the annealing of the overlapping region. Following annealing the DNA polymerase extends 3' ends filling in gaps within each annealed fragment. Finally, DNA ligase seals the cuts in the assembled DNA resulting in a fully sealed double-stranded DNA molecule (Figure 11)(Gibson *et al.*, 2008).

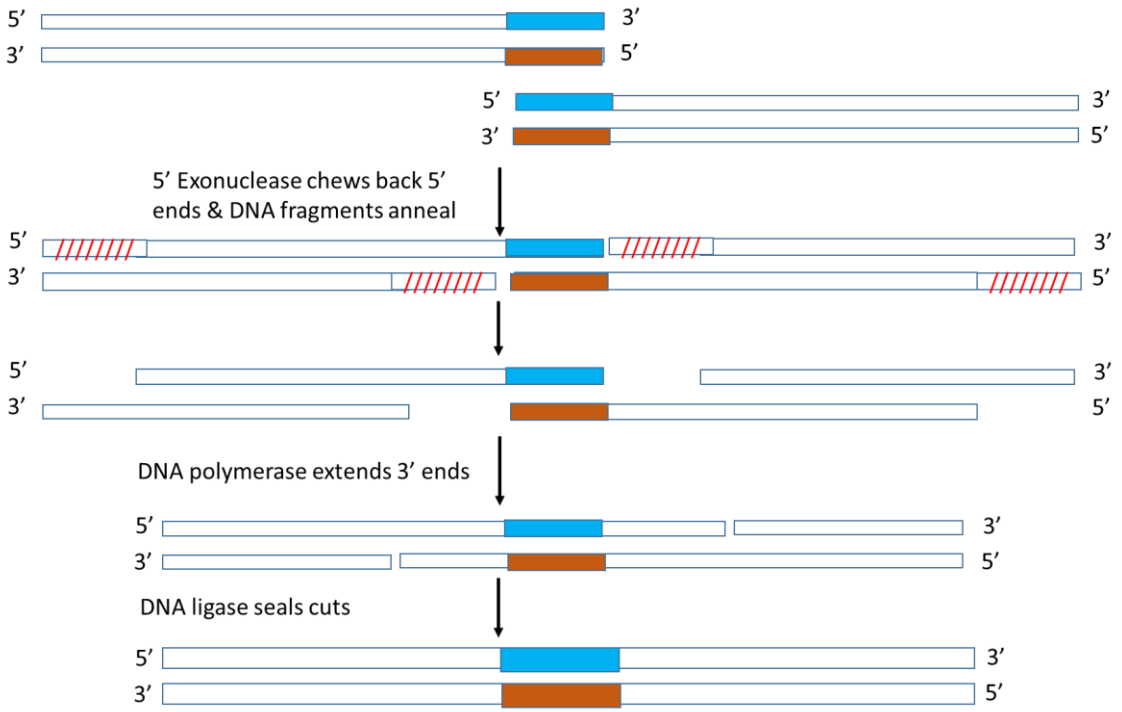

Figure 11 Overview of Gibson isothermal assembly.

5' Exonuclease cuts back the 5' ends and the DNA fragments with overlapping regions anneal. The DNA polymerase fills the gaps by extending the 3' ends of the annealed fragments. The cuts are sealed by DNA ligase within the mixture forming a double stranded DNA molecule.

Adapted from (Gibson et al., 2008).

Isothermal assembly was used to put together multiple fragments into plasmids. For isothermal assembly 50-100ng of the vector with 3-fold excess insert and combined with 1:1 volume of 2x Gibson Assembly master mix (NEB). The mixture was incubated at 50°C for 1 hour. After the incubation period, the mixture was kept at -20°C for subsequent transformation of chemically competent E. *coli* DH5α following supplier's guidelines (NEB).

2.12 Preparation of deoxycholate-extracted outer membrane vesicles (dOMVs)

The sodium deoxycholic acid method was adapted from (Fredriksen *et al.*, 1991; Mukhopadhyay *et al.*, 2005; Vaughan *et al.*, 2010) in order to prepare the outer membrane vesicles. Bacterial lawns were grown on TSB+ agar plates using 200µl of bacterial glycerol stock. Bacteria were transferred from plates to 30 ml of MC.7 in 50 ml tubes. The tubes were incubated overnight at 37°C, 5% CO_2 shaking at 350RPM. Next day 2 ml of this bacterial culture was used to inoculate 150ml of MC.7 in a baffled bottle and cultured for 8 hours. Afterwards, the culture was divided into 3 bottles and volume was made up to 150 ml each. The bacteria were cultured until the turbidity had reached an OD_{600nm} of 2.0 followed by heat killing in a water bath at 56°C for 45 minutes. The bacteria were then centrifuged at 4,500 x g for 1 hour at 20°C to pellet. The wet mass was measured, and the pellets were homogenised in buffer 1 (0.1M Tris-HCl pH 8.6, 10mM EDTA, 0.5% (W/V) deoxycholic acid) using a ratio of buffer to a biomass of 5:1 (V/W). The homogenates were ultracentrifuged at 20,000 x g for 30 minutes at 4°C in order to separate the cell fragments. The supernatant was retained and ultracentrifuged at 100,000 x g for 2 hours at 4°C in order to pellet the dOMV. The dOMV pellet was suspended in 2.5ml of buffer 2 (50mM Tris-HCl pH 8.6, 2mM EDTA, 1.2% deoxycholic acid, 20% sucrose (W/V)) and ultracentrifuged again at 100,000 x g for 2 hours at 4°C. The acquired dOMV pellet was suspended in 2ml of buffer 3 (0.2M glycine, 3% sucrose). The protein concentration of the dOMV suspension was calculated using Bradford protein assay and the dOMV suspension was stored at -20°C.

2.13 Sodium Dodecyl Sulphate Polyacrylamide Gel Electrophoresis (SDS-PAGE) and silver staining

5µg of bacterial dOMV was mixed with 4x Laemmli loading buffer (0.5 M Tris HCl, pH 6.8, 1% bromophenol blue) (Laemmli, 1970). The lysates were reduced using 10% (v/v) 2-Mercaptoethanol, by heating the mixture at 100°C for 5 minutes on a hot plate. 25µl of each sample was loaded into the wells of the NuPAGE™ Novex™ 4-12% Bis-Tris, 1.0

mm, 10-well Protein Gel (Thermo scientific). SDS-PAGE was run at 125 constant voltage in Invitrogen™ Novex™ XCell SureLock™ Mini-Cell Electrophoresis System (Thermo Scientific) using SDS MOPS buffer (1M MOPS, 1M Tris base, 70mM SDS, 20nM EDTA).

The Gel was stained using Invitrogen™ Novex™ SilverQuest™ Silver Staining Kit (Thermo Scientific) following the instructions provided by the manufacturer. The gel was removed from the cassette, rinsed with ultrapure water and fixed for an hour in ultrapure water containing 40% ethanol and 10% acetic acid (Both from Thermo scientific). The gel was then washed with 30% ethanol for 10 minutes before sensitizing for 10 minutes in ultrapure water containing 30% ethanol and 10% sensitizing solution. Next, the gel was washed a second time followed by rinsing with ultrapure water for 10 minutes before incubating the gel for 15 minutes in ultrapure water containing 1% stainer. This was followed by a wash with ultrapure water before incubating the gel ultrapure water containing 10% developer until the desired band intensity was achieved. Then the development was stopped immediately using the stopper solution. After 10 minutes, the gel was washed with ultrapure water for 10 minutes.

2.14 Isolation of Peripheral Blood mononuclear cells (PBMC)

Human Peripheral blood mononuclear cells were isolated from healthy donor leukocyte cones (NHS Blood and Transplant (NHSBT) Service, Southampton, UK) by density gradient sedimentation using Lymphoprep (Stemcell Technologies). Leukocytes were mixed with 10% Foetal Calf Serum (FCS) (Life technologies), 1 x PBS (Severn Biotech Ltd), 2mM EDTA (Thermo scientific). The diluted leukocyte mixture was gently layered on top of lymphoprep solution in a 50ml tube. The tubes were centrifuged at 800 x g for 30 minutes at room temperature. Next, the plasma layer was removed and discarded followed by the collection of mononuclear cell layer (MNC) at the plasma: lymphoprep interface without disrupting the erythrocyte/granulocyte pellet. Next, the collected MNCs were washed 4 times with 1 x PBS, 2mM EDTA and the mixture was centrifuged at 300 x g for 5 minutes at 4°C. The supernatant was discarded, the cells were counted and resuspended in storing solution (10% DMSO in FCS) at 1 x 10^8 cells/ml. The cells were transferred in sterile cryogenic vials, stored at -80°C for 24 hours before transferring them to liquid nitrogen.

2.15 Lymphoblastoid cell lines

Lymphoblastoid cell lines (LCLs) are human peripheral blood B cell line that has been immortalised by transfection with Epstein Barr Virus resulting in a continuous source,

bearing negligible genetic and phenotypic variations. LCLs expressing IgDλ +ve, IgDIgMλ +ve, or IgDIgMκ +ve were kindly provided by Dr Andrew Vaughan. All LCL were cultured in complete cell culture media and were maintained in T75cm^2 flasks in a humidified atmosphere at 37°C, 5% CO2 unless otherwise stated. Once 70-80% confluency was reached, cells were sub-cultured.

2.16 Antibodies

2.16.1 Fluorochrome conjugates

The following antihuman antibody fluorochrome conjugates were used to stain 1x10^6 PBMC in order to gate on specific cell populations: APC anti-human CD19 Ab (clone HIB19) (1 µg/ml), APC/Cy7 anti-human IgM Ab (clone MHM-88) (0.5 µg/ml), Brilliant Violet 421™ anti-human IgD Ab (clone LA6-2) (0.5 µg/ml), PE anti-human Ig light chain λ Ab (clone MHL-38) (2 µg/ml) and PerCP/Cy5.5 anti-human Ig light chain κ Ab (clone MHK-9) (1 µg/ml) (All 5 from Biolegend).

2.16.2 Anti-IgM, anti-IgD, anti-lambda and anti-kappa treatment of peripheral blood mononuclear cells

PBMC were pre-treated with 10 µg/ml of F(ab')$_2$ polyclonal goat anti-human IgM, IgD, λ light chain and k light chain antibodies (All four from Bio-Rad Abd Serotec) for 1 hour at 37°C in order to block specific cell surface receptors and assess its effect on B cell proliferation.

2.17 Proliferation assay

To identify the proliferating cells subset in response to mitogens PBMC were thawed in 1 x PBS (Severn Biotech Ltd), washed and resuspended at 1x10^8 cells/ml in complete cell culture media (RPMI 1640, 10% Foetal Calf Serum (FCS), 2mM L-glutamine, 1mM sodium pyruvate, 100 U/ml penicillin-streptomycin) at 20°C. PBMC were labelled with 25µM carboxyfluorescein succinimidyl ester (CFSE) and incubated at 20°C for 5 minutes. The cells were then washed with complete cell culture medium and resuspended at 1x10^6 cells/ml in complete cell culture medium and plated into 24 well flat-bottom plates. The PBMC were then cultured at 37°C 5% CO_2 for 4 days in complete cell culture medium alone or with 1µg/ml protein (quantified using Bradford protein assay) of OMVs.

On day 4 the cells were washed with complete cell culture medium, stained with appropriate fluorochrome-conjugated antibodies and incubated at 4°C for 30 mins. The

cells were then washed with FACS wash (1 x PBS, 1% BSA, 0.05% sodium azide (NaN_3)) and fixed with fixative (4% paraformaldehyde in PBS). Finally, a FACSAria flow cytometer was used to analyse the proliferation of cells by measuring the decrease in CFSE intensity. Each repeat was performed on PBMCs from different donor leukocyte cones.

2.18 Alexa Fluor 488 labelling of dOMVs

Deoxycholate-extracted dOMVs were injected into dialysis cassettes using a sterile 21G needle and a sterile 1ml syringe. The dialysis cassettes were made to float using buoys and placed in the dialysis solution (10% 0.27M sodium carbonate (Na_2CO_3), 90% 0.1M sodium bicarbonate ($NaHCO_3$)). Ultrapure water was used for the preparation of dialysis solution and the pH was adjusted to pH 9.

The dOMVs were dialysed for 2 hours at 4°C followed by another 2-hour dialysis at 4°C in fresh dialysis solution and a final overnight dialysis in fresh dialysis solution at 4°C.

After the completion of dialysis, the dOMV suspension was transferred from the dialysis cassettes to a universal and labelled with 0.2mg of Alexa Fluor™ 488 Carboxylic Acid, 2,3,5,6-Tetrafluorophenyl Ester, 5-isomer (A488) (suspended in DMSO). Next, the A488-labelled dOMV suspension was transferred to fresh dialysis cassettes and made to float in buffer 3 (0.2M glycine, 3% sucrose). The dOMVs were dialysed for 2 hours at 4°C followed by another 2-hour dialysis in a fresh buffer at 4°C. Finally, the dOMVs were dialyzed overnight in fresh buffer at 4°C and transferred to cryogenic vials for storage at -20°C.

2.19 Fluorescence assay

PBMC were thawed in 1 x PBS (Severn Biotech Ltd), washed and resuspended at $5x10^6$ cells/ml in complete cell culture media at 20°C. $1x10^6$ cells were plated into 96 well flat bottom plate. The PBMC were then cultured at 37°C 5% CO_2 for 2 hours in complete cell culture medium alone or with 10µg/ml protein (quantified using Bradford protein assay) of A488-labelled dOMVs. After the 2-hour incubation period, the cells were washed with complete cell culture medium, stained with appropriate fluorochrome-conjugated antibodies and incubated at 4°C for 30 mins. The cells were then washed with FACS wash (1 x PBS, 1% BSA, 0.05% sodium azide (NaN_3)) and fixed with fixative (4% paraformaldehyde in PBS). Finally, the mean fluorescence intensity of the B cells was analysed using a FACSAria flow cytometer.

2.20 Fluorescence Confocal Microscopy

10µg/ml protein (quantified using Bradford protein assay) of A488-labelled Nlac dOMVs were co-incubated with $1x10^6$ IgDλ +ve, IgDIgMλ +ve, or IgDIgMκ +ve LCLs at 37°C 5% CO_2 for 0 and 2 hours in the complete cell culture medium. After incubation periods the cells were washed with complete cell culture medium, fixed and permeabilized with Cytofix/Cytoperm™ solution (BD Biosciences). Next, the cells were stained with Brilliant Violet 421™ anti-human IgD Ab (clone LA6-2) (0.5 µg/ml), and A568 biotin-conjugated anti-human CD107a (LAMP-1) Ab (All 3 from Biolegend). The cells were mounted onto a 1mm microscope slide with mounting media (polyvinyl alcohol) and sealed under a coverslip (Both from Thermo scientific). The samples were analysed on Leica TCS SP5 Confocal Laser Scanning Microscope. Compensation was used to account for wavelength interference for samples in which two different colour stains were used.

2.21 RNA Extraction and Purification

Bacteria were grown to log phase in MC.7 media and RNA was isolated using PureLink RNA mini kit (Thermo Scientific) according to the manufacturer's instructions. On-column PureLink DNase treatment was performed on the samples to remove contaminating DNA from RNA preparations. RNA concentrations were estimated using a NanoDrop ND-1000 spectrophotometer (Thermo Scientific). RNA concentration was measured at a 260nm absorbance. The peak absorption of RNA with DNA contamination was calculated by the ratio of Abs260: Abs280, with 280nm being the peak absorption of DNA. A 260/280 ratio of 1.9-2.1 was considered adequately clear of DNA contaminants. Samples were stored at -80°C.

2.22 RNA Reverse Transcription

SensiFAST cDNA synthesis kit (Bioline) was used for reverse transcription of total RNA. 1 µg of total RNA was mixed with 1x TransAmp Buffer, dinucleotide triphosphates (dNTPs) 500 µM, random hexamer primers 50 µM and Reverse transcriptase 200 U in RNAse free H_20. The reaction mixtures were incubated in the thermocycler with the conditions mentioned below (Table 15) and RNA was reverse transcribed to generate complementary DNA (cDNA). Samples were stored at -20°C.

Table 15 Overview of Reverse transcription steps

RT steps	Temperature	Time
Primer annealing	25°C	10 min
Reverse transcription	42°C	30 min
Inactivation	85°C	5 min
Hold	4°C	-

2.23 Reverse transcription-polymerase chain reaction (RT-PCR)

cDNA generated by reverse transcription of RNA was amplified using specific primers. Next, the Products were run on a 1% agarose electrophoresis gel (Sigma-Aldrich) and the DNA bands were visualised at set exposure time across all samples.

2.24 Data analysis

Acquisition of gel images was performed on Gel Doc™ XR+ Imager (Bio-Rad) and quantification of the bands was performed on Image Lab software 6.0.1(Bio-Rad).
BD FACSDIVA software (BD Biosciences) was used to acquire flow cytometry data and the analysis was performed with FlowJo version 10.1 software for Windows (FlowJo LLC, Ashland, Oregon).
Statistical analysis was performed with GraphPad Prism version 7 for Windows (GraphPad Software, Inc., California).

3. Investigating the proliferative response to *N. lactamica* and *N. cinerea* outer membrane vesicles

3.1 Introduction

It has previously been shown that *N. lactamica* outer membrane vesicles induce proliferation in CD19+ cells derived from the mucosa and periphery (Vaughan *et al.*, 2010). Native OMVs are spherical buds produced by Gram-negative bacteria (Figure 12). Bacterial OMVs are ~20–250 nm in diameter proteoliposomes that bud and detach from the cell during active growth. OMVs are composed of lipids, protein, endotoxic lipopoly- or lipooligosaccharide and periplasmic content of the outer membrane embedded in the phospholipids but lack the cytoplasmic component (McBroom and Kuehn, 2005; Schwechheimer and Kuehn, 2015).

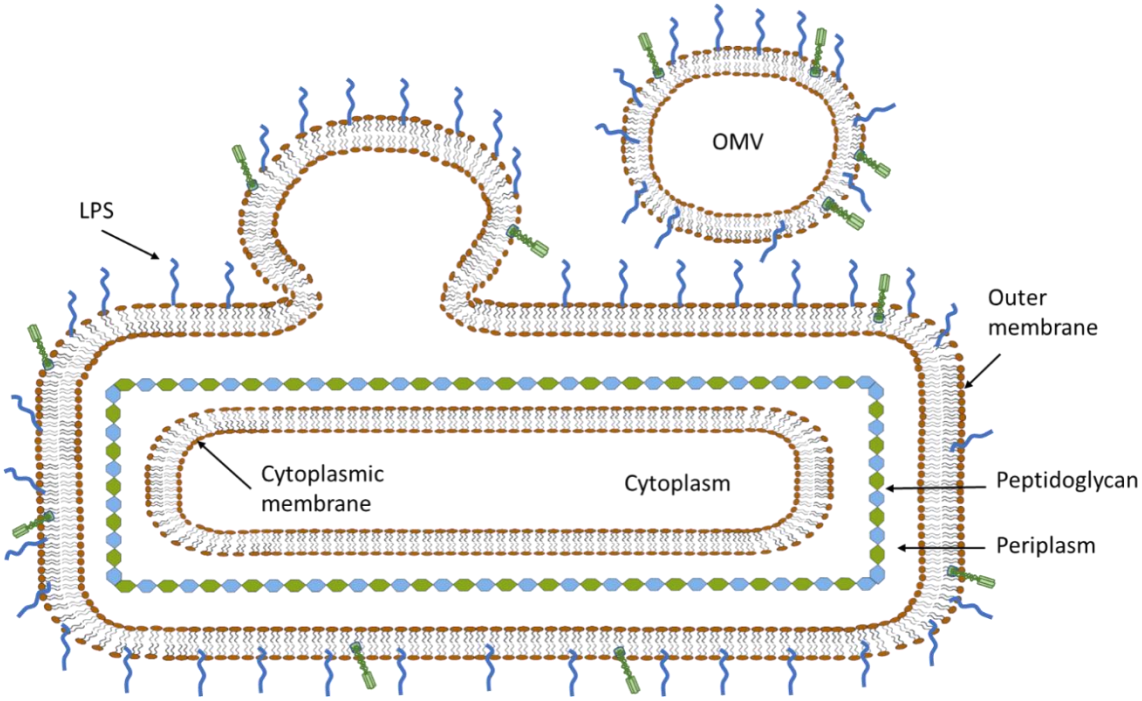

Figure 12 Diagram depicting native outer membrane vesicle production.

Bacterial native OMVs are ~20–250 nm in diameter proteoliposomes that bud and detach from the cell during active growth. OMVs can be considered as representative samples of bacterial outer membrane as they contain numerous MAMPs, including membrane bound and periplasmic proteins, lipopolysaccharide (LPS) or lipooligosaccharide (LOS), adhesins, toxins, enzymes (i.e. autolysins), phospholipids and peptidoglycan.

Artificially generated dOMVs prepared using the sodium deoxycholic acid method were used in order to investigate the immune response towards the *Neisseria* species as they represent many of the major bacterial antigens that may be involved in host interactions. Additionally, dOMVs have been extensively used to investigate acquired immunity to *Neisseria* spp. (Davenport *et al.*, 2003; McBroom and Kuehn, 2005; Sardinas *et al.*, 2006; Vaughan *et al.*, 2009; Santos *et al.*, 2012)

Prior research into *N. lactamica* has shown that stimulating tonsillar mononuclear cells with *N. lactamica* Y92-1009 dOMV induces a proliferative response in CD19+ cells, in contrast to *N. meningitidis* H44/76 dOMV. It was speculated that the B cell proliferative response was dependent on the B cell receptor (BCR) as treatment of BCR with BCR-specific antibodies resulted in inhibition of the proliferative response (Vaughan *et al.*, 2010).

I postulate that the B cell proliferative response to *N. lactamica* is due to the interaction between the IgD cell surface receptor and a putative IgD binding protein present on *N. lactamica* dOMV. This interaction of Nlac seems to be restricted to λ light chain-expressing IgD+ B cells (*Vaughan et al.,* unpublished data).

To confirm whether *N. lactamica* dOMV-induced B cell proliferation is restricted to λ light chain-expressing B cells, I investigated the proliferative response of PBMC using a CFSE proliferation assay. In proliferating cells, the concentration of CFSE is halved between daughter cells during mitosis, resulting in decreased fluorescence intensity, which can be used to distinguish them from non-proliferating cells using flow cytometry (Tung *et al.*, 2004; Tuominen-Gustafsson *et al.*, 2006).

3.2 Aims

- To verify the presence of mitogenic IgD binding protein or proteins.
- To confirm that the proliferation induced by *N. lactamica* dOMVs in CD19+IgD+ B cells is higher in λ light chain-expressing B cells compared to κ light expressers.

3.3 Results

3.3.1 Gating plan

PBMC isolated from leukocytes of healthy individuals were stained with CFSE on day 0 and cultured in the presence of media only or with *N. lactamica* Y92-1009*, N. cinerea* 346T*, N. meningitidis* H44/76 dOMVs or Pokeweed mitogen for 4 days. In order to analyse the data, singlets were gated on using forward scatter and forward scatter high (Figure 13A). Next, lymphocytes were gated on using forward and side scatter (Figure 13B), followed by gating on CD19+ events (Figure 13C) using anti-CD19 Ab-fluorochrome. Next using anti-IgM and anti-IgD monoclonal Ab conjugated fluorochromes IgD+IgDIgM+ events were specifically gated on (Figure 13D). Next, fluorochrome-conjugated anti-λ and anti-k light chain Ab markers were used to differentiate between λ light chain and k light chain-expressing B cells (Figure 13D). Finally, using the CFSE histogram of the non-treated sample CFSE low population were gated on to identify dividing cells (Figure 13F).

From this point onwards throughout this thesis, the IgD+IgDIgM+ events will be referred to as CD19+IgD+ population.

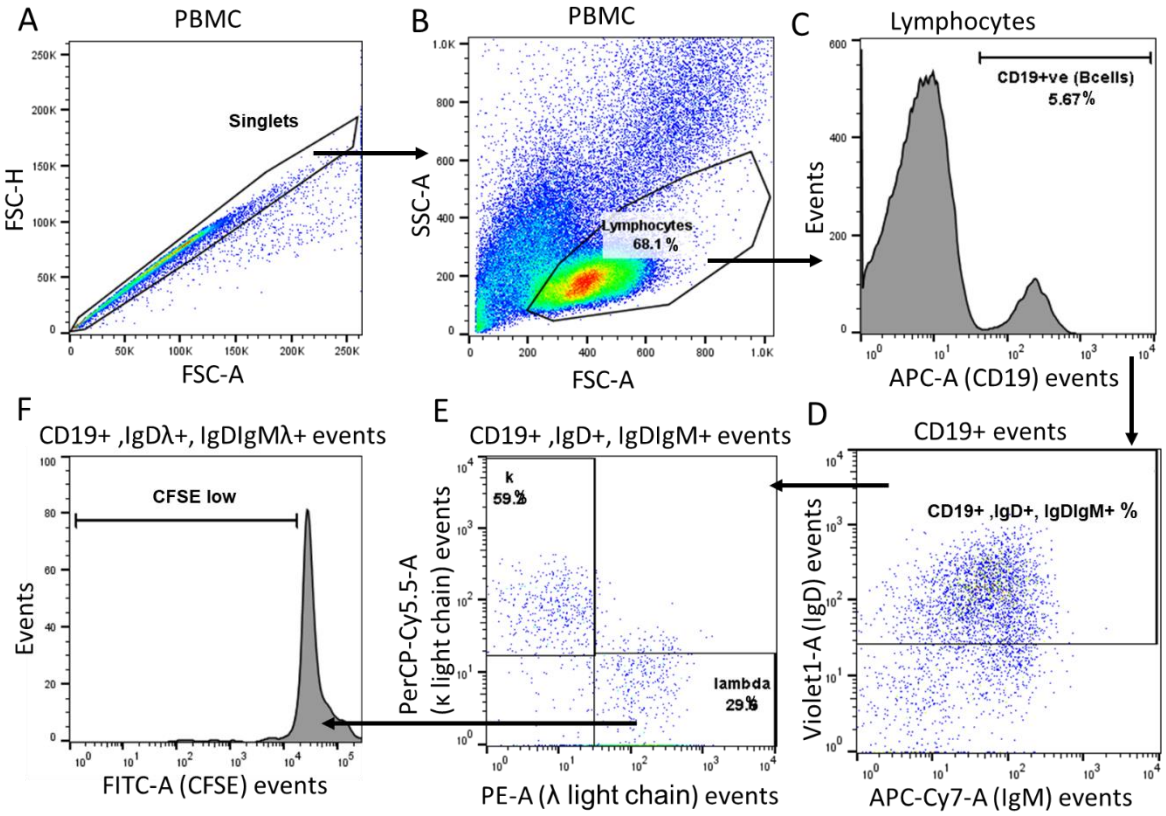

Figure 13 Gating plan.

(A) A representative dot plot displaying forward scatter (FSC) vs forward scatter high (FSC-H) used for gating singlets. (B) A representative dot plot displaying forward scatter (FSC) vs side scatter (SSC) of the PBMC used for gating lymphocytes. (C) A representative histogram displaying CD19 association of the lymphocytes used for gating CD19+ cells. (D) A representative dot plot displaying IgM vs IgD expression on CD19+ cells used to gate on IgD+IgDIgM+ cells (CD19+IgD+ cells). (E) A representative dot plot displaying λ light chain vs κ light chain-expressing population used to gate on λ or κ light chain-expressing CD19+IgD+IgDIgM+ cells (CD19+IgDλ+ cells). (F) A representative histogram displaying CFSE+ events in control sample used for gating on CFSE low population.

3.3.2 B cell proliferation in response to *N. lactamica* Y92-1009, *N. cinerea* 346T and *N. meningitidis* H44/76 dOMVs

Flow cytometric analysis of CFSE labelled PBMC cultured in the presence of *N. lactamica* Y92-1009 dOMVs showed a CFSE response in the CD19+IgD+ population that was mostly restricted to **λ** light chain-expressing B cells (Figure 14). In response to Nlac dOMVs, the median percentage of proliferating IgDλ+ B cells was significantly higher compared to IgDκ+ B cells (Figure 15). Furthermore, compared to Nlac, Nmen dOMVs induced a significantly reduced proliferative response in IgDλ+ B cells. This established the previous data (Vaughan et al unpublished data) suggesting the presence of a mitogenic IgD λ light chain binding protein in *N. lactamica* dOMVs.

For this proliferation assay Pokeweed mitogen (PWM) was used as a positive control because of its ability to trigger mitosis by activating signalling transduction pathways (Bekeredjian-Ding *et al.*, 2012). Results showed that PWM induced proliferation in both λ and κ light chain-expressing B cells. Furthermore, in response to PWM, there was no significant difference between the levels of proliferation in IgDλ+ B cells compared to IgDκ+ B cells (Figure 15). The fact that PWM displayed high levels of proliferation in both IgDλ and IgDκ expressing B cells suggests that perhaps Nlac dOMVs are specifically targeting the IgDλ+ B cells rather than λ light chain-expressing cells being more prone to proliferation compared to κ light chain expressers.

It was hypothesised that the ability to induce B cell proliferation might be a shared property among commensal *Neisseria* spp. According to the Core Genome Multilocus Sequence Typing (cgMLST) of 246 concatenated core gene sequences, Ncin is closely related to Nlac (Bennett *et al.*, 2012). Furthermore, OMV analysis of these two species by SDS-PAGE has shown that they have a very similar protein profile with multiple shared bands (Figure 16). Therefore, in addition to researching the association between the putative IgD binding protein and mitogenic property of Nlac, the mitogenicity of *Neisseria cinerea* 346T, a commensal of the URT, was also investigated. Since Ncin is closely related to Nlac, it may also share the ability to activate B cells expressing IgDλ. In accordance with this hypothesis, results indicated that the B cells stimulated with Ncin dOMVs also proliferated. The median proliferative response to Ncin dOMVs in IgD**λ**+ B cells was significantly higher compared to IgDκ+ B cells, suggesting the existence of a mitogenic IgD **λ** light chain binding protein (Figure 15). All antigen treated cells displayed a significantly higher proliferation in IgD λ and κ light chain-expressing B cells compared to untreated cells.

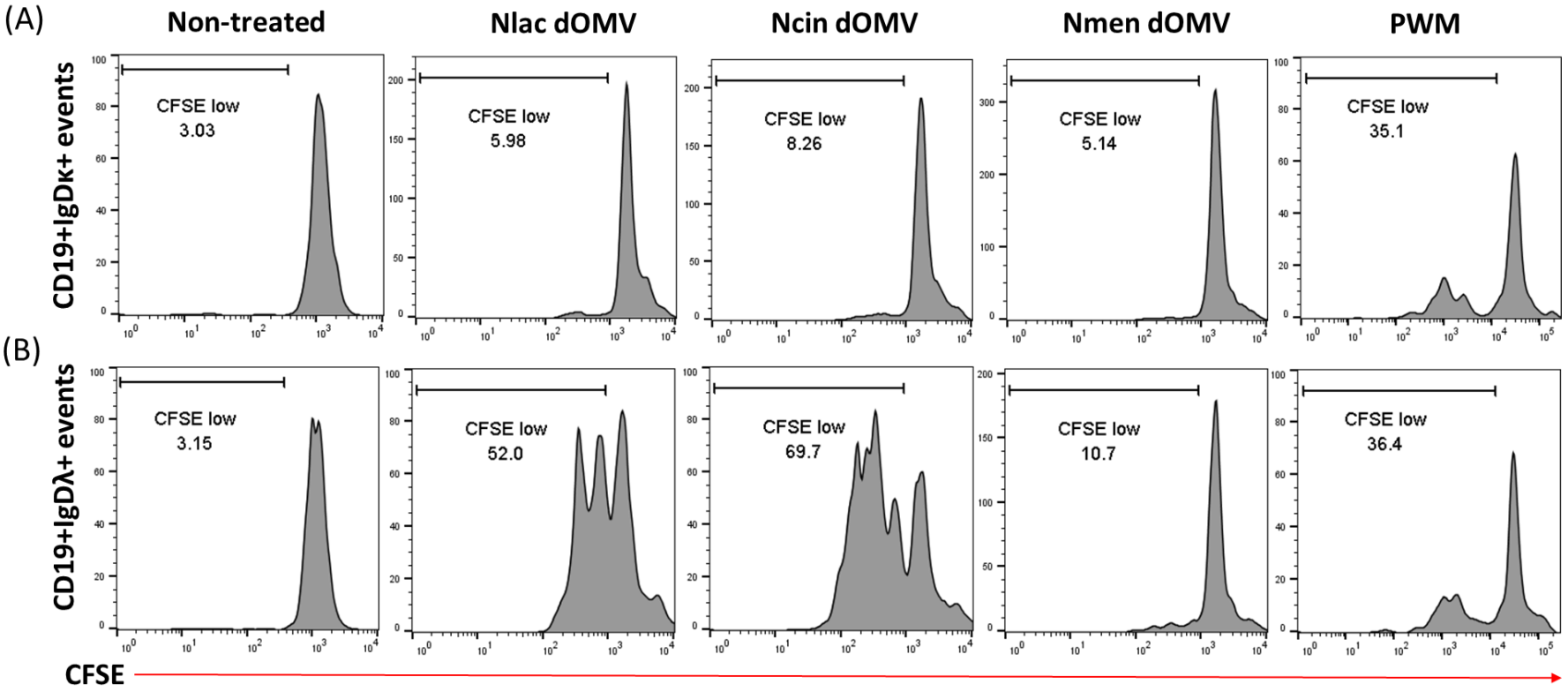

Figure 14 Nlac and Ncin dOMV induces proliferation in IgDλ+ B cells.

PBMC were stained with CFSE on day 0 and cultured in the presence of media only or with *N. lactamica* Y92-1009, *N. cinerea* 346T, *N. meningitidis* H44/76 dOMVs and pokeweed mitogen for 4 days. On day 4 cells were washed and analysed by flow cytometry. Proliferating cells were differentiated by a reduction in CFSE intensity compared to CFSE intensity of the non-treated cells. Representative histograms showing fluorescence intensity of CFSE staining in CD19+IgD+ events expressing (A) k light chain and (B) λ light chain. Values in the histograms refers to percentage of population with reduced CFSE intensity. One representative experiment of six.

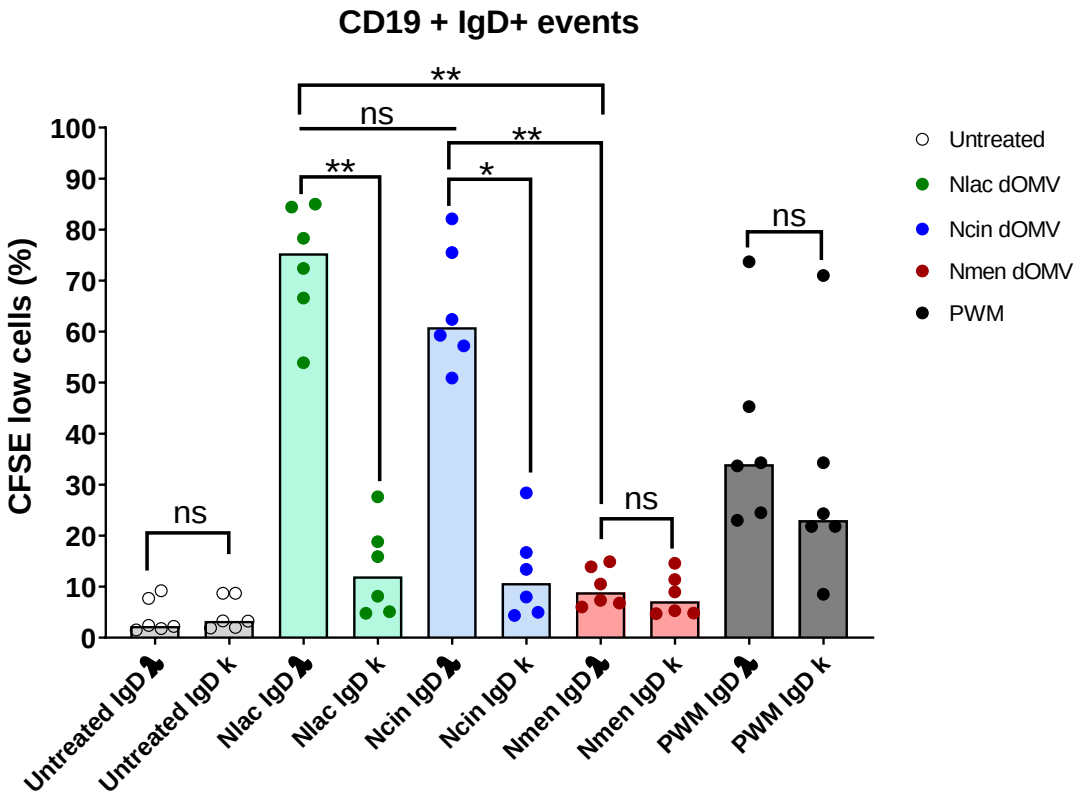

Figure 15 Nlac and Ncin dOMV induces proliferation in IgDλ+ B cells.

Collated data showing percentage of CFSE low CD19+IgD+ cells expressing k or λ light chain in response to stimulation with *N. lactamica* Y92-1009, *N. cinerea* 346T, *N. meningitidis* H44/76 dOMVs and pokeweed mitogen for 4 days. Results were acquired on day 4 using a flow cytometer. Proliferating cells were differentiated by a reduction in CFSE intensity compared to CFSE intensity of the non-treated cells. The peak height of the bars represents the median values of 6 repeated experiments on PBMCs from individual donors. Groups were analysed using Friedman test with Dunn's correction for multiple comparisons. * $P \leq 0.05$, ** $P \leq 0.01$ and not significant (ns), $P > 0.05$.

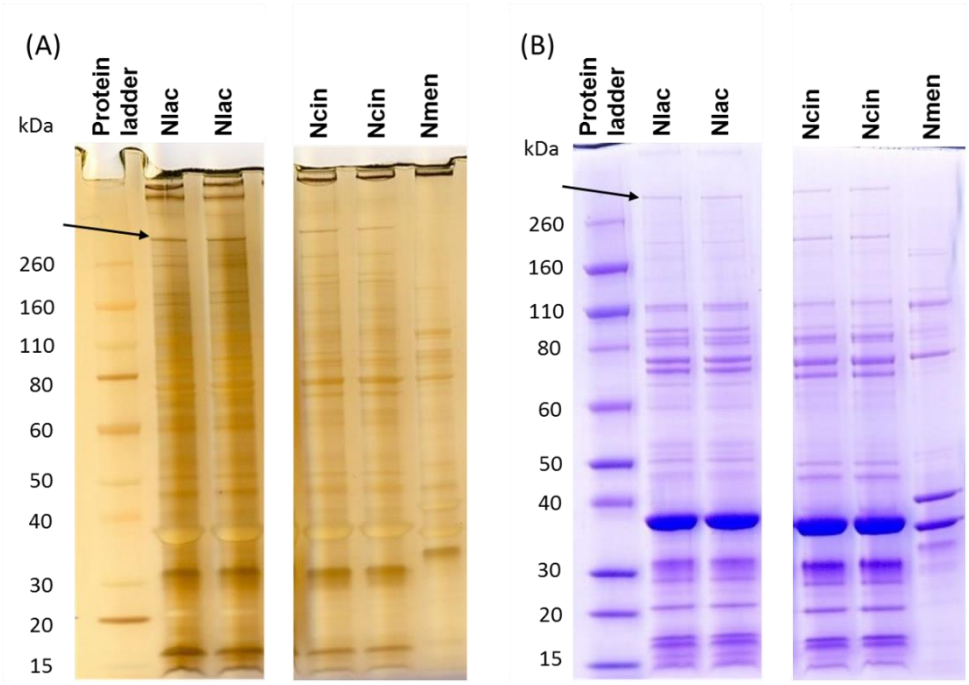

Figure 16 Protein profile of *N. lactamica*, *N. cinerea* and Nmen.

SDS-PAGE of dOMVs prepared from *N. lactamica* Y92-1009, *N. cinerea* 346T and *N. meningitidis* H44/76 strains. 5µg of OMV was applied to each lane and OMVs were visualised using (A) silver staining and (B) coomassie blue staining. Molecular weight markers are indicated on the left hand side. The putative IgDbp is illustrated by the arrows.

3.3.3 Investigating the proliferation of CD19+IgDλ+ cells pre-treated with anti-BCR Igs in response to *N. lactamica* and *N. cinerea* dOMVs

To determine that the B cell proliferative response to *N. lactamica* and *N. cinerea* dOMVs was reliant on the IgD BCR and specifically IgD+ B cells expressing λ light chain, PBMCs were treated with $F(ab')_2$ polyclonal goat anti-human IgM, IgD, λ or k Abs in order to prevent ligand binding. These pre-treated PBMCs were then cultured in the medium alone or in the presence of *N. lactamica* Y92-1009 dOMV, *N. cinerea* 346T dOMV or PWM for 4 days. Nmen was not tested for the abrogation of B cell proliferation as its induced proliferation was negligible compared to Nlac. Finally, on day 4 the cells were washed, and the proliferation was measured by flow cytometry.

Results showed that proliferation in CD19+IgDλ+ cells in response to Nlac dOMV was reduced significantly when treated with anti-IgD Ab compared to WT Nlac whereas treatment with anti-IgM had no significant impact on the proliferation. Treatment with anti-λ light chain Ab significantly inhibited the proliferation and treatment with anti-k light chain Ab had no significant reduction in proliferation (Figure 18).

The proliferation in CD19+IgDλ+ cells in response to Ncin dOMV exhibited a similar relationship where treatment with anti-IgD Ab caused a significant reduction in proliferation compared to WT Ncin but treatment with anti-IgM had no significant effect on proliferation. Treatment with anti-λ light chain Ab also significantly reduced proliferation and anti-κ light chain Ab caused no significant reduction in proliferation (Figure 18).

PWM was used as a control in this assay to ensure the trend in reduction of proliferation in response to anti-IgD and anti-λ Ab treatment is indeed exclusive to Nlac and Ncin dOMVs. CD19+IgD+ λ light chain-expressing cells in response to PWM exhibited a significant increase in proliferation when treated with anti-IgD Ab compared to WT Nlac. Treatment with anti-IgM Ab also resulted in significantly increased proliferation. Treatment with anti- λ light chain Ab or anti-k light chain Ab had no significant effect on proliferation. The proliferation induced by PWM increased when cells were pre-treated with anti-IgM and anti-IgD Abs compared to non-pre-treated cells (Figure 18). This could be due to the anti-IgM and anti-IgD Abs providing stimulatory signals in addition to the PWM. Both anti-IgM and anti-IgD Abs have been shown to stimulate human B cells (Gergely, Cook and Agnello, 1997) and used in combination with PWM would result in a higher response compared to PWM alone. The lack of any significant effect on proliferation when cells were pre-treated with anti-λ or anti-k light chain Ab could be explained by the fact that PWM induced proliferation in both λ and k light chain-expressing CD19+ B cells (Figure 15), albeit at different levels. Therefore, pre-treatment of CD19+ B cells with only anti-λ or anti-k light chain Ab will not result in a significantly reduced proliferation.

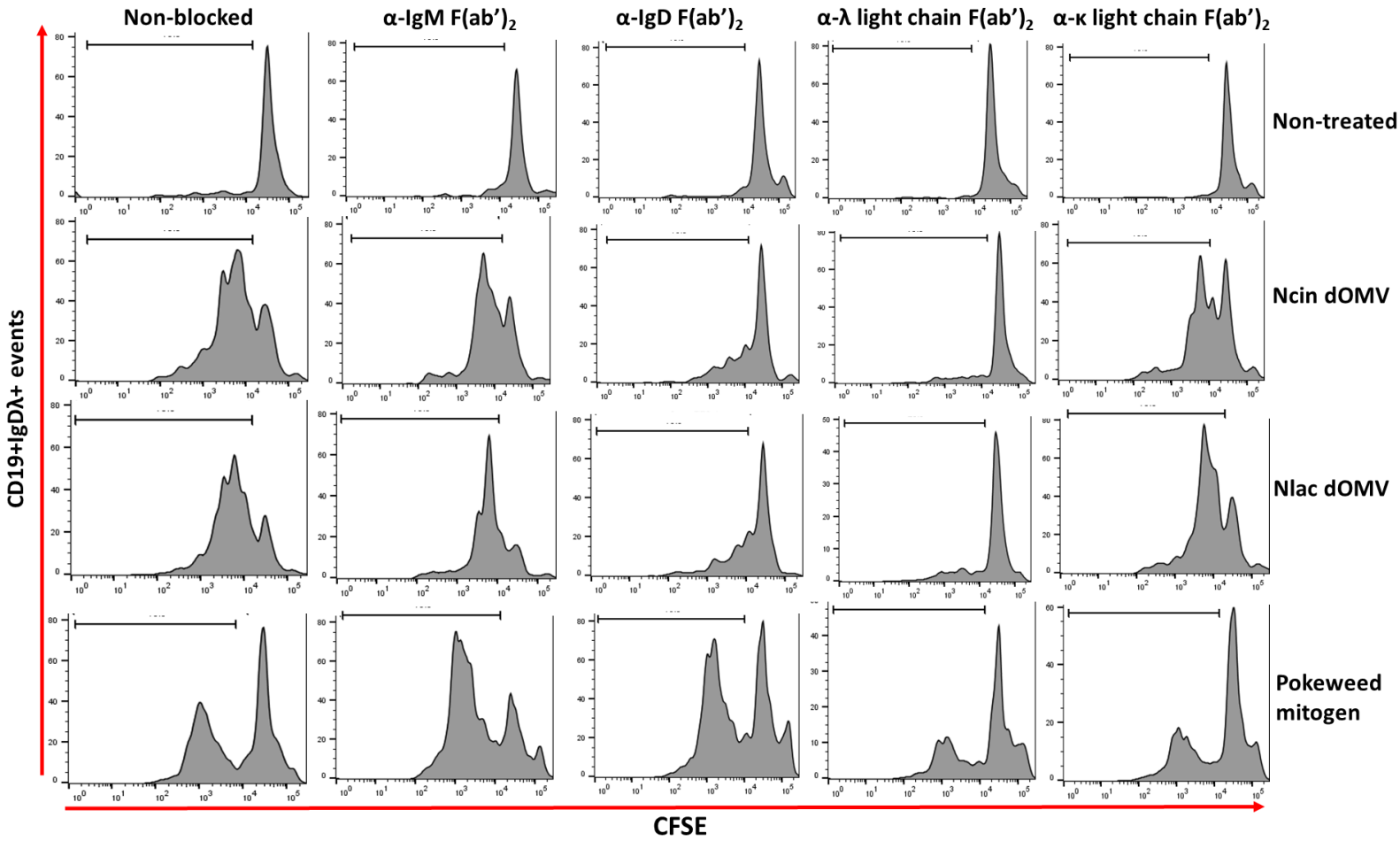

Figure 17 Blocking of λ light chain and IgD cell surface receptor causes a reduction in the percentage of proliferating cells in response to Nlac and Ncin dOMVs.

CFSE stained PBMC were either treated with $F(ab')_2$ polyclonal goat anti-human IgM, IgD, λ light chain, k light chain Ab or left untreated. All 5 conditioned PBMC were cultured in medium alone or in the presence of antigens. On day 4, cells were washed and stained with fluorochrome-conjugated monoclonal antibodies and analysed by flow cytometry. Proliferating cells were differentiated by the decreased fluorescence intensity of CFSE staining. Representative histograms showing fluorescence intensity of CFSE staining in λ light chain-expressing CD19+IgD+ events. One representative experiment of six.

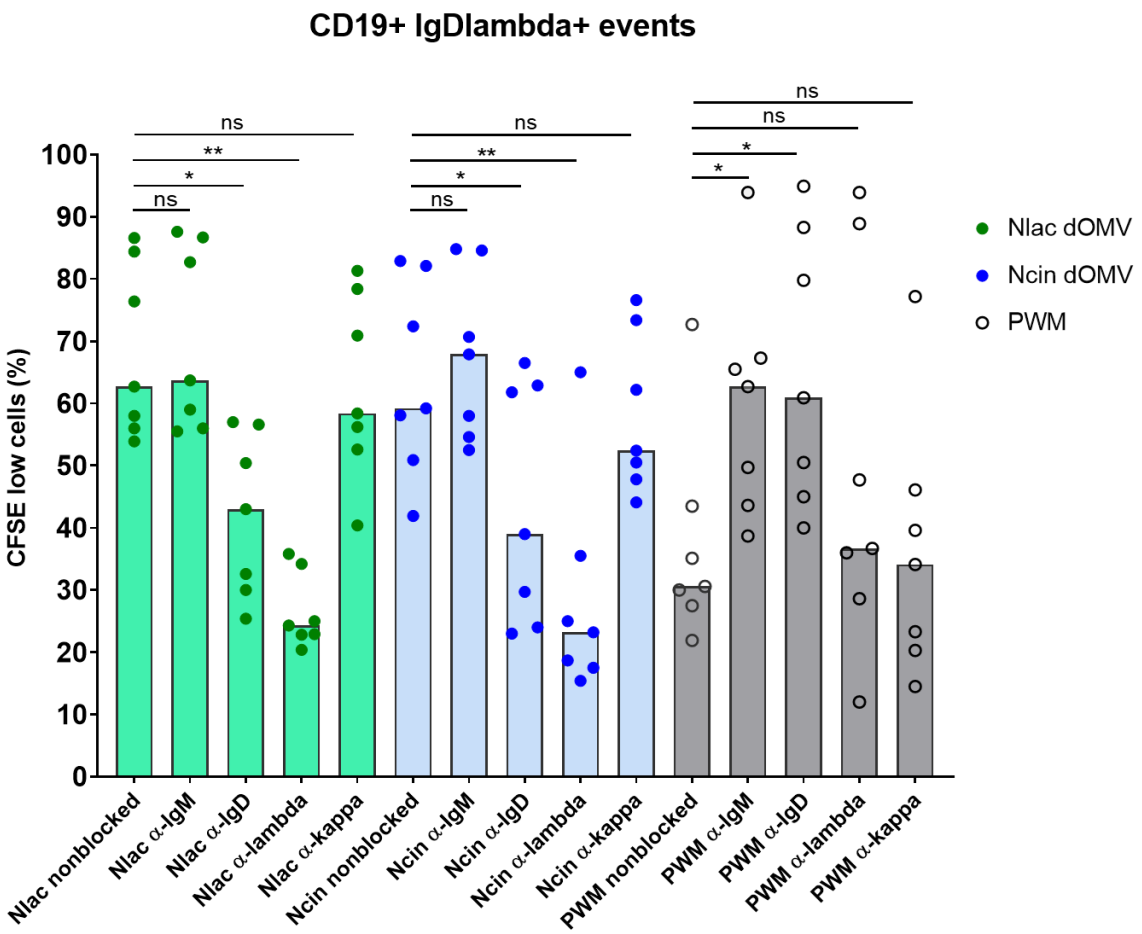

Figure 18 The percentage of proliferating cells in response to Nlac and Ncin is significantly reduced in IgDλ+ B cells upon blocking λ light chain and IgD cell surface receptors.

Compiled data showing the effect of treating PBMC with F(ab')$_2$ polyclonal goat anti-human IgM, IgD, λ light chain and k light chain Ab on the percentage of dividing cells in the presence or absence of *N. lactamica* Y92-1009, *N. cinerea* 346T, and pokeweed mitogen. Results were acquired on day 4 using a flow cytometer. Proliferating cells were differentiated by a reduction in CFSE intensity compared to CFSE intensity of the non-treated cells. The peak height of the bars represents the median values of 7 repeated experiments on PBMCs from individual donors. Groups were analysed using Friedman test with Dunn's correction for multiple comparisons. * $P \leq 0.05$, ** $P \leq 0.01$ and ns $P > 0.05$.

3.3.4 Interaction and co-localisation of Nlac dOMV and IgDλ+ B cells

It is unclear whether the induced proliferative response is due to the direct or indirect association of dOMV with the B cells. To investigate whether the dOMV colocalises with the B cells an interaction assay was performed. PBMC were cultured in the presence of Alexa Fluor 488 labelled dOMVs for 2 hours, followed by washing and flow cytometry analysis. The mean fluorescence intensity (MFI) of the B cells cultured in the presence of A488-labelled dOMV was compared to non-treated cells. It was reasoned that in the event of a positive association between the fluorescently labelled dOMV and B cells, the bound B cells should exhibit a higher MFI compared to non-treated cells. BCR was blocked with pre-treatment of $F(ab')_2$ polyclonal goat anti-human IgM, IgD, λ or k Abs in order to prevent specific ligand interaction. It was hypothesised that the blocking of only IgD and λ light chain on B cells would abrogate the interaction and result in reduced detected MFI.

Incubation of Nlac A488-labelled dOMVs with PBMCs demonstrated that CD19+IgDλ+ and CD19+IgDκ+ displayed a higher level of MFI compared to non-treated cells (Figure 20). Furthermore, CD19+IgDλ+ cells displayed a significantly higher level of MFI compared to CD19+IgDκ+ when incubated with A488-labelled Nlac or Ncin but not Nmen dOMVs (Figure 20, Figure 19, Figure 21).

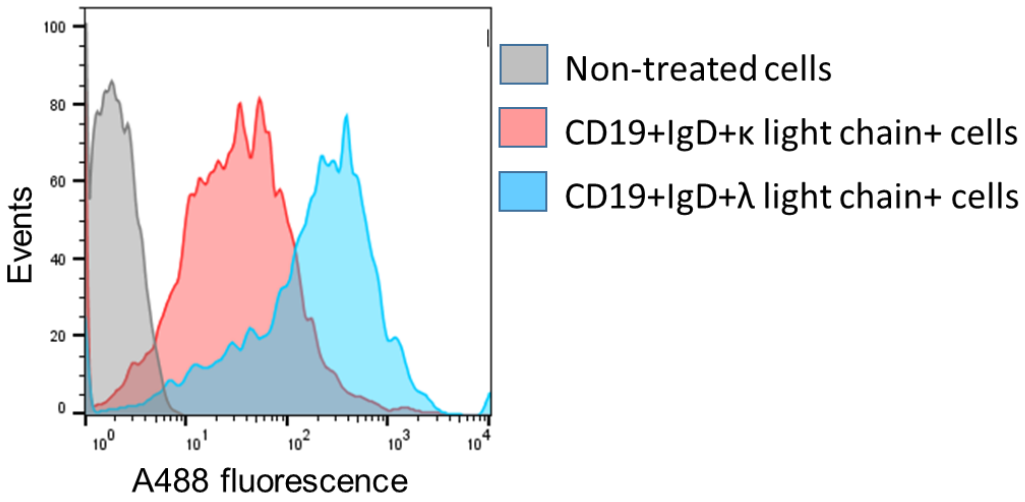

Figure 20 Nlac A488-labelled dOMVs colocalises with CD19+IgDλ+ B cells compared to CD19+IgDκ B cells.

PBMCs were cultured in medium alone or in the presence of A488-labelled dOMV. After 2 hours cells were washed and stained with fluorochrome-conjugated monoclonal antibodies and analysed by flow cytometry. Representative histogram showing MFI CD19+IgD+λ light chain+ and CD19+IgD+κ light chain+ cells in response to co-incubation with A488-labelled Nlac dOMVs.

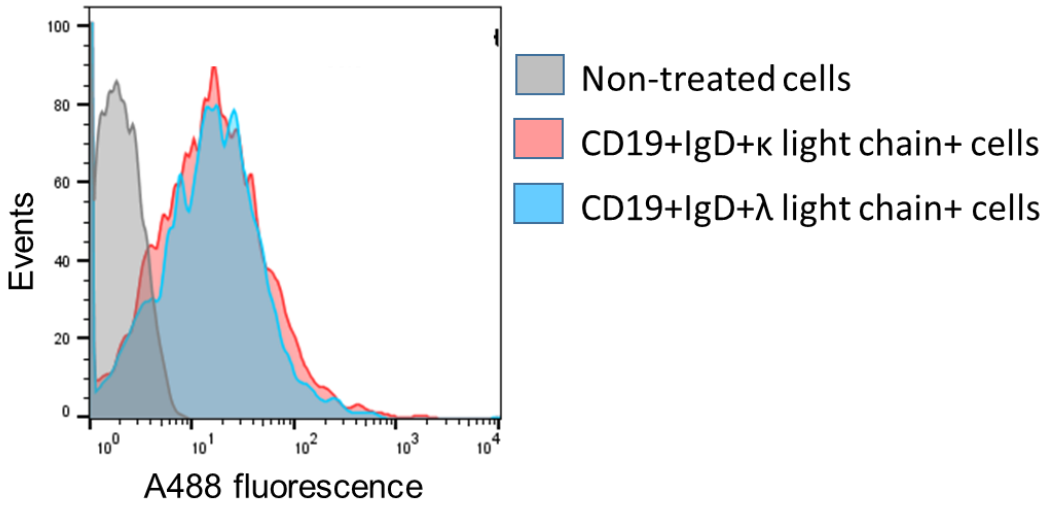

Figure 19 Nmen A488-labelled dOMVs does not colocalises with CD19+IgDλ+ B cells.

PBMCs were cultured in medium alone or in the presence of A488-labelled dOMV. After 2 hours cells were washed and stained with fluorochrome-conjugated monoclonal antibodies and analysed by flow cytometry. Representative histogram showing MFI of CD19+IgD+λ light chain+ and CD19+IgD+κ light chain+ cells in response to co-incubation with A488-labelled Nmen dOMVs.

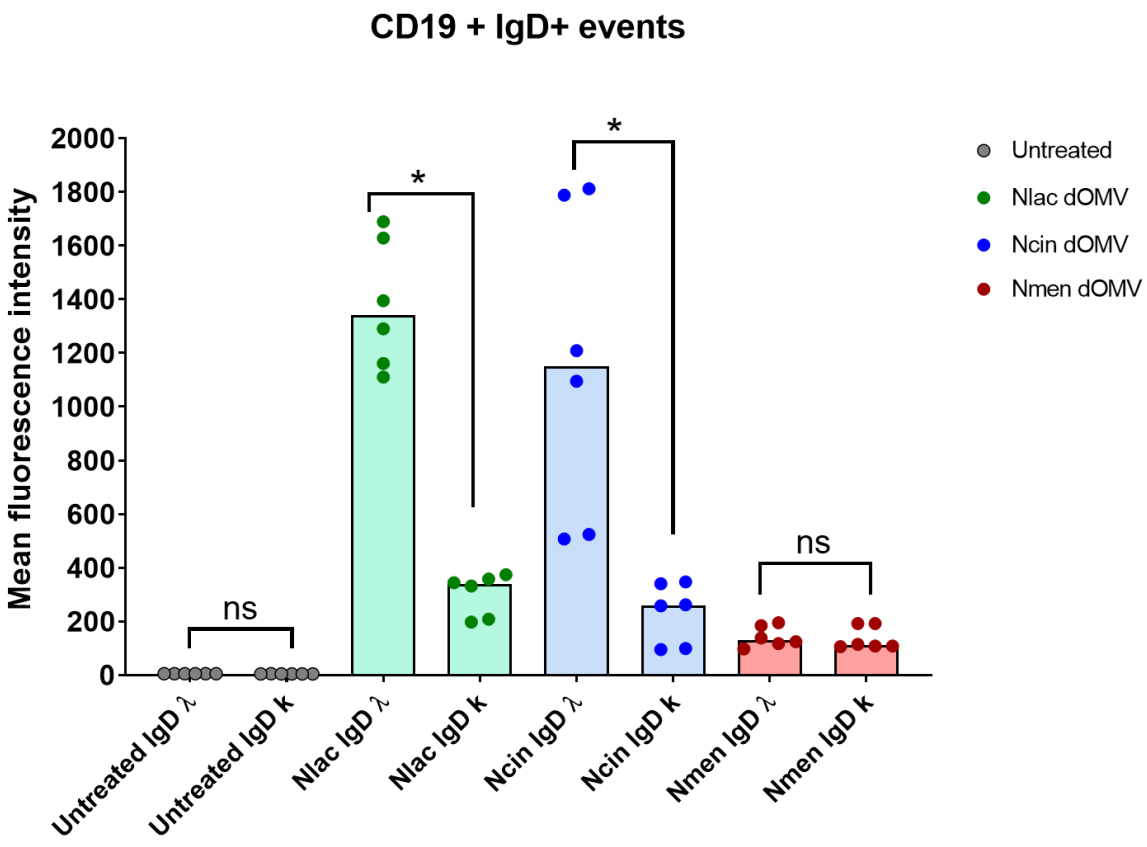

Figure 21 CD19+IgD+ cells express a higher mean fluorescence intensity in response to A488-labelled Nlac, Ncin and Nmen dOMVs.

Compiled data showing the level of detected MFI in CD19+IgD+ cells in response to coincubation with A488-labelled Nlac, Ncin and Nmen dOMVs for 2 hours at 37°C. After 2 hours cells were washed, and results were acquired using a flow cytometer. When possible 10,000 CD19+ events were analysed and the mean fluorescent intensity (MFI) was measured. The peak height of the bars represents the median values of 6 repeated experiments on PBMCs from individual donors. Groups were analysed using the Wilcoxon matched-pairs signed rank test. * $P \leq 0.05$, ns $P > 0.05$.

To investigate OMV-B cell interactions further, the BCR was blocked with pre-treatment of $F(ab')_2$ polyclonal goat anti-human IgM, IgD, λ or k Abs to prevent specific ligand interaction. Experiments showed a decreased MFI in IgDλ+ B cells co-incubated with A488-labelled Nlac or Ncin dOMVs when pre-treated with anti-IgD, anti-IgM, anti-λ or anti-κ light chain Ab. However, the decrease in MFI was significantly lower in cells pre-treated with anti-IgD or anti-λ Ab compared to pre-treatment with anti-IgM or anti-κ Ab (Figure 21, Figure 22).

The collated data in (Figure 23) indicates a significantly higher MFI in IgDλ+ cells co-incubated with A488-labelled Nlac and Ncin dOMVs compared to Nmen dOMVs. Furthermore, pre-treatment with anti-IgD or anti-IgM Ab resulted in a significantly reduced MFI in IgDλ+ cells co-incubated with A488-labelled Nlac and Ncin dOMVs but not Nmen dOMVs. However, the difference between the levels of reduction in MFI was significantly higher when treated with anti-IgD compared to anti-IgM Ab. Similarly, cells pre-treated with anti-λ or anti-κ Ab resulted in significantly reduced MFI in IgDλ+ cells. Furthermore, the difference between the levels of reduction in MFI was significantly higher when treated with anti-λ compared to anti-κ light chain Ab (Figure 23).

Finally, pre-treatment of cells co-incubated with A488-labelled Nmen dOMVs did not show any significant reduction in MFI when pre-treated with anti-IgD, IgM, λ light chain or κ light chain Ab (Figure 23).

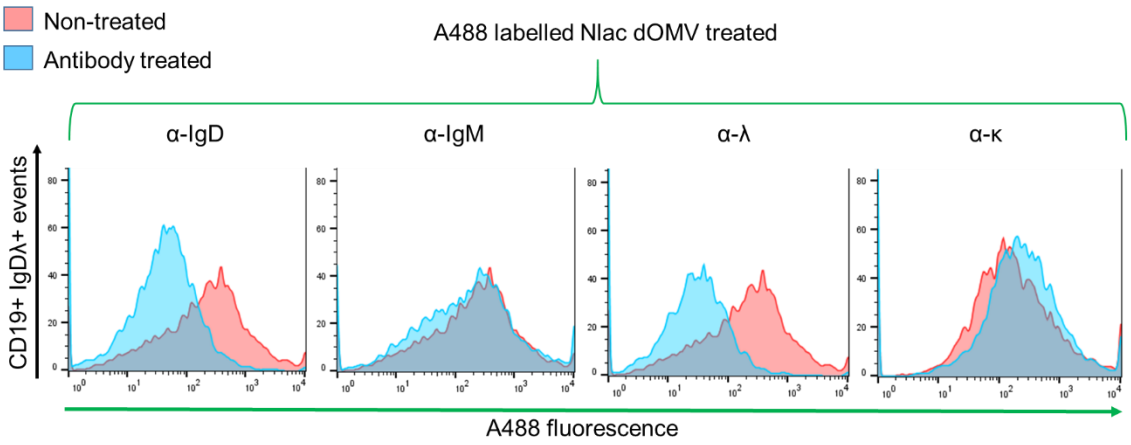

Figure 22 Blocking of only IgD and λ light chain on B cells resulted in reduced MFI.

Representative histograms showing MFI of CD19+IgDλ+ cells in response to coincubation with A488-labelled Nlac dOMVs. PBMCs were either treated with $F(ab')_2$ polyclonal goat anti-human IgM, IgD, λ light chain, k light chain Ab or left untreated. All 5 conditioned PBMCs were cultured in medium alone or in the presence of A488-labelled dOMVs. After 2 hours cells were washed and stained with fluorochrome-conjugated monoclonal antibodies and analysed by flow cytometry. One representative experiment of six.

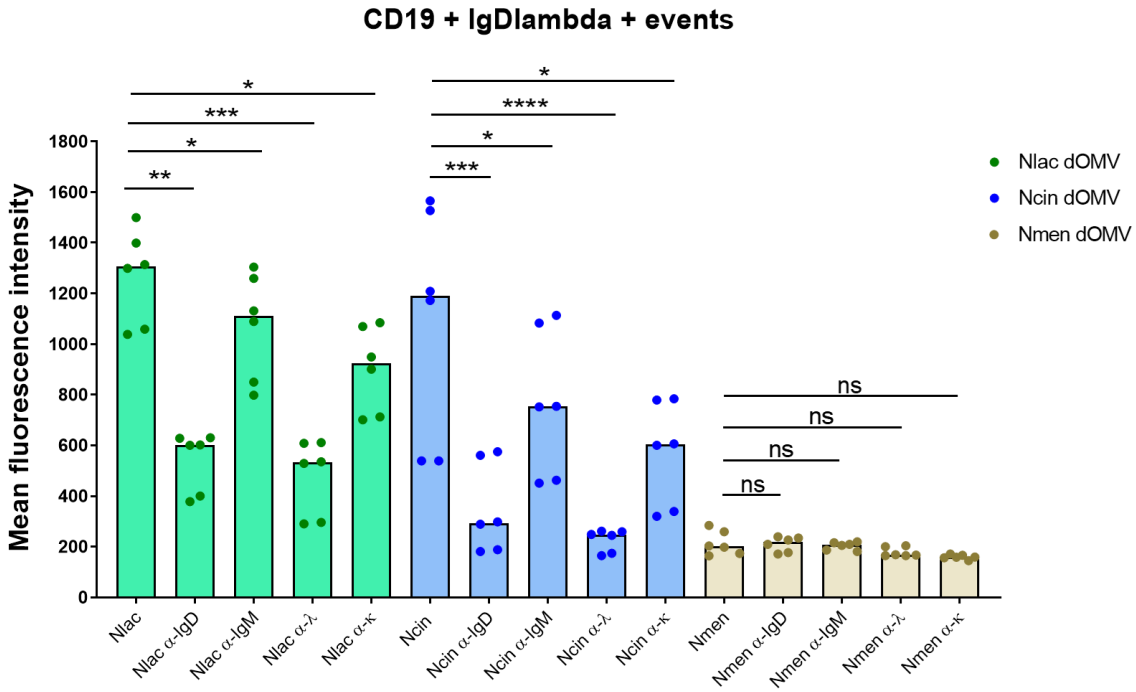

Figure 23 Mean fluorescence intensity of CD19+IgDλ+ cells in response to A488-labelled Nlac, Ncin and Nmen dOMVs is reduced more upon pre-treatment with anti-λ light chain Ab and anti-IgD Ab compared to pre-treatment with anti-k light chain Ab and anti-IgM Ab.

Compiled data showing the effect of treating PBMC with $F(ab')_2$ polyclonal goat anti-human IgM, IgD, λ light chain and k light chain Ab on MFI of IgDλ+ B cells in the presence of A488-labelled Nlac, Ncin and Nmen dOMVs for 2 hours at 37°C. After 2 hours cells were washed and results were acquired using a flow cytometer. When possible 10,000 CD19+ events were analysed and the mean fluorescent intensity (MFI) was measured. The peak height of the bars represents the median values of 6 repeated experiments on PBMCs from individual donors. Groups were analysed using Friedman test with Dunn's correction for multiple comparisons. * $P \leq 0.05$, ** $P \leq 0.01$, *** $P \leq 0.001$, **** $P \leq 0.0001$, and ns $P > 0.05$.

3.3.5 Investigating the internalization of A488-labelled mitogenic *Neisseria* dOMVs by CD19+IgDλ+ B cells.

Flow cytometry data presented in this thesis has shown that the incubation of CD19+IgDλ+ B cells in the presence of A488 dOMVs results in an increased MFI in the gated population suggesting interaction and co-localization between the mitogenic dOMVs and IgDλ+ B cells. However, it is not clear whether the dOMVs are adhering to the surface of these B cells or whether the B cells are internalizing these dOMVs. Since B cells are APC, they do partake in low-level phagocytosis in order to digest the foreign antigen and present the epitopic peptide fragment on the MHC class II. To further investigate this colocalization IgDλ+ cells were incubated with A488-labelled Nlac dOMVs for 0 and 2 hours and confocal microscopy was used to confirm the internalization of dOMVs by IgDλ+ cells.

Antigen-induced clustering of the BCR is normally followed by BCR internalization and movement to endosomal compartments. Lysosomal associated membrane protein 1 (LAMP-1) is an integral membrane glycoprotein on lysosomes. Thus, the use of fluorochrome-conjugated anti-human LAMP-1 Ab made it possible to investigate the endocytosis of dOMVs into lysosomes by IgDλ+ cells.

Lymphoblastoid cell lines (LCLs) expressing IgDλ +ve, IgDIgMλ +ve, or IgDIgMκ +ve LCLs were co-incubated with10µg/ml protein of A488-labelled Nlac dOMVs at 37°C 5% CO_2 for 2 hours in the complete cell culture medium. After incubation, the cells were washed with complete cell culture medium, fixed and permeabilized with Cytofix/Cytoperm™ solution. Next, the cells were stained with fluorochrome-conjugated anti-human IgD and anti-human CD107a (LAMP-1) Abs. The cells were washed and mounted onto a 1mm microscope slide with mounting media and sealed under a coverslip. Compensation was used on a Leica TCS SP5 Confocal Laser Scanning Microscope to account for wavelength interference and prevent fluorophore overspill before finally analysing the samples.

Results showed that at 2-hour time point the Nlac dOMV staining (green) and LAMP-1 staining (Red) was highly punctate for IgDλ +ve and IgDIgMλ +ve LCLs. Whereas in IgDIgMκ +ve LCLs only the LAMP-1 staining was punctate. In contrast, IgD BCR staining (Blue) was less punctate and more diffuse in all 3 LCLs. Furthermore, the Nlac dOMV staining co-localized the LAMP-1 staining in IgDλ +ve and IgDIgMλ +ve LCLs but not in IgDIgMκ +ve LCLs (Figure 24). No A488-labelled Nlac dOMVs were observed in any test conditions at baseline (data not shown).

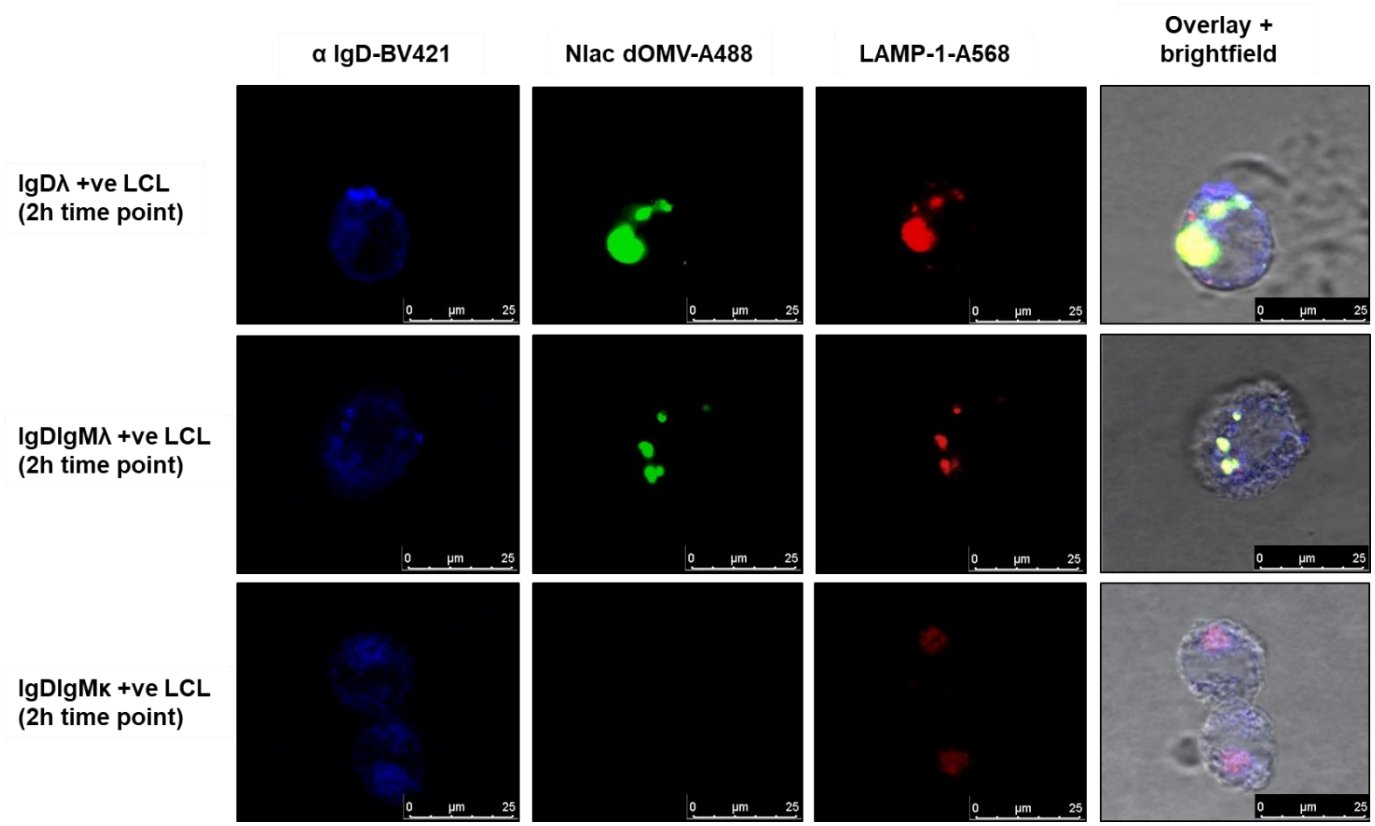

Figure 24 Nlac dOMVs traffics to lysosomes in IgDλ +ve LCLs.

Confocal fluorescence microscopy analysis of A488-labelled Nlac dOMVs (green) co-incubated with $1x10^6$ IgDλ +ve, IgDIgMλ +ve, or IgDIgMκ +ve LCLs at 37°C 5% CO_2 for 2 hours in complete cell culture medium. After incubation, the cells were washed, fixed and permeabilized. Next, the cells were stained with Brilliant Violet 421™ anti-human IgD Ab (Blue) and A568 biotin-conjugated anti-human CD107a (LAMP-1) Ab (Red). The cells were mounted onto a 1mm microscope slide, sealed under a cover slip, and analysed on a Confocal Laser Scanning Microscope. Data represents 3 identical experiments.

3.4 Discussion

It has previously been demonstrated that *N. lactamica* dOMVs induce a proliferative response in naive B cells that is independent of T cells (Vaughan *et al.*, 2010). It was postulated that this B cell proliferation is in response to a direct interaction between the dOMVs and IgD expressed on the surface of the B cell, suggesting the presence of a putative IgD-binding protein in *N. lactamica* dOMV. In accordance with this hypothesis, proliferation assays showed that *N. lactamica* dOMV induces a mitogenic response in IgD+ B cells. Furthermore, λ light chain-expressing B cells display significantly higher proliferation compared to κ light chain-expressing cells. This bias is significant and consistent with all repeats. Therefore, it can be deduced that either the putative IgD-binding protein is, in fact, an IgD λ binding protein, or that the λ light chain-expressing B cells are more susceptible to proliferation.

To further study and verify the role of IgD λ BCR in orchestrating the proliferative response to *N. lactamica* dOMV, the BCR was blocked with anti-BCR Abs and the change in proliferation was compared to non-treated cells. Previously Vaughan *et al,* showed that blocking of BCR by pre-treatment with anti-IgM and anti-IgD Abs abrogated the proliferative response, suggesting the involvement of IgD B cell surface receptor in this activity. The same study showed that blocking IgM also partially inhibited the proliferative response, suggesting IgM BCR may also have a role in inducing proliferation (Vaughan *et al.*, 2010). However, that study used whole Ig for blocking which has been shown to reduce the Ca^{2+} signalling (Tutt *et al.*, 2015). The whole Ig will largely also interact with and activate the inhibitory FcγRIIb via the Fc domain, triggering negative signalling which may be the reason for the suppressed activity shown by treatment with the anti-IgM antibody (Vaughan *et al.*, 2014; Tutt *et al.*, 2015).

In order to eliminate this possibility, instead of pre-treating with whole Ig, $F(ab')_2$ fragments of antibodies were used. $F(ab')_2$ fragments are generated using the enzyme pepsin in order to cleave the Ig below the hinge region, removing most of the Fc region. Since $F(ab')_2$ fragment antibodies lack Fc portions, it can only interact with cell surface Ig via the antigen-binding domain, therefore eliminating any binding between Fc portions of antibodies and Fc receptors on cells such as macrophages, dendritic cells, neutrophils, NK cells and B cells (Murphy *et al.*, 2012). Using $F(ab')_2$ fragments instead of whole Ig to block the BCR demonstrated that only blocking IgD or λ light chain inhibited the proliferation of B cells in response to *N. lactamica* dOMV. Conversely, blocking IgM or κ light chain did not inhibit proliferation.

3.4.1 Presence of putative mitogenic trimeric autotransporter adhesin in *N. cinerea*

Based on the whole genomic multilocus sequence typing (wgMLST) approach to molecular typing of *Neisseria* phylogeny, Ncin is closely related to Nlac (Bennett *et al.*, 2012). It is possible Ncin may also be mitogenic for B cells due to its similarity to Nlac. Therefore, in addition to Nlac, *N. cinerea* 346T was also investigated for mitogenic activation of B cells. The results showed that like Nlac, Ncin also induces a mitogenic proliferative response in IgD+ λ light chain+ B cells.

Furthermore, in response to Nlac and Ncin dOMVs pre-treatment of CD19+IgDλ+ cells with anti-IgD and anti-λ light chain Ab, but not anti-IgM and anti-κ light chain Ab resulted in a reduced percentage of proliferation compared to non-pre-treated cells. However, the level of inhibition differed between pre-treatment with anti-IgD and anti-λ Ab as anti-λ pre-treatment resulted in significantly lower proliferation compared to pre-treatment with anti-IgD Ab (Figure 18). This could be due to different affinities of anti-IgD and anti-λ Ab for the binding site, or it could be due to a higher competition for anti-IgD compared to anti-λ Ab. Another reason for this difference in levels of inhibition could be due to anti-IgD Ab resulting in a higher level of calcium flux compared to anti-λ Ab and thus resulting in the lower level of inhibition of proliferation with anti-IgD Ab compared to anti-λ Ab.

Based on these data it can be hypothesised that similar to *M. catarrhalis* (Forsgren *et al.*, 2001), *N. cinerea* 346T may also contain an IgD-binding protein triggering proliferation in this B cell subset. Furthermore, like Nlac, Ncin IgD-binding protein may also target IgDλ BCR.

Previously it has been proposed that interactions between bacterial antigen and IgD on lymphocytes play a role in pathogenesis and host defence in URT infections (Janson *et al.*, 1991; Forsgren *et al.*, 2001). However, since Nlac and Ncin both interact with IgDλ BCR and induce proliferation, this suggests that, contrary to the previous notion the ability of URT bacterial colonisers to interact with IgD and induce proliferation may be a feature of commensalism, rather than mediating virulence. These results also show that Nlac is not the only commensal *Neisseria* spp. to be mitogenic for IgDλ+ B cell. It was therefore hypothesised that the ability to interact with and activate B cells expressing IgDλ may be a conserved property within commensal *Neisseria* spp. that inhabit the URT. Therefore, in later sections of this thesis it will be shown which other URT colonising *Neisseria* spp. are also mitogenic for B cells and if so, whether it is due to an IgDλ binding protein.

3.4.2 Interaction of A488-labelled Nlac, Ncin and Nmen dOMVs with IgDλ+ B cells.

Another question addressed in this chapter is whether dOMVs from Nlac or Ncin colocalise with the IgDλ+ B cell population. The results in (Figure 21) showed that incubation of PBMCs with either Nlac or Ncin A488-labelled dOMVs results in a higher MFI in CD19+IgD+λ light chain+ cells compared to CD19+IgDκ light chain+ cells. This indicates that Nlac and Ncin A488-labelled dOMVs colocalise with CD19+IgD+λ light chain+ cells rather than CD19+IgDκ light chain+ cells. However, CD19+IgDκ+ cells did display a higher MFI value when compared to the non-treated cells (Figure 20, Figure 19, Figure 21). This could be due to non-specific interactions between dOMV and CD19+IgDκ+. Alternatively, it could be that the Nlac putative IgDbp binds to IgDλ and IgDκ but is internalised only by IgDλ expressing cells which results in accumulation of the A488-labelled dOMV inside the cells leading to a higher MFI. Moreover, this co-localisation is absent when PBMCs were incubated in the presence of Nmen A488-labelled dOMVs (Figure 19).

3.4.3 Effect of blocking IgM, IgD, λ or k BCR on the interaction with Nlac, Ncin and Nmen dOMVs

In order to investigate the effect of blocking IgM, IgD, λ or k BCR, PBMCs cells were pre-treated with $F(ab')_2$ polyclonal goat anti-human IgM, IgD, λ or k Abs. The cells were incubated with A488-labelled Nlac or Ncin dOMVs and MFI was measured. A reduction in MFI was observed across all conditions. The decrease in MFI upon pre-treatment with anti-IgM could be due to anti-IgM preventing the IgDbp from getting access to the IgD BCR, as both IgD and IgM are co-expressed on the surface of the B cells.

λ and κ expressing cells can adhere to each other by cell-cell adhesion or they can both attach to the same antigen resulting in adherence to each other. This could explain the decreased MFI in cells pre-treated with anti-κ Ab as pre-treatment of κ expressing B cells could be preventing the attachment to λ expressing B cells. Furthermore, the reduction upon pre-treatment with anti-IgM or anti-k Ab could simply be due to non-specific adherence. This reduction is in agreement with the previous data in (Figure 20, Figure 22), as there was a higher level of MFI in CD19+IgDk+ B cells compared to non-treated cells, which upon pre-treatment with anti-k Ab would result in a reduced MFI in CD19+IgD+ B cells. There was a significant reduction in detected MFI when cells were pre-treated with anti-IgD and anti-λ. Moreover, this reduction was significantly lower when compared to cells that were pre-treated with anti-IgM or anti- k light chain Ab. This suggests that the putative IgDbp is more specific to IgDλ+ B cells.

A question raised by the experiments in this chapter relates to the high level of MFI displayed by CD19+IgD+ B cells in response to A488-labelled Nlac and Ncin dOMVs. The interaction between the dOMVs and B cells requires further work to investigate whether these dOMVs are adhering to the surface of the B cells or whether they are internalised by the B cells. Phagocytosis, the engulfment and destruction of antigen, is essential in the instigation and development of mammalian adaptive immunity. In mammals, phagocytosis is chiefly carried out by “professional phagocytes” such as monocytes, macrophages, neutrophils and dendritic cells. However, it has been demonstrated that non-professional phagocytes such as B cells may also partake in low-level phagocytosis (Parra *et al.*, 2012; Nygaard *et al.*, 2016). This has been shown for Mcat where binding of an antigen to the BCR leads to the internalisation of the antigen-BCR complex and movement to the endosome (Perez Vidakovics *et al.*, 2010; Schaar *et al.*, 2011). B cells have also been shown to internalize *Salmonella typhimurium* (Verjans *et al.*, 1994; Rosales-Reyes *et al.*, 2005; Souwer *et al.*, 2009). In accordance with these studies, it is suggested here that the Nlac and Ncin dOMV interaction with the IgD-BCR results in internalisation of the antigen-BCR complex leading to downstream signalling and proliferation. Alternatively, the dOMV might not be internalised and simply the association of the Nlac or Ncin dOMV with the IgD-BCR could be instigating a signal for B cell proliferation resulting in high MFI (Figure 23). In order to test these hypotheses, confocal microscopy was utilized to clarify whether Nlac OMV is internalised by IgDλ cells or if it only co-localizes the outer surface of the B cells.

The use of LCLs expressing only IgDλ, IgDIgMλ or IgDIgMκ enabled investigation of the co-localization to specific cell types. Observation of highly punctate A488 stain (from A488-labelled Nlac dOMVs) co-localizing the A568 stain (from A568 biotin-conjugated anti-human LAMP-1 Ab) in IgDλ and IgDIgMλ LCLs, but not in IgDIgMκ, suggests the endocytosis of Nlac dOMVs in IgDλ+ cells only. These results, in conjunction with the MFI data, suggest that Nlac dOMVs bind the IgDλ BCR and are endocytosed. It is possible that in vivo, after endocytosis by B cells, Nlac may survive intracellularly similar to *Salmonella typhimurium* (Verjans *et al.*, 1994; Rosales-Reyes *et al.*, 2005; Souwer *et al.*, 2009). Alternatively, Nlac might behave similar to Mcat, resulting in death upon internalization of B cells and therefore uses its OMV to avoid being internalized by B cells. (Jendholm *et al.*, 2008).

In summary, these experiments support the hypothesis that Nlac dOMVs containing the putative IgDbp act in a similar way to MID protein, causing internalization by B cells and the mediation of TLR2/9 signalling eventually results in the secretion of IgM Ab.

4. Investigating various *Neisseria* spp. for the presence of MID homologues and their ability to induce B cell proliferation.

4.1 Introduction

In chapter 3 it was shown that dOMV from Ncin is also mitogenic for CD19+IgD+ cells and similar to Nlac, Ncin dOMVs induced significantly higher proliferation in CD19+IgDλ+ B cells compared to CD19+IgDκ+ B cells. This suggests that Ncin may also express an IgDλ binding protein.

The fact that both Nlac and Ncin induces proliferation in IgDλ+ B cell suggests mitogenicity is not strictly a pathogenic property as previously suggested (Janson *et al.*, 1991). These results also demonstrate that Nlac is not the only commensal *Neisseria* to be mitogenic for CD19+IgDλ+ B cells and that other commensal species may also have this property.

In this chapter, a survey of other *Neisseria* spp. colonizing humans was carried out, for the potential mitogenic ability towards B cells.

4.1.1 *Neisseria* candidates to be surveyed for mitogenicity

Phylogenetic taxonomy based on the whole genome of *Neisseria* was used to select bacterial strains for mitogenicity testing (Bennett *et al.*, 2012). Each strain from different *Neisseria* spp. was chosen from a different branch of the phylogenetic tree in order to obtain a range of strains that represents the *Neisseria* spp. colonizing humans (Table 16). Where possible, strains with available complete genome sequences were chosen for investigation. Subsequently, these genome sequences were used for comprehensive homology search against the amino acid sequence of the MID protein.

As previously discussed in chapter 1.4.3 *Moraxella catarrhalis* contains a trimeric autotransporter protein MID which binds to the IgD expressed on the surface of B cells resulting in activation and proliferation of B cells.

The IgD binding region (IgDbr) of MID protein has been discovered by expressing truncated fragments of MID in *E. coli* followed by confirmation of the IgD binding by Western blot. This study discovered that the smallest fragment with conserved IgD binding function was composed of 238 amino acid (AA) residues (MID 962-1200 amino acids) (Figure 25) (Forsgren *et al.*, 2001; Nordstrom, Forsgren and Riesbeck, 2002).

Based on the known function of MID as a TI B cell mitogen, it was decided to use MID (aa962-1200) sequence as a search query for the investigation of MID homologues/putative IgDbp in the genome of *Neisseria* spp.

GHALSQGLANDTDKTRAASIGDVLNAGFNLQGNGEAKDFVSTYDTVNFIDGNATT
AKVTYDDTKQTSTVTYDVNVDNKTLEVTGDKKLGVKTTTLTKTSANGNATKFSAA
DGDALVKASDIATHLNTLAGDIQTAKGASQASSSASYVDADGNKVIYDSTDKKYY
QVNEKGQVDKTKEVTKDKLVAQAQTPDGTLAQMNVKSVINKEQVNDANKKQGINE
DNAFVKGLEKAASDNKTKN

Figure 25 The amino acid sequence of the IgDbr (962-1200) of the MID protein

Taken from (Forsgren *et al.*, 2001; Nordstrom, Forsgren and Riesbeck, 2002).

Table 16 List of *Neisseria* species to be assessed for B cell mitogenicity

Species
CCUG 50858T *Neisseria bacilliformis*
CCUG 2043T *Neisseria elongata ss elongata*
CCUG 17913T *Neisseria flavescens*
CCUG 41451T *Neisseria macacae*
CCUG 26878T *Neisseria mucosa ss Heidelbergensis*
CCUG 18031T *Neisseria polysaccharea*
CCUG 23930T *Neisseria subflava*
Neisseria gonorrhoeae MS11

4.2 Aims

- To perform a comprehensive homology search in order to identify MID aa962-1200 homologous genes in *Neisseria* spp. colonising humans.
- To extract dOMVs from the commensal *Neisseria* strains and to investigate their ability to activate IgDλ expressing B cells.
- Identify the conserved domains present in the MID homologues present in various commensal *Neisseria* strains.
- Investigate the expression of putative TAAs present in various commensal *Neisseria* strains.

4.3 Hypotheses

- The ability to induce proliferation in IgDλ+ B cell is shared among commensal *Neisseria* spp.

4.4 Homology search

The genome sequence of various *Neisseria* strains from the PubMLST Bacterial Isolate Genome Sequence Database was investigated for the presence of homology to MID aa962-1200. Protein-Protein and Nucleotide-Nucleotide BLAST tools from the NCBI website: https://blast.ncbi.nlm.nih.gov/Blast.cgi were used for the homology search.

Homology is deduced from excess similarity, and excess similarity is inferred from statistical E values of BLAST search. The E value is a parameter used in the BLAST homology search as a significance threshold for reporting homology results, and it describes the number of hits one can expect to see by chance with a database of a specific size. Max score is also considered when working out an E value. The E value decreases exponentially as the max score increases. In this report, an E value of < 0.001 or lower was set as an acceptable threshold for reporting the blast results (Pearson, 2013; Ladunga, 2017). Furthermore, NCBI rounds off E values of ~1e-250 to 0 and in case of retrieving an E value of 0, ‡ symbol was used to indicate significance.

It was also decided to use a 30% identity, which is also used by other homology focused studies (Bennett *et al.*, 2012; Pearson, 2013). Two sequences are considered homologous if they are 30% identical over their entire lengths (much higher identities are seen by chance in short alignments). While percentage identity alone is not a reliable measure of homology it can be a reasonable proxy for evolutionary distance after the establishment of homology. As it is possible to get false positive results based on percentage identity, the max score was also used when inferring homology. A max score or bit score is the highest alignment score between the query sequence and the database sequence segment. It does not depend on the size of the query sequence length or the size of the database and would give the same value for hits in databases of varied sizes. Based on the literature review a max score of ≥ 50 is considered significant enough to assume homology. However, a max score of > 40 can be considered significant in combination with an E value < 0.001. Individually or collectively these criteria are commonly used to identify homologous sequences (Pertsemlidis and Fondon, 2001; Pearson, 2013), therefore, in our search for homology between MID and *Neisseria* spp. colonising humans, we also utilised these criteria to avoid false-positive results.

In order to perform a comprehensive homology search, the search was divided into three stages comprising an extensive BLAST, a strain-specific BLAST and a confirmatory BLAST to identify the true homology. First, the amino acid sequence of the IgDbr (962-1200) of the MID protein (Figure 25) was used as the search query using the web-based Protein-Protein BLAST tool from the NCBI website: https://blast.ncbi.nlm.nih.gov/Blast.cgi. Where possible the query (MID aa962-1200) was searched against the database of whole species in order to perform a broad search and identify any possible MID aa962-1200

homologues within that species. However, where the search against a database of whole species retrieved a large number of possible homologues, the search was performed against at least two strains. Next, a BLAST search was performed on the nucleotide CDS of MID aa962-1200 homologues identified in the whole species against nucleotide CDS of the specific strain (strain chosen for investigation from that species). Finally, a BLAST search was performed on the protein CDS of MID aa962-1200 against MID aa962-1200 homologues which passed the homology criteria and were present in our chosen strain. This permitted identification of the true percentage homology between the IgDbp of MID and its homologues present in *Neisseria* spp. colonising humans.

4.4.1 Results

4.4.1.1 *Neisseria lactamica*

The BLAST search of the amino acid sequence of the IgDbr of the MID protein (aa962-1200) against *N. lactamica* Y92-1009 revealed two hits (Table 17). Both hits fulfil the homology criteria and therefore were considered homologous to MID protein (aa962-1200).

The BLAST search of the amino acid sequence of the IgDbr of the MID protein (aa962-1200) against a strain of *N. lactamica* (ATCC 23970) revealed 5 genes possibly encoding a putative IgDbp (Table 18). All five genes fulfil the homology criteria and were considered to be homologous to MID protein (aa962-1200).

In order to check whether MID (aa962-1200) homologues present in *N. lactamica* ATCC 23970 are also present in *N. lactamica* Y92-1009 a BLAST search of the nucleotide CDS of all five MID (aa962-1200) homologues present in *N. lactamica* 223970 was performed against *N. lactamica* Y92-1009 nucleotide CDS (Table 19). Results showed that DR91_346, NEILACOT_03494 and NEILACOT_04187 present in *N. lactamica* ATCC 23970 shares the same locus as the NLY_36660 in *N. lactamica* Y92-1009. Whereas DR91_RS03790 and NEILACOT_04186 from *N. lactamica* ATCC 23970 shares same locus as the NLY_37260 in *N. lactamica* Y92-1009.

Finally, a BLAST search was performed on the protein CDS of MID aa962-1200 homologues that passed the homology criteria and were present in *N. lactamica* Y92-1009 against MID aa962-1200 in order to find the percentage identity of homology between MID homologues present in *N. lactamica* Y92-1009 (Table 20). Results showed that MID aa962-1200 shares 47% identity with NLY_36660 and 52% identity with NLY_37260. Both of these hits passed the pre-specified homology criteria and can be considered homologous to MID aa962-1200. It is hypothesised that identification of these homologues suggests the presence of one or multiple putative IgDbp which would result in inducing proliferation in IgDλ+ B cells.

Table 17 *N. lactamica* Y92-1009 homologues to MID aa962-1200: NCBI.

No.	Description	Locus tag	Accession	No. of base pairs	No. of amino acids	Max score	Query coverage	E value	Identity	Passed homology criteria
1	Unnamed protein product	NLY_36660 (Vaughan *et al*) (13627-23904)	CBX21664.1	10278	3425	70.5	38%	$4e^{-15}$	47%	Yes
2	Hypothetical protein	NLY_37260 (Vaughan *et al*) (55410-65606)	WP_003712364.1	10197	3398	46.2	57%	$5e^{-07}$	31%	Yes

Table 18 *N. lactamica* ATCC 23970 homologues to MID aa962-1200: NCBI.

No.	Description	Locus tag	Accession	No. of base pairs	No. of amino acids	Max score	Query coverage	E value	Identity	Passed homology criteria
1	Adhesin	DR91_346 (Minogue *et al*) (391775-401872)	KFJ35963.1	10097	3365	72.8	40%	$9e^{-16}$	46%	YES
2	YadA-like domain protein	NEILACOT_03494 (Fulton *et al*) (9983-17674)	EEZ76379.1	7691	2563	72.4	40%	$1e^{-15}$	46%	YES
3	Adenoviral fibre protein (repeat/shaft region)	NEILACOT_04187 (Fulton *et al*) (30266-36430)	EEZ75770.1	6164	2054	55.1	48%	$7e^{-10}$	68%	YES
4	Hypothetical protein	DR91_RS03790 (Minogue *et al*) (811177-821073)	WP_036475096.1	9896	3298	55.1	49%	$8e^{-10}$	68%	YES
5	Hep/Hag repeat protein	NEILACOT_04186 (Fulton *et al*) (26536-30231)	EEZ75769.1	3695	1231	45.1	25%	$1e^{-06}$	50%	YES

Table 19 *N. lactamica* Y92-1009 homologues to *N. lactamica* ATCC 23970 putative IgDbp candidates. Nucleotide CDS vs nucleotide CDS.

‡ indicates an E value of ~1e-250.

No.	Description	Locus tag	Location in Y92-1009 complete genome	No. of base pairs	No. of amino acids	Max score	Query coverage	E value	Identity	Passed homology criteria
1	Adhesin (This gene shares the same locus as the unnamed protein product NLY_36660)	DR91_346 (Minogue *et al*)	(1660714-1670991) REV	10278	3425	5463	91%	‡	98%	YES
2	YadA-like domain protein (This gene shares the same locus as the unnamed protein product NLY_36660)	NEILACOT_03494 (Fulton *et al*)	(1660714-1670991) REV	10278	3425	5463	89%	‡	98%	YES
3	Adenoviral fibre protein (repeat/shaft region) (This gene shares the same locus as the unnamed protein product NLY_36660)	NEILACOT_04187 (Fulton *et al*)	(1660714-1670991) REV	10278	3425	4329	81%	‡	98%	YES
4	Hypothetical protein (This gene shares the same locus as the hypothetical protein NLY_37260)	DR91_RS03790 (Minogue *et al*)	(1702497-1712693) FOR	10197	3399	6822	86%	‡	90%	YES
5	Hep/Hag repeat protein (This gene shares the same locus as the hypothetical protein NLY_37260)	NEILACOT_04186 (Fulton *et al*)	(1702497-1712693) FOR	10197	3399	2955	96%	‡	95%	YES

Table 20 Homology search of *N. lactamica* Y92-1009 putative IgDbp candidates against MID aa962-1200: protein CDS.

No.	Description	Locus tag	Location in Y92-1009 complete genome	No. of base pairs	No. of amino acids	Max score	Query coverage	E value	Identity	Passed homology criteria
1	Unnamed protein product	NLY_36660 (Vaughan *et al*)	(1660714-1670991) REV	10278	3425	70.5	83%	$2e^{-17}$	47%	Yes
2	Hypothetical protein	NLY_37260 (Vaughan *et al*)	(1702497-1712693) FOR	10197	3398	50.4	79%	$1e^{-10}$	52%	Yes

4.4.1.2 *Neisseria cinerea*

The BLAST search of MID aa962-1200 against *N. cinerea* whole species revealed nineteen homologues (Table 21). All hits in the list fulfil the homology criteria except for the last two hits which have E values >0.001 and max scores <40. Additionally, NEICINOT_RS03205 is a fragment of NEICINOT_03770 and shares the same locus therefore NEICINOT_RS03205 was not considered a separate homologue.

Next, a BLAST search was performed on the nucleotide CDS of MID aa962-1200 homologues identified in the *N. cinerea* whole species database against *N. cinerea* 346T nucleotide CDS (Table 22). Results showed that DBY94_RS04140, DQM57_RS03620, DBZ01_RS07140, DBY98_RS09210, DBY88_RS04835 and DBY98_RS09205 shares the same locus as NEICINOT_04577_346 in *N. cinerea* 346T. Whereas DQM57_RS08900, DBY98_RS02130, DBZ01_RS03935, DBY88_RS07265, DBY94_RS08785, NEICINOT_RS03205, NEICINOT_03771, DBY98_RS02115, DQM57_RS08905, NEICINOT_05179 and DBZ01_RS03930 shares the same locus as NEICINOT_03770_346 in *N. cinerea* 346T.

Finally, a BLAST search was performed on the protein CDS of MID aa962-1200 homologues that passed the homology criteria and were present in *N. cinerea* 346T against MID aa962-1200 in order to find the true percentage identity between MID aa962-1200 homologues present in *N. cinerea* 346T (Table 23). Results showed that MID aa962-1200 shares 51% identity with NEICINOT_04577_346 and 63% identity with NEICINOT_03770_346. Both of these hits passed our set homology criteria and can be considered homologous to MID aa962-1200. It is hypothesised that these homologues encode a putative IgDbp which would result in inducing proliferation in IgDλ+ B cells.

Table 21 *N. cinerea* ATCC 14685 homologues to MID aa962-1200: NCBI.

No.	Description	Locus tag	Accession	No. of base pairs	No. of amino acids	Max score	Query coverage	E value	Identity	Passed homology criteria
1	Hep_Hag family protein	NEICINOT_04577 (Weinstock *et al*) (50810-56488)	WP_003677430.1	5679	1892	81.3	51%	4e-18	50.00%	Yes
2	Hypothetical protein	DBY94_RS04140 (Nichols *et al*) (262708-268434)	WP_108043721.1	5727	1908	81.3	51%	4e-18	50.00%	Yes
3	Hypothetical protein	DQM57_RS08900 (Doyle *et al*) (1707763-1719516)	WP_111727535.1	11754	3917	80.9	33%	5e-18	54.32%	Yes
4	Hypothetical protein	DQM57_RS03620 (Doyle *et al*) (1154474-1160131)	WP_111726921.1	5658	1885	79.3	51%	2e-17	49.09%	Yes
5	Hypothetical protein	DBY98_RS02130 (Nichols *et al*) (403996-414975)	WP_107996471.1	10980	3659	77	33%	1e-16	55.56%	Yes
6	Hypothetical protein	DBZ01_RS03935 (Nichols *et al*) (737440-749196)	WP_107859595.1	11575	3918	75.9	32%	2e-16	60.00%	Yes
7	Peptidase propeptide and YPEB domain protein	NEICINOT_03770 (Weinstock *et al*) (18281-27937)	WP_003675924.1	9657	3218	75.5	33%	3e-16	54.32%	Yes
8	Hypothetical protein	DBY88_RS07265 (Nichols *et al*) (74096-84757)	WP_107960884.1	10662	3553	73.9	33%	1e-15	55.07%	Yes
9	Hypothetical protein	DBY94_RS08785 (Nichols *et al*)	WP_108044334.1	4317	1438	72	23%	4e-15	61.40%	Yes

		(6071-10387)								
10	Hypothetical protein	DBZ01_RS07140 (Nichols *et al*) (517232-522226)	WP_107860082.1	4995	1664	72	38%	5e-15	47.50%	Yes
11	Hypothetical protein (This gene is a fragment of NEICINOT_03771 and shares the same locus)	NEICINOT_RS03205 (Weinstock *et al*) (28515-31103)	WP_039854152.1	2589	862	71.6	28%	7e-15	56.72%	Yes
12	Peptidase propeptide and YPEB domain protein	NEICINOT_03771 (Fulton *et al*) (28515-32327)	EEZ71940.1	3813	1270	71.2	28%	8e-15	56.72%	Yes
13	Hypothetical protein	DBY98_RS02115 (Nichols *et al*) (398031-402452)	WP_107996465.1	4422	1473	70.9	29%	1e-14	55.71%	Yes
14	Hypothetical protein	DBY98_RS09210 (Nichols *et al*) (71667-74063)	WP_107997459.1	2397	798	70.9	29%	1e-14	51.35%	Yes
15	Hypothetical protein	DBY88_RS04835 (Nichols *et al*) (311871-316853)	WP_107960539.1	4983	1660	69.7	27%	4e-14	53.03%	Yes
16	Hypothetical protein	DBY98_RS09205 (Nichols *et al*) (68708-71479)	WP_107997458.1	2772	923	68.9	38%	5e-14	43.96%	Yes
17	Hypothetical protein	DQM57_RS08905 (Doyle *et al*) (1720082-1725412)	WP_111727536.1	53331	1776	68.9	29%	6e-14	54.29%	Yes
18	Hypothetical protein	NEICINOT_05179 (Fulton *et al*) (1-1336)	EEZ70713.1	1338	445	35.8	8%	0.004	75.00%	No

19	Hypothetical protein	DBZ01_RS03930 (Nichols *et al*) (731562-736862)	WP_107859594.1	5301	1766	25.8	8%	9.1	60.00%	No

Table 22 *N. cinerea* 346T homologues to *N. cinerea* ATCC 14685 putative IgDbp candidates. Nucleotide CDS vs nucleotide CDS.

‡ indicates an E value of ~1e-250.

No.	Description	Locus tag	Accession	No. of base pairs	No. of amino acids	Max score	Query coverage	E value	Identity	Passed homology criteria
1	Hep_Hag family protein	NEICINOT_04577_346 (Weinstock *et al*)	NODE 3 (681-6023) REV	5343	1780	3230	68%	‡	89%	Yes
2	Hypothetical protein (This gene is a fragment of NEICINOT_04577 and shares the same locus)	DBY94_RS04140_346 (Nichols *et al*)	NODE 3 (681-6023) REV	5343	1780	3397	66%	‡	90.36%	Yes
3	Hypothetical protein (This gene is a fragment of NEICINOT_03770 and shares the same locus)	DQM57_RS08900_346 (Doyle *et al*)	NODE 12 (18204-29351) REV	11148	3715	2916	81%	‡	93.97%	Yes
4	Hypothetical protein (This gene is a fragment of NEICINOT_04577 and shares the same locus)	DQM57_RS03620_346 (Doyle *et al*)	NODE 3 (681-6023) REV	5343	1780	3330	66%	‡	90.48%	Yes
5	Hypothetical protein (This gene is a fragment of NEICINOT_03770 and shares the same locus)	DBY98_RS02130_346 (Nichols *et al*)	NODE 12 (18204-29351) REV	11148	3715	4898	75%	‡	96.68%	Yes
6	Hypothetical protein (This gene is a fragment of NEICINOT_03770 and shares the same locus)	DBZ01_RS03935_346 (Nichols *et al*)	NODE 12 (18204-29351) REV	11148	3715	6348	86%	‡	97.43%	Yes
7	Peptidase propeptide and YPEB domain protein	NEICINOT_03770_346 (Weinstock *et al*)	NODE 12 (18204-29351) REV	11148	3715	2916	71%	‡	94%	Yes
8	Hypothetical protein	DBY88_RS07265_346 (Nichols *et al*)	NODE 12 (18204-29351)	11148	3715	9097	73%	‡	94.81%	Yes

	(This gene is a fragment of NEICINOT_03770 and shares the same locus)		REV							
9	Hypothetical protein (This gene is a fragment of NEICINOT_03770 and shares the same locus)	DBY94_RS08785_346 (Nichols *et al*)	NODE 12 (18204-29351) REV	11148	3715	632	34%	‡	98.87%	Yes
10	Hypothetical protein (This gene is a fragment of NEICINOT_04577 and shares the same locus)	DBZ01_RS07140_346 (Nichols *et al*)	NODE 3 (681-6023) REV	5343	1780	7829	100%	‡	94.94%	Yes
11	Peptidase propeptide and YPEB domain protein (This gene is a fragment of NEICINOT_03770 and shares the same locus)	NEICINOT_03771_346 (Fulton *et al*)	NODE 12 (29925-35201) REV	5277	1758	627	13%	‡	99%	Yes
12	Hypothetical protein (This gene is a fragment of NEICINOT_03770 and shares the same locus)	DBY98_RS02115_346 (Nichols *et al*)	NODE 12 (29925-35201) REV	5277	1758	678	54%	‡	84.70%	Yes
13	Hypothetical protein (This gene is a fragment of NEICINOT_04577 and shares the same locus)	DBY98_RS09210_346 (Nichols *et al*)	NODE 3 (681-6023) REV	5343	1780	3685	100%	‡	94.51%	Yes
14	Hypothetical protein (This gene is a fragment of NEICINOT_04577 and shares the same locus)	DBY88_RS04835_346 (Nichols *et al*)	NODE 3 (681-6023) REV	5343	1780	1559	23%	‡	94.22%	Yes
15	Hypothetical protein (This gene is a fragment of NEICINOT_04577 and shares the same locus)	DBY98_RS09205_346 (Nichols *et al*)	NODE 3 (681-6023) REV	5343	1780	4265	100%	‡	94.45%	Yes
16	Hypothetical protein (This gene is a fragment of NEICINOT_03770 and shares the same locus)	DQM57_RS08905_346 (Doyle *et al*)	NODE 12 (29925-35201) REV	5277	1758	712	48%	‡	85.61%	Yes

17	Hypothetical protein (This gene is a fragment of NEICINOT_03770 and shares the same locus)	NEICINOT_05179_346 (Fulton *et al*)	NODE 12 (29925-35201) REV	5277	1758	737	57%	‡	86.21%	Yes
18	Hypothetical protein (This gene is a fragment of NEICINOT_03770 and shares the same locus)	DBZ01_RS03930_346 (Nichols *et al*)	NODE 12 (29925-35201) REV	5277	1758	7491	100%	‡	92.26%	Yes

Table 23 Homology search of *N. cinerea* 346T putative IgDbp candidates against MID aa962-1200: protein CDS.

No.	Description	Locus tag	Location in CCUG 346T genome	No. of base pairs	No. of amino acids	Max score	Query coverage	E value	Identity	Passed homology criteria
1	Hep_Hag family protein	NEICINOT_04577_346 (Weinstock *et al*)	NODE 3 (681-6023) REV	5343	1780	68.2	60%	$7e^{-17}$	51%	Yes
2	Peptidase propeptide and YPEB domain protein	NEICINOT_03770_346 (Weinstock *et al*)	NODE 12 (18204-29351) REV	11148	3715	74.7	88%	$8e^{-19}$	63%	Yes

4.4.1.3 *Neisseria flavescens*

The BLAST search of MID aa962-1200 against *N. flavescens* whole species database revealed five homologues (Table 24). All hits fulfil the homology criteria and therefore were considered homologous to MID protein (aa962-1200). Additionally, NEIFLAOT_RS05735 is a fragment of NEIFLAOT_01374 and shares the same locus therefore NEIFLAOT_RS05735 was not considered a separate homologue.

Next, a BLAST search was performed on the nucleotide CDS of MID aa962-1200 homologues identified in the *N. flavescens* whole species database against *N. flavescens* CCUG 17913 nucleotide CDS (Table 25). Results showed that NEIFLAOT_01375 and NEIFLAOT_01374 share the same locus as DYC64_RS10620_17913 in *N. flavescens* CCUG 17913.

Finally, a BLAST search was performed on the protein CDS of MID aa962-1200 homologues that passed the homology criteria and were present in *N. flavescens* CCUS 17913, against MID aa962-1200 in order to find the true percentage identity between MID aa962-1200 homologues present in *N. flavescens* CCUS 17913 (Table 26). Results showed that MID aa962-1200 shares 55% identity with DYC64_RS10620_17913 and 36% identity with NEIFLAOT_01884_17913. Both of these hits passed our set homology criteria and can be considered homologous to MID aa962-1200. We hypothesised that these homologues might encode a putative IgDbp which would result in inducing proliferation in IgDλ+ B cells.

Table 24 *N. flavescens* whole taxid homologues to MID aa962-1200: NCBI.

No.	Description	Locus tag	Accession	No. of base pairs	No. of amino acids	Max score	Query coverage	E value	Identity	Passed homology criteria
1	Hypothetical protein	DYC64_RS10620 (Doyle *et al*) (22475-237731)	WP_115287662.1	12978	4325	82	37%	$3e^{-16}$	55%	Yes
2	Hypothetical protein	NEIFLAOT_01375 (Fulton *et al*) (3249-13100)	WP_003680603.1	9852	3283	82	34%	$2e^{-16}$	55%	Yes
3	YadA-like domain protein	NEIFLAOT_01374 (Fulton *et al*) (79-3228)	EEG33524.1	3150	1049	75.9	33%	$4e^{-12}$	56%	Yes
4	Hypothetical protein (This gene is a fragment of NEIFLAOT_01374 and shares the same locus)	NEIFLAOT_RS05735 (Fulton *et al*) (79-2502)	WP_100066428.1	2424	807	71.6	33%	$8e^{-15}$	54%	Yes
5	MULTISPECIES: Hypothetical protein	NEIFLAOT_01884 (Fulton *et al*) (182-6934)	WP_003681270.1	6753	2250	64.7	61%	$2e^{-12}$	36%	Yes

Table 25 *N. flavescens* CCUG 17913 homologues to *N. flavescens* whole taxid putative IgDbp candidates. Nucleotide CDS vs nucleotide CDS.

‡ indicates an E value of ~1e-250.

No.	Description	Locus tag	Location in CCUG 17913T genome	No. of base pairs	No. of amino acids	Max score	Query coverage	E value	Identity	Passed homology criteria
1	Hypothetical protein	DYC64_RS10620_17913 (Doyle *et al*)	(1996246-2009223) FOR	12978	4325	7521	100%	‡	90%	Yes
2	Hypothetical protein (This gene is a fragment of DYC64_RS10620_17913 and shares the same locus)	NEIFLAOT_01375_17913 (Fulton *et al*)	(1996246-2006053) FOR	9808	3269	15285	99%	‡	99%	Yes
3	YadA-like domain protein (This gene is a fragment of DYC64_RS10620_17913 and shares the same locus)	NEIFLAOT_01374_17913 (Fulton *et al*)	(2006074-2009223) FOR	3150	1049	5818	100%	‡	100%	Yes
4	MULTISPECIES: Hypothetical protein	NEIFLAOT_01884_17913 (Fulton *et al*)	(573174-579926) FOR	6753	2250	12471	100%	‡	100%	Yes

Table 26 Homology search of *N. flavescens* CCUG 17913T putative IgDbp candidates against MID aa962-1200: protein CDS.

No.	Description	Locus tag	Location in CCUG 17913T genome	No. of base pairs	No. of amino acids	Max score	Query coverage	E value	Identity	Passed homology criteria
1	Hypothetical protein	DYC64_RS10620_17913 (Doyle *et al*)	(1996246-2009223) FOR	12978	4325	82	92%	$3e^{-21}$	55%	Yes
2	MULTISPECIES: Hypothetical protein	NEIFLAOT_01884_17913 (Fulton *et al*)	(573174-579926) FOR	6753	2250	64.7	83%	$1e^{-15}$	36%	Yes

4.4.1.4 *Neisseria mucosa*

The BLAST search of MID aa962-1200 against *N. mucosa* whole species database retrieved two hits (Table 27). Results showed that both hits failed to fulfil the homology criteria. Therefore, HMPREF0604_01528 and ES17_05175 were not considered MID aa962-1200 homologues as they had E values >0.001 and max scores <40.

Next, a BLAST search was performed on the nucleotide CDS of MID aa962-1200 homologues identified in the *N. mucosa* whole species database against *N. mucosa* 26878 nucleotide CDS (Table 28). Results showed that *N. mucosa* 26878 genome lacks homology to MID aa962-1200 homologues found in *N. mucosa* whole species. Therefore, it is hypothesised that *N. mucosa* 26878 lacks a putative IgDbp and dOMVs extracted from this strain will lack the ability to induce proliferation in IgDλ+ B cells.

Table 27 *N. mucosa* whole taxid homologues to MID aa962-1200: NCBI.

*** indicates end of contig.**

No.	Description	Locus tag	Accession	No. of base pairs	No. of amino acids	Max score	Query coverage	E value	Identity	Passed homology criteria
1	hypothetical protein HMPREF0604_01528, partial	HMPREF0604_01528 (Earl *et al*) (464206-467864*)	EFV80256.1	3660	1220	34.7	30%	0.022	37%	No
2	hypothetical protein ES17_05175, partial	ES17_05175 (Chong *et al*) (*1-2137)	KGJ31917.1	2137	712	3.1	30%	0.059	37%	No

Table 28 *N. mucosa* 26878 homologues to *N. mucosa* whole taxid putative IgDbp candidates. Nucleotide CDS vs nucleotide CDS.

No.	Description	Locus tag	Location in CCUG 26878T genome	No. of base pairs	No. of amino acids	Max score	Query coverage	E value	Identity	Passed homology criteria
1	hypothetical protein HMPREF0604_01528, partial	HMPREF0604_01528 (Earl *et al*)	No homologues to hypothetical protein (HMPREF0604_01528) (partial) were found in the genome of *N. mucosa* 26878T strain							
2	Hypothetical protein encompassing MULTISPECIES: adhesin	ES17_05175 (Chong *et al*)	No homologues to Hypothetical protein encompassing MULTISPECIES: adhesin (ES17_05175) were found in the genome of *N. mucosa* 26878T strain							

4.4.1.5 *Neisseria macacae*

The BLAST search of MID aa962-1200 as the query against *N. macacae* whole species database retrieved zero hits, suggesting an absence of a putative IgDbp.

4.4.1.6 *Neisseria gonorrhoeae*

The BLAST search of MID aa962-1200 as the query against *N. gonorrhoeae* whole species database retrieved zero hits, suggesting an absence of a putative IgDbp.

4.4.1.7 *Neisseria subflava*

The BLAST search of MID aa962-1200 against *N. subflava* whole species database revealed four homologues (Table 29). All four hits failed to fulfil the homology criteria and therefore were not considered true MID aa962-1200 homologues.

Next, a BLAST search was performed on the nucleotide CDS of MID aa962-1200 homologues identified in the *N. subflava* whole species database (despite failing the homology criteria) were searched against *N. subflava* CCUG 23930 nucleotide CDS (Table 30). Results showed that except for DBY81_RS00565 similar versions of DV114_RS07825, NEISUBOT_05623 and DBY97_RS02575 were present in *N. subflava* CCUG 23930. Additionally, NEISUBOT_05623_23930 is a fragment of DBY97_RS02575_23930 and shares the same locus in *N. subflava* CCUG 23930. Whereas, DV114_RS07825_23930 is a fragment of FAH66_RS06750_23930 and shares the same locus in *N. subflava* CCUG 23930.

Finally, a BLAST search was performed on the protein CDS of MID aa962-1200 against MID aa962-1200 homologues that were present in *N. subflava* CCUG 23930. This allowed us to find the true percentage identity of MID aa962-1200 homologues present in *N. subflava* CCUG 23930 (Table 31). Results showed that FAH66_RS06750_23930 had a max score of <40 and therefore was not considered a true MID aa962-1200 homologue. Whereas, DBY97_RS02575_23930 passed our homology criteria and shares 42% identity with MID aa962-1200. It is hypothesised that *N. subflava* CCUG 23930T contains a putative IgDbp and dOMVs extracted from *N. subflava* CCUG 23930T will induce proliferation in IgDλ+ B cells.

Table 29 *N. subflava* whole taxid homologues to MID aa962-1200: NCBI.

No.	Description	Locus tag	Accession	No. of base pairs	No. of amino acids	Max score	Query coverage	E value	Identity	Passed homology criteria
1	Hypothetical protein	DV114_RS07825 (Topaz *et al*) (1640340-1642841)	WP_114926330.1	2502	833	34.3	30%	0.032	37%	No
2	Hep/Hag repeat protein, partial	NEISUBOT_05623 (Fulton *et al*) (*1-4451)	EFC50946.1	4452	1483	33.9	30%	0.044	37%	No
3	Hypothetical protein	DBY97_RS02575 (Nichols *et al*) (148925-156448)	WP_107857326.1	7524	2507	34.3	24%	0.044	43%	No
4	Hypothetical protein	DBY81_RS00565 (Nichols *et al*) (121621-124395)	WP_107791837.1	2775	924	33.1	14%	0.093	43%	No
5	Hypothetical protein	FAH66_RS06750 (Streich *et al*) (1390190-1391710)	WP_137041115.1	1521	506	32.3	30%	0.15	37%	No

Table 30 *N. subflava* CCUG 23930 homologues to *N. subflava* whole taxid putative IgDbp candidates. Nucleotide CDS vs nucleotide CDS.

*** indicates the end of the contig. ‡ indicates an E value of ~1e-250.**

No.	Description	Locus tag	Location in CCUG 23930T genome	No. of base pairs	No. of amino acids	Max score	Query coverage	E value	Identity	Passed homology criteria
1	Hypothetical protein	DV114_RS07825_23930 (Topaz *et al*)	(1390190-1391710) FOR	948	316	669	32%	‡	89%	N/A
2	Hep/Hag repeat protein, partial (This gene is a fragment of hypothetical protein DBY97_RS02575_23930)	NEISUBOT_05623_23930 (Fulton *et al*)	(1392048-1401554) FOR	9507	3169	1674	27%	‡	96%	N/A
3	Hypothetical protein	DBY97_RS02575_23930 (Nichols *et al*)	(1392048-1401554) FOR	9507	3169	3402	41%	‡	95%	N/A
4	Hypothetical protein	DBY81_RS00565 (Nichols *et al*)	No homologues to Hypothetical protein DBY81_RS00565 were found in the genome of *N. subflava* 23930T strain							
5	Hypothetical protein	FAH66_RS06750_23930 (Streich *et al*)	(1390190-1391710) FOR	1521	506	2809	100%	‡	100%	N/A

Table 31 Homology search of *N. subflava* CCUG 23930T putative IgDbp candidates against MID aa962-122: protein CDS.

*** indicates the end of the contig.**

No.	Description	Locus tag	Location in CCUG 23930T genome	No. of base pairs	No. of amino acids	Max score	Query coverage	E value	Identity	Passed homology criteria
1	Hypothetical protein	DBY97_RS02575_23930 (Nichols *et al*)	(1392048-1401554) FOR	9507	3169	56.2	56%	$1e^{-12}$	42%	Yes
2	Hypothetical protein	FAH66_RS06750_23930 (Streich *et al*)	(1390190-1391710) FOR	1521	506	32	30%	$1e^{-05}$	37%	No

4.4.1.8 *Neisseria bacilliformis*

The BLAST search of MID aa962-1200 against *N. bacilliformis* whole species database revealed one homologue; Hypothetical protein (HMPREF9123_2960) (Table 32). This candidate does fulfil the set homology criteria and therefore was considered a true MID aa962-1200 homologue.

Next, a BLAST search was performed on the nucleotide CDS of MID aa962-1200 homologues identified in the *N. bacilliformis* whole species database against *N. bacilliformis* CCUG 50858T nucleotide CDS (Table 33). Results showed that *N. bacilliformis* CCUG 50858T does contain a similar version of HMPREF9123_2960.

Finally, a BLAST search was performed on the protein CDS of MID aa962-1200 against MID aa962-1200 homologues that were present in *N. bacilliformis* CCUG 50858T. This allowed us to find the true percentage identity of MID aa962-1200 homologues present in *N. bacilliformis* CCUG 50858T (Table 34). Results showed an absence of homology between HMPREF9123_2960_50858 and MID aa962-1200. It is hypothesised that *N. bacilliformis* CCUG 50858T lacks a putative IgDbp and dOMVs extracted from *N. bacilliformis* CCUG 50858T will lack the ability to induce proliferation in IgDλ+ B cells.

Table 32 *N. bacilliformis* whole taxid homologues to MID aa962-1200: NCBI.

*** indicates the end of the contig.**

No.	Description	Locus tag	Accession	No. of base pairs	No. of amino acids	Max score	Query coverage	E value	Identity	Passed homology criteria
1	hypothetical protein HMPREF9123_2960, partial	HMPREF9123_2960 (Muzny *et al*) (*1-1108*)	EGF04938.1	1107	369	58.2	20%	$9e^{-11}$	60%	Yes

Table 33 *N. bacilliformis* CCUG 50858T homologues to *N. bacilliformis* whole taxid putative IgDbp candidates. Nucleotide CDS vs nucleotide CDS.

*** indicates the end of the contig. ‡ indicates an E value of ~1e-250.**

No.	Description	Locus tag	Location in CCUG 50858T genome	No. of base pairs	No. of amino acids	Max score	Query coverage	E value	Identity	Passed homology criteria
1	hypothetical protein HMPREF9123_2960, partial	HMPREF9123_2960_50858 (Muzny *et al*)	NODE 918 (*3-944*)	942	314	1903	99%	‡	100%	Yes

Table 34 Homology search of *N. bacilliformis* CCUG 50858T putative IgDbp candidates against MID aa962-1200: protein CDS.

*** indicates the end of the contig.**

No.	Description	Locus tag	Location in CCUG 50858T genome	No. of base pairs	No. of amino acids	Max score	Query coverage	E value	Identity	Passed homology criteria
1	hypothetical protein HMPREF9123_2960, partial	HMPREF9123_2960_ 50858 (Muzny *et al*)	NODE 918 (*3-944*)	942	314	No homology to IgD binding region of MID				

4.4.1.9 *Neisseria polysaccharea*

The BLAST search of MID aa962-1200 against *N. polysaccharea* whole species database revealed eight homologues (Table 35). All hits fulfil the set homology criteria and therefore were considered MID protein aa962-1200 homologues.

Next, a BLAST search was performed on the nucleotide CDS of MID aa962-1200 homologues identified in the *N. polysaccharea* whole species database that passed homology criteria were searched against *N. polysaccharea* CCUG 18031T nucleotide CDS

Table 36). Results showed that *N. polysaccharea* CCUG 18031T genome lacks homology to DBZ13_RS11025, DV116_RS04120 and NPLS3_RS0111260. Furthermore, NPLS3_RS0111140, DV116_RS03990, DBZ13_RS02755 and CX323_RS11530 shares the same locus as NEIPOLOT_RS07545_18031 (NODE 130) in *N. polysaccharea* CCUG 18031T. Therefore *N. polysaccharea* CCUG 18031T contains one MID (aa962-1200) homologue.

Finally, a BLAST search was performed on the protein CDS of MID aa962-1200 against MID aa962-1200 homologues that were present in *N. polysaccharea* CCUG 18031 T. This allowed us to find the true percentage identity of MID aa962-1200 homologues present in *N. polysaccharea* CCUG 18031 T (Table 37). Results showed that MID aa962-1200 shares 51% identity with NEIPOLOT_RS07545_18031. NEIPOLOT_RS07545_18031 passed our set homology criteria and can be considered homologous to MID aa962-1200. It is hypothesised that this homologue might encode a putative IgDbp which would result in inducing proliferation in IgDλ+ B cells.

Table 35 *N. polysaccharea* whole taxid homologues to MID aa962-1200: NCBI.

No.	Description	Locus tag	Accession	No. of base pairs	No. of amino acids	Max score	Query coverage	E value	Identity	Passed homology criteria
1	Peptidase M10	NEIPOLOT_RS07545 (Weinstock *et al*) (181-11316)	WP_003751070.1	11135	3711	79	47%	$2e^{-17}$	51%	Yes
2	Peptidase M10	NPLS3_RS0111140 (Stein *et al*) (23242-34659)	WP_042508591.1	11417	3805	88.6	47%	$1e^{-20}$	55%	Yes
3	Peptidase M10	DV116_RS03990 (Topaz *et al*) (82995-94244)	WP_118997216.1	11249	3749	75.5	47%	$4e^{-16}$	49%	Yes
4	Hypothetical protein	DBZ13_RS11025 (Nichols *et al*) (14296-24111)	WP_107863896.1	9815	3271	55.1	27%	$3e^{-09}$	68%	Yes
5	Hypothetical protein	DBZ13_RS02755 (Nichols *et al*) (158863-171570)	WP_107862818.1	12707	4235	82	34%	$2e^{-18}$	55%	Yes
6	Hypothetical protein	DV116_RS04120 (Topaz *et al*) (116707-126531)	WP_118997229.1	9824	3274	53.1	61%	$1e^{-08}$	31%	Yes
7	Hypothetical protein	NPLS3_RS0111260 (Stein *et al*) (57926-67780)	WP_025458501.1	9854	3284	46.6	27%	$2e^{-06}$	46%	Yes
8	MULTISPECIES: adhesin [*Neisseria*]	CX323_RS11530 (Green *et al*) (1160-2938)	WP_002235721.1	1778	592	47	51%	$1e^{-06}$	32%	Yes

Table 36 *N. polysaccharea* CCUG 18031T homologues to *N. polysaccharea* whole taxid putative IgDbp candidates. Nucleotide CDS vs nucleotide CDS.

‡ indicates an E value of ~1e-250.

No.	Description	Locus tag	Location in CCUG 18031T genome	No. of base pairs	No. of amino acids	Max score	Query coverage	E value	Identity	Passed homology criteria
1	Peptidase M10	NEIPOLOT_RS07545_18031 (Weinstock *et al*)	NODE 130 (149052-160187) REV	11136	3711	20565	100%	‡	100%	Yes
2	Peptidase M10 (This gene is identical to NEIPOLOT_RS07545_18031 and shares the same locus)	NPLS3_RS0111140_18031 (Stein *et al*)	NODE 130 (149052-160187) REV	11136	3711	2992	61%	‡	98%	Yes
3	Peptidase M10 (This gene is identical to NEIPOLOT_RS07545_18031 and shares the same locus)	DV116_RS03990_18031 (Topaz *et al*)	NODE 130 (149052-160187) REV	11136	3711	4987	64%	‡	92%	Yes
4	Hypothetical protein	DBZ13_RS11025_18031 (Nichols *et al*)	No homologues to DBZ13_RS11025_1803 were found in the genome of *N. polysaccharea* 18031T strain							
5	Hypothetical protein (This gene is identical to NEIPOLOT_RS07545_18031 and shares the same locus)	DBZ13_RS02755_18031 (Nichols *et al*)	NODE 130 (149052-160187) REV	11136	3711	1086	27%	‡	94%	Yes
6	Hypothetical protein	DV116_RS04120_18031 (Topaz *et al*)	No homologues to DV116_RS04120_18031 were found in the genome of *N. polysaccharea* 18031T strain							

7	Hypothetical protein	NPLS3_RS0111260_18031 (Stein *et al*)	No homologues to NPLS3_RS0111260_18031 were found in the genome of *N. polysaccharea* 18031T strain							
8	MULTISPECIES: adhesin (This gene is a fragment of NEIPOLOT_RS07545_18031 and shares the same locus)	CX323_RS11530_18031 (Green *et al*)	NODE 130 (149052-149701) REV	11136	3711	1009	36%	‡	95%	Yes

Table 37 Homology search of *N. polysaccharea* CCUG 18031T putative IgDbp candidates against MID aa962-1200: protein CDS.

No.	Description	Locus tag	Location in CCUG 18031T genome	No. of base pairs	No. of amino acids	Max score	Query coverage	E value	Identity	Passed homology criteria
1	Peptidase M10	NEIPOLOT_RS07545_18031 (Weinstock *et al*)	NODE 130 (149052-160187) REV	11136	3711	79	77%	$3e^{-20}$	51%	Yes

4.4.1.10 *Neisseria elongata*

The BLAST search of MID aa962-1200 against *N. elongata* whole species database revealed fourteen hits (Table 38). All hits in the list fulfil the homology criteria except for the last three hits which have E values >0.001 and max scores <40. Furthermore, DBZ15_RS07785 and DBZ11_RS07115 are fragments of DBZ17_RS07175 and share the same locus. Whereas, NCTC10660_01758 is a fragment of DYA92_RS09215 and shares the same locus.

Next, a BLAST search was performed on the nucleotide CDS of MID aa962-1200 homologues identified in the *N. elongata* whole species against *N. elongata* CCUG 2043T nucleotide CDS. Results showed that *N. elongata* CCUG 2043T genome lacks homology to NEIELOOT_01063, NELON_05740, NELON_RS11650, NELON_05745 and NCTC11050_01479 (Table 39). Furthermore, DV445_RS01490_2043, DBZ12_RS09010_2043, DBZ17_RS07175_2043, SAMN05421815_11543 and DYA92_RS09215_2043 are all fragments of DV446_RS08075_2043 and shares the same locus in *N. elongata* CCUG 2043T.

Finally, a BLAST search was performed on the protein CDS of MID aa962-1200 against MID aa962-1200 homologues that were present in *N. elongata* CCUG 2043T. This allowed us to find the true percentage identity of MID aa962-1200 homologues present in *N. elongata* CCUG 2043T (Table 40). Results showed that MID aa962-1200 shares 48% identity with DYA92_RS09215_2043. DYA92_RS09215_2043 passed our set homology criteria and can be considered homologous to MID aa962-1200. It is hypothesised that this homologue might encode a putative IgDbp which would result in inducing proliferation in IgDλ+ B cells.

Table 38 *N. elongata* whole taxid homologues to MID aa962-1200: NCBI.

No.	Description	Locus tag	Accession	No. of base pairs	No. of amino acids	Max score	Query coverage	E value	Identity	Passed homology criteria
1	Hemagglutinin, partial	NEIELOOT_01063 (Weinstock *et al*) (1531218-1535459)	EFE50161.1	4242	1414	60.8	18%	$5e^{-11}$	64	Yes
2	Hypothetical protein	NELON_05740 (Veyrier *et al*) (1104610-1108851)	WP_041961374.1	4241	1413	61.2	17%	$5e^{-11}$	65	Yes
3	Hypothetical protein (This gene is a fragment of Hypothetical protein DBZ17_RS07175 and shares the same locus)	DBZ15_RS07785 (Nichols *et al*) (31888-37635)	WP_107885654.1	5747	1915	57.4	23%	$9e^{-10}$	54	Yes
4	Hypothetical protein (This gene is a fragment of Hypothetical protein DBZ17_RS07175 and shares the same locus	DBZ11_RS07115 (Nichols *et al*) (32262-37916)	WP_107919106.1	5654	1884	56.2	23%	$3e^{-09}$	52	Yes
5	Hypothetical protein	DV445_RS01490 (Topaz *et al*) (282613-289767)	WP_114921484.1	7154	2384	55.8	23%	$3e^{-09}$	52	Yes
6	Hypothetical protein	DBZ12_RS09010 (Nichols *et al*) (43578-49430)	WP_107971514.1	5852	1950	55.8	23%	$3e^{-09}$	52	Yes
7	Hypothetical protein	DBZ17_RS07175 (Nichols *et al*) (31456-38610)	WP_107854335.1	7154	2384	55.8	23%	$3e^{-09}$	52	Yes

8	Coiled stalk of trimeric autotransporter adhesin, partial	SAMN05421815_11543 (Varghese *et al*) (39309-40352)	SFH22707.1	1043	347	51.6	23%	$6e^{-08}$	48	Yes
9	Hypothetical protein	DV446_RS08075 (Topaz *et al*) (1594554-1602851)	WP_114910528.1	8298	2765	52	23%	$6e^{-08}$	48	Yes
10	Hypothetical protein	DYA92_RS09215 (Doyle *et al*) (1560482-1568806)	WP_115275811.1	8324	2774	52	23%	$7e^{-08}$	48	Yes
11	Adhesin (This gene is a fragment of Hypothetical protein DYA92_RS09215 and shares the same locus)	NCTC10660_01758 (Doyle *et al*) (1560482-1564699)	STZ68251.1	4218	1405	52	17%	$7e^{-08}$	56	Yes
12	Hypothetical protein	NELON_RS11650 (Doyle *et al*) (1108667-1110814)	WP_003774309.1	2147	715	32.7	17%	0.095	42	No
13	Hypothetical protein	NELON_05745 (Veyrier *et al*) (1108700-1110814)	AJE18443.1	2114	704	32.7	17%	0.096	42	No
14	Adhesin	NCTC11050_01479 (Doyle *et al*) (1535518-1537422)	SQH50306.1	1904	634	32.7	17%	0.11	42	No

Table 39 *N. elongata* CCUG 2043T homologues to *N. elongata* whole taxid putative IgDbp candidates. Nucleotide CDS vs nucleotide CDS.

*** indicates the end of the contig. ‡ indicates an E value of ~1e-250.**

No.	Description	Locus tag	Location in CCUG 2043T genome	No. of base pairs	No. of amino acids	Max score	Query coverage	E value	Identity	Passed homology criteria
1	Hemagglutinin, partial	NEIELOOT_01063 (Weinstock *et al*)	No homologues to Hemagglutinin NEIELOOT_01063 were found in the genome of *N. elongata* 2043T strain							
2	Hypothetical protein	NELON_05740 (Veyrier *et al*)	No homologues to Hypothetical protein NELON_05740 were found in the genome of *N. elongata* 2043T strain							
3	Hypothetical protein (This gene is a fragment of DV446_RS08075_2043 and shares the same locus)	DV445_RS01490_2043 (Topaz *et al*)	(1594554-1602851) FOR	8298	2765	7496	67%	‡	96%	Yes
4	Hypothetical protein (This gene is a fragment of DV446_RS08075_2043 and shares the same locus)	DBZ12_RS09010_2043 (Nichols *et al*)	(1594554-1602851) FOR	8298	2765	3585	60%	‡	98%	Yes
5	Hypothetical protein (This gene is a fragment of DV446_RS08075_2043 and shares the same locus)	DBZ17_RS07175_2043 (Nichols *et al*)	(1594554-1602851) FOR	8298	2765	7502	67%	‡	96%	Yes
6	Coiled stalk of trimeric autotransporter adhesin, partial (This gene is a fragment of DV446_RS08075_2043 and shares the same locus)	SAMN05421815_11543 (Varghese *et al*)	(1594554-1602851) FOR	8298	2765	1432	74%	‡	100%	Yes
7	Hypothetical protein	DV446_RS08075_2043 (Topaz *et al*)	(1594554-1602851)	8298	2765	8399	60%	‡	100%	Yes

			FOR							
8	Hypothetical protein (This gene is a fragment of DV446_RS08075_2043 and shares the same locus)	DYA92_RS09215_2043 (Doyle *et al*)	(1594554-1602851) FOR	8298	2765	8468	61%	‡	100%	Yes
9	Hypothetical protein	NELON_RS11650 (Doyle *et al*)	No homologues to Hypothetical protein NELON_RS11650 were found in the genome of *N. elongata* 2043T strain							
10	Hypothetical protein	NELON_05745 (Veyrier *et al*)	No homologues to Hypothetical protein NELON_05745 were found in the genome of *N. elongata* 2043T strain							
11	Adhesin	NCTC11050_01479 (Doyle *et al*)	No homologues to Adhesin NCTC11050_01479 were found in the genome of *N. elongata* 2043T strain							

Table 40 Homology search of *N. elongata* CCUG 2043T putative IgDbp candidates against MID aa962-1200: protein CDS.

*** indicates the end of the contig.**

No.	Description	Locus tag	Location in CCUG 2043T genome	No. of base pairs	No. of amino acids	Max score	Query coverage	E value	Identity	Passed homology criteria
1	Hypothetical protein	DYA92_RS09215_2043 (Doyle *et al*)	(1594554-1602851) FOR	8325	2775	52	72%	$3e^{-11}$	48%	Yes

4.4.1.11 *Neisseria meningitidis*

As stated at the beginning of this chapter, where the search against the whole species database retrieved a large number of possible homologues, the search was performed against at least two strains. In the case of *N. meningitidis,* the search was performed against *N. meningitidis* H44/76, *N. meningitidis* MC58 and *N. meningitidis* ATCC 13091.

The BLAST search of MID aa962-1200 against *N. meningitidis* H44/76 revealed one homologue; MULTISPECIES: adhesin (nhhA) (DV147_RS09460) (Table 41). This candidate does fulfil the set homology criteria and therefore was considered a true MID aa962-1200 homologue.

The BLAST search of MID aa962-1200 against *N. meningitidis* MC58 retrieved the same homologue as *N. meningitidis* H44/76; MULTISPECIES: adhesin (nhhA) (DV147_RS09460) (Table 42). This candidate does fulfil the set homology criteria and therefore was considered a true MID aa962-1200 homologue.

The BLAST search of MID aa962-1200 against *N. meningitidis* ATCC 13091 revealed one homologue; adhesin (DV147_RS09460) (Table 43). This candidate does fulfil the set homology criteria and therefore was considered a true MID aa962-1200 homologue.

Next, a BLAST search was performed on the nucleotide CDS of MID aa962-1200 homologues identified in various strains of *N. meningitidis* were searched against *N. meningitidis* H44/76 nucleotide CDS (Table 44). Results showed that a similar version of DV147_RS09460 and HMPREF0602_RS108910 was present in *N. meningitidis* H44/76.

Finally, a BLAST search was performed on the protein CDS of MID aa962-1200 homologues present in *N. meningitidis* H44/76 against MID aa962-1200 in order to find the true percentage identity. Results showed that MID aa962-1200 shares 38% identity with DV147_RS09460_H44/76 (Table 45). DV147_RS09460_H44/76 passed our set homology criteria and can be considered homologous to MID aa962-1200. It is hypothesised that this homologue might encode a putative IgDbp which would result in inducing proliferation in IgDλ+ B cells.

Table 41 *N. meningitidis* H44/76 homologues to MID aa962-1200: NCBI.

No.	Description	Locus tag	Accession	No. of base pairs	No. of amino acids	Max score	Query coverage	E value	Identity	Passed homology criteria
1	MULTISPECIES: adhesin (nhhA)	DV147_RS09460 (Topaz *et al*) (30789-32564)	WP_002222588.1	1776	591	45.8	35%	$8e^{-07}$	38%	Yes

Table 42 *N. meningitidis* MC58 homologues to MID aa962-1200: NCBI.

No.	Description	Locus tag	Accession	No. of base pairs	No. of amino acids	Max score	Query coverage	E value	Identity	Passed homology criteria
1	MULTISPECIES: adhesin (nhhA)	DV147_RS09460 (Topaz *et al*) (30789-32564)	WP_002222588.1	1776	591	45.8	35%	$6e^{-07}$	38%	Yes

Table 43 *N. meningitidis* ATCC 13091 homologues to MID aa962-1200: NCBI.

No.	Description	Locus tag	Accession	No. of base pairs	No. of amino acids	Max score	Query coverage	E value	Identity	Passed homology criteria
1	Adhesin [*Neisseria* meningitidis]	HMPREF0602_RS108910 (Muzny *et al*) (1033262-1035031)	WP_002213712.1	1773	590	48.9	51%	$6e^{-08}$	34%	Yes

Table 44 *N. meningitidis* H44/76 homologues to *N. meningitidis* putative IgDbp candidates. Nucleotide CDS vs nucleotide CDS.

‡ indicates an E value of ~1e-250.

No.	Description	Locus tag	Location in H44/76 genome	No. of base pairs	No. of amino acids	Max score	Query coverage	E value	Identity	Passed homology criteria
1	MULTISPECIES: adhesin [*Neisseria meningitidis* MC58] (This is the same gene as DV147_RS09460 Found in H44/76)	DV147_RS09460 _H44/76 (Topaz *et al*)	(1292481-1294256) FOR	1776	591	3192	100%	‡	100%	Yes
2	Adhesin [*Neisseria meningitidis* ATCC 13091] (This is the same gene as DV147_RS09460 Found in H44/76)	HMPREF0602_R S108910_H44/76 (Muzny *et al*)	(1292481-1294256) FOR	1776	591	3192	100%	‡	100%	Yes
3	MULTISPECIES: adhesin [*Neisseria meningitidis* H44/76]	DV147_RS09460 _H44/76 (Topaz *et al*)	(1292481-1294256) FOR	1776	591	3192	100%	‡	100%	Yes

Table 45 Homology search of *N. meningitidis* H44/76 putative IgDbp candidates against MID aa962-1200: protein CDS.

No.	Description	Locus tag	Location in H44/76 genome	No. of base pairs	No. of amino acids	Max score	Query coverage	E value	Identity	Passed homology criteria
1	MULTISPECIES: adhesin (nhhA)	DV147_RS09460_H44/76 (Topaz *et al*)	(1292481-1294256) FOR	1776	591	45.8	35%	$6e^{-10}$	38%	Yes

4.4.1.12 MID homologues

The data from the comprehensive homology search in chapter 4.4.1.1-10 revealed that several *Neisseria* spp. contains MID homologues. The identified MID homologues and their relevant strains are listed in (Table 46).

Table 46 List of MID homologues identified through comprehensive homology search.

No.	Mid homologue	Strain
1	Unnamed protein product NLY_36660	Y92-1009 *N. lactamica*
2	Hypothetical protein NLY_37260	Y92-1009 *N. lactamica*
3	Hep_Hag family protein NEICINOT_04577_346	CCUG 346T *N. cinerea*
4	Peptidase propeptide and YPEB domain protein NEICINOT_03770_346	CCUG 346T *N. cinerea*
5	Hypothetical protein DYC64_RS10620_17913	CCUG 17913T *N. flavescens*
6	MULTISPECIES: Hypothetical protein NEIFLAOT_01884_17913	CCUG 17913T *N. flavescens*
7	Hypothetical protein DBY97_RS02575_23930	CCUG 23930T *N. subflava*
8	Peptidase M10 NEIPOLOT_RS07545_18031	CCUG 18031T *N. polysaccharea*
9	Hypothetical protein DYA92_RS09215_2043	CCUG 2043T *N. elongata ss elongata*
10	MULTISPECIES: adhesin (nhhA) DV147_RS09460	MC58 *N. meningitidis*

4.4.2 Investigating the proliferation of CD19+IgDλ+ cells in response to dOMVs from various *Neisseria* species

In chapter 3 it was shown that dOMVs from Nlac and Ncin induce a proliferative response in CD19+IgDλ+ B cells compared to CD19+IgDκ+ B cells. Results from chapter 4.4.1.1-2 showed that both Nlac and Ncin contains MID homologues. It was therefore hypothesised that the MID homologues identified in chapter 4.4.1 (Table 46) could be putative IgDbps and the strains containing a MID homologue(s) might induce proliferation of IgDλ+ B cells. To test this hypothesis dOMVs were generated from the chosen *Neisseria* spp., for use in proliferation assays. The quality of the dOMVs was checked by running an SDS-PAGE and the protein profile was analysed (Figure 26).

Results showed the presence of several protein bands in all strains, consistent with the presence of abundant proteins in the vesicles. Some strains had a very similar protein profile with a number of shared bands and a few deviations in bands. The major band at ~38 kDa shared by all strains is likely to be the PorB protein band (Mukhopadhyay *et al.*, 2005; Toussi *et al.*, 2012). Whereas the band at ~40 kDa present in Nmen is likely to be the PorA protein band (Behrouzi *et al.*, 2014).

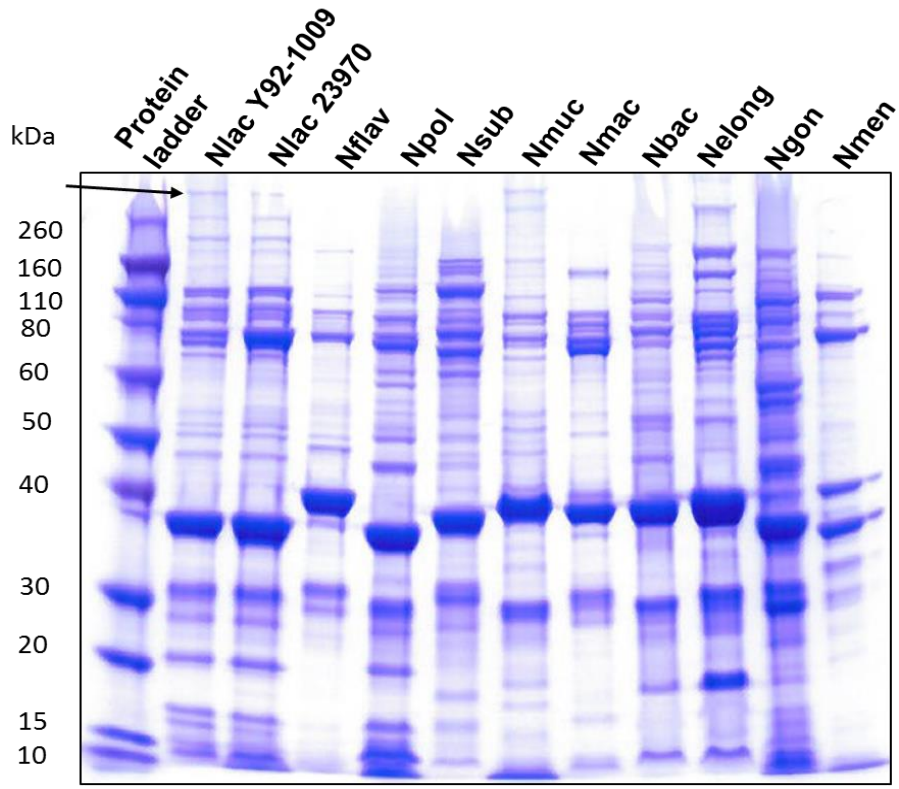

Figure 26 Protein profile of candidate *Neisseria* strains.

SDS-PAGE of dOMVs prepared from *N. lactamica* Y92-1009, *N. lactamica* 23970, *N. flavescens* 17913T, *N. polysaccharea* 18031T, *N. subflava* 23930T, *N. mucosa ss Heidelbergensis* 26878T, *N. macacae* 41451T, *N. bacilliformis* 50858T, *N. elongata ss elongata* 2043T, *N. gonorrhoeae* MS11 and *N. meningitidis* H44/76 strains. 5µg of dOMV was applied to each lane and protein bands were visualised using the Coomassie blue staining. Molecular weight markers are indicated on the left-hand side.

Once dOMV quality had been verified, they were used in B cell proliferation assay. Flow cytometric analysis was performed on CFSE labelled PBMC cultured in the presence of *N. lactamica* Y92-1009*, N. cinerea* 346T*, N. flavescens* 17913T*, N. polysaccharea* 18031T*, N. bacilliformis* 50858T*, N. elongata ss elongata* 2043T*, N. macacae* 41451T*, N. mucosa ss Heidelbergensis* 26878T*, N. subflava* 23930T*, N. gonorrhoeae* MS11 and *N. meningitidis* H44/76 dOMVs for 4 days. Results showed that dOMVs from all strains induced significant proliferation compared to the background in both IgDλ+ or κ+ B cells. However, there was no significant difference between the proliferation induced in IgDλ+ or κ+ B cells. Furthermore, only dOMVs from Nlac, Ncin, Nflav and Npol induced a higher level of proliferation in IgDλ+ B cells compared to IgDκ+ B cells (Figure 27).

In response to Nlac, Ncin, Nflav and Npol dOMVs, the median percentage of proliferating IgDλ+ B cells was significantly higher compared to IgDκ+ B cells. Whereas, the median proliferative response induced by other strains was not biased towards IgDλ+ B cells as there was no significant difference between the percentage of the proliferative population expressing λ or κ light chains (Figure 27).

The results of comprehensive MID homology search in the context of B cell mitogenicity are summarized in (Table 47).

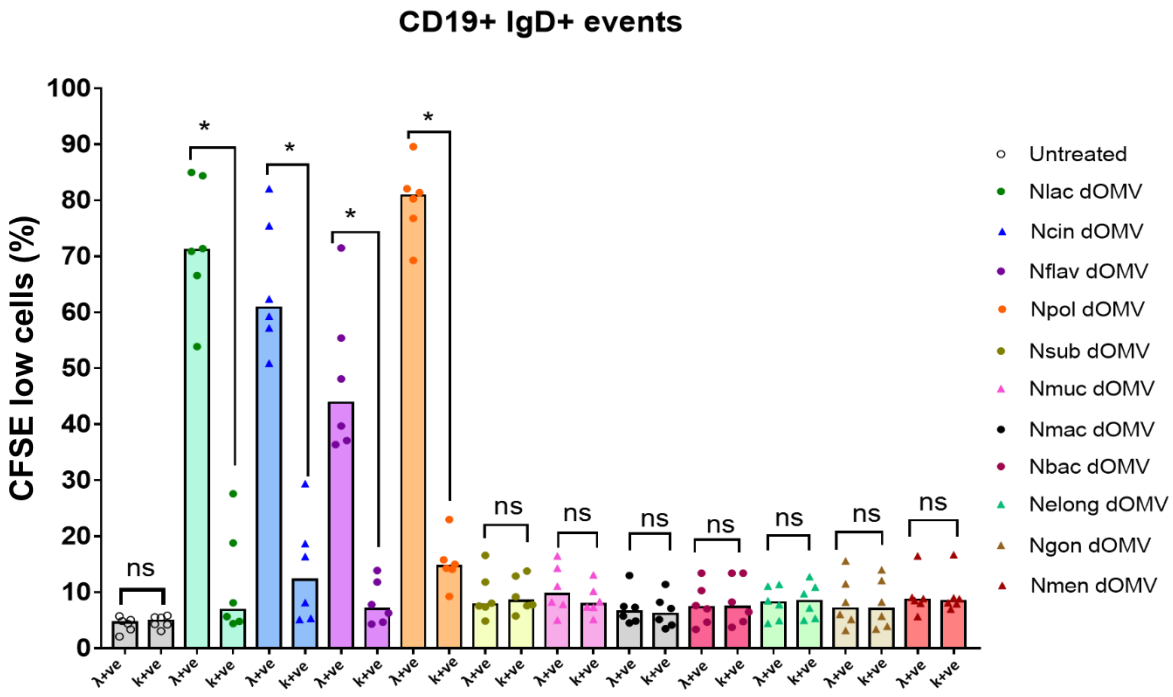

Figure 27 Nlac, Ncin, Nflav and Npol dOMV induces proliferation of IgDλ+ B cells.

Collated data showing percentage of CFSE low CD19+IgD+ cells expressing k or λ light chain in response to 4 day stimulation with *N. lactamica Y92*-1009, *N. cinerea* 346T, *N. flavescens* 17913T, *N. polysaccharea* 18031T, *N. bacilliformis* 50858T, *N. elongata ss elongata* 2043T, *N. macacae* 41451T, *N. mucosa ss Heidelbergensis* 26878T, *N. subflava* 23930T, *N. gonorrhoeae* MS11 and *N. meningitidis* H44/76 dOMVs. Results were acquired on day 4 using a flow cytometer. Proliferating cells were differentiated by a reduction in CFSE intensity compared to CFSE intensity of the non-treated cells. The peak height of the bars represents the median values of 6 repeated experiments on PBMCs from individual donors. Groups were analysed using the Wilcoxon matched-pairs signed rank test. * $P \leq 0.05$, ns $P > 0.05$.

Table 47 Summary of the *Neisseria* spp. survey for the ability to induce B cell proliferation, and its relationship with MID homologue(s)

No.	Strain	Mid homologue(s)	Mitogenic for B cells
1	Y92-1009 *Neisseria. lactamica*	• Unnamed protein product NLY_36660 • Hypothetical protein NLY_37260	Yes
2	CCUG 346T *Neisseria. cinerea*	• Hep_Hag family protein NEICINOT_04577_346 • Peptidase propeptide and YPEB domain protein NEICINOT_03770_346	Yes
3	CCUG 17913T *Neisseria flavescens*	• Hypothetical protein DYC64_RS10620_17913 • MULTISPECIES: Hypothetical protein NEIFLAOT_01884_17913	Yes
4	CCUG 18031T *Neisseria polysaccharea*	• Peptidase M10 NEIPOLOT_RS07545_18031	Yes
5	MC58 *Neisseria. meningitidis*	• MULTISPECIES: adhesin (nhhA) DV147_RS09460	No
6	CCUG 23930T *Neisseria subflava*	• Hypothetical protein DBY97_RS02575_23930	No
7	CCUG 2043T *Neisseria elongata ss elongata*	• Hypothetical protein DYA92_RS09215_2043	No
8	CCUG 26878T *Neisseria mucosa ss Heidelbergensis*	Lacks MID homologue	No
9	CCUG 41451T *Neisseria macacae*	Lacks MID homologue	No
10	CCUG 50858T *Neisseria bacilliformis*	Lacks MID homologue	No
11	*Neisseria gonorrhoeae* MS11	Lacks MID homologue	No

4.4.3 Investigating the proliferation of CD19+IgDλ+ cells pre-treated with anti-IgD, anti-IgM, anti-λ or anti-κ antibodies in response to *N. flavescens* and *N. polysaccharea* dOMVs

In order to confirm that the B cell proliferative response is dependent upon the IgDλ BCR, CFSE labelled PBMC were pre-treated with $F(ab')_2$ polyclonal goat anti-human IgM, IgD, λ or κ Abs to prevent ligand binding. Non-pre-treated and pre-treated PBMCs were cultured in the medium alone or in the presence of Nlac, Ncin, Nflav and Npol dOMVs for 4 days. On day 4 cells were washed and proliferation was measured by flow cytometry.

Results showed that the proliferation of CD19+IgDλ+ cells in response to Nlac dOMV was reduced significantly when treated with anti-IgD Ab, whereas treatment with anti-IgM had no significant impact on the proliferation. Treatment with anti-λ light chain Ab significantly inhibited the proliferation and treatment with anti-κ light chain Ab caused no significant change in proliferation compared to non-anti-Ig treated cells (Figure 28).

Incubation of PBMCs in the presence of Ncin dOMVs showed no significant difference in proliferation of IgDλ+ cells when pre-treated with anti-IgM Ab, but did display a significant difference when treated with anti-IgD Ab. Treatment with anti-λ also resulted in a significant reduction of proliferation in IgDλ+ B cells and this significant reduction was absent from cells treated with anti-κ Ab (Figure 28).

Culturing of PBMCs in the presence of Nflav dOMV displayed a similar trend to Nlac and Ncin as the proliferation was reduced when pre-treated with anti-IgD Ab in comparison to non-pre-treated cells, whereas treatment with anti-IgM had no significant impact on the proliferation. Treatment with anti-λ light chain Ab significantly inhibited proliferation, while treatment with anti-k light chain Ab caused no significant change in proliferation compared to non-anti-immunoglobulin treated (Figure 28).

The fourth mitogen, Npol dOMVs, displayed a similar proliferation profile to Nlac, Ncin and Nflav. There was no significant difference in proliferation when pre-treated with anti-IgM Ab when compared to non-pre-treated, but a significant reduction was observed when treated with anti-IgD Ab. Treatment with anti-λ also resulted in a reduction of proliferation in IgDλ+ B cells. This significant reduction was absent from cells treated with anti-κ Ab (Figure 28).

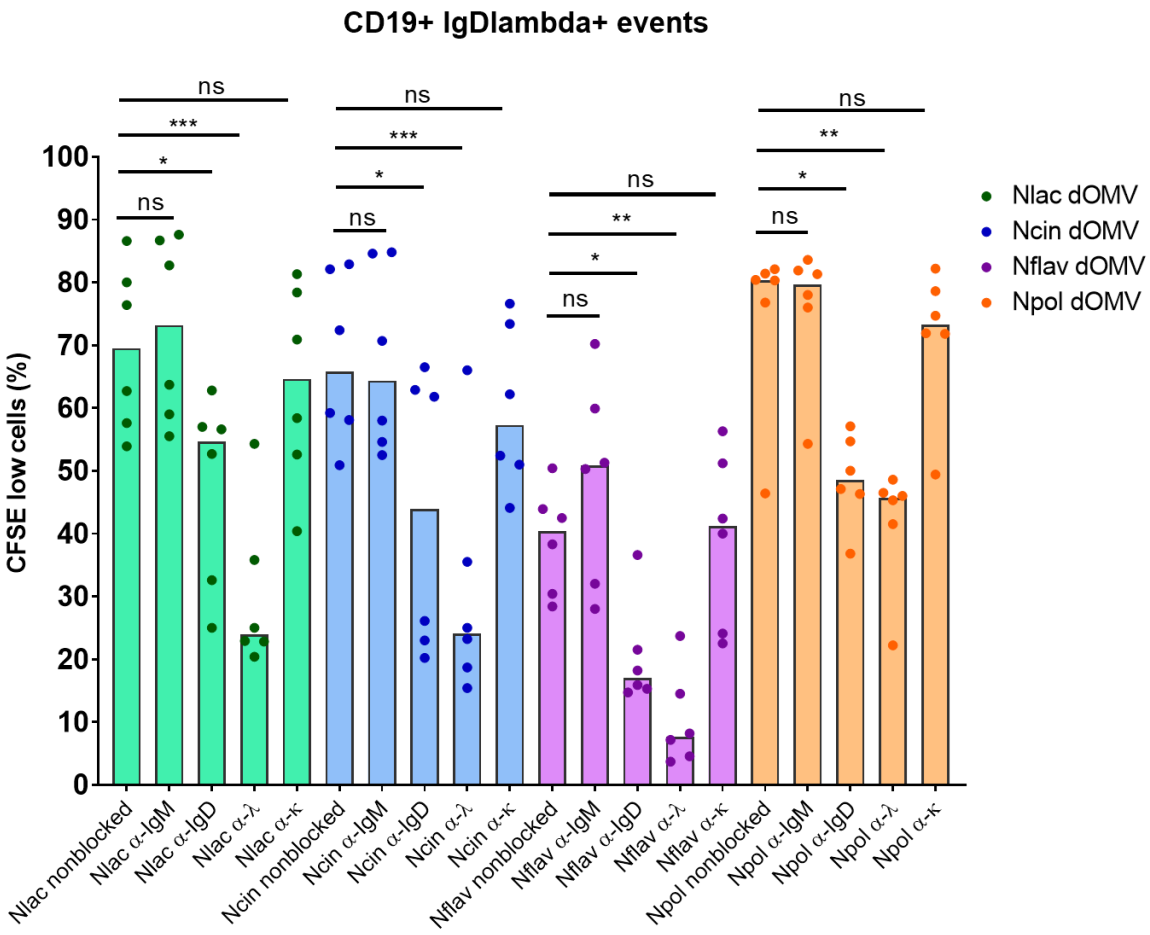

Figure 28 The percentage of proliferating cells in response to Nlac, Ncin, Nflav and Npol dOMV is significantly reduced in IgDλ+ B cells upon blocking λ light chain and IgD cell surface receptors.

Compiled data showing the effect of treating PBMC with F(ab')$_2$ polyclonal goat anti-human IgM, IgD, λ light chain and k light chain Ab on proliferation in the presence or absence of *N. lactamica* Y92-1009, *N. cinerea* 346T, *N flavescens* 17913T and *N polysaccharea* 18031T. Results were acquired on day 4 using a flow cytometer. Proliferating cells were differentiated by a reduction in CFSE intensity compared to CFSE intensity of the non-treated cells. The peak height of the bars represents the median values of 6 repeated experiments on PBMCs from individual donors. Columns were analysed using Friedman test with Dunn's correction for multiple comparisons. * $P \leq 0.05$, ** $P \leq 0.01$, *** $P \leq 0.001$ and ns $P > 0.05$.

4.4.4 Protein domains

Protein domains are distinct conserved parts of protein sequences and their tertiary structures. They are usually responsible for a particular function and contributes to the overall role of a protein. They can exist, function, be stable and fold independently of the rest of the protein. Various TAAs have been well studied in terms of their structure, function and domains (Nummelin *et al.*, 2004; Meng *et al.*, 2006) *etc.* Several known domains are frequent in TAAs (Table 48).

Table 48 Conserved domains found in trimeric autotransporter adhesins

Name	Accession	Description
ESPR	pfam13018	Extended Signal Peptide (ESPR) of the type V secretion system. ESPR aids the inner membrane translocation by acting as a temporary tether thus preventing the accumulation of misfolded protein (Desvaux *et al.*, 2006).
HiaBD2	Pfam15403	HiaBD2 represents the GIN (Glycine Isoleucine Asparagine) motif of the head domain of Trimeric autotransporter adhesin. GIN domains are repetitive in structure but not in sequence (Yeo *et al.*, 2004).
LbR_YadA-like head	Cd12820	Left-handed beta roll_YadA like head domains are the most common head domains. They are repetitive in structure and sequence (Bassler *et al.*, 2015).
TAA-Trp-ring	Pfam15401	The tryptophan-ring motif of the head of Trimeric autotransporter adhesin, named for a highly conserved tryptophan ring found in the C-terminal part of the head domain (Bassler *et al.*, 2015).
YadA_anchor	Pfam03895	YadA-like membrane anchor domain. The membrane anchor domain aids the translocation of the polypeptide chain of the coiled-coil stalk domain through the cell membrane via its beta-barrel lumen. Additionally, it also anchors the whole protein to the bacterial OM (Mikula *et al.*, 2012)
YadA_stalk	Pfam05662	The coiled stalk of trimeric autotransporter adhesins. These domains can be found in repetitive numbers and their length can differ among different species. They act as spacers by moving the head domains away from the bacterial cell surface and toward the extracellular matrix of the host (Mikula *et al.*, 2012).

Using the data available from various crystal structures of TAA fragments such as (Nummelin *et al.*, 2004; Meng *et al.*, 2006) *etc.* has made it possible to identify TAAs from the analysis of sequence data.

Conserved Domain Database (CDD) is a protein annotation resource that consists of a collection of well-annotated multiple sequence alignment models. CDD includes domains curated at NCBI as well as data imported from the external sources. The current CDD version, v3.17 includes a total of 57,242 protein and protein-domain models (Lu *et al.*, 2019).

Using the NCBI's CD-search interface accessible at https://www.ncbi.nlm.nih.gov/Structure/cdd/wrpsb.cgi website, the sequence motifs of specific TAA domains were compared against the protein sequences of MID aa962-1200 homologues found in human colonizing *Neisseria* spp. The results for the presence or absence of TAA conserved domains are summarised in (Table 49) (For raw data, see Appendix A).

Table 49 Conserved domains located in MID homologues found in human colonising *Neisseria* spp.

No.	Description	Conserved domains found in trimeric autotransporter adhesins					
		ESPR (pfam13018)	**HiaBD2** (pfam15403)	**LbR_YadA-like head** (cd12820)	**TAA-Trp-ring** (pfam15401)	**YadA_stalk** (pfam05662)	**YadA_anchor** (pfam03895)
1	Unnamed protein product NLY_36660 (*N. lactamica*)	+	-	+	-	+	+
2	Hypothetical protein NLY_37260 (*N. lactamica*)	+	+	+	+	+	+
3	Hep_Hag family protein NEICINOT_04577_346 (*N. cinerea*)	+	-	+	-	+	+

4	Peptidase propeptide and YPEB domain protein NEICINOT_03770_346 (*N. cinerea*)	+	-	+	+	+	+
5	Hypothetical protein DYC64_RS10620_17913 (*N. flavescens*)	+	-	+	+	+	+
6	MULTISPECIES: Hypothetical protein NEIFLAOT_01884_17913 (*N. flavescens*)	+	+	-	+	+	+
7	Hypothetical protein DBY97_RS02575_23930 (*N. subflava*)	+	-	+	-	+	+
8	Peptidase M10 NEIPOLOT_RS07545_18031 (*N. polysaccharea*)	+	-	+	-	+	+
9	Hypothetical protein DYA92_RS09215_2043 (*N. elongata*)	-	-	+	-	+	+
10	MULTISPECIES: adhesin (nhhA) DV147_RS09460 (*N. meningitidis*)	+	-	+	+	+	+

4.4.5 Investigating expression levels of the putative IgDbp gene

I have shown that some of the *Neisseria* strains lack the ability to induce proliferation in IgDλ+ B cells despite the presence of a putative IgDbp gene (Table 51). This difference in function might be due to the lack of or reduced level of IgDbp gene expression. Therefore, strains containing the MID homologue CDS that lacked the ability to induce proliferation in IgDλ+ B cells were investigated.

Gene expression is the process by which information from a gene is used to synthesise a functional gene product, such as proteins or functional RNA. Gene expression is tightly regulated, and the level of expression of a specific gene can increase or decrease depending upon the extracellular milieu (Wang *et al.*, 2016).

Ideally, the measurement of expression is done by detecting the final gene product i.e. protein using methods such as Western Blotting. However, these methods often require detection antibodies specific for the protein of interest. In the absence of specific antibody, it is often easier to detect mRNA and to infer gene-expression levels from these measurements. Therefore, in order to investigate whether MID homologous genes are transcribed, and to compare the levels of gene expression between *Neisseria* spp., a Semi-quantitative Reverse Transcription Polymerase Chain Reaction (SQRT-PCR) was used. The SQRT-PCR approach used here was modified from that used in similar studies (Rio, 2014; Antiabong, Ngoepe and Abechi, 2016). SQRT-PCR technique involved combining reverse transcription of RNA into complementary DNA (cDNA) and the amplification of specific DNA targets using the polymerase chain reaction (PCR). The amplified samples were run on an agarose gel and the intensity of DNA bands was measured using Image Lab.

EtBr works by intercalating itself in the DNA molecule in a concentration-dependent manner, which when exposed to UV light exhibits fluorescence. This allows for an estimation of the amount of DNA in any particular DNA band based on its intensity (Lee *et al.*, 2012).

In order to standardize the design of the assay and avoid inconsistent results, the data were normalized to housekeeping genes (HKGs). According to a 2009 guideline called “Minimum Information for Publication of Quantitative Real-Time PCR” the use of a single, unvalidated reference gene for normalization is not acceptable, as normalization with a single HKG can falsely bias the results (Kozera and Rapacz, 2013). Therefore, two validated HKGs with stable expression from a list of invariable genes presented by Rocha et al were used (Rocha, Santos and Pacheco, 2015). SecA and gyrB were chosen as an internal standard to normalize the expression levels of the target gene of interest as the

nucleotide sequence for these two genes are present in the genome of all the candidate strains of interest.

UV transilluminator emits high levels of UV radiation on the gel and in the presence of UV light, the dye bound to the DNA exhibits fluorescence. Since this experiment relies on the accurate measurement of the target band intensity, it was important to obtain equivalent signals when running identical samples on different gels or different wells of the same gel. Due to the nonuniformity of UV transilluminators and variation between gels (Chakravarti *et al.*, 2008), the signal was investigated by running the same samples across entire gel lanes and also on different gels.

A region of SecA (HKG) was amplified using the gDNA at 40 cycles in order to obtain a large quantity of PCR product. The PCR product was then applied to 6 lanes on 4 different gels in order to compare the band intensity across gels. The samples were also run in triplicates on the different areas of the same gel in order to investigate the difference between intensity across different lanes of the same gel. The gels were imaged with a Gel Doc imager and the acquired gel images were analysed by Image Lab volume tools. A rectangle was drawn just large enough to include the largest band and the same rectangle was then copied and pasted over other DNA bands. The intensity of each DNA band (calculated as the volume in Image Lab) was measured and recorded as optical intensity units (OU). This allowed estimation of the level of expression based on the intensity of the target DNA bands.

Results showed that for the same PCR product there was no significant difference between the median intensity of bands in area 1, area 2, area 3 and area 4 (Figure 29). Whereas the comparison of the same PCR product across different gels showed significant differences between the median intensities of bands (Figure 30). The median intensity of bands on gel 1 was significantly different compared to gel 2 and gel 4. Furthermore, the median intensity of bands on gel 2 was significantly different compared to gel 3, and the median intensity of bands of gel 3 was significantly different from bands on gel 4. However, there was no significant difference between the median intensity of bands on gel 1 compared to bands on gel 3, and gel 2 compared to gel 4 (Figure 30).

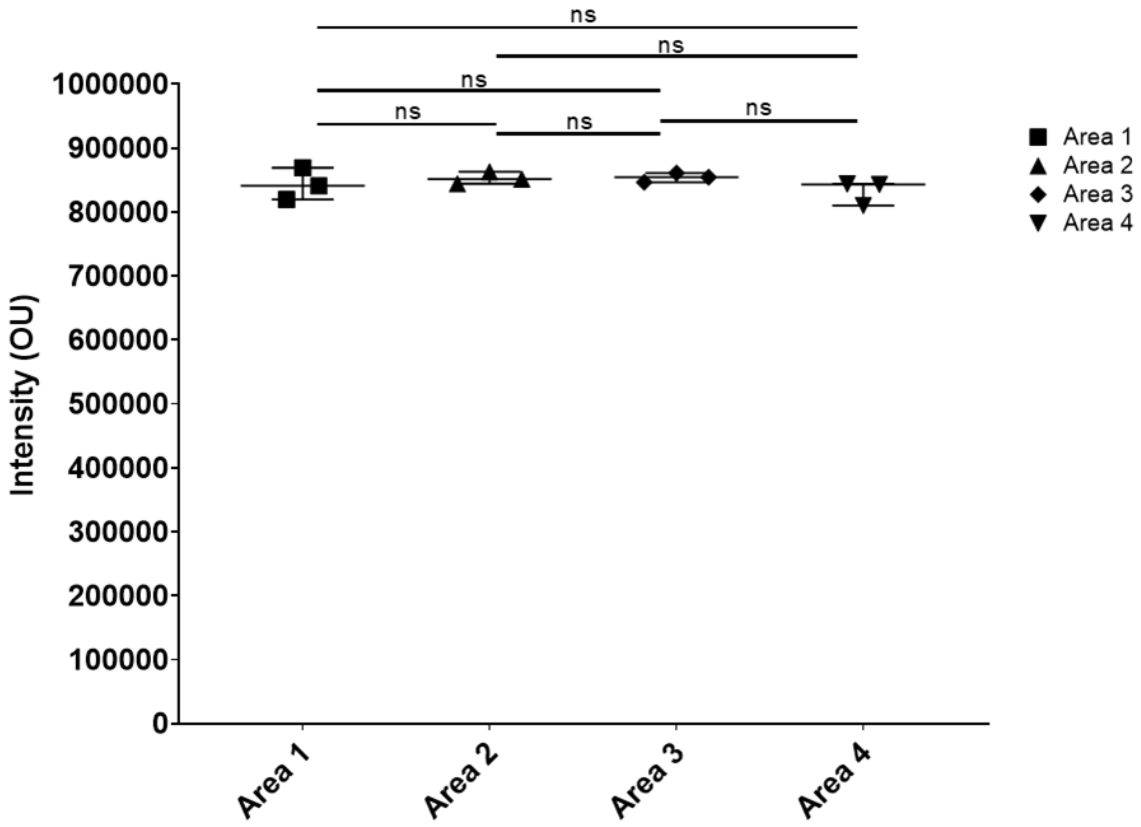

Figure 29 Band intensity of the same PCR product does not differ significantly across different lanes of the same gel.

Collated data showing the band intensity of the same PCR product across different areas of the same gel. Same PCR product was pipetted in triplicates in different areas across the same gel and the band intensity of the PCR product was analysed. Peak height of horizontal bars represents the median band intensity of the PCR product. Groups were analysed using Friedman test with Dunn's correction for multiple comparisons. * $P \leq 0.05$, ** $P \leq 0.01$, *** $P \leq 0.001$ and ns $P > 0.05$.

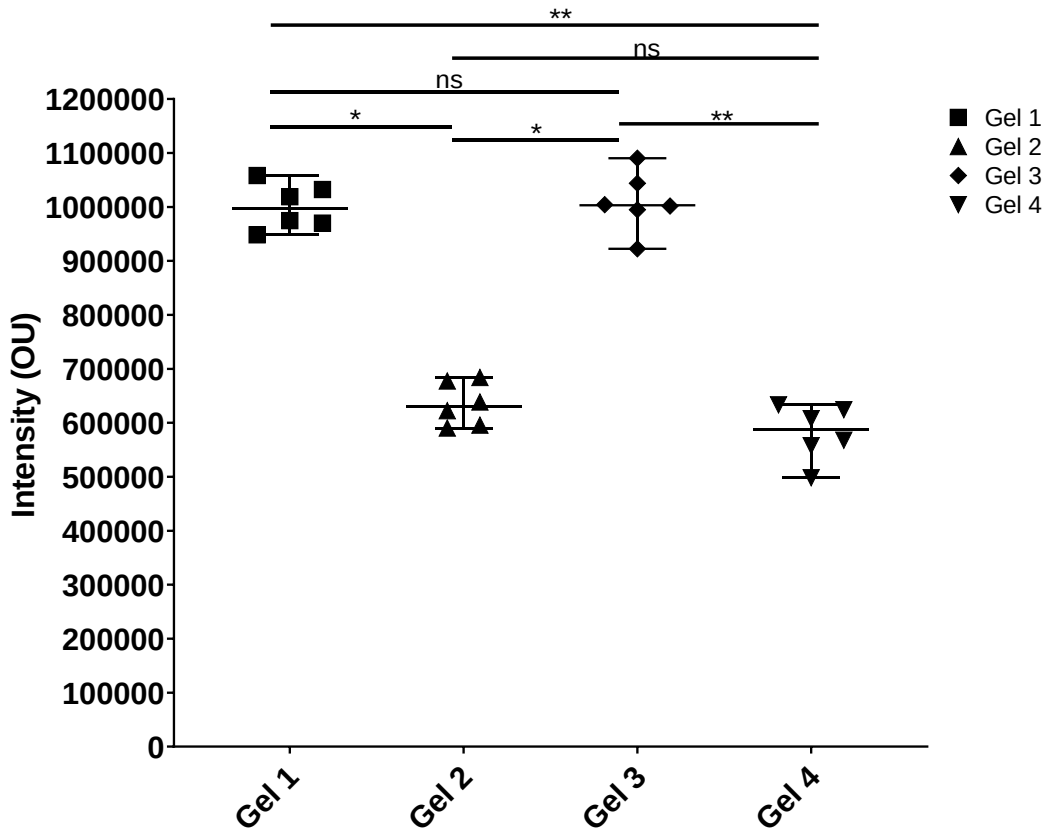

Figure 30 The intensity of the same PCR product varies significantly when analysed on different gels.

Collated data showing the band intensity of the same PCR product across different gels. Same PCR product was pipetted in 6 successive lanes on four different gels and the band intensity of the PCR product was analysed. Peak height of horizontal bars represents the median band intensity of the PCR product. Groups were analysed using Friedman test with Dunn's correction for multiple comparisons. * $P \leq 0.05$, ** $P \leq 0.01$, *** $P \leq 0.001$ and ns $P > 0.05$.

The results demonstrate that the band intensity of the same sample does not differ significantly across different lanes of a gel (Figure 29). However, the intensity of the same sample varies significantly when analysed on different gels (Figure 30). Since there is nonuniformity between different gels it was decided to run samples on the same gel when making a direct comparison.

Another factor that affects the intensity of the target band is UV exposure time. With a low exposure time, the DNA bands would be faint, whereas high exposure time would result in pixel saturation and high background signal. It is important to obtain the highest signal to noise ratio as possible for the accurate estimation of the intensity of DNA bands. In order to find the best exposure time for the highest signal to noise ratio gels were exposed to various UV exposure times while imaging the gel in the transilluminator.

RNA and reverse transcribed cDNA from the RNA of all 6 strains were used as a template and the SecA region was amplified by PCR at 30, 35 and 40 PCR cycles. The amplified product was run on a 1% agarose gel and the gel was imaged at 0.2, 0.4, 0.6, and 0.8 seconds UV exposure time. Finally, the intensity of the bands was calculated using Image lab software. Signal-to-Noise Ratios (SNR) were calculated for all samples by dividing the intensity of each cDNA amplified product with the RNA amplified product for all exposure times.

Results showed that 0.8 seconds exposure to UV light during gel imaging gave the best SNR for most samples. Furthermore, the highest SNR at 0.8 sec exposure time was consistent with 30, 35 and 40 PCR cycles (Figure 31).

After a certain number of cycles when any of reagents become limited the PCR amplification reaches a plateau (Kainz, 2000). At this plateau, the differences between test samples may be obscured. For example, at a plateau, the RNAs initially present at high levels may give products of equal intensity to low abundant RNAs. This makes it difficult to accurately quantify the initial DNA concentrations in different test samples in an endpoint PCR (Antiabong, Ngoepe and Abechi, 2016). In order to compensate for this effect, the number of PCR cycles was optimized. The HKGs were amplified at various numbers of PCR cycles using the cDNA from the samples as a template. This allowed the identification of the minimum number of cycles required for sufficient amplified PCR product to be visible upon imaging the agarose gel. This also permitted identification of the number of PCR cycles at which the amplified product saturates DNA bands. Based on the optimization data it was decided to run all samples at 30, 35 and 40 cycles as this would permit intensity reading at different stages of amplification. However, for simplicity, only the results from 35 cycles are shown for these experiments as this gave the best SNR.

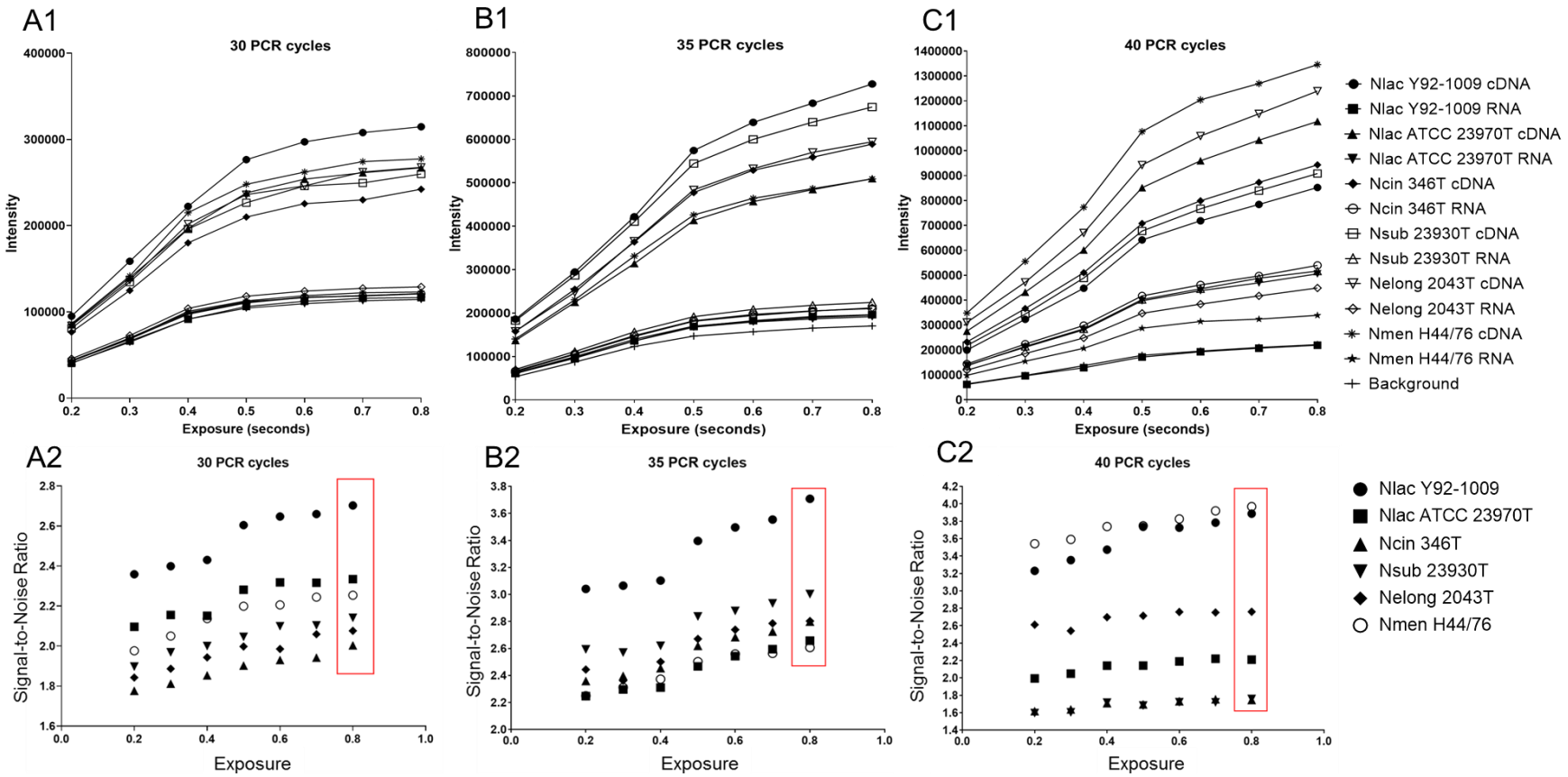

Figure 31 UV exposure time can affect Signal-to-Noise Ratio of DNA band intensity.

RNA and reverse transcribed cDNA from the RNA of all 6 strains were used as template and SecA region was amplified by PCR at (A1) 30 PCR cycles, (B1) 35 PCR cycles and (C1) 40 PCR cycles. The amplified products were run on a 1% agarose gel and the gel was imaged at 0.2, 0.4, 0.6, and 0.8 seconds UV exposure time. The band intensities were analysed and SNRs were calculated for all samples by dividing the intensity of each cDNA amplified product with the RNA amplified product for all exposure times. Graphs showing the SNRs for various samples at 0.2, 0.4, 0.6 and 0.8 seconds of UV exposure time at (B1) 30 PCR cycles, (B2) 35 PCR cycles and (B3) 40 PCR cycles.

A total of 6 strains *N. lactamica* Y92-1009, *N. lactamica* ATCC 23970, *N. cinerea* 346T, *N. subflava* 23930T, *N. elongata* 2043T and *N. meningitidis* H44/76 were chosen to be tested for the expression of MID homologues. *N. cinerea* and both *N. lactamica* strains induce proliferation in IgDλ+ B cells, albeit at different levels. Whereas *N. subflava*, *N. elongata* and *N. meningitidis* does not induce proliferation in IgDλ+ B cells despite the presence of a MID homologue. SecA and gyrB were chosen as internal standards to normalize the expression levels of the target gene of interest.

RNA was extracted from all 6 strains and reverse transcribed to cDNA. Regions of SecA, gyrB and 2 regions from each MID homologue were amplified at 30, 35 and 40 PCR cycles using the cDNA as template (Table 50). The intensity corresponding to the gene of interest was divided by the intensity corresponding to the HKGs to obtain a ratio of the target gene to HKGs. Since expression levels for all gene of interests were normalized to mean expression levels of secA and gyrB genes, a comparison can be made between the estimated expression levels of MID homologous present in all 6 *Neisseria* strains.

Table 50 Semi-quantitative Reverse Transcription Polymerase Chain Reaction overview

Strain	Gene	Regions tested using gDNA, cDNA and RNA as template
N. lactamica Y92-1009	secA	~450 bp region from the middle of the ORF
	gyrB	~450 bp region from the middle of the ORF
	NLY_37260	~450 bp region near 5' end of the ORF
		~450 bp region near 3' end of the ORF
	NLY_36660	~450 bp region near 5' end of the ORF
		~450 bp region near 3' end of the ORF
N. lactamica ATCC 23970	secA	~450 bp region from the middle of the ORF
	gyrB	~450 bp region from the middle of the ORF
	NLY_37260	~450 bp region near 5' end of the ORF
		~450 bp region near 3' end of the ORF
	NLY_36660	~450 bp region near 5' end of the ORF
		~450 bp region near 3' end of the ORF
N. cinerea 346T	secA	~450 bp region from the middle of the ORF
	gyrB	~450 bp region from the middle of the ORF
	NEICINOT_03770	~450 bp region near 5' end of the ORF
		~450 bp region near 3' end of the ORF
	NEICINOT_04577	~450 bp region near 5' end of the ORF
		~450 bp region near 3' end of the ORF
N. subflava 23930T	secA	~450 bp region from the middle of the ORF
	gyrB	~450 bp region from the middle of the ORF
	DBY97_RS02575_ 23930	~450 bp region near 5' end of the ORF
		~450 bp region near 3' end of the ORF
N. elongata 2043T	secA	~450 bp region from the middle of the ORF
	gyrB	~450 bp region from the middle of the ORF
	DYA92_RS09215_ 2043	~450 bp region near 5' end of the ORF
		~450 bp region near 3' end of the ORF
N. meningitidis H44/76	secA	~450 bp region from the middle of the ORF
	gyrB	~450 bp region from the middle of the ORF
	DV147_RS09460 (nhhA)	~450 bp region near 5' end of the ORF
		~450 bp region near 3' end of the ORF

Results showed that the NLY_37260 gene displayed a higher band intensity when reverse-transcribed cDNA from *N. lactamica* Y92-1009 was used as the template for PCR amplification compared to the RNA (-ve control). The NLY_36660 gene also displayed a higher band intensity for the cDNA template compared to the RNA template. Furthermore, the median band intensity of NLY_37270 was significantly higher than the median intensity of NLY_36660 (Figure 32).

Results for *N. lactamica* ATCC 23970 showed a similar trend for the intensity of PCR products. The NLY_37260 gene displayed a higher intensity for the PCR product amplified from the cDNA template compared to the RNA template. The NLY_36660 gene also displayed a higher intensity for the cDNA template compared to the RNA template. Furthermore, the median intensity of NLY_37270 was significantly higher than the median intensity of NLY_36660 (Figure 33).

Analyses of the samples from the *N. cinerea* 346T strain showed that the NEICINOT_03770 gene displayed a higher intensity for PCR product amplified from cDNA template compared to the RNA template. The NEICINOT_04577 gene also displayed a higher intensity for product amplified from cDNA template compared to the RNA template. However, there was no significant difference between the median intensity of NEICINOT_03770 and NEICINOT_04577 PCR products amplified from cDNA (Figure 34).

As for the samples from the *N. subflava* 23930T strain, the results showed that the BY97_RS02575_23930 gene displayed a higher intensity for the PCR product amplified from the cDNA template compared to the PCR product amplified from the RNA template (Figure 35).

Samples from the *N. elongata* 2043T strain also displayed a higher intensity for the PCR product amplified from the cDNA template compared to the PCR product amplified from the RNA template (Figure 36).

Finally, the samples from *N. meningitidis* also displayed a higher intensity for the PCR product amplified from the cDNA template compared to the PCR product amplified from the RNA template (Figure 37).

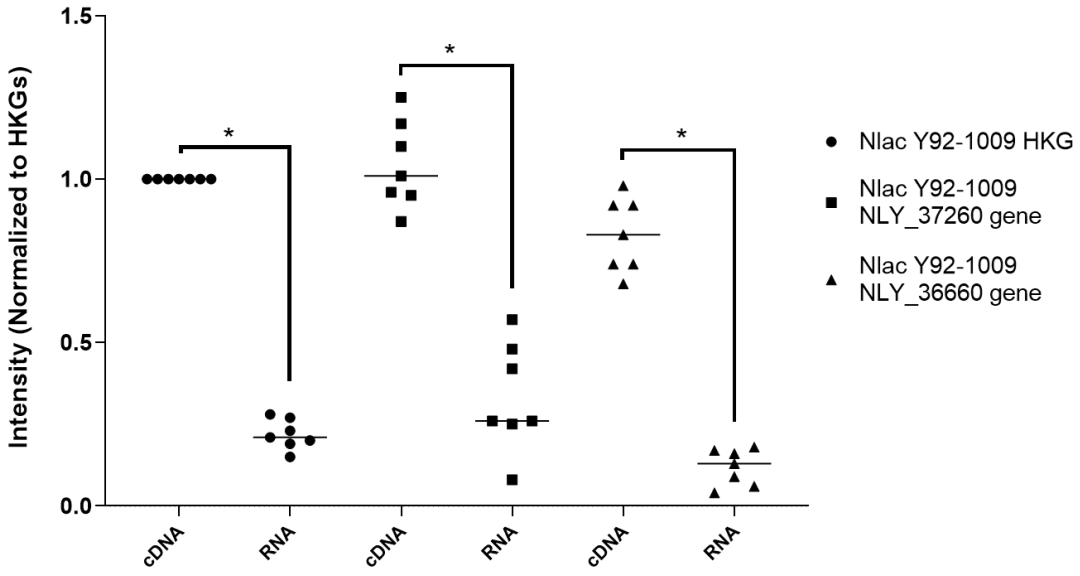

Figure 32 NLY_37260 and NLY_36660 genes are transcribed in *N. lactamica* Y92-1009.

Collated data showing the estimated median expression levels of HKGs and MID homologue NLY_37260 and NLY_36660 genes present in *N. lactamica Y92-1009.* RNA was extracted and reverse transcribed into cDNA. The extracted cDNA was used as template to amplify a region of both HKGs (secA and gryB), and 2 regions in each MID homologue by PCR at 35 cycles. The amplified product was run on a 1% agarose gel, the gel was imaged by a gel Doc system and the band intensities were analysed. The mean band intensity of the 2 regions of each MID homologue was normalized to the mean intensity of the 2 HKGs. Horizontal bars represent the median intensity (normalized to HKGs) of 7 repeated experiments. Groups were analysed using the Wilcoxon matched-pairs signed rank test. * $P \leq 0.05$, ns $P > 0.05$.

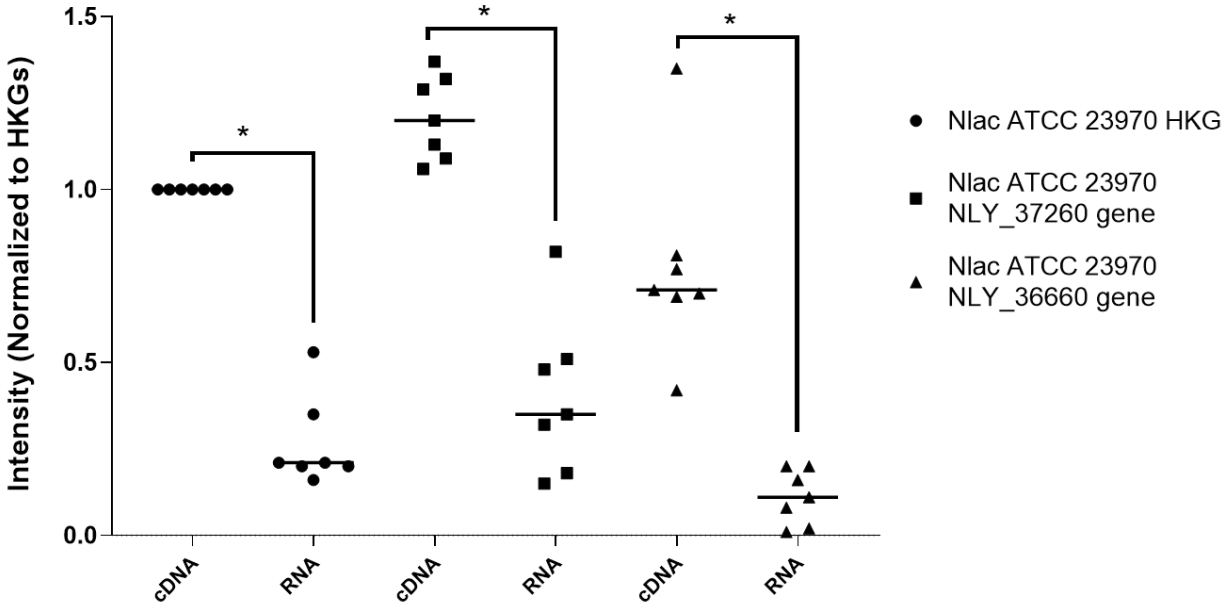

Figure 33 NLY_37260 and NLY_36660 genes are transcribed in *N. lactamica* ATCC 23970.

Collated data showing the estimated median expression levels of HKGs and MID homologues NLY_37260 and NLY_36660 genes present in *N. lactamica* ATCC 23970. RNA was extracted and reverse transcribed into cDNA. The extracted cDNA was used as template to amplify a region of both HKGs (secA and gryB), and 2 regions in each MID homologue by PCR at 35 cycles. The amplified product was run on a 1% agarose gel, the gel was imaged by a gel Doc system and the band intensities were analysed. The mean band intensity of the 2 regions of each MID homologue was normalized to the mean intensity of the 2 HKGs. Horizontal bars represent the median intensity (normalized to HKGs) of 7 repeated experiments. Groups were analysed using the Wilcoxon matched-pairs signed rank test. * $P \leq 0.05$ and ns $P > 0.05$.

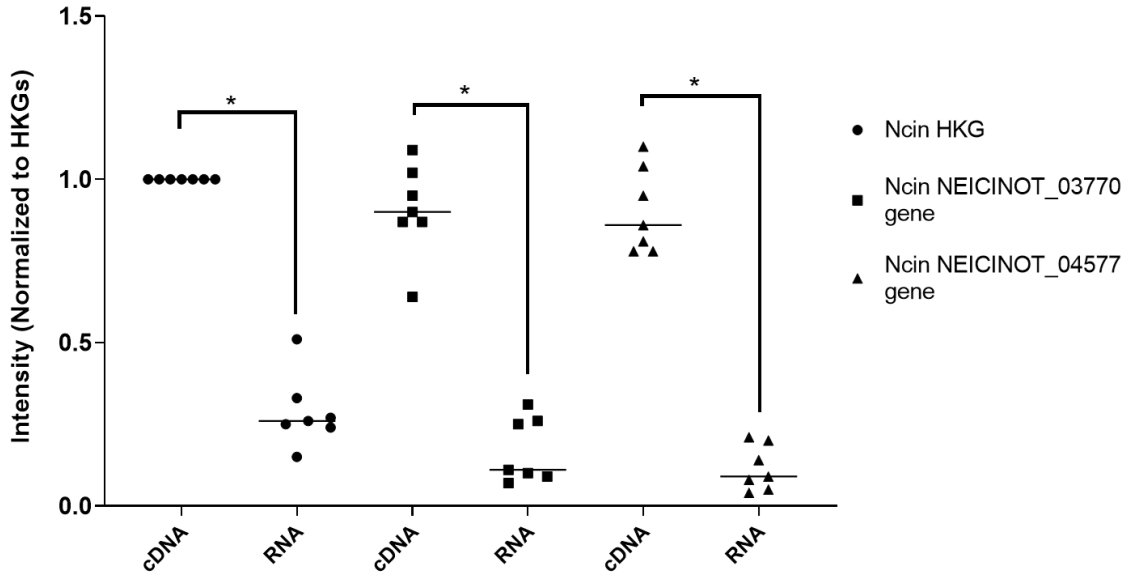

Figure 34 NEICINOT_03770 and NEICINOT_04577 genes are transcribed in *N. cinerea* 346T.

Collated data showing the estimated median expression levels of HKGs and MID homologues NEICINOT_03770 and NEICINOT_04577 genes present in *N. cinerea.* RNA was extracted and reverse transcribed into cDNA. The extracted cDNA was used as template to amplify a region of both HKGs (secA and gryB), and 2 regions in each MID homologue by PCR at 35 cycles. The amplified product was run on a 1% agarose gel, the gel was imaged by a gel Doc system and the band intensities were analysed. The mean band intensity of the 2 regions of each MID homologue was normalized to the mean intensity of the 2 HKGs. Horizontal bars represent the median intensity (normalized to HKGs) of 7 repeated experiments. Groups were analysed using the Wilcoxon matched-pairs signed rank test. * $P \leq 0.05$ and ns $P > 0.05$.

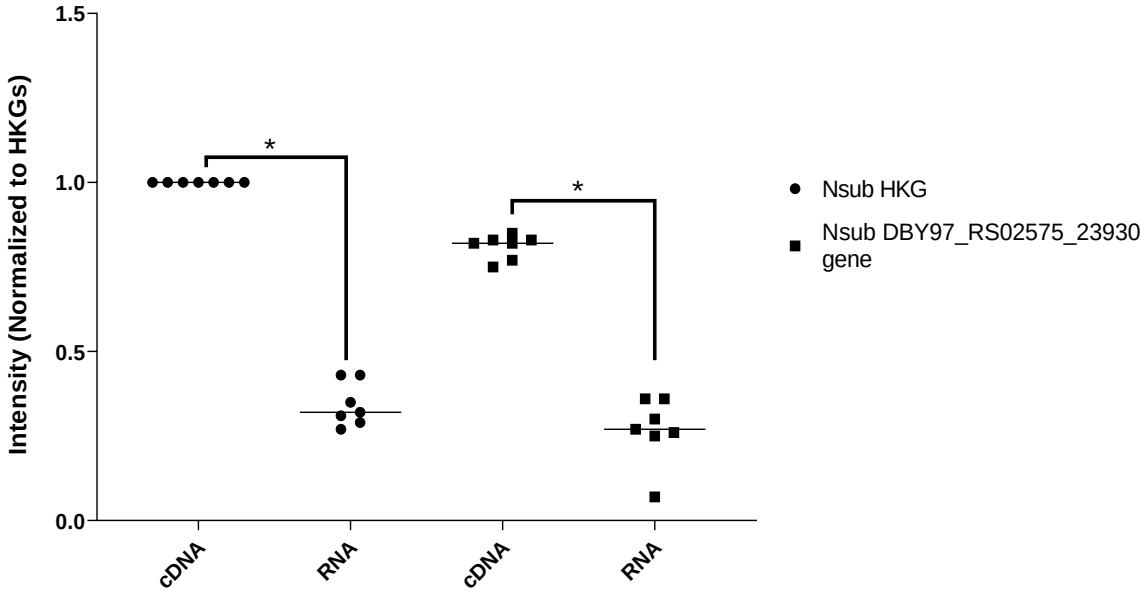

Figure 35 DBY97_RS02575_23930 gene is transcribed in *N. subflava* 23930T.

Collated data showing the estimated median expression levels of HKGs and MID homologue DBY97_RS02575_23930 genes present in *N. subflava.* RNA was extracted and reverse transcribed into cDNA. The extracted cDNA was used as template to amplify a region of both HKGs (secA and gryB), and 2 regions in the MID homologue by PCR at 35 cycles. The amplified product was run on a 1% agarose gel, the gel was imaged by a gel Doc system and the band intensities were analysed. The mean band intensity of the 2 regions of the MID homologue was normalized to the mean intensity of the 2 HKGs. Horizontal bars represent the median intensity (normalized to HKGs) of 7 repeated experiments. Groups were analysed using the Wilcoxon matched-pairs signed rank test. * $P \leq 0.05$ and ns $P > 0.05$.

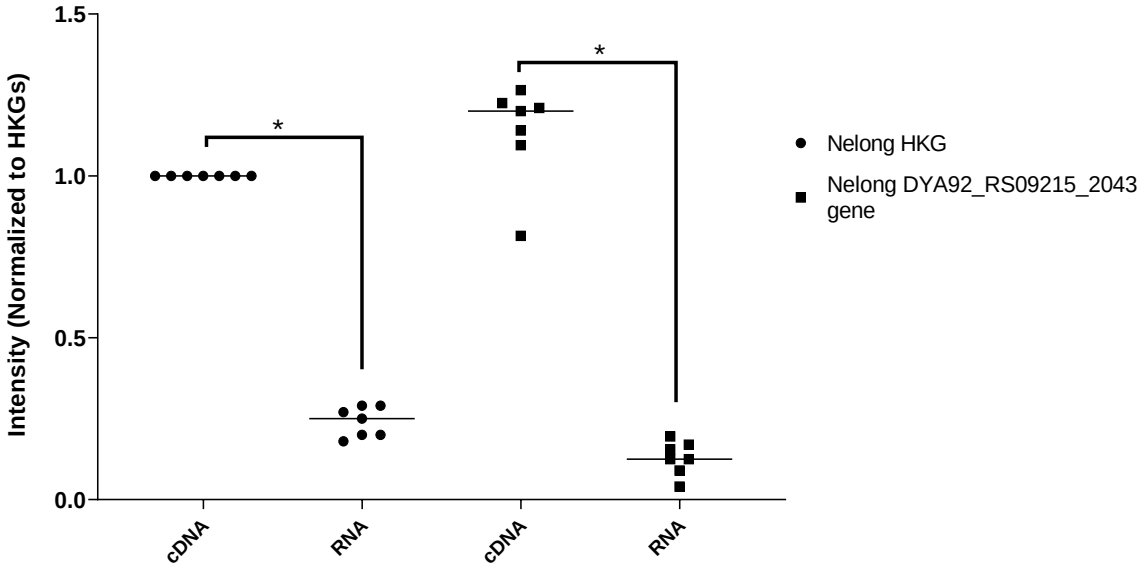

Figure 36 DYA92_RS09215_2043 gene is transcribed in *N. elongata* 2043T.

Collated data showing the estimated median expression levels of HKGs and MID homologue DYA92_RS09215_2043 genes present in *N. elongata*. RNA was extracted and reverse transcribed into cDNA. The extracted cDNA was used as template to amplify a region of both HKGs (secA and gryB), and 2 regions in the MID homologue by PCR at 35 cycles. The amplified product was run on a 1% agarose gel, the gel was imaged by a gel Doc system and the band intensities were analysed. The mean band intensity of the 2 regions of the MID homologue was normalized to the mean intensity of the 2 HKGs. Horizontal bars represent the median intensity (normalized to HKGs) of 7 repeated experiments. Groups were analysed using the Wilcoxon matched-pairs signed rank test. * $P \leq 0.05$ and ns $P > 0.05$.

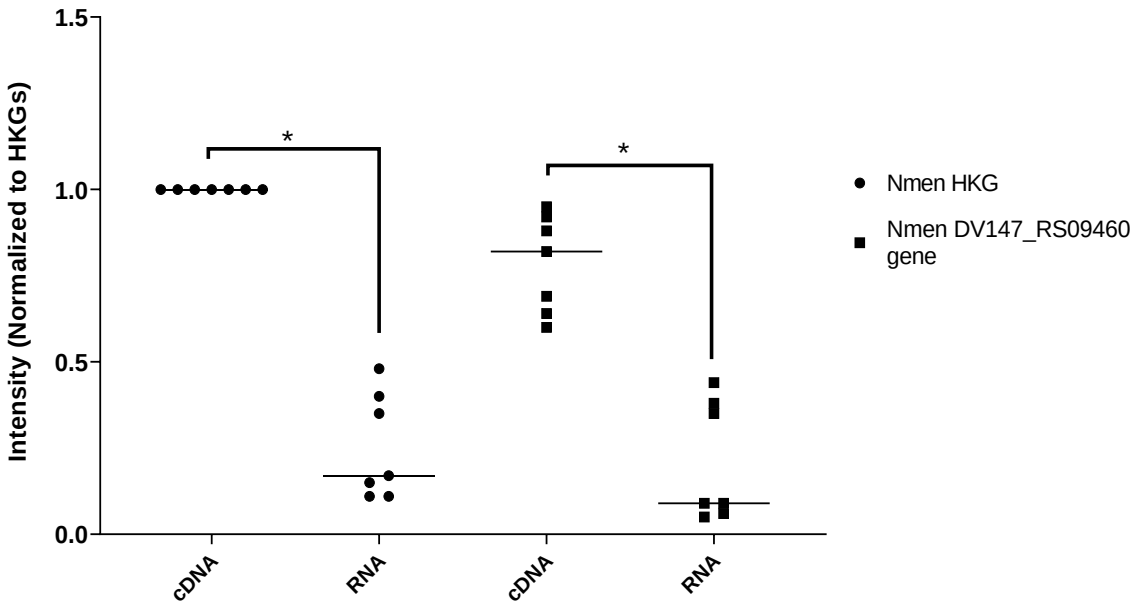

Figure 37 DV147_RS09460 (nhhA) gene is transcribed in *N. meningitidis* H44/76.

Collated data showing the estimated median expression levels of HKGs and MID homologue DV147_RS09460 (nhhA) genes present in *N. meningitidis*. RNA was extracted and reverse transcribed into cDNA. The extracted cDNA was used as template to amplify a region of both HKGs (secA and gryB), and 2 regions in the MID homologue by PCR at 35 cycles. The amplified product was run on a 1% agarose gel, the gel was imaged by a gel Doc system and the band intensities were analysed. The mean band intensity of the 2 regions of the MID homologue was normalized to the mean intensity of the 2 HKGs. Horizontal bars represent the median intensity (normalized to HKGs) of 7 repeated experiments. Groups were analysed using the Wilcoxon matched-pairs signed rank test. * $P \leq 0.05$ and ns $P > 0.05$.

4.4.6 Comparing the gene expression levels of MID homologues in various *Neisseria* spp.

Results above showed that all MID homologues were transcribed in all *Neisseria* spp. tested. However, despite the transcription of MID homologues, *N. subflava*, *N. elongata* and *N. meningitidis*, lacked the ability to induce proliferation in IgDλ+ B cells (see section 4.4.12). It was hypothesised that this could be due to lower levels of expression in these spp.

Therefore, it was decided to compare the gene expression levels of MID homologues of *N. lactamica* ATCC 23970, *N. cinerea* 346T, *N. subflava* 23930T, *N. elongata* 2043T and *N. meningitidis* H44/76 against the MID homologues found in *N. lactamica* Y92-1009. RNA was extracted from all 6 strains and reverse transcribed into cDNA. The extracted cDNA was used as a template to amplify a region of both HKGs (secA and gyrB), and 2 regions of each MID homologue by PCR at 35 cycles. Amplified products from each MID homologue were run on the same gel with Nlac MID homologues for direct comparison. The amplified product was run on a 1% agarose gel, the gel was imaged by a Gel Doc system and the band intensities were analysed. The mean band intensity of the 2 regions of the MID homologue was normalized to the mean intensity of the 2 HKGs.

Results showed that there was no significant difference between the median band intensity measured for NLY_37260 in *N. lactamica* ATCC 23970, NEICINOT_03770 and NEICINOT_04577 in *N. cinerea* 346T, DBY97_RS02575_23930 in *N. subflava* 23930T, DYA92_RS09215_2043 in *N. elongata* 2043T, and DV147_RS09460 in *N. meningitidis* H44/76 compared to NLY_37260 in *N. lactamica* Y92-1009. However, the median band intensity of NLY_36660 in *N. lactamica* ATCC 23970 was significantly lower compared to NLY_37260 in *N. lactamica* Y92-1009 (Figure 38A).

Further analysis showed that there was no significant difference between the median band intensity of NLY_36660 in *N. lactamica* ATCC 23970, NEICINOT_03770 and NEICINOT_04577 in *N. cinerea* 346T, DBY97_RS02575_23930 in *N. subflava* 23930T and DV147_RS09460 in *N. meningitidis* H44/76 compared to NLY_36660 in *N. lactamica* Y92-1009. However, the median band intensity of NLY_37260 in *N. lactamica* ATCC 23970 and DYA92_RS09215_2043 in *N. elongata* 2043T was significantly higher compared to NLY_36660 in *N. lactamica* Y92-1009 (Figure 38B).

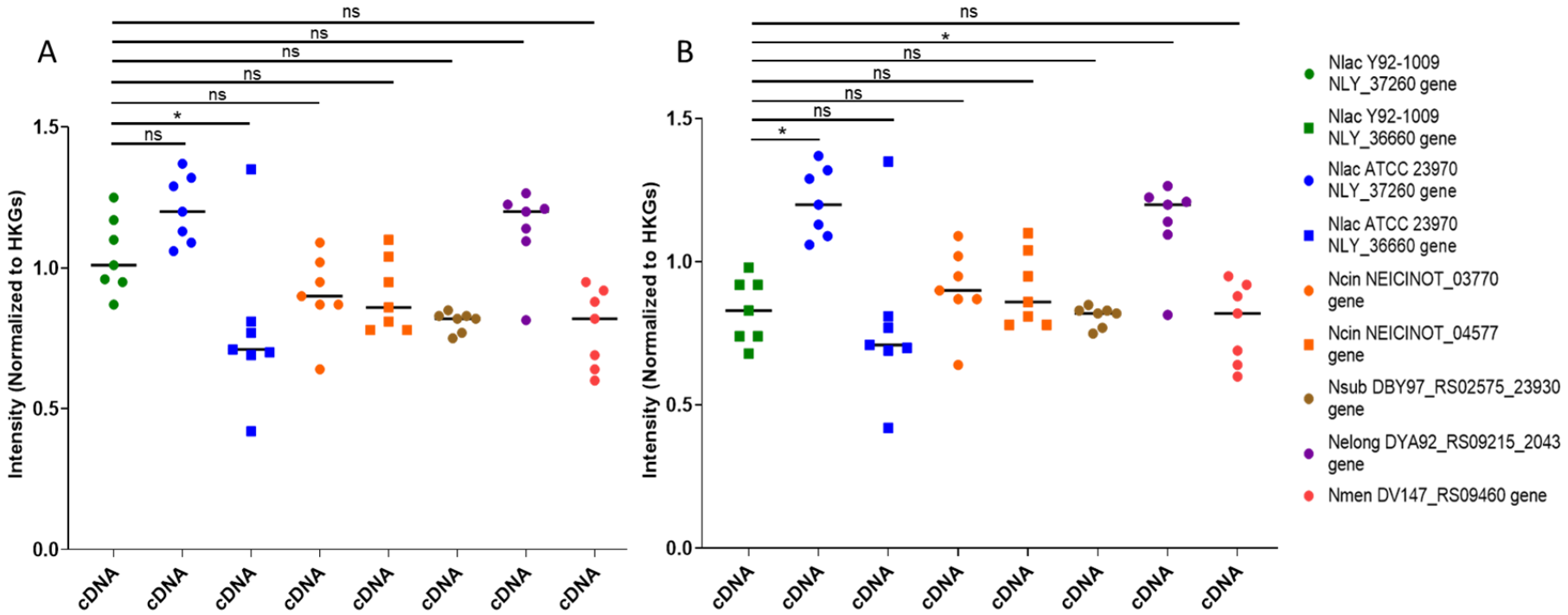

Figure 38 Comparison of estimated levels of gene expression of MID homologues present in several *Neisseria* species that colonize humans, against MID homologues present in *N. lactamica* Y92-1009.

RNA was extracted and reverse transcribed into cDNA. The extracted cDNA was used as template to amplify a region of both HKGs (secA and gryB), and 2 regions of each MID homologue by PCR at 35 cycles. The amplified product was run on a 1% agarose gel, the gel was imaged by a gel Doc system and the band intensities were analysed. The mean band intensity of the 2 regions of the MID homologue was normalized to the mean intensity of the 2 HKGs. **(A)** Comparison of estimated levels of gene expression of MID homologues present in Nlac, Ncin, Nsub, Nelong and Nmen against NLY_37260 gene. **(B)** Comparison of estimated levels of gene expression of MID homologues present in in Nlac, Ncin, Nsub, Nelong and Nmen against NLY_36660 gene. Each sample was run with HKGs and Nlac MID homologues for comparison. Horizontal bars represent the median intensity (normalized to HKGs) of 7 repeated experiments. Groups were analysed using Kruskal-Wallis test with Dunn's correction for multiple comparisons. * $P \leq 0.05$ and ns $P > 0.05$.

4.5 Discussion

4.5.1 Presence of MID aa 962-1200 homologues in various *Neisseria* species

In this chapter, the genome sequence of various *Neisseria* strains was investigated for the presence of homology to the MID aa962-1200. The amino acid sequence of the IgD binding region (aa962-1200) of MID was used as a search query, using the web-based Protein-Protein BLAST tool.

It was shown that *N. mucosa, N. macacae, N. bacilliformis* and *N. gonorrhoeae* either completely lack MID homologues or are very weakly homologous. In contrast, *N. lactamica, N. cinerea, N. flavescens, N. polysaccharea, N. subflava, N. elongata* and *N. meningitidis* displayed at least one or in some cases multiple MID homologues.

The presence of these MID homologues suggests expression of a putative TAA, which in the case of MID is an IgDbp. It was hypothesised that all strains that possess these homologues could induce the proliferation of IgDλ+ B cells, while those lacking them may not.

Various TAAs have been studied in terms of their structure, function and domains (Nummelin *et al.*, 2004; Meng *et al.*, 2006). All TAAs share a similar trimeric surface structure, consisting of N-terminal head, a stalk and a C-terminal anchor domain (Hoiczyk *et al.*, 2000; Leo *et al.*, 2011). Furthermore, several known domains are frequent in TAAs (Table 48), therefore we also investigated the amino acid sequence of these putative TAAs for the presence of domains that are frequent in TAAs (Table 49).

The C-terminus anchor domain is responsible for translocation through the outer membrane and is highly conserved between all TAAs, whereas stalk and head domains can be found in different orientations (Koretke *et al.*, 2006; Linke *et al.*, 2006b; Fialho and Mil-Homens, 2011). Our domain search also revealed that YadA_anchor and YadA_stalk domains were conserved in all MID homologues present in *Neisseria* spp. Furthermore, the head domains differed between different putative *Neisseria* TAAs. The most widespread head domains are LbR_YadA-like head, HiaBD2 (GIN) and TrpRing domain (Bassler *et al.*, 2015). Since the BLAST search revealed that all MID homologues of *Neisseria* spp. contain the domains that are frequent in TAAs, it strengthens the claim that these MID homologues present in various *Neisseria* spp. are putative TAAs, and analogous to MID protein might be mitogenic for B cells.

4.5.2 Various B cell mitogens found in *Neisseria* species

In this section of the chapter it was shown that in addition to *N. lactamica and N. cinerea* 346T*, N. flavescens* 17913T and *N. polysaccharea* 18031T are mitogenic for CD19+IgDλ+ cells. All *Neisseria* mitogenic strains investigated so far induced higher proliferation in λ light chain-expressing B cells compared to κ light chain-expressing B cells.

Furthermore, pre-treatment of CD19+IgDλ+ cells with anti-IgD and anti-λ light chain Ab but not anti-IgM and anti-κ light chain Ab resulted in a reduced percentage of proliferation compared to non-pre-treated cells. However, the level of inhibition differed between pre-treatment with anti-IgD and anti-λ Ab as anti-λ pre-treatment resulted in significantly lower proliferation compared to pre-treatment with anti-IgD Ab (Figure 28). This could be due to different affinities of anti-IgD and anti-λ Ab for the binding site or it could be due to higher competition for anti-IgD compared to anti-λ Ab. Another mechanism for this difference in levels of inhibition could be anti-IgD Ab causing a higher level of calcium flux compared to anti-λ Ab and thus resulting in the lower level of inhibition of proliferation with anti-IgD Ab compared to anti-λ Ab.

In general, strains lacking MID homologues failed to induce proliferation in CD19+IgDλ+ B cells, whilst strains exhibiting MID homologues did induce proliferation in the expected B cell population. The only discrepancy observed was in case of *N. subflava, N. elongata* and *N. meningitidis,* where despite the presence of MID homologues the dOMVs from these strains do not induce proliferation in CD19+IgDλ+ B cells.

It was hypothesised that the lack of proliferation despite the presence of MID homologue could be due to the putative IgDbp gene not being expressed resulting in failure to induce proliferation in IgDλ+ B cells.

In order to investigate this, gene expression was measured employing an SQRT-PCR technique.

4.5.3 Expression of MID homologues in *Neisseria* species

Previously I showed that some of the *Neisseria* strains lack the ability to induce proliferation in IgDλ+ B cells despite the presence of a putative IgDbp gene. We speculated that this difference in phenotype is due to the lack of, or reduced level of expression of putative TAA.

Transcription is the process of copying a gene's DNA sequence to make mRNA. The transcribed mRNA migrates to the cytoplasm where it is used in translation for protein synthesis (Slobodin *et al.*, 2017). Therefore, successful replication of target genes by using cDNA reverse transcribed from the RNA would confirm the target gene being

transcribed. Furthermore, the estimated levels of expression can be compared to investigate whether a low expression level is a reason for lack of ability to induce proliferation in IgDλ+ B cells.

I demonstrated that all MID homologues present in *N. lactamica* Y92-1009, *N. lactamica* ATCC 23970, *N. cinerea* 346T, *N. subflava* 23930T, *N. elongata* 2043T and *N. meningitidis* H44/76 are transcribed, and I was able to amplify multiple regions of target genes using reverse-transcribed cDNA as template. Further analysis revealed that most MID homologues present in the tested strains were expressed at similar levels as NLY_37260 in *N. lactamica* Y92-1009. Furthermore, none of the homologues were expressed at lower levels than NLY_36660 present in *N. lactamica* Y92-1009.

An important paradox is that the MID homologues present in non-mitogenic strains are transcribed at similar levels to MID homologues present in mitogenic Nlac. However, this could still be explained by the lack of or low level of protein expression as these data only confirms the transcription of target genes and perhaps the disparity in phenotype occurs during or post-translation.

Proteins are synthesized by ribosomes via translation of mRNA into polypeptide chains, which may then undergo post-translational modification (PTM) to form the protein product. PTMs facilitates the folding of the polypeptide chain into its functional 3-dimensional (3D) structure. The correct 3D structure is essential to the protein function, and protein misfolding may result in protein inactivation or instability (Sabate, de Groot and Ventura, 2010), leading to loss of function or degradation (Baneyx and Mujacic, 2004). Furthermore, many proteins are destined for specific sites, for example, secretory proteins must be translocated to the secretory pathway. If the protein is not translocated to the environment in which it operates it will not be able to perform its intended function. Finally, the enzymatic breakdown is another factor that could result in the degradation of the protein.

Any of the gene expression steps, from translation to post-translational modification, could result in a lack of, or low level of functional putative TAA expression on the surface of non-proliferating *Neisseria* strains. It can be hypothesised that due to the lack of TAA protein expression various strains of *Neisseria* are unable to attach to the BCR, and therefore are unable to induce proliferation via the BCR. Therefore, as part of future work, the protein expression of putative TAA proteins could be investigated by a more specific technique such as Western blotting.

5. Knocking out and investigating the role of putative TAAs from various *Neisseria* species and strains that induce proliferation in CD19+IgDλ+ B cells

5.1 Investigating the ability of *N. lactamica* Y92-1009 ΔNLY_36660, ΔNLY_37260 and Δ3660 ΔNLY_37260 to induce proliferation in IgDλ+ B cells

One of the objectives of this study was to confirm that NLY-36660 (3,425aa, mass: ~353.4KDa, 47% identical to IgD binding part of MID) and NLY-37260 (3,398aa, mass: ~351KDa, 52% identical to IgD binding part of MID) genes indeed encode the IgD binding protein. These two putative IgDbp candidates were identified in chapter 4 by performing comprehensive BLAST search of the amino acid sequence of the IgD binding part of the MID protein against *N. lactamica* Y92-1009.

Having successfully identified putative IgDbp candidates, *N. lactamica* ΔNLY_36660, ΔNLY_37260, and Δ3660 ΔNLY_37260 Double Mutant (DM) were generated by Dr Jay Laver. NLY_37260 and NLY_36660 ORF were knocked out replacing them with spectinomycin resistance gene aadA1 or kanamycin resistance gene aphA3.

5.2 Aims

- Compare the protein profile of *N. lactamica* Y92-1009 dOMV with *N. lactamica* Y92-1009 ΔNLY_36660, ΔNLY_37260 and DM dOMV.
- To knock out MID aa962-1200 homologues from strains that induce proliferation in B cells.
- To investigate the ability of dOMVs extracted from the knockout strains to induce proliferation in CD19+IgDλ+ population.

5.3 Hypotheses

- dOMVs from the Knockout strains that lack all MID homologues will lack the ability to induce proliferation in IgDλ+ B cells.
- dOMVs from the mutant strains where a single MID homologue is knocked out will still induce proliferation in IgDλ+ B cells.

5.4 Results

5.4.1 Protein profile of *N. lactamica* Y92-1009, ΔNLY_36660 ΔNLY_37260, ΔNLY_37260, ΔNLY_36660, *N. cinerea* 346T and *N. meningitidis* H44/76 dOMV

The effect of knocking out *N. lactamica* genes on the protein profile was assessed by SDS-PAGE, dOMVs were applied to each lane and protein bands were visualised using silver and coomassie blue staining (Figure 39). The profile revealed numerous shared bands evidently visible in all OMVs and some bands limited to certain strains. *N. lactamica* Y92-1009, ΔNLY_36660 ΔNLY_37260 (DM), ΔNLY_37260, ΔNLY_36660 and *N. cinerea* 346T OMVs had very similar protein profiles with a few variations in bands. There was a clear band present at approximately 42 kDa in Nmen, which was absent from the remainder of the strains. This major band is likely to be the class 1 outer membrane protein PorA (Behrouzi *et al.*, 2014). Bands around 20 and 70 kDa were shared by all strains except for Nmen. Both Nmen and DM strains were missing a band at 180 kDa, which was present in all other strains.

Furthermore, the knockout strains displayed a different protein profile than WT *N. lactamica,* as there was a clear lack of a band in DM and ΔNLY_37260 over 260 kDa, as illustrated by the arrow (Figure 39). This is consistent with the predicted ~350 kDa of the putative IgD binding protein. In contrast, ΔNLY_36660 did not show a clear difference in protein bands, suggesting a need for a more specific technique such as western blotting in order to distinctly detect a lack of protein in the knockout strains.

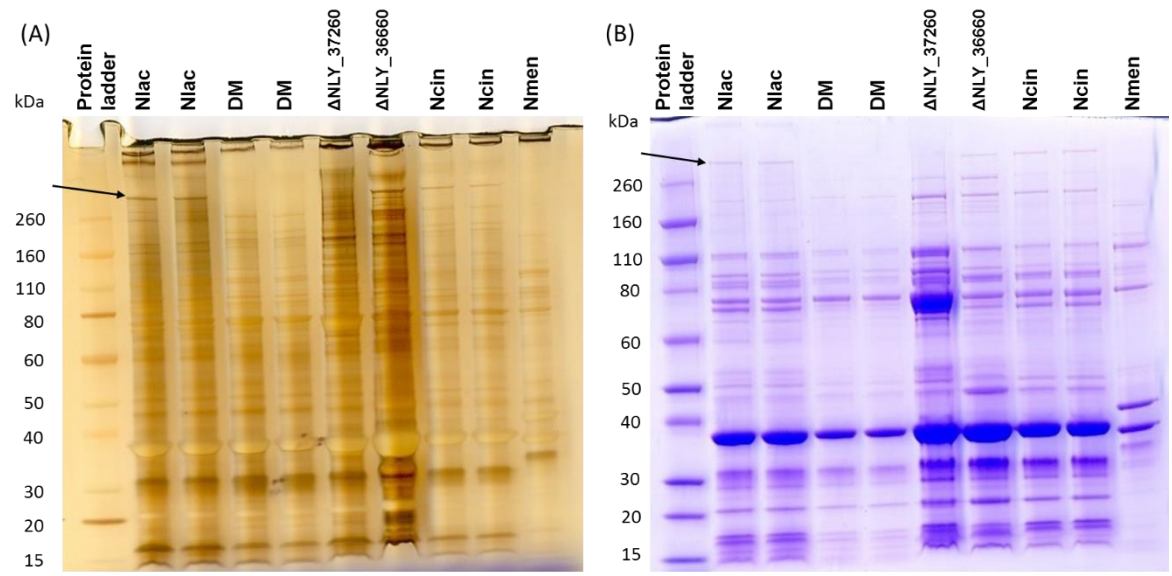

Figure 39 Protein profile of Nlac, Ncin, Nmen, DM, ΔNLY_37260 and ΔNLY_36660.

SDS-PAGE of dOMVs prepared from *N. lactamica* Y92-1009, ΔNLY_36660 ΔNLY_37260 (DM), ΔNLY_37260, ΔNLY_36660, *N. cinerea* 346T and *N. meningitidis* H44/76 strains. 5µg of OMV was applied to each lane and OMVs were visualised using (A) silver staining and (B) coomassie blue staining. Molecular weight markers are indicated on the left hand side. The putative IgDbp is illustrated by the arrows.

5.4.2 B cell proliferation in response to *N. lactamica* Y92-1009, ΔNLY_36660 ΔNLY_37260, ΔNLY_37260, ΔNLY_36660 and *N. meningitidis* H44/76 dOMV

In order to compare the proliferation in CD19+IgD+ cells in response to *N. lactamica* knockout strains, CFSE labelled PBMC were cultured in either media only or in the presence of *N. lactamica* Y92-1009, ΔNLY_36660 ΔNLY_37260 aadA1 (DM), ΔNLY_37260, ΔNLY_36660, *N. meningitidis* H44/76 dOMVs or PWM for 4 days. Results were acquired on day 4 using a flow cytometer (Figure 40). The results showed a clear loss of mitogenicity in DM as the levels of proliferation induced in CD19+IgDλ+ population by DM dOMVs was significantly lower than WT Nlac dOMVs. However, dOMVs from the ΔNLY_37260 and ΔNLY_36660 knockout Nlac strains continued to induce proliferation of the CD19+IgDλ+ population. Furthermore, similar to WT Nlac, both ΔNLY_37260 and ΔNLY_36660 dOMVs induced a higher level of proliferation in λ light chain-expressing CD19+IgD+ cells. Results also showed that there was no significant difference between the proliferation induced by the two knockout strains (Figure 40).

The induction of B cell proliferation by ΔNLY_37260 and ΔNLY_36660 single knockouts but not DM suggests that both genes could encode an IgD binding protein. This also explains the lower proliferative response of IgDλ+ B cells to dOMV from single knockout strains compared to the wild-type, where lack of one IgD binding protein-encoding gene causes lower IgD binding protein expression which in turn is inducing lower proliferation.

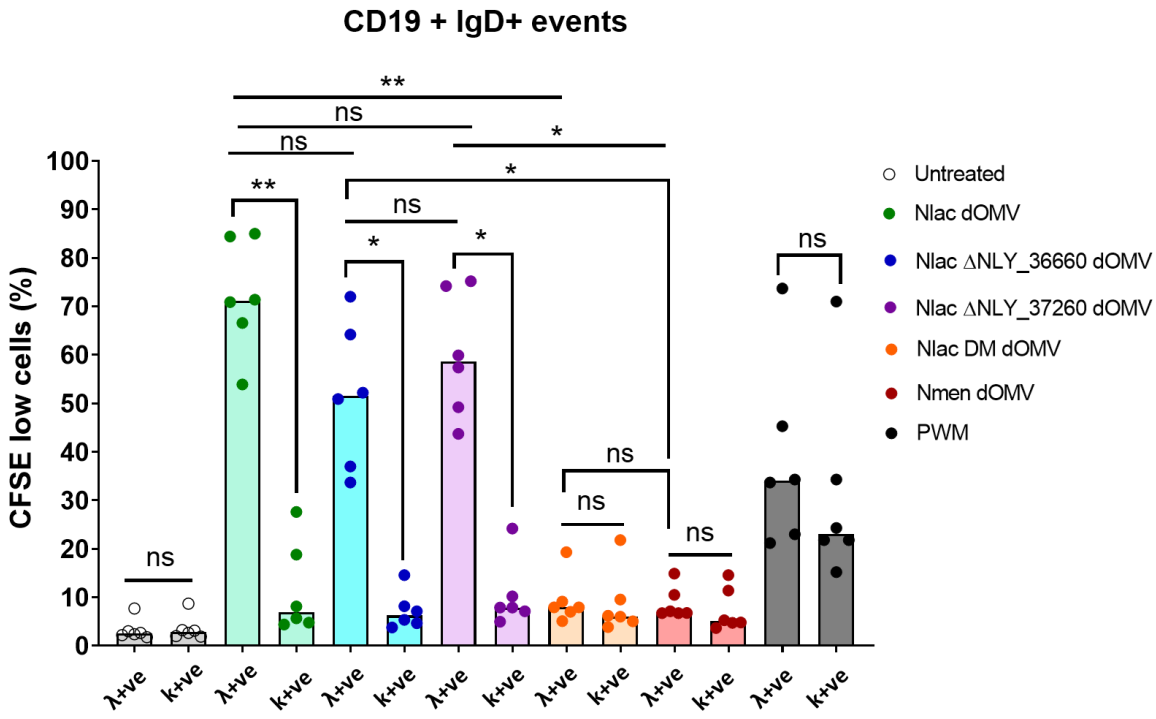

Figure 40 Nlac ΔNLY_37260 and Nlac ΔNLY_36660 dOMV induced proliferation of CD19+IgDλ+ cells compared to CD19+IgDκ+ cells.

Percentage of CFSE low CD19+IgD+ cells expressing κ or λ light chain in response to culturing with *N. lactamica* Y92-1009, *N. lactamica* ΔNLY_36660 ΔNLY_37260 (DM), *N. lactamica* ΔNLY_37260, *N. lactamica* ΔNLY_36660, *N. meningitidis* H44/76 dOMVs and pokeweed mitogen for 4 days. Results were acquired on day 4 using a flow cytometer. Proliferating cells were differentiated by a reduction in CFSE intensity compared to CFSE intensity of the non-treated cells.The peak height of the bars represents the median values of 6 repeated experiments on PBMCs from individual donors. Groups were analysed using Friedman test with Dunn's correction for multiple comparisons. * $P \leq 0.05$, ** $P \leq 0.01$, and ns $P > 0.05$.

5.4.3 Investigating co-localisation of dOMVs from *N. lactamica* IgDbp knockout strains, with IgDλ+ B cells by mean fluorescence intensity

Based on the observation that *N. lactamica* dOMVs contain IgDbps which binds to IgD on the surface of the CD19+IgD+ cells, the dOMVs from knockout strains lacking the IgDbp should not be able to bind to IgD expressed on the surface of the B cells.

To investigate this, PBMCs were incubated in the presence of fluorescently labelled dOMVs from *N. lactamica* Y92-1009, *N. lactamica* ΔNLY_36660 ΔNLY_37260 (DM), *N. lactamica* ΔNLY_37260, *N. lactamica* ΔNLY_36660 and *N. meningitidis* H44/76 dOMVs for 2 hours at 37°C. In the event of an association between the fluorescently labelled dOMVs and B cells, the bound B cells would exhibit a higher MFI compared to non-treated cells.

Results showed that IgDλ+ cells incubated with A488-labelled WT *N. lactamica* displayed the highest level of MFI (Figure 41) compared to non-treated cells. Compared to *N. lactamica* WT, *N. lactamica* ΔNLY_36660 displayed a significantly reduced MFI in IgDλ+ B cells. *N. lactamica* ΔNLY_37260 also demonstrated a significantly reduced MFI in IgDλ+ B cells. Finally, the cells incubated with A488-labelled DM displayed the lowest level of MFI when compared with A488 WT *N. lactamica*. While the MFI of IgDλ+ cells incubated with *N. lactamica* ΔNLY_36660 and *N. lactamica* ΔNLY_37260 were significantly lower than treatment with WT *N. lactamica*, they were significantly higher compared to cells incubated with A488-labelled Nmen. However, there was no significant difference between the MFI of cells incubated with DM and Nmen dOMVs (Figure 41).

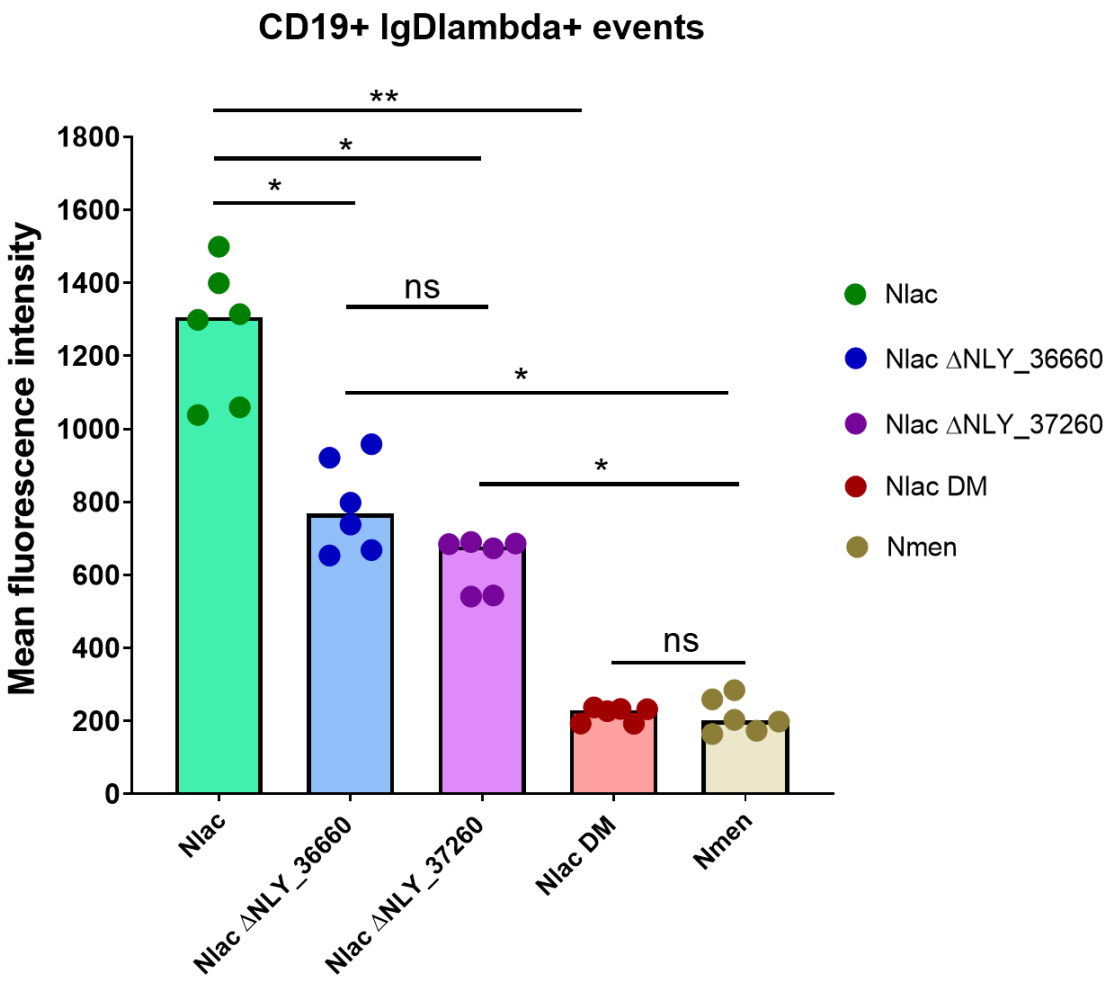

Figure 41 Mean fluorescence intensity of CD19+IgDλ+ cells co-incubated with A488-labelled *N. lactamica* ΔNLY_37260, *N. lactamica* ΔNLY_36660 and *N. lactamica* DM dOMV is reduced compared to cells co-incubated with A488-labelled dOMV from WT *N. lactamica*.

Data showing A488 MFI of CD19+IgDλ+ cells following incubation with A488-labelled dOMV from *N. lactamica* Y92-1009, *N. lactamica* ΔNLY_36660 ΔNLY_37260 (DM), *N. lactamica* ΔNLY_37260, *N. lactamica* ΔNLY_36660 and *N. meningitidis* H44/76 for 2 hours at 37°C. After 2 hours cells were washed and results were acquired using a flow cytometer. When possible 10,000 CD19+ events were analysed and the mean fluorescent intensity (MFI) was measured. The peak height of the bars represents the median values of 6 repeated experiments on PBMCs from individual donors. Groups were analysed using Friedman test with Dunn's correction for multiple comparisons. * $P \leq 0.05$, ** $P \leq 0.01$ and ns $P > 0.05$.

To further confirm that surface IgD is required for the association of *N. lactamica* dOMV with IgDλ+ B cells, PBMC were pre-treated with F(ab')2 polyclonal goat anti-human IgM, IgD, λ or k Abs in order to prevent ligand binding. Non-pre-treated and pre-treated PBMC were cultured in the presence of A488-labelled *N. lactamica* ΔNLY_36660, *N. lactamica* ΔNLY_37260, *N. lactamica* DM and Nmen dOMVs for 2 hours. Following incubation cells were washed and the MFI of IgDλ+ B cells was measured by flow cytometry.

Results showed that IgDλ+ cells co-incubated with A488-labelled *N. lactamica* ΔNLY_36660 had a significant reduction of MFI when pre-treated with anti-IgD Ab compared to anti-IgM Ab. The difference in the level of MFI reduction was also observed when cells were pre-treated with anti-λ light chain Ab compared to anti-κ light chain Ab (Figure 42).

Similarly, IgDλ+ cells co-incubated with A488-labelled *N. lactamica* ΔNLY_37260 also showed a significantly larger reduction in MFI when pre-treated with anti-IgD Ab compared to anti-IgM Ab. Furthermore, pre-treatment with anti-λ light chain Ab compared to anti-κ light chain Ab revealed a significantly increased level of reduction in MFI (Figure 42).

Finally, IgDλ+ cells co-incubated with A488-labelled DM or Nmen did not show any significant difference between the MFI when pre-treated with anti-IgD, anti-IgM, anti-λ light chain and anti-κ light chain Ab (Figure 42).

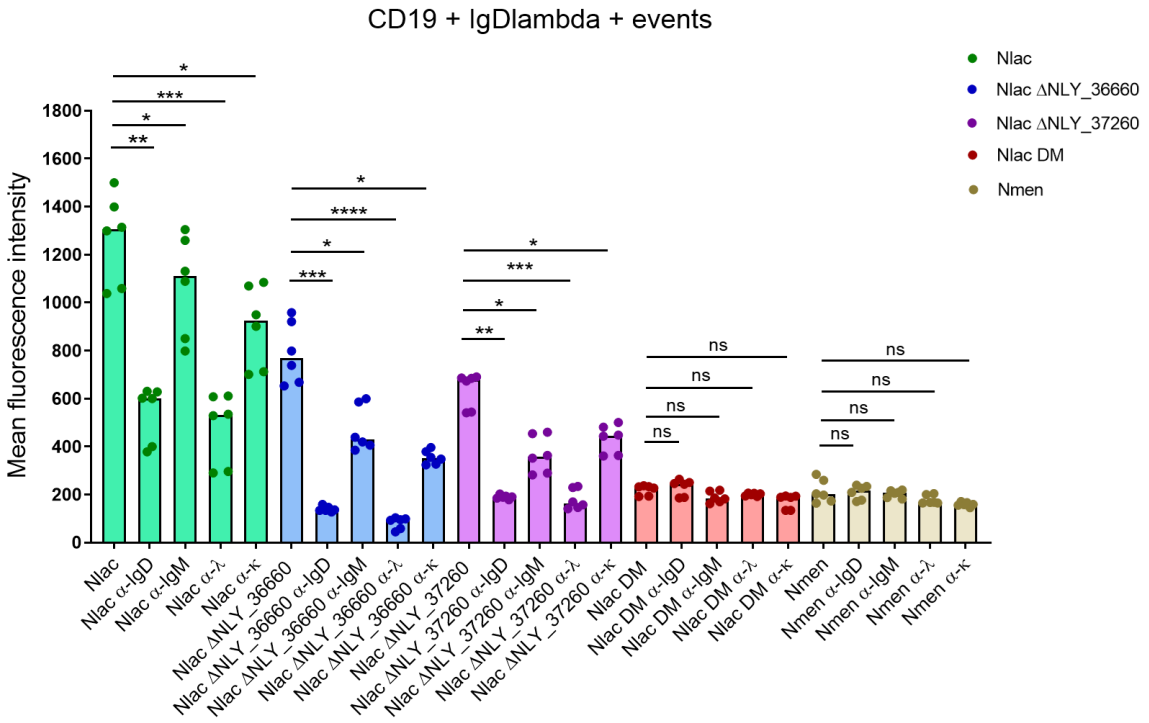

Figure 42 Mean fluorescence intensity of CD19+IgDλ+ cells in response to A488-labelled *N. lactamica* ΔNLY_36660, *N. lactamica* ΔNLY_37260, *N. lactamica* DM and *N. meningitidis* dOMVs is reduced more upon pre-treatment with anti-λ light chain Ab and anti-IgD Ab compared to pre-treatment with anti-k light chain Ab and anti-IgM Ab.

Data showing the effect of treating PBMC with F(ab')$_2$ polyclonal goat anti-human IgM, IgD, λ light chain and k light chain Ab on MFI of IgDλ+ B cells in the presence of A488-labelled *N. lactamica* ΔNLY_36660*, N. lactamica* ΔNLY_37260*, N. lactamica* DM and *N. meningitidis* dOMVs for 2 hours at 37°C. After 2 hours cells were washed and results were acquired using a flow cytometer. When possible 10,000 CD19+ events were analysed and the mean fluorescent intensity (MFI) was measured. The peak height of the bars represents the median values of 6 repeated experiments on PBMCs from individual donors. Groups were analysed using Friedman test with Dunn's correction for multiple comparisons. * P ≤ 0.05, ** P ≤ 0.01, *** P ≤ 0.001, **** P ≤ 0.0001 and ns P > 0.05.

5.4.4 Knocking out MID homologues from *N. cinerea*, *N. flavescens* and *N. polysaccharea* and investigating the proliferation of CD19+IgDλ+ cells in response to dOMVs of these knockout strains

N. cinerea is a non-encapsulated commensal of the URT but is sometimes isolated from the urogenital tract. It is commonly found in the oropharynx of 20% of the healthy adult population (Knapp and Hook, 1988).

N. flavescens is a non-encapsulated bacterium that resides in the mucosal membranes of the URT. *N. flavescens* has been reported in cases of infections (Wertlake and Williams, 1968), however, under normal circumstances, it is classified as a non-pathogenic bacterium.

N. polysaccharea is also a non-encapsulated commensal of URT. It can produce polysaccharide from sucrose. It is found in ~3 % of healthy children. Genetically it is most closely related to Nmen (Bennett *et al.*, 2012) and is often misidentified as Nmen because it can also produce acid from glucose and maltose (Cunningham, Mainella and Patel, 2014).

Since all *Neisseria* spp. excluding Nmen and Ngon colonise the URT of healthy individuals, development of disease in most cases is likely due to enhanced virulence of that particular strain or host being immunocompromised (Johnson, 1983).

5.4.5 *Neisseria cinerea* ΔNEICINOT_03770

NEICINOT_03770 5’ end fragment was amplified with primers 1 and 2 (Table 7) and NEICINOT_03770 3’ end fragment was amplified with primers 3 and 4 (Table 7) using Ncin genomic DNA as the template. The primers were designed to ensure a misalignment between the primer and the template to cause a frameshift in the fragments. An extra nucleotide “A” was added to the forward primer at the 5th position at the 3’ end.

In order to knock out NEICINOT_03770 a cassette containing spectinomycin resistance gene aadA1 flanked by 5’ end and 3’ end fragments of NEICINOT_03770 ORF was combined with PUC19 plasmid using Gibson isothermal assembly. The assembled plasmid with ΔNEICINOT_03770_aadA1 was transformed into and maintained in *E. coli* DH5α. Plasmids were extracted and used as the template DNA for amplification of ΔNEICINOT_03770_aadA1 by HM-PCR. The PCR product of ΔNEICINOT_03770_aadA1 was used to transform *N. cinerea* (Figure 43). Successful transformants were selected on TSB plates containing spectinomycin. The size of ΔNEICINOT_03770_aadA1 was confirmed by PCR amplification using *N. cinerea* ΔNEICINOT_03770_aadA1 genomic DNA as the template with primers 9 and 10 (Table 7). Gel electrophoresis demonstrated that the size of the target gene in *N. cinerea* ΔNEICINOT_03770 was approximately ~3000 bp compared to ~11000 bp in WT (Figure 44). The observed bands were of the expected size, confirming successful transformation and the integration of ΔNEICINOT_03770 at the correct locus.

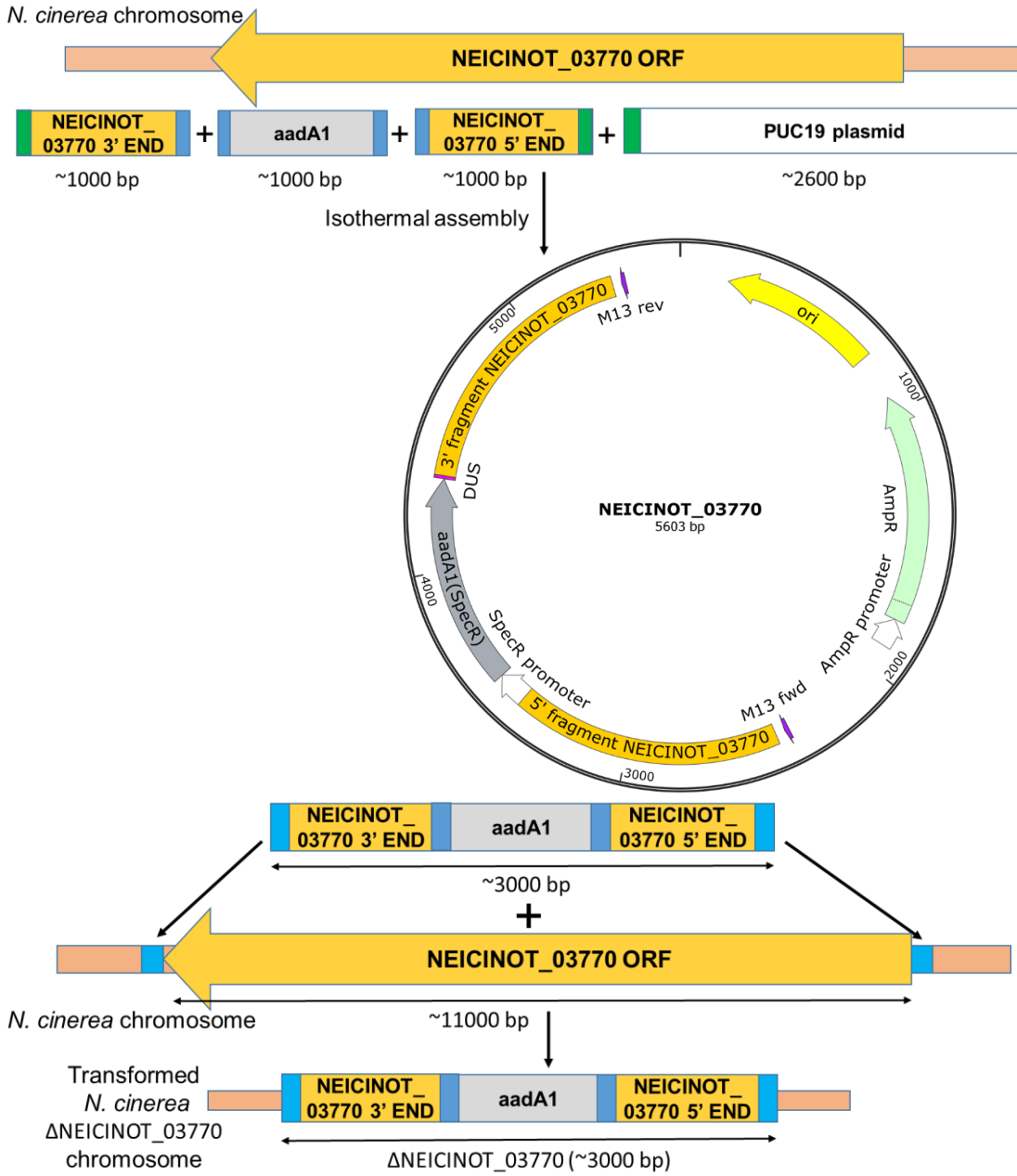

Figure 43 Overview of *N. cinerea* 346T ΔNEICINOT_03770 transformation strategy.

A cassette containing spectinomycin resistance gene aadA1, flanked by 5' end NEICINOT_03770 and 3' end NEICINOT_03770 fragments were combined with PUC19 plasmid by isothermal assembly and maintained in *E. coli* DH5α. ΔNEICINOT_03770_aadA1 gene was amplified by HM-PCR and the PCR product was used for transformation of *N. cinerea*. Transformed colonies were selected on spectinomycin + TSB plates.

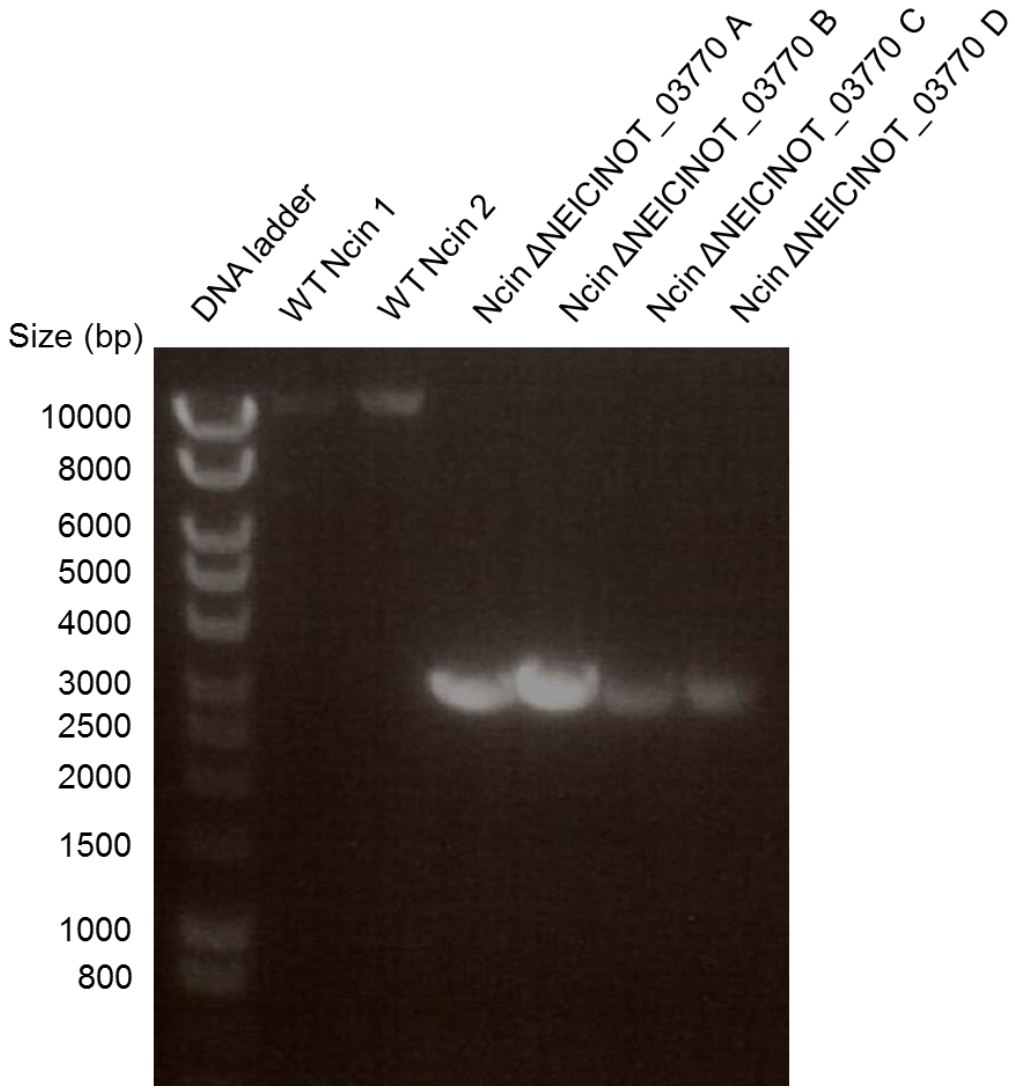

Figure 44 PCR products amplified from genomic DNA of wild-type *N. cinerea* and *N. cinerea* ΔNEICINOT_03770 A, B, C, D.

Four transformed colonies were grown overnight in the presence of spectinomycin and genomic DNA was extracted from overnight cultures. Extracted DNA from four candidates (ΔNEICINOT_03770 A, B, C and D) (lane 4, 5, 6 and 7) was used as template for the PCR amplification of ΔNEICINOT_03770 gene with primers flanking ΔNEICINOT_03770 gene. PCR product of WT *N. cinerea* was used for comparison (lane 2 and 3). A DNA ladder with known sequence length was added in lane 1 to confirm the approximate size of the PCR products.

5.4.6 *Neisseria flavescens* ΔDYC64_RS10620

DYC64_RS10620 5’ end fragment (~1000 bp) was amplified with primers 1 and 2 (Table 8) and DYC64_RS10620 3’ end fragment (~1000 bp) was amplified with primers 3 and 4 (Table 8) using Nflav genomic DNA as the template. The primers were designed to ensure a misalignment between the primer and the template to cause a frameshift in the fragments. An extra nucleotide “A” was added to the forward primer at the 4th position at the 3’ end.

In order to knockout DYC64_RS10620 gene from *N. flavescens* chromosome, the procedure outlined in (Figure 45) was followed, resulting in the generation of *N. flavescens* ΔDYC64_RS10620 knockouts. Transformed colonies were selected on kanamycin + TSB plates. To confirm the integration of ΔDYC64_RS10620_aphA3 into the correct locus, primers flanking the target ORF (primer 9 and 10, Table 8) were used to PCR amplify the target sequence using chromosomal DNA from the four successful transformants. Analysis of the PCR product by gel electrophoresis revealed a truncated size band in *N. flavescens* ΔDYC64_RS10620 of approximately ~3000 bp compared to ~13000 bp in WT (Figure 46). The observed bands were of the expected size, confirming successful transformation and the integration of ΔDYC64_RS10620 at the correct locus.

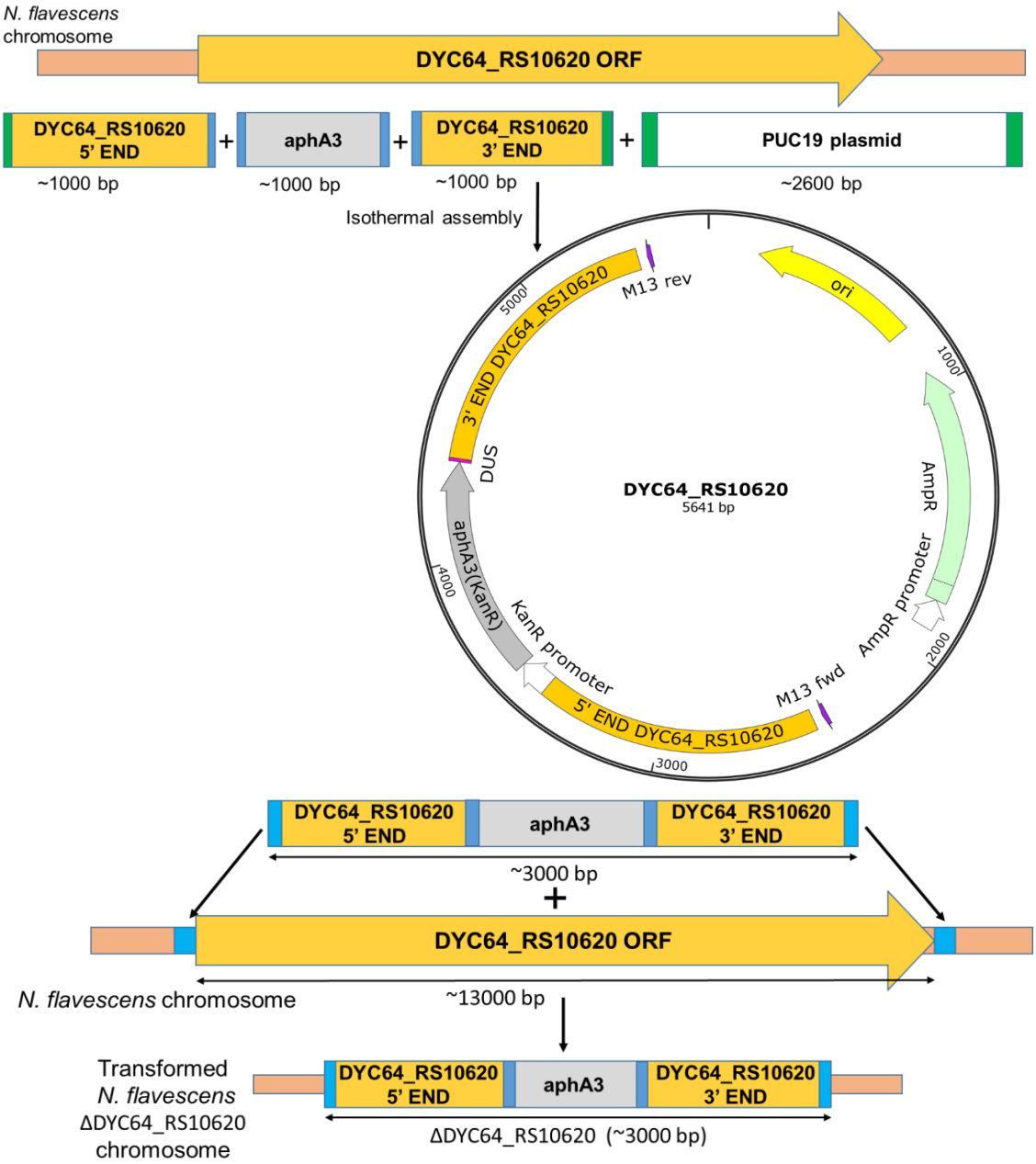

Figure 45 Overview of *N. flavescens* ΔDYC64_RS10620 transformation strategy.

A cassette containing kanamycin resistance gene aphA3, flanked by 5' end DYC64_RS10620 and 3' end DYC64_RS10620 fragments were combined with PUC19 plasmid by isothermal assembly and maintained in *E. coli* DH5α. ΔDYC64_RS10620_aphA3 gene was amplified by HM-PCR and the PCR product was used for transformation of *N. flavescens*. Transformed colonies were selected on spectinomycin + TSB plates.

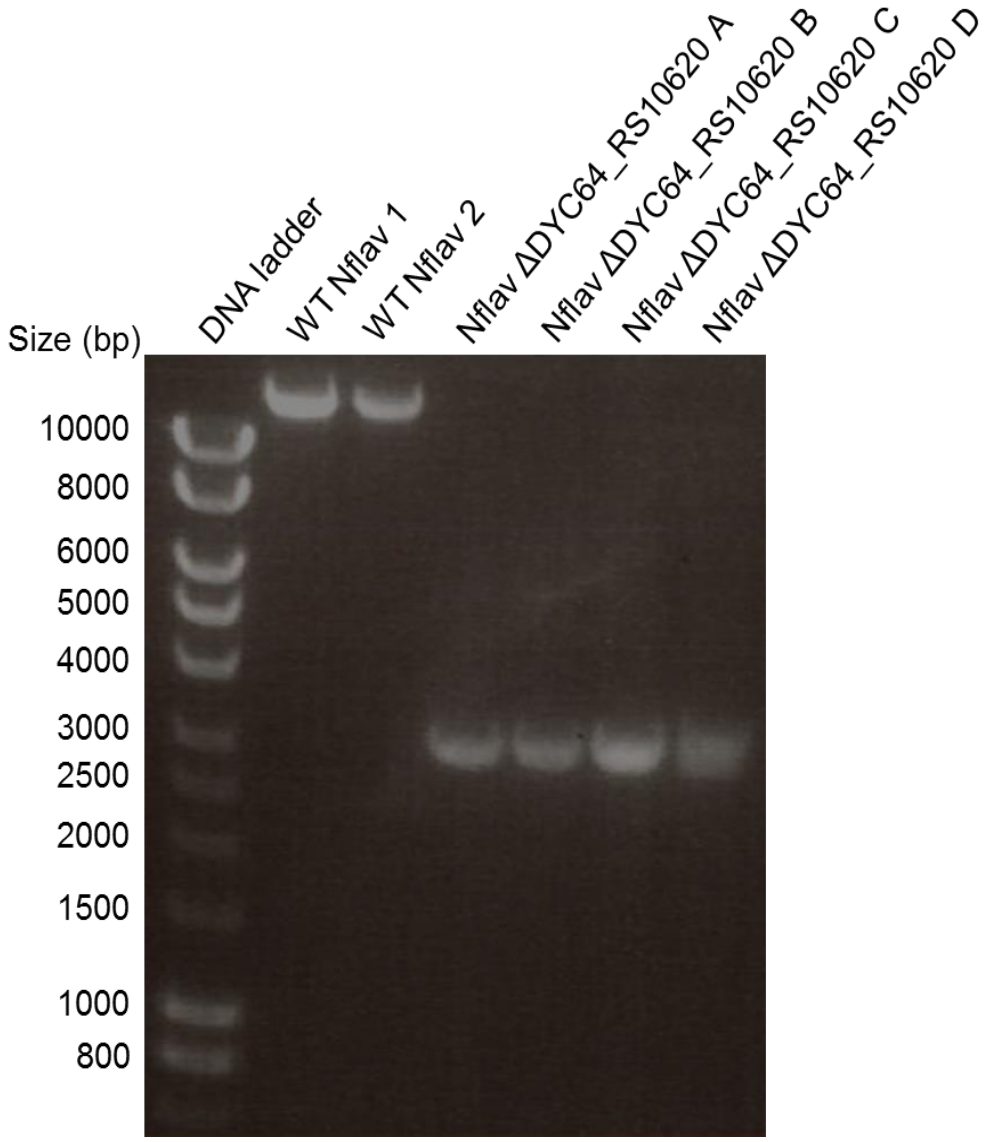

Figure 46 PCR products amplified from genomic DNA of wild-type *N. flavescens* and *N. flavescens* ΔDYC64_RS10620 A, B, C, D.

Four transformed colonies were grown overnight in the presence of kanamycin and genomic DNA was extracted from overnight cultures. Extracted DNA from the four candidates (ΔDYC64_RS10620 A, B, C and D) (lane 4, 5, 6 and 7) was used as template for the PCR amplification of the knocked-out ORF with primers flanking ΔDYC64_RS10620 ORF. PCR product of WT *N. flavescens* was used for comparison (lane 2 and 3). A DNA ladder with known sequence length was added in lane 1 to confirm the approximate size of the PCR products.

5.4.7 *Neisseria polysaccharea* ΔNEIPOLOT_RS07545

NEIPOLOT_RS07545 5’ end fragment was amplified with primers 1 and 2 (Table 9) and NEIPOLOT_RS07545 3’ end fragment was amplified with primers 3 and 4 (Table 9) using Npol genomic DNA as the template. The primers were designed to ensure a misalignment between the primer and the template to cause a frameshift in the fragments. An extra nucleotide “A” was added to the forward primer at the 4th position at the 3’ end.

Following the generation of 5’ end and 3’ end fragments, *N. polysaccharea* ΔNEIPOLOT_RS07545 was knocked out following the steps outlined in (Figure 47). Successful transformants were selected on spectinomycin + TSB. In order to further confirm the success of the knockout and to ensure the cassette was inserted in the correct place, primers flanking NEIPOLOT_RS07545 (primer 9 and 10, Table 9) were used to PCR amplify the NEIPOLOT_RS07545 ORF using genomic DNA from the knockout strains as the template DNA. Subsequently, the amplified PCR product was analysed by gel electrophoresis (Figure 48). Results demonstrated that the size of the target sequence for all four *N. polysaccharea* ΔNEIPOLOT_RS07545 were truncated (~3000 bp) compared to WT *N. polysaccharea* (~11000 bp), suggesting a successful integration of ΔNEIPOLOT_RS07545 into the *N. polysaccharea* genome at the target locus.

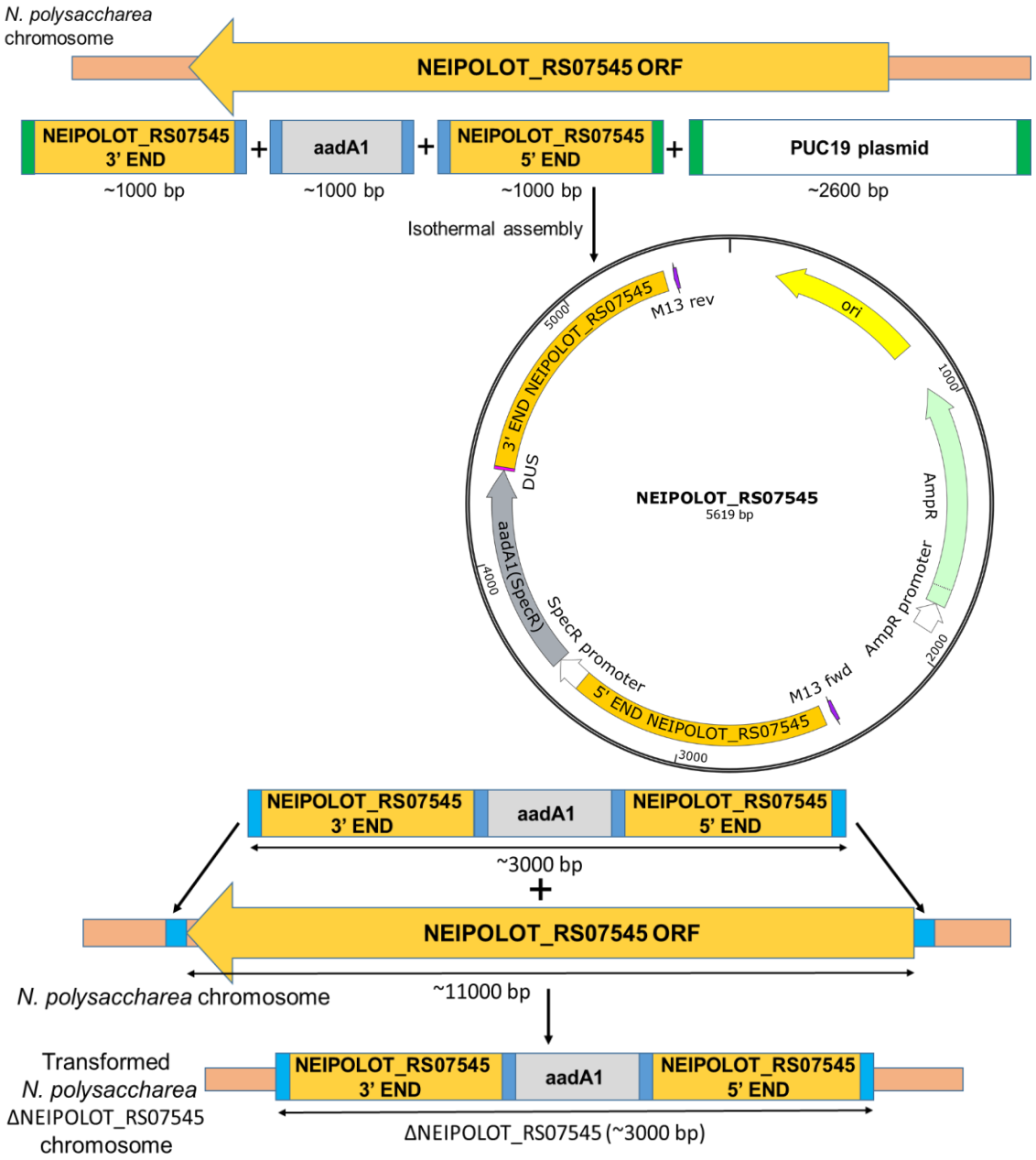

Figure 47 Overview of *N. polysaccharea* ΔNEIPOLOT_RS07545 transformation strategy.

A cassette containing spectinomycin resistance gene aadA1, flanked by 5' end NEIPOLOT_RS07545 and 3' end NEIPOLOT_RS07545 fragments were combined with PUC19 plasmid by isothermal assembly and maintained in *E. coli* DH5α. ΔNEIPOLOT_RS07545_aadA1 ORF was amplified by HM-PCR and the PCR product was used for transformation of *N. polysaccharea*. Transformed colonies were selected on spectinomycin + TSB plates.

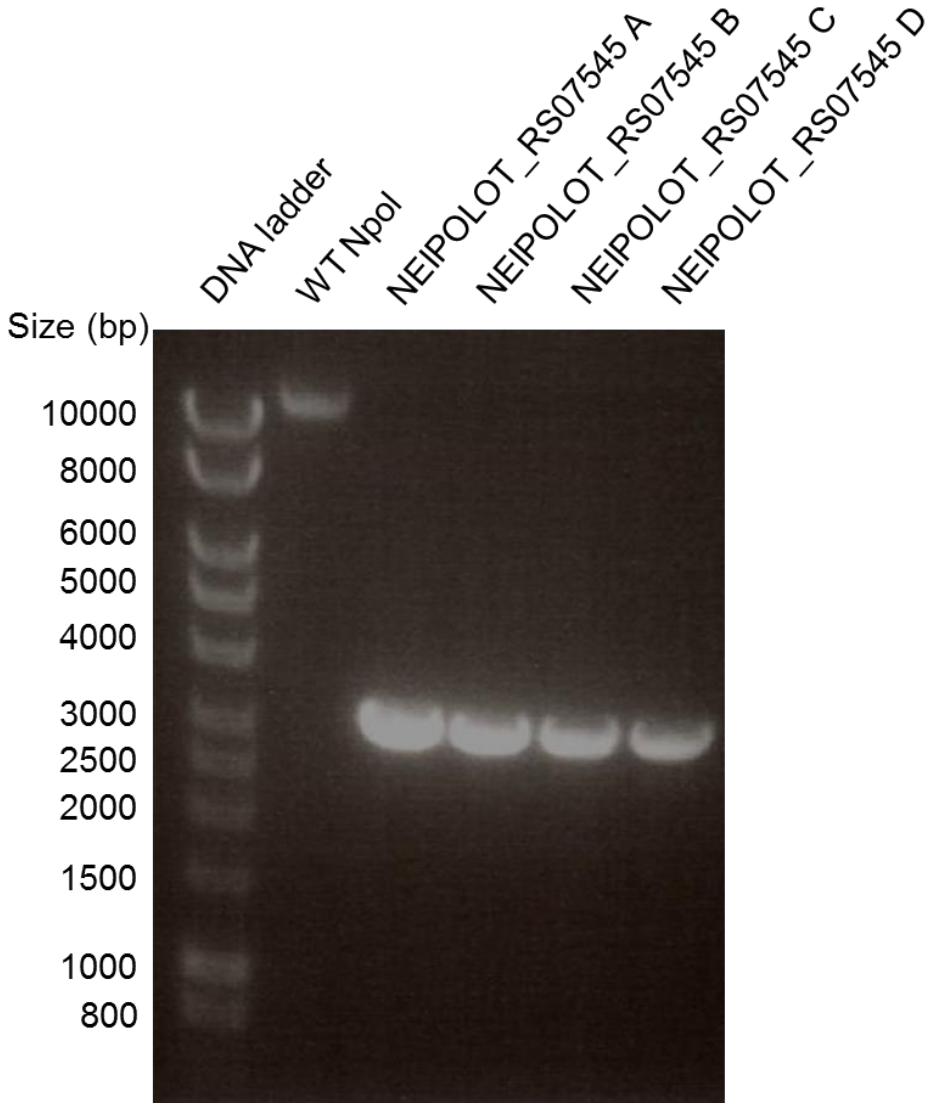

Figure 48 PCR products amplified from genomic DNA of wild-type *N. polysaccharea* and *N. polysaccharea* ΔNEIPOLOT_RS07545 A, B, C, D.

Four transformed colonies were grown overnight in the presence of spectinomycin and the genomic DNA was extracted from overnight cultures. Extracted DNA from four candidates (ΔNEIPOLOT_RS07545 A, B, C and D) (lane 3, 4, 5 and 6) was used as the template for the PCR amplification of the knocked out gene, with primers flanking ΔNEIPOLOT_RS07545. The PCR product of WT *N. polysaccharea* was used for comparison (lane 2). A DNA ladder with known sequence length was added in lane 1 to confirm the approximate size of the PCR products.

5.4.8 Further knockouts

NEICINOT_03770, DYC64_RS10620 and NEIPOLOT_RS07545 were considered to be the only MID homologues present in *N. cinerea*, *N. flavescens* and *N. polysaccharea* respectively. However, when a more comprehensive homology search was performed in chapter 4.4, it was discovered that other MID homologues NEICINOT 04577 and NEIFLAOT 01884, were present in *N. cinerea* and *N. flavescens* respectively. Therefore, these homologues were also knocked out to investigate their effects on the ability to induce proliferation of IgDλ+ B cells. Furthermore, NEICINOT_03770 was also knocked out, by completely replacing the ORF with an antibiotic resistance gene to show that there was no significant difference between the knockouts generated by frameshift or complete removal of the ORF.

5.4.8.1 *Neisseria cinerea* ΔNEICINOT_03770

The ~500 bp sequence upstream of NEICINOT_03770 5' end was amplified with primers 1 and 2 (Table 10) and the ~500 bp sequence downstream of NEICINOT_03770 3' end was amplified with primers 3 and 4 (Table 10) using Ncin genomic DNA as the template.

In order to knock out NEICINOT_03770 a cassette containing spectinomycin resistance gene aadA1 flanked by the ~500 bp sequence upstream of NEICINOT_03770 ORF and the ~500 bp sequence downstream of NEICINOT_03770 ORF was combined with PUC19 plasmid using Gibson isothermal assembly. The assembled plasmid with ΔNEICINOT_03770_aadA1 was transformed into and maintained in *E. coli* DH5α. Plasmids were extracted and used as the template DNA for amplification of ΔNEICINOT_03770_aadA1 by HM-PCR. The PCR product of ΔNEICINOT_03770_aadA1 was used to transform WT *N. cinerea* (Figure 49). Successful transformants were selected on TSB plates containing spectinomycin. The size of ΔNEICINOT_03770_aadA1 was confirmed by PCR amplification using *N. cinerea* ΔNEICINOT_03770_aadA1 genomic DNA as the template with primers 9 and 10 (Table 10). Gel electrophoresis demonstrated that the size of the target ORF in *N. cinerea* ΔNEICINOT_03770 was ~2500 bp compared to ~12000 bp in WT (Figure 50). The observed bands are of expected size suggesting the transformation has been successful and the cassette has been inserted in the correct locus.

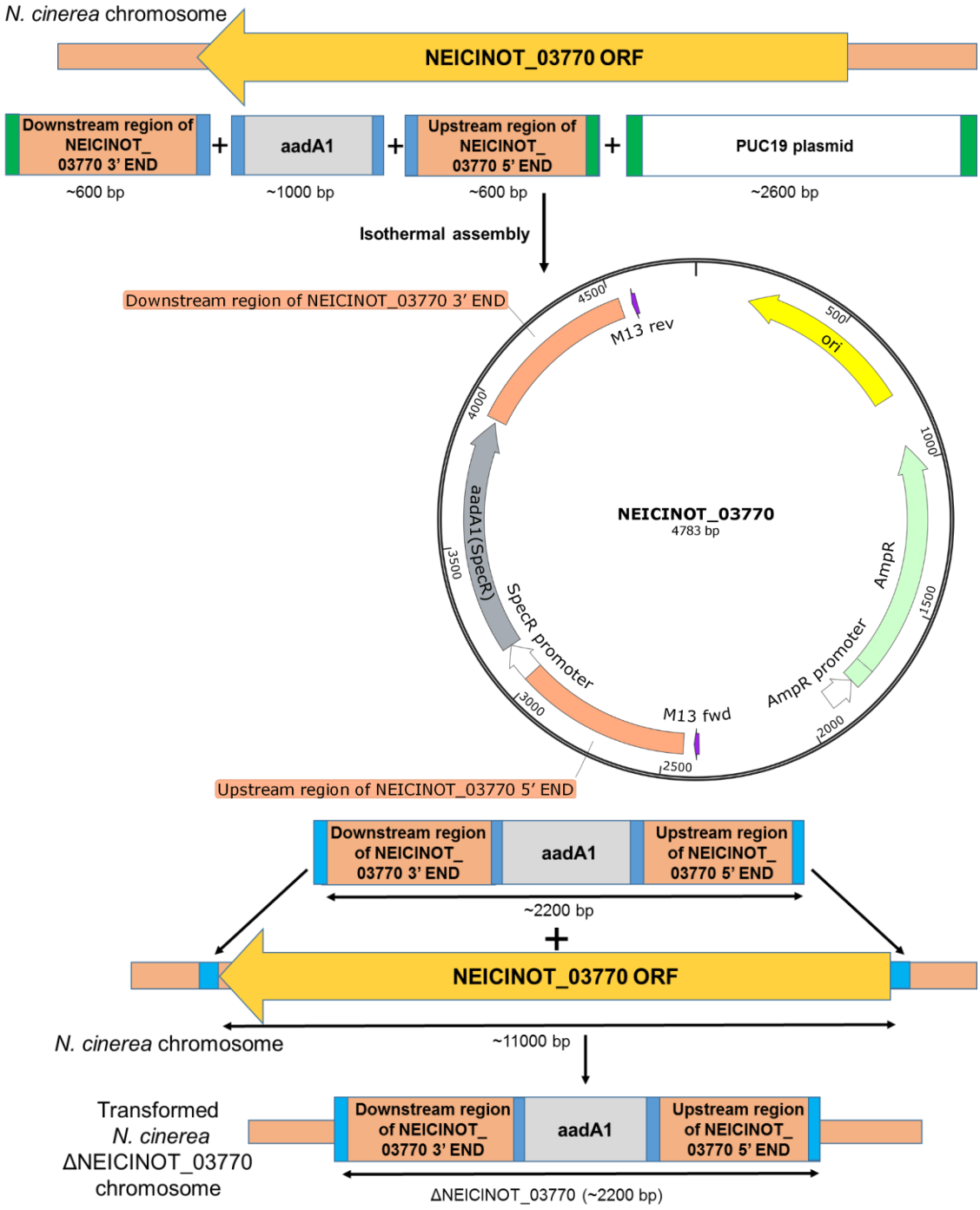

Figure 49 Overview of *N. cinerea* 346T ΔNEICINOT_03770 transformation strategy.

A cassette containing spectinomycin resistance gene aadA1, flanked by the upstream region of NEICINOT_03770 5' end and downstream region of NEICINOT_03770 3' end fragments were combined with PUC19 plasmid by isothermal assembly and maintained in *E. coli* DH5α. ΔNEICINOT_03770_aadA1 gene was amplified by HM-PCR and the PCR product was used for transformation of *N. cinerea*. Transformed colonies were selected on spectinomycin + TSB plates.

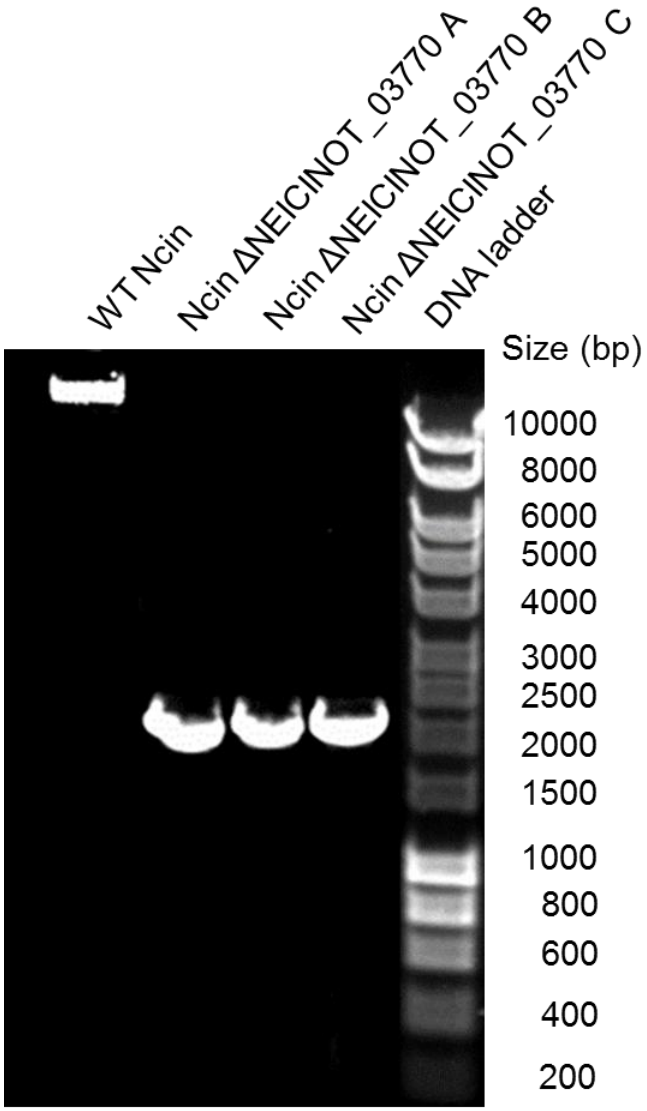

Figure 50 PCR products amplified from genomic DNA of wild-type *N. cinerea* and *N. cinerea* ΔNEICINOT_03770 A, B and C.

Three transformed colonies were grown overnight in the presence of spectinomycin and genomic DNA was extracted from overnight cultures. Extracted DNA from three candidates (ΔNEICINOT_03770 A, B and C) (lane 2, 3 and 4) was used as a template for the PCR amplification of ΔNEICINOT_03770 ORF with primers flanking ΔNEICINOT_03770 ORF. PCR product of WT *N. cinerea* was used for comparison (lane 1). A DNA ladder with known sequence length was added in lane 5 to confirm the approximate size of the PCR products.

5.4.8.2 *Neisseria cinerea* ΔNEICINOT_04577

The ~500 bp sequence upstream of NEICINOT_04577 5' end was amplified with primers 1 and 2 (Table 11) and the ~500 bp sequence downstream of NEICINOT_04577 3' end was amplified with primers 3 and 4 (Table 11) using Ncin genomic DNA as the template.

In order to knock out NEICINOT_04577 a cassette containing spectinomycin resistance gene aadA1 flanked by the ~500 bp sequence upstream of NEICINOT_04577 ORF and the ~500 bp sequence downstream of NEICINOT_04577 ORF was combined with PUC19 plasmid using Gibson isothermal assembly. The assembled plasmid with ΔNEICINOT_04577_aadA1 was transformed into and maintained in *E. coli* DH5α. Plasmids were extracted and used as the template DNA for amplification of ΔNEICINOT_04577_aadA1 by HM-PCR. The PCR product of ΔNEICINOT_04577_aadA1 was used to transform *N. cinerea* (Figure 51). Successful transformants were selected on TSB plates containing spectinomycin. The size of ΔNEICINOT_04577_aadA1 was confirmed by PCR amplification using *N. cinerea* ΔNEICINOT_04577_aadA1 genomic DNA as the template with primers 9 and 10 (Table 11). Gel electrophoresis demonstrated that the size of the target ORF in *N. cinerea* ΔNEICINOT_04577 was ~2500 bp compared to ~6000 bp in WT (Figure 52). The observed bands are of the expected size, suggesting that the transformation has been successful, and the cassette has been inserted into the correct locus.

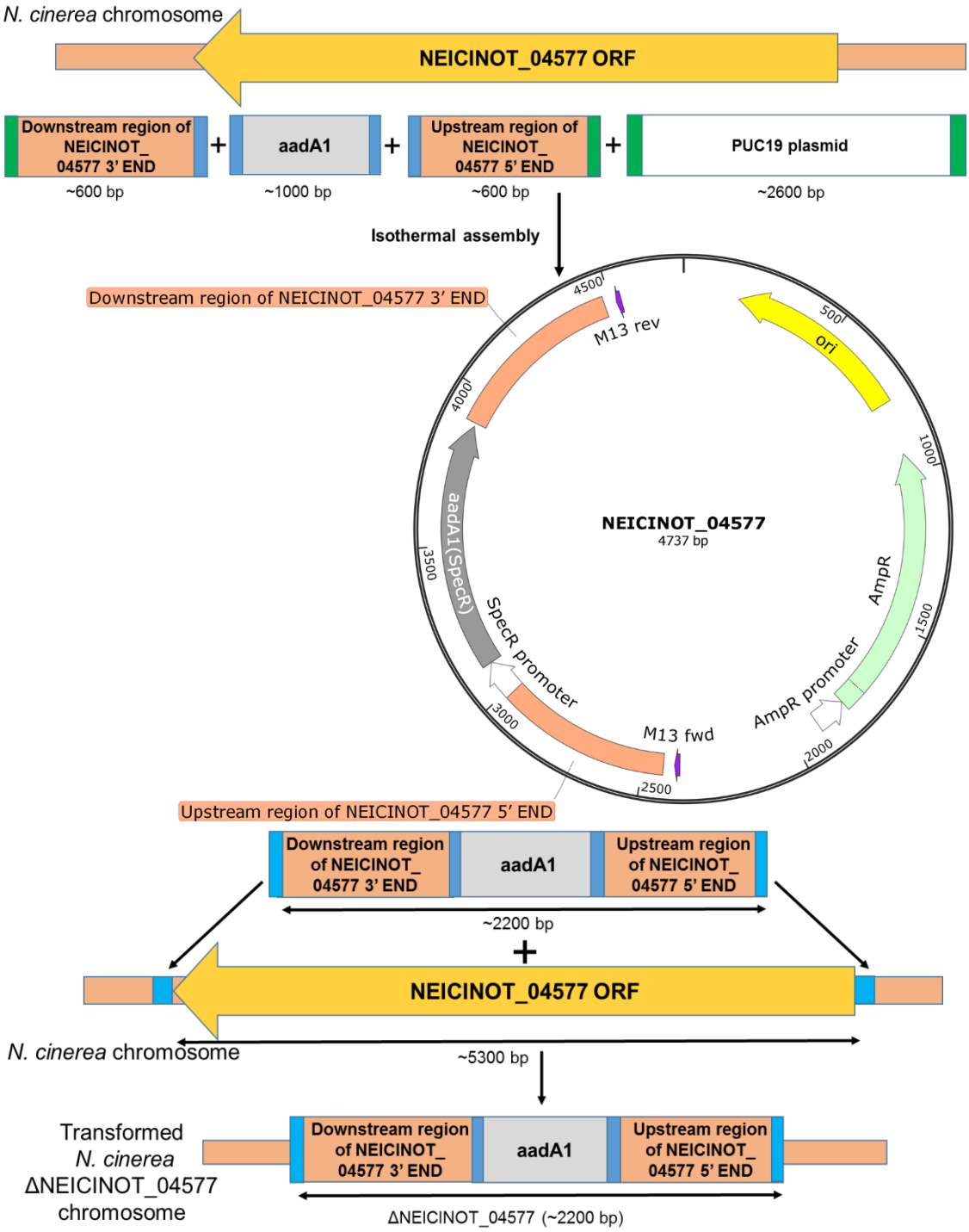

Figure 51 Overview of *N. cinerea* 346T ΔNEICINOT_04577 transformation strategy.

A cassette containing spectinomycin resistance gene aadA1, flanked by the upstream region of NEICINOT_04577 5' end and downstream region of NEICINOT_04577 3' end fragments, were combined with PUC19 plasmid by isothermal assembly and maintained in *E. coli* DH5α. ΔNEICINOT_04577_aadA1 gene was amplified by HM-PCR and the PCR product was used for transformation of *N. cinerea*. Transformed colonies were selected on spectinomycin + TSB plates.

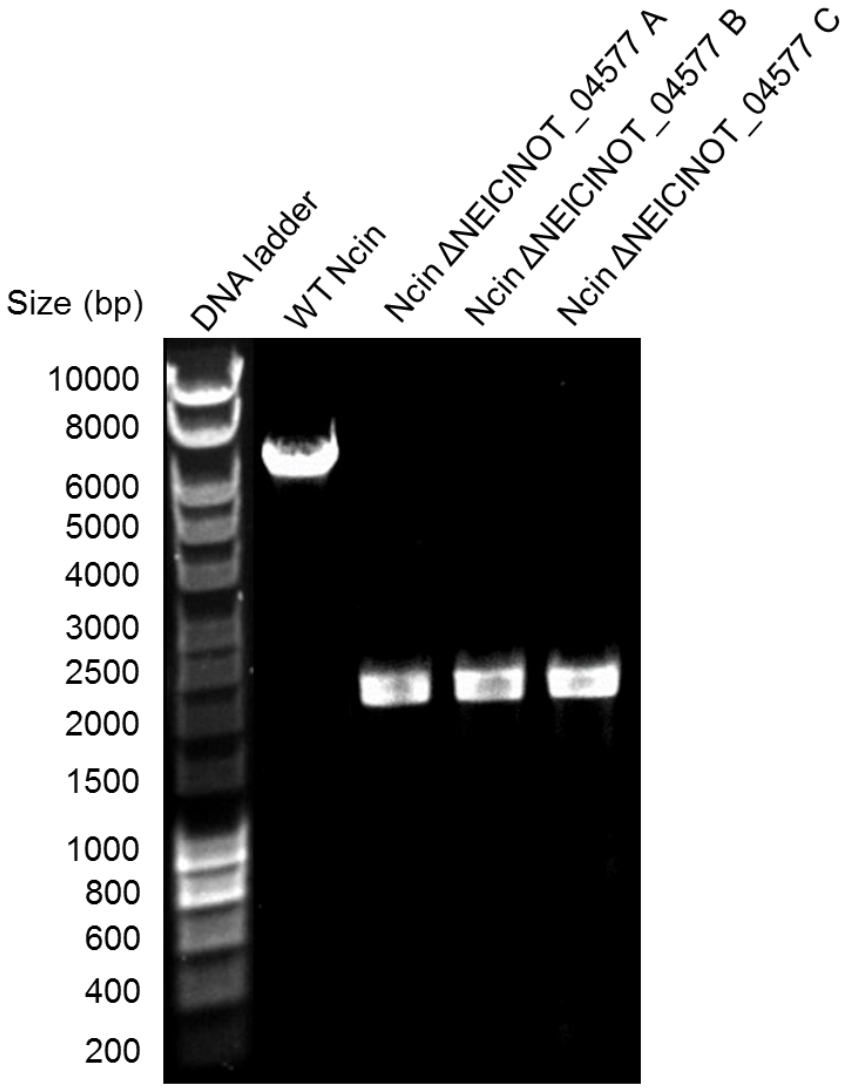

Figure 52 PCR products amplified from genomic DNA of wild-type N. *cinerea* and *N. cinerea* ΔNEICINOT_04577 A, B and C.

Three transformed colonies were grown overnight in the presence of spectinomycin and genomic DNA was extracted from overnight cultures. Extracted DNA from three candidates (ΔNEICINOT_04577 A, B and C) (lane 3, 4 and 5) was used as a template for the PCR amplification of ΔNEICINOT_04577 ORF, with primers flanking ΔNEICINOT_04577 ORF. The PCR product of WT *N. cinerea* was used for comparison (lane 2). A DNA ladder with known sequence length was added in lane 1 to confirm the approximate size of the PCR products.

5.4.8.3 *Neisseria flavescens* ΔNEIFLAOT_01884

The ~500 bp sequence upstream of ΔNEIFLAOT_01884 5' end was amplified with primers 1 and 2 (Table 12) and the ~500 bp sequence downstream of ΔNEIFLAOT_01884 3' end was amplified with primers 3 and 4 (Table 12) using Nflav genomic DNA as the template.

In order to knock out NEIFLAOT_01884 a cassette containing spectinomycin resistance gene aadA1 flanked by ~500 bp sequence upstream of ΔNEIFLAOT_01884 ORF and ~500 bp sequence downstream of ΔNEIFLAOT_01884 ORF was combined with PUC19 plasmid using Gibson isothermal assembly. The assembled plasmid with ΔNEIFLAOT_01884_aadA1 was transformed into and maintained in *E. coli* DH5α. Plasmids were extracted and used as the template DNA for amplification of ΔNEIFLAOT_01884_aadA1 by HM-PCR. The PCR product of ΔNEIFLAOT_01884_aadA1 was used to transform *N. flavescens* (Figure 53). Successful transformants were selected on TSB plates containing spectinomycin. The size of ΔNEIFLAOT_01884_aadA1 was confirmed by PCR amplification using *N. flavescens* ΔNEIFLAOT_01884_aadA1 genomic DNA as the template with primers 9 and 10 (Table 12). Gel electrophoresis demonstrated that the size of the target ORF in *N. flavescens* ΔNEIFLAOT_01884 was ~2500 bp compared to ~8000 bp in WT (Figure 54). The observed bands are of the expected size, suggesting that the transformation has been successful, and the cassette has been inserted into the correct locus.

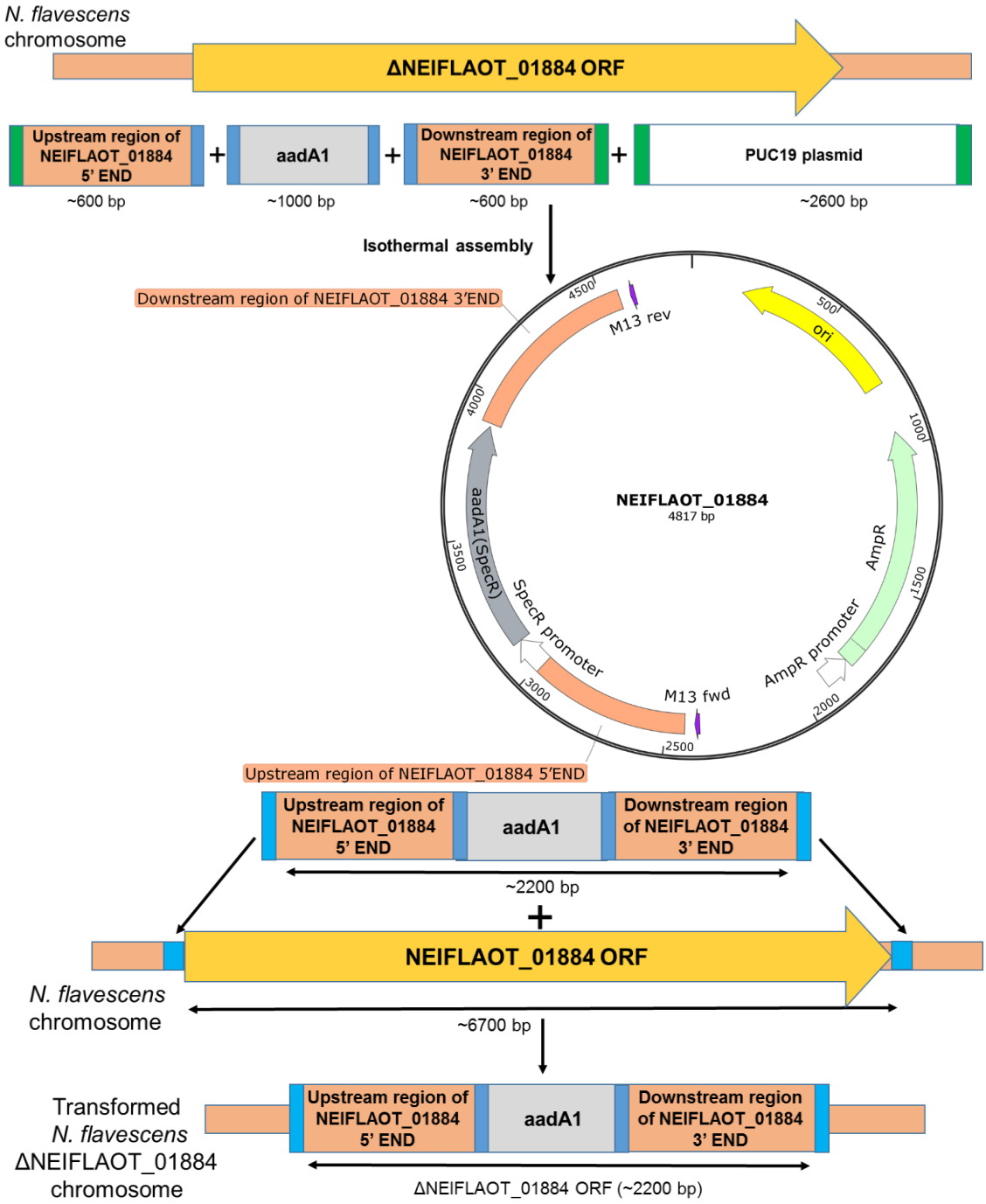

Figure 53 Overview of *N. cinerea* 346T ΔNEIFLAOT_01884 transformation strategy.

A cassette containing spectinomycin resistance gene aadA1, flanked by upstream region of NEIFLAOT_01884 5' end and downstream region of NEIFLAOT_01884 3' end fragments were combined with PUC19 plasmid by isothermal assembly and maintained in *E. coli* DH5α. ΔNEIFLAOT_01884 _aadA1 gene was amplified by HM-PCR and the PCR product was used for transformation of *N. cinerea*. Transformed colonies were selected on spectinomycin + TSB plates.

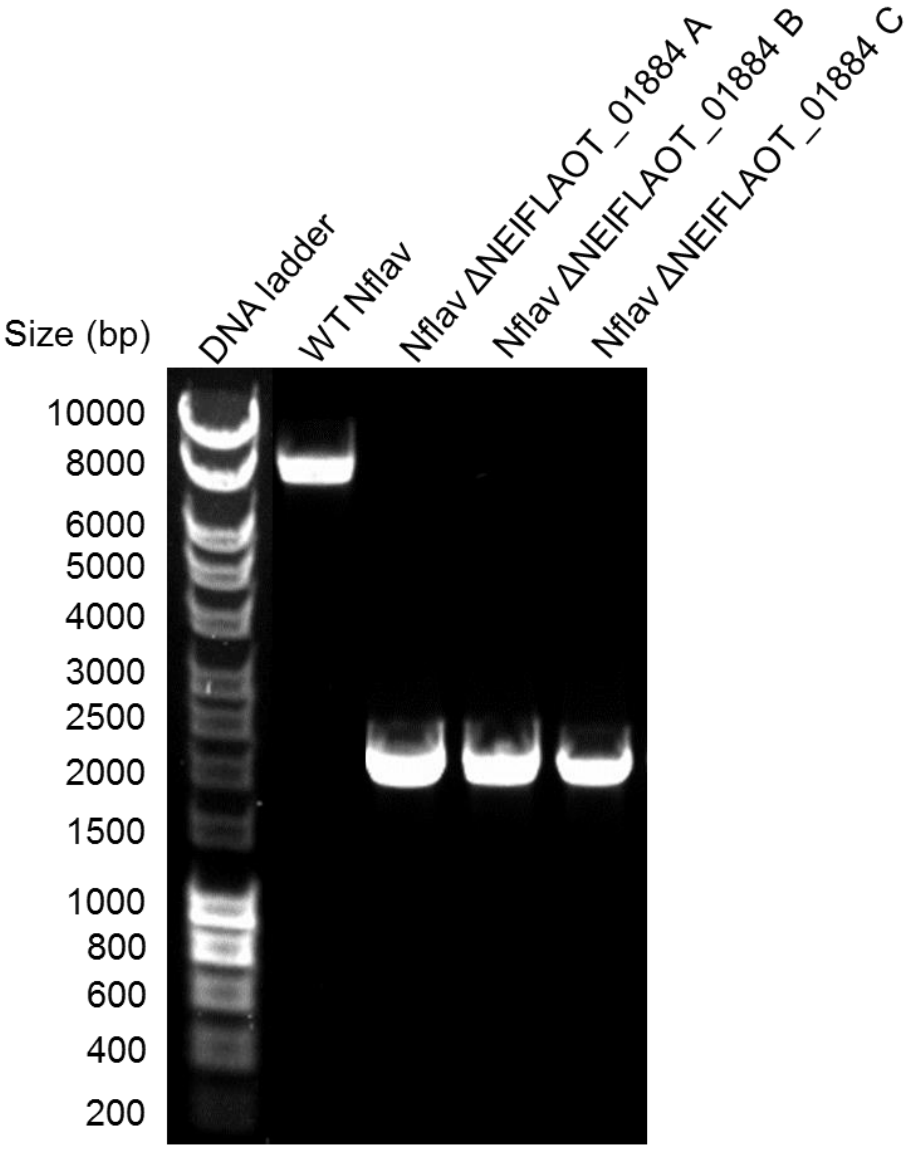

Figure 54 PCR products amplified from genomic DNA of wild-type *N. flavescens* and *N. flavescens* ΔNEIFLAOT_01884 A, B and C.

Three transformed colonies were grown overnight in the presence of spectinomycin and genomic DNA was extracted from overnight cultures. Extracted DNA from three candidates (ΔNEIFLAOT_01884 A, B and C) (lane 3, 4 and 5) was used as the template for the PCR amplification of ΔNEIFLAOT_01884 ORF with primers flanking ΔNEIFLAOT_01884 ORF. The PCR product of WT *N. flavescens* was used for comparison (lane 2). A DNA ladder with known sequence length was added in lane 1 to confirm the approximate size of the PCR products.

5.4.9 Investigating the proliferation of CD19+ IgDλ+ cells in response to dOMVs from knockout strains *N. cinerea* ΔNEICINOT_03770, *N. flavescens* ΔNF_12978 and *N. polysaccharea* ΔNP_11136

Following the isolation of successful knockouts, the mitogenic properties of *N. cinerea* ΔNEICINOT_03770, *N. flavescens* ΔDYC64_RS10620 and *N. polysaccharea* ΔNEIPOLOT_RS07545 dOMVs were tested, to find out whether the knocked-out genes play a role in the induction of proliferation in CD19+IgDλ+ B cells.

CFSE labelled PBMC were cultured in either media alone or in the presence of *N. cinerea* 346T, *N. cinerea* 346T ΔNEICINOT_03770, *N. flavescens* 17913T*, N. flavescens* 17913T ΔDYC64_RS10620*, N. polysaccharea* 18031T*, N. polysaccharea* 18031T ΔNEIPOLOT_RS07545 or *N. meningitidis* H44/76 dOMVs for 4 days. Results were acquired on day 4 using a flow cytometer.

Analysis of data from flow cytometry showed a clear loss of mitogenicity in *N. cinerea* ΔNEICINOT_03770 as ΔNEICINOT_03770 dOMVs resulted in significantly reduced levels of CD19+IgDλ+ B cell proliferation compared WT Ncin dOMVs (Figure 55).

dOMVs from *N. flavescens* ΔDYC64_RS10620 also lost the ability to induce proliferation in CD19+IgDλ+ and resulted in significantly reduced CD19+IgDλ+ B cell proliferation compared to WT Ncin dOMVs (Figure 55).

Similar to *N. cinerea* ΔNEICINOT_03770 and *N. flavescens* ΔDYC64_RS10620, *N. polysaccharea* ΔNEIPOLOT_RS07545 also displayed a clear loss of mitogenicity and resulted in a significantly reduced proliferation of CD19+IgDλ+ B cell population compared to WT Npol dOMVs (Figure 55).

Furthermore, dOMV from all 3 knockout strains did not induce significantly higher proliferation in λ light chain-expressing CD19+IgD+ cells compared to κ light chain expressers (Figure 55).

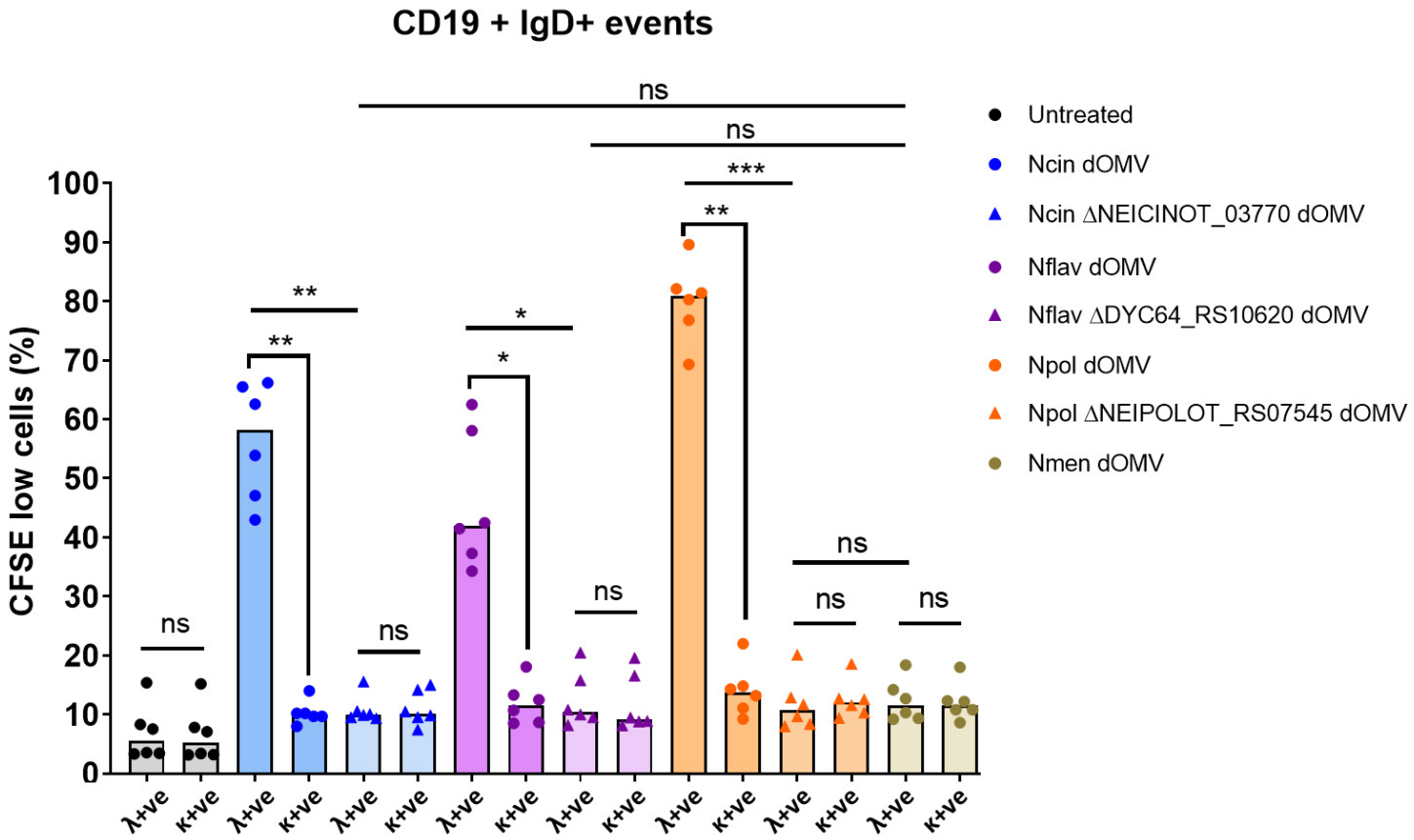

Figure 55 *N. cinerea* ΔNEICINOT_03770, *N. flavescens* ΔDYC64_RS10620 and *N. polysaccharea* ΔNEIPOLOT_RS07545 dOMVs do not induce proliferation in IgDλ+ B cells.

Percentage of dividing CD19+IgD+ cells expressing k or λ light chain in response to stimulation with *N. cinerea* 346T, *N. cinerea* 346T ΔNEICINOT_03770, *N. flavescens* 17913T, *N. flavescens* 17913T ΔDYC64_RS10620, *N. polysaccharea* 18031T, *N. polysaccharea* 18031T ΔNEIPOLOT_RS07545 and *N. meningitidis* H44/76 dOMVs. Results were acquired on day 4 using a flow cytometer. The peak height of the bars represents the median values of 6 repeated experiments on PBMCs from individual donors. Groups were analysed using Friedman test with Dunn's correction for multiple comparisons. * P ≤ 0.05, ** P ≤ 0.01, *** P ≤ 0.001 and ns P > 0.05.

5.4.10 Investigating the proliferation of CD19+ IgDλ+ cells in response to dOMVs from knockout strains *N. cinerea* ΔNEICINOT_03770, *N. cinerea* ΔNEICINOT_04577 and *N. flavescens* Δ01884

Deoxycholate-extracted OMVs from *N. cinerea* ΔNEICINOT_03770, *N. cinerea* ΔNEICINOT_04577 and *N. flavescens* Δ01884 were tested for the ability to induce proliferation in CD19+IgDλ+ B cells.

CFSE labelled PBMC were cultured in either media alone or in the presence of *N. lactamica* Y92-1009, *N. meningitidis* H44/76, *N. cinerea* 346T, *N. cinerea* 346T ΔNEICINOT_03770, *N. cinerea* 346T ΔNEICINOT_04577, *N. flavescens* 17913T or *N. flavescens* 17913T Δ01884 dOMVs for 4 days. Results were acquired on day 4 using a flow cytometer.

Analysis of data from flow cytometry showed a clear loss of mitogenicity in *N. cinerea* ΔNEICINOT_03770 as ΔNEICINOT_03770 dOMVs resulted in significantly reduced levels of CD19+IgDλ+ B cell proliferation compared WT Ncin dOMVs (Figure 56).

dOMVs from *N. cinerea* ΔNEICINOT_04577 also displayed loss of mitogenicity and resulted in significantly reduced CD19+IgDλ+ B cell proliferation compared to WT Ncin (Figure 56).

N. flavescens Δ01884 dOMVs also lost the ability to induce proliferation and induced significantly low-level CD19+IgDλ+ B cell proliferation compared to WT Nflav dOMVs (Figure 56).

Furthermore, dOMV from all 3 knockout strains did not induce significantly higher proliferation in λ light chain-expressing CD19+IgD+ cells compared to κ light chain expressers (Figure 56).

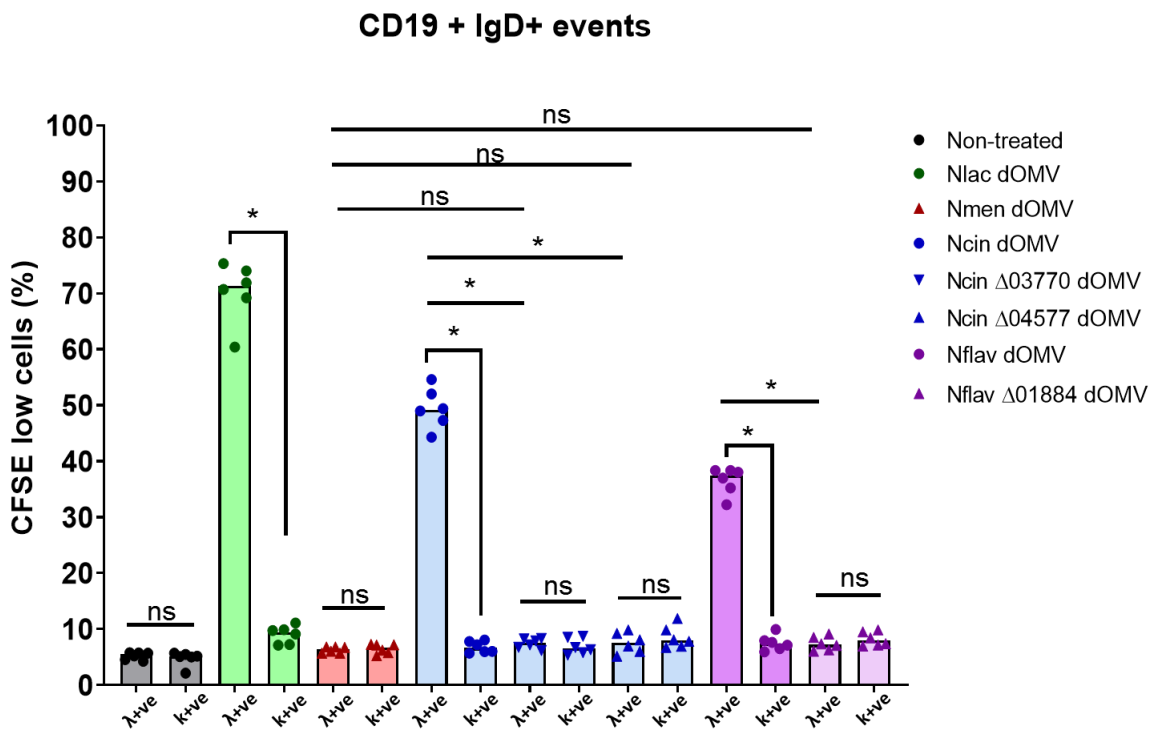

Figure 56 *N. cinerea* ΔNEICINOT_03770, *N. cinerea* ΔNEICINOT_04577 and *N. flavescens* Δ01884 dOMVs do not induce proliferation in IgDλ+ B cells.

Collated data showing percentage of dividing CD19+IgD+ cells expressing k or λ light chain in response to stimulation with *N. lactamica* Y92-1009, *N. meningitidis* H44/76, *N. cinerea* 346T, *N. cinerea* 346T ΔNEICINOT_03770, *N. cinerea* 346T ΔNEICINOT_04577, *N. flavescens* 17913T and *N. flavescens* 17913T Δ01884 dOMVs. Results were acquired on day 4 using a flow cytometer. The peak height of the bars represents the median values of 6 repeated experiments on PBMCs from individual donors. Groups were analysed using Friedman test with Dunn's correction for multiple comparisons. * $P \leq 0.05$ and ns $P > 0.05$.

5.4.11 Summation of knockout data

It was decided to knock out the MID homologues identified in chapter 4.4.1, from the strains that were mitogenic for CD19+IgDλ+ B cells. Subsequently, the dOMVs from the knockout strains was tested for their ability to induce proliferation of CD19+IgDλ+ B cells. The knockout strains generated throughout this project are listed in Table 51. The results showed that in the case of *N. lactamica* double mutants were needed for full inhibition of B cell proliferation, but single mutants were sufficient in *N. cinerea* and *N. flavescens* spp. Moreover, *N. polysaccharea* also lost the ability to induce proliferation upon knockout of its only MID homologue.

Table 51 Summary of the generated knockout strains and their mitogenic property.

No.	Knockout strain	Mitogenic for B cells
1	*Neisseria lactamica* Y92-1009 ΔNLY_37260	Yes
2	*Neisseria lactamica* Y92-1009 ΔNLY_36660	Yes
3	*Neisseria Lactamica* Y92-1009 ΔNLY_37260, ΔNLY_36660 (DM)	No
4	*Neisseria cinerea* 346T ΔNEICINOT_03770	No
5	*Neisseria cinerea* 346T ΔNEICINOT_04577	No
6	*Neisseria flavescens* 17913T ΔDYC64_RS10620	No
7	*Neisseria flavescens* 17913T ΔNEIFLAOT_01884	No
8	*Neisseria polysaccharea* 18031T ΔNEIPOLOT_RS07545	No

5.4.12 Insertion of NLY_37260 gene back in *N. lactamica* ΔNLY_36660 ΔNLY_37260 DM strain complementation

It was decided to insert NLY_37260 gene into ΔNLY_36660 ΔNLY_37260 DM strain as it has a higher percentage identity with MID (aa962-1200) compared to NLY_36660 gene. In order to insert the NLY_37260 gene into the chromosome of *N. lactamica* DM by homologous recombination, the procedure outlined in (Figure 57) was followed. Insert containing a promoter, NLY_37260 gene, chloramphenicol resistance gene for selection and homologous regions flanking the insertion site was designed. The insert was combined with PUC19 plasmid by the isothermal assembly and transformed in *E. coli* DH5α. The plasmid from the transformed *E. coli* was used for complementation of 37260 gene. However, attempts to complement NLY_37260 gene were unsuccessful as no colonies were observed on the selection plate.

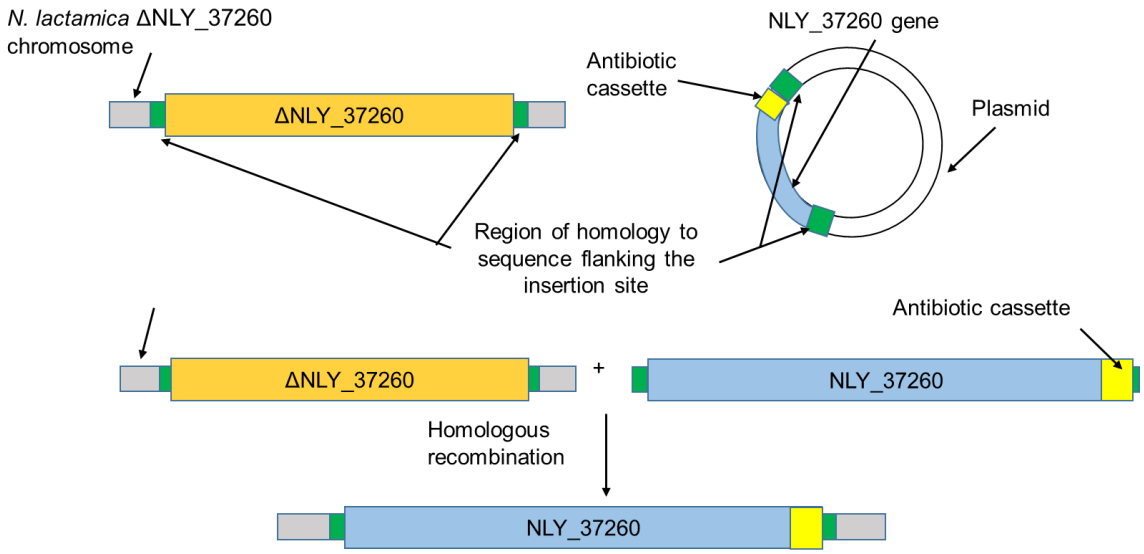

Figure 57 Overview of *N. lactamica* NLY_37260 complementation strategy.

An insert containing the chloramphenicol resistance gene + NLY_37260 incorporated within the homologous sequence to the region flanking the insertion site on the chromosome of *N. lactamica* Δ3660 ΔNLY_37260 DM was designed. The insert was combined with PUC19 plasmid by isothermal assembly and transformed in *E. coli* DH5α. The plasmid from the transformed *E. coli* was used to attempt insertion of NLY_37260 into the chromosome of *N. lactamica* Δ3660 ΔNLY_37260 DM. Transformed colonies were selected on chloramphenicol + TSB plates.

5.5 Discussion

5.5.1 Putative trimeric autotransporter adhesins in *N. lactamica* Y92-1009 and their effect on the ability to induce proliferation in IgDλ+ B cells

A particular asset in the research described in this chapter is the availability of *N. lactamica* ΔNLY_36660, *N. lactamica* ΔNLY_37260 and *N. lactamica* ΔNLY_36660 ΔNLY_37260 DM strains. It was postulated that both 36660 (3,425aa, mass: ~353.4KDa, 47% identical to IgD binding part of MID) and ΔNLY_37260 (3,398aa, mass: ~351KDa, 31% identical to IgD binding part of MID) genes encode an IgD binding protein. In accordance with this hypothesis, the DM strain failed to stimulate B cells while both knockout strains continued to induced B cell proliferation. This suggests that *N. lactamica* contains two IgD binding proteins, with redundancy between them. Furthermore, A488-labelled dOMV from *N. lactamica* ΔNLY_36660 induced a significantly reduced MFI in IgDλ+ B cells compared to ΔNLY_37260. However, there was no significant difference in the percentage of proliferation induced by the dOMV of these strains suggesting the difference in MFI between the two knockout strains is probably due to the level of adhesin expression.

5.5.2 Putative trimeric autotransporter adhesins in *N. cinerea*, *N. flavescens* and *N. polysaccharea* and their effect on the ability to induce proliferation in IgDλ+ B cells

Having observed a phenotypic change in the Nlac knockout strains the effect of knocking out MID homologues on mitogenic strains from various *Neisseria* species was investigated. MID homologous genes in mitogenic *Neisseria* were knocked out and putative ΔIgDbp *Neisseria* strains (Ncin ΔNEICINOT_03770, Ncin ΔNEICINOT_04577, Nflav ΔDYC64_RS10620, Nflav Δ01884 and Npol ΔNEIPOLOT_RS07545) were successfully generated. Strikingly, dOMVs from all knockouts lack the ability to induce proliferation in CD19+IgD+ cells. It is therefore deduced that there is an association between MID homologous genes present in the mitogenic *Neisseria* spp and the ability to induce proliferation in CD19+IgD+ cells.

However, an important point to be noted is that unlike *N. lactamica* knockouts where single knockouts continued to be mitogenic and only DM lost the ability to induce proliferation in CD19+IgD+ cells, in Ncin and Nflav knocking out either MID homologue resulted in failure to induce proliferation despite retaining the second MID homologue. Perhaps, Ncin and Nflav require the presence of both putative TAA proteins might be

required for the proteins to function correctly. Alternatively, the TAAs present in Ncin and Nflav might have low affinity for the target site compared to Nlac TAAs. This would imply that only in the presence of the two TAAs is the bacterium able to reach the required threshold to induce proliferation in IgDλ+ B cells and loss of either gene would result in the failure to reach that threshold.

5.5.3 Complementation of NLY_37260

The *Neisseriaceae* are naturally competent and undergo natural transformation due to horizontal gene transfer (Hamilton and Dillard, 2006; Duffin and Seifert, 2010; Spencer-Smith *et al.*, 2016). Naturally-competent bacteria take up the insert DNA and incorporate it in its chromosome via homologous recombination resulting in transformed colonies. However, the understanding of genetic competence in *Neisseria* is predominantly based on research performed using *N. meningitidis* and *N.gonorrhoeae* and does not necessarily apply to *N. lactamica*. Furthermore, genetic manipulation of *N. lactamica* is very challenging using the protocol that was successful for other *Neisseria* spp*. as in vitro* attempts to transfer pMIDG100 into a total of 53 *N. lactamica* strains were unsuccessful (O'Dwyer C *et al.*, 2004). Therefore, in order to complement NLY_37260 gene similar procedure to gene knock-out experiments (section 5.4.4-8) was adapted. However, attempts to complement NLY_37260 gene were unsuccessful.

Several factors affect the efficiency with which DNA can be transformed and recombined. The lack of DNA uptake sequences, length of sequence homology necessary for efficient recombination and restriction enzymes can degrade unmethylated or improperly methylated DNA in the cytoplasm before its recombination into the genome (Matsumoto and Igo, 2010; Kung *et al.*, 2013). However, since the construct was designed considering these factors, the reason for unsuccessful transformation is most likely due to the large size (~10000 bp) of the gene. The total size of transforming DNA can also affect recombination efficiency as it has been shown in *R. solanacearum* which can naturally transform and recombine 90 kb of DNA, but efficiencies were 3-fold lower than when the transforming DNA was 1 kb in length (Coupat *et al.*, 2008).

6. Final Discussion

In this project, the following discoveries have been made:

- Deoxycholate-extracted OMVs from *N. lactamica, N. cinerea, N. flavescens* and *N polysaccharea* induce proliferation in CD19+IgDλ+ B cells.
- Deoxycholate-extracted OMVs from *N. elongata, N. subflava, N. mucosa, N. macacae, N. gonorrhoea* and *N. meningitidis* are unable to induce a mitogenic response in B cells.
- The proliferative response in IgDλ+ B cells is dependent upon interaction with IgDλ BCR, as blocking of IgD and λ light chain with Ab results in a significant reduction in dOMV-induced proliferation.
- Incubation with A488-labelled dOMVs of Nlac and Ncin results in a significantly higher MFI in IgDλ+ B cells compared to IgDκ+ B cells. Whereas, PBMC incubation with A488-labelled dOMVs from Nmen does not achieve high MFI suggesting the response is specific to proliferation-inducing *Neisseria* spp.
- *N. lactamica, N. cinerea. N. flavescens, N. polysaccharea, N. subflava, N. elongata* and *N. meningitidis* contain at least one MID homologue. Whereas, *N. mucosa, N. macacae, N. bacilliformis* and *N. gonorrhoeae* either completely lack MID homologues or are very weakly homologous.
- The MID homologues present in *N. lactamica* Y92-1009, *N. lactamica* ATCC 23970, *N. cinerea* 346T, *N. subflava* 23930T, *N. elongata* 2043T and *N. meningitidis* H44/76 are transcribed. Furthermore, the level of transcription is similar or higher than that of NLY_37260 (*N. lactamica* Y92-1009).
- Knockout strains lacking MID homologue/s lack the ability to induce B cell proliferation. However, in the case of *N. lactamica* single knockout retained the ability to induce proliferation in IgDλ+ B cells, albeit at lower levels.

6.1 Importance of understanding mechanisms of *N. lactamica* commensalism in the prevention of meningitis

From birth, mucosal epithelia of human beings are colonised by diverse commensal organisms, which reside in the mucosae for prolonged periods without causing disease in healthy individuals. The colonisation of human mucosal surfaces by commensal bacteria is believed to protect against potentially pathogenic bacteria by presenting competition for nutrients, environmental niche and cognate receptors (Turnbaugh *et al.*, 2007; Zhang and He, 2015; Bosch *et al.*, 2016; Blacher *et al.*, 2017). *Neisseria m*eningitidis is carried asymptomatically by 10% of the adult population but under certain circumstances can

cause invasive disease leading to septicaemia and meningitis (Bernardini *et al.*, 2004; Lo, Tang and Exley, 2009; Aspholm *et al.*, 2010). *N. meningitidis* has been shown to down-regulate various host defence genes, such as those encoding antimicrobial peptides (e.g. PI3 and LCN2) and complement components (e.g. C1S), as a strategy to maintain colonisation (Wong *et al.*, 2011). This may also explain why *N. meningitidis* has the potential to cause invasive disease in an environment where host defences are compromised. In contrast, *Neisseria lactamica* is a commensal bacterium that resides in the URT of healthy infants and children without causing disease. The benign nature of *N. lactamica* infection is principally due to the lack of a polysaccharide capsule, which is the major virulence determinant of the meningococcus. *N. lactamica* is remarkable in that it can colonise the nasopharynx of infants and adults for prolonged periods. Furthermore, unlike *N. meningitidis*, *N. lactamica* does not downregulate the host defence genes, as indicated by activation of genes such as TNF-α, IL1A and IL-8, and that the expression of these cytokines may alert the host to its presence and potentially prevent or limit the bacterium from entering the blood and causing invasive disease (Wong *et al.*, 2011). Despite this response, *N. lactamica* continues to colonise the URT, likely due to an upregulation of genes such as KLF6 that regulate and prevent an over activation of the proinflammatory response so that the commensal is not cleared completely by the host (Wong *et al.*, 2011).

Data from carriage studies have demonstrated an inverse relationship between URT carriage of *N. lactamica* and *N. meningitidis.* In contrast to the carriage of *N. lactamica* which is high in young children but declines with age, meningococcal carriage increases (Gold *et al.*, 1978; Cartwright *et al.*, 1987). It has been theorized that this inverse relationship was due to the development of SBA to *N. lactamica* antigens that are cross-reactive to MenB antigens (Goldschneider, Gotschlich and Artenstein, 1969a;b; Kremastinou et al., 1999; Troncoso et al., 2002). Cross-reactive immunity has been shown in mice where immunization by *N. lactamica* OMV-based vaccine protected the mice against lethal challenge with serogroup B and C meningococcal isolates, however, this effect was not due to the induction of cross-reactive SBA (Oliver *et al.*, 2002). Furthermore, experimental data from the mouse studies have shown that *N. lactamica* vaccines comprising OMVs or whole killed bacterial cells elicit protection in mice against disseminated meningococcal disease without detectable SBA (Li *et al.*, 2006). Based on the previous studies it can be purported that *N. lactamica* induces a humoral immune response, but in contrast to the carriage of the meningococcus, *N. lactamica* carriage does not induce bactericidal antibodies, although the opsonophagocytic activity of serum is elicited (Evans *et al.*, 2008; Evans *et al.*, 2011).

Understanding the mechanism(s) through which *N. lactamica* prevents meningococcal colonisation would allow the development of new approaches to protect against meningococcal disease. If the mechanism is revealed to be cross-reactive immunity, this knowledge could be utilized to develop vaccines that could prevent meningococcal colonisation and thereby also prevent meningococcal disease.

6.2 The potential role of mitogenic responses in maintaining homeostasis of commensal bacteria

In this thesis, it has been argued that *N. lactamica* induces a mitogenic response in B cells which generates immunoglobulin capable of coating the surface of commensals. Whether this occurs *in vivo* has not been shown.

I have shown that there is a B cell proliferative response to *N. lactamica* which is due to the interaction between a putative IgD binding protein present on the surface of *N. lactamica* and IgD on the surface of the B cell. Other bacteria with known IgD binding proteins such as *Moraxella catarrhalis*, induce T independent B cell proliferation via the IgD binding protein. This B cell activation results in the production of IgM Abs, which are not directed against *Moraxella* suggesting this IgM secretion has a facilitatory role in Mcat pathogenesis (Perez Vidakovics *et al.*, 2010). *Haemophilus influenzae* dOMVs have also been shown to induce proliferation in B cell, which is abrogated upon pre-treatment with anti-IgD Ab. Furthermore, OMVs from both strains have been shown to bind to B cells. However, pre-treatment of B cells with anti-IgD Ab failed to inhibit the binding of dOMV from NTHi KR403. This suggests that another molecule on the surface of B lymphocyte might contribute to the binding of OMV derived from NTHi KR403 (Deknuydt, Nordstrom and Riesbeck, 2014). Furthermore, it has been shown that myeloma proteins bind strongly to type b MinnA strain but failed to bind to *E. coli* expressing recombinant protein D from *H. influenzae* suggests that protein D is not sufficient for IgD binding to type b strains (Sasaki and Munson, 1993).

My early results suggest that Nlac and Ncin both commensal species belonging to the *Neisseria* genus are also B cell activators. I have shown that dOMVs from *N. lactamica* induce proliferation in IgDλ+ B cells. This suggests that either the putative IgDbp specifically targets the λ light chain-expressing CD19+IgD+ cells or it could be the case that λ light chain-expressing B cells are more prone to proliferation by mitogens. Furthermore, PWM induced high levels of proliferation in both IgDλ and IgDκ expressing B cells suggests that perhaps Nlac dOMVs are specifically targeting the IgDλ+ B cells rather than λ light chain-expressing cells being more prone to proliferation compared to κ light

chain expressers (Figure 16). Based on the co-localisation fluorescence assay (Figure 20; Figure 23), I hypothesise that *N. lactamica* expressing a putative IgDbp co-localises with both λ and κ light chain-expressing B cells but is endocytosed by only λ light chain-expressing B cells. This results in accumulation of dOMV or whole bacteria inside the B cells providing a prolonged signal resulting in proliferation.

I also surveyed the other commensal species in the genus *Neisseria* and showed that in addition to *N. lactamica* and *N. cinerea* 346T*, N. flavescens* 17913T and *N. polysaccharea* 18031T are also capable of inducing proliferation in CD19+IgDλ+ cells. The ability to induce proliferation in CD19+IgDλ+ cells by other commensal *Neisseria* spp. suggests that mitogenicity is not strictly a pathogenic property as previously suggested (Janson *et al.*, 1991). Furthermore, conservation of this property in other *Neisseria* spp. implies that it may play a key role in the host-commensal interactions, and may benefit the bacteria, as otherwise this property would not have been conserved due to metabolic burden.

Of great interest, controlled human infection with *N. lactamica* (Deasy *et al.*, 2015) and subsequent investigation of its genome has shown mutation in the large hypothetical protein NLY_37260 in 27% of the human subjects who were colonised (Pandey *et al.*, 2018). This large hypothetical protein includes regions homologous to MID binding protein. Furthermore, NLY_37260 and NLY_36660 genes both induce proliferation in IgDλ B cells. Together, these data indicate that the NLY_37260 gene might be an important gene for the initial colonization period. However, since there is redundancy between NLY_37260 and NLY_36660 gene after initial colonization there is a reduced focus on the conservation of NLY_37260 gene.

In the gut, B cell mitogens present in the commensal flora are responsible for mediating the T-independent IgA response in the intestine which prevents overgrowth of flora and maintains homeostasis in the gut (Hooper and Gordon, 2001). Similarly, activating naive B cells using IgD binding protein by the commensal flora of URT could be a strategy to evade the adaptive immune system.

In contrast to memory B cells which can be activated by cytokines and CPG without any BCR stimulation, human naïve B cells depend on BCR signalling. Previous studies have shown that naïve B cells fail to proliferate only in the presence CPG, However, the same cells are activated when BCR is stimulated in conjunction with CPG (Bernasconi, Traggiai and Lanzavecchia, 2002; Jiang *et al.*, 2007). Upon invasion by a foreign antigen, the professional APCs such as dendritic cells and macrophages engulf the antigen, resulting in an immune response by producing various cytokines and by presenting antigen to T cells in the context of MHC. BAFF is one of the main cytokines that activate B cells and is also activated by TLR9 activation (Schneider and Tschopp, 2003). BAFF-induced B cell

proliferation has been observed in the presence of *M. catarrhalis* OMVs, as the OMVs containing DNA-induced TLR9 signalling, which was found to synergise with antigen-induced BCR signalling (Perez Vidakovics *et al.*, 2010). More evidence for TLR9-induced B cell proliferation comes from a study where B cell proliferation induced by *H. influenzae* OMV was shown to decrease by >50% in the presence of TLR9 antagonist, suggesting a key role for TLR9 in the OMV-dependent B cell proliferative response (Deknuydt, Nordstrom and Riesbeck, 2014). In another study, it was shown that BCR crosslinking induces up-regulation of TLR9 on naive B cells, which consequently makes B cells more sensitive to CpG motifs (Bernasconi, Onai and Lanzavecchia, 2003).

It is proposed here that interaction between the IgDbp present in Nlac, Ncin, Nflav and Npol OMVs with IgD-BCR induces B cell activation. The interaction between the putative IgDbp and the IgD-BCR would result in the antigen-BCR complex being internalised by the B cell. Studies have shown that in addition to deoxycholate-extracted OMVs, naturally secreted OMVs also contain bacterial DNA (Renelli *et al.*, 2004; Perez-Cruz *et al.*, 2015; Bitto *et al.*, 2017) and that the internalized BCR signals recruit TLR-containing endosomes to the autophagosome (Chaturvedi, Dorward and Pierce, 2008). As discussed earlier, in the endosome, the DNA containing dOMVs would activate TLR9 providing a supplementary signal in addition to the BCR signal. This may cause the B cells to proliferate and differentiate into short-lived plasma cells (Jendholm *et al.*, 2008). Short-lived plasma cells secrete IgM Ab which may bind to Nlac OMV or whole bacteria on the nasopharyngeal epithelium, preventing overgrowth and maintaining homeostasis in the same way as sIgA binds to commensal spp. to maintain homeostasis of the intestinal epithelium (Macpherson *et al.*, 2000; Macpherson, Geuking and McCoy, 2005).

The functional importance of IgD has been shown in a study exploring the relationship between the CXCR4 signal and IgD-BCR. Their investigation revealed that the B cells from IgD-deficient but not IgM-deficient mice displayed abrogation of CXCL12-mediated CXCR4 signalling and B-cell migration (Becker *et al.*, 2017). The fact that CXCR4 function is hindered in the absence of IgD-BCR suggests that IgD plays an important role in maintaining homeostasis of the B cells.

It has been shown that a B cell population expressing IgD+IgM-CD38+ cell markers are resident in the respiratory mucosal environments and can be found in the lymphoid tissues, tonsils, nasal cavities, lachrymal gland and salivary gland (Vladutiu, 2000; Chen and Cerutti, 2010). Furthermore, human but not mouse IgD+IgM− B cells have been shown to preferentially utilize the λ light chain instead of the more common κ light chain (Gutzeit, Chen and Cerutti, 2018). These IgD+IgM− B cells differentiate into antibody-secreting cells, producing soluble IgD (Chen *et al.*, 2009; Loh, Vale and McLean-Tooke,

2013). In normal serum, IgD concentration is only 0.2% of total Ig molarity, (Loh, Vale and McLean-Tooke, 2013). However, large numbers of local IgD secreting plasma cells have been observed in human bronchus-associated lymphoid tissue and tonsils (Forsgren and Grubb, 1979). In tonsils, the IgD+IgM−ve B cell subgroup accounts for up to 20-25% of plasma cells and about 1.5-5% of total CD19+ B cells (Chen *et al.*, 2009). This compartmentalisation suggests that IgD might be involved in the local immune response. The secreted IgD or IgM in response to IgDbp perhaps coats the bacteria thereby shielding its MAMPs, which reduces the cellular activation and prevents the stimulation of a prolonged adaptive immune response. This is beneficial to the host as this would prevent induction of local inflammatory cytokine production which could otherwise cause damage to the host tissue. As discussed in chapter 1, sIgA provides a defence against harmful gut microbiota by limiting bacterial association with the epithelium and preventing bacterial penetration of host tissue. Similarly, IgM Ab bound to Nlac dOMV or whole bacteria would also partake in complement fixation resulting in marking the bacterium with C3b for phagocytosis by macrophages (Figure 58). Both these strategies would keep the bacterial population in check and prevent it from appearing as a threat, thus allowing it to evade a prolonged adaptive immune response and complete elimination.
It is apparent that colonisation by *N. lactamica* protects against meningococcal disease and results in a humoral immune response that is qualitatively different from the immune response to *N. meningitidis* (Gold *et al.*, 1978; Cartwright *et al.*, 1987; Olsen *et al.*, 1991; Kremastinou *et al.*, 2003; Gorringe, 2005). I hypothesise that an adaptive cross-reactive immune mechanism, independent of SBA, is responsible for *N. lactamica* protection against meningococcal disease.

Nlac dOMV induced B cell proliferation has been shown to be T-independent (Vaughan *et al.*, 2010) which suggests that similar to Mcat dOMV induced TI B cell proliferation (Perez Vidakovics *et al.*, 2010) Nlac might also utilize the simultaneous signal from BCR and activation of TLR9 in order to induce B cell proliferation in a T-independent manner (Figure 58). Furthermore, there is also evidence suggesting that the human innate B cell subset are able to produce other Ig classes besides IgM in a T-independent manner, as studies using *SCID* mice repopulated with human IgM memory B cells showed that both IgM and IgG were produced in response to vaccination with either polysaccharide vaccine or heat-killed bacteria (Moens *et al.*, 2008). However, B cells also partake in antigen presentation to CD4 T cells so the initial TI B cell stimulation could lead to T-dependent B cell proliferation and class switch Abs (Figure 59). It has been shown that protection against URT colonisation with *S. pneumoniae* in mice is instead dependent upon the induction of CD4+ T-cell responses of Th17 effector phenotype (Malley et al., 2005; Moffitt et al., 2011; Trzcinski et al., 2005; Zhang et al., 2009). In a similar way, colonisation by

Nlac resulting in the priming of TI B cell proliferation could lead to T cell-dependent B cell proliferation resulting in class switching of secreted immunoglobulin. Alternatively, the TI B cell response primed by Nlac colonisation resulting in low-level antibody-mediated response could be shielding the bacterium from complement-mediated-killing. In this thesis, various hypotheses relating to commensal Nlac behaviour whilst remaining colonised (despite inducing a proliferative response) have been tested. However, to narrow down these hypotheses the Ig class secreted in response to Nlac colonisation needs to be investigated. This paradigm could be tested in a human challenge model, but for now, will have to remain a hypothesis.

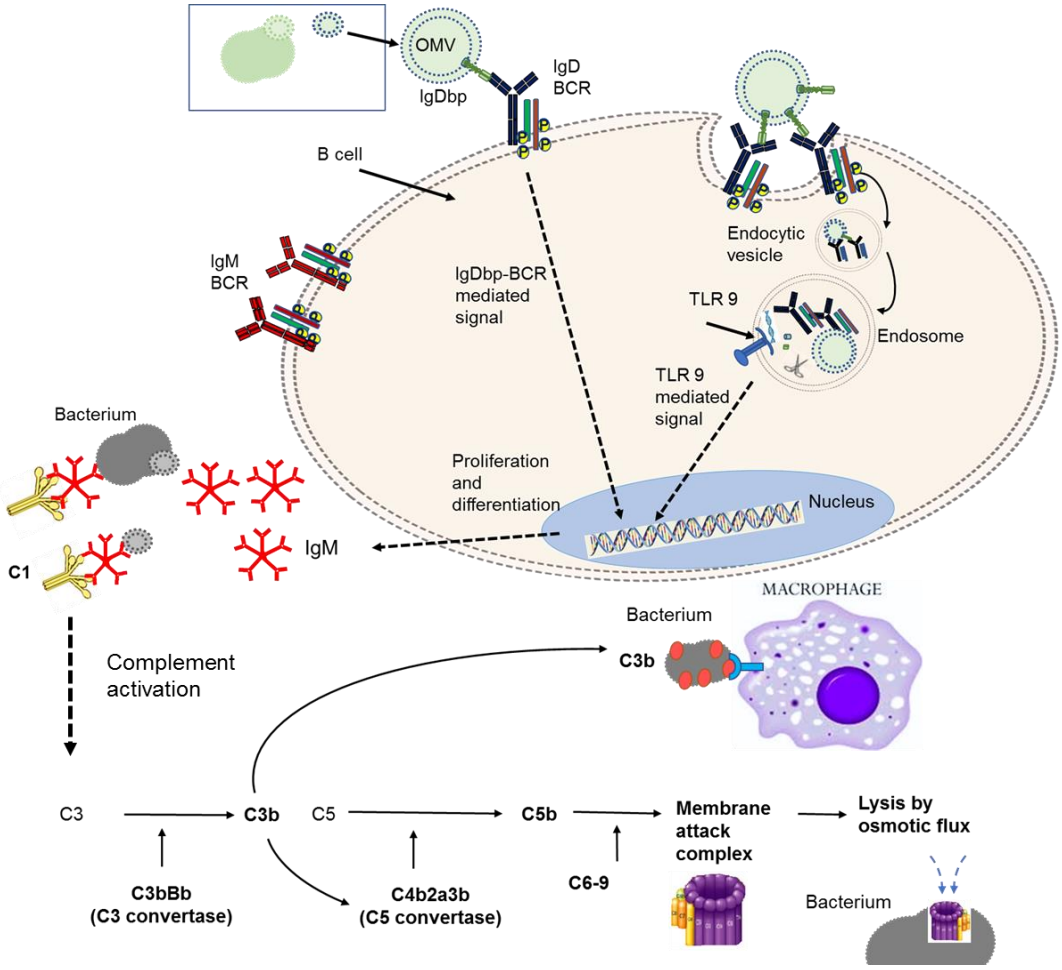

Figure 58 Hypothetical model to explain the B cell proliferation in response to *N. lactamica*, *N. cinerea*, *N. flavescens* and *N. polysaccharea* and its potential downstream role.

Binding of IgDbps present on the dOMV from *N. lactamica, N. cinerea, N. flavescens* or *N. polysaccharea* with IgD-BCR results in internalisation of the antigen-BCR complex by receptor-mediated endocytosis. The IgD-BCR complex is transported to the endosome where it is degraded by lysosomal enzymes. In the endosome, the DNA-containing dOMV activates TLR9 providing a supplementary signal in addition to the initial signal caused by BCR activation. Together these signals are enough to drive B cells to proliferate and differentiate into short-lived plasma cells in a T-independent manner. Short-lived plasma cells could secrete IgM Ab which could partake in complement fixation. IgM Ab binds via its Fc region to the C1 complex resulting in the initiation of the Classical pathway of complement. Complement activation results in the formation of C3 convertase which cleaves C3b. C3b coats the bacterium allowing it to be recognised by macrophages for phagocytosis. Complement activation also results in the formation of C5 convertase which cleaves C5b which joins with C6-9 forming membrane attack complex (MAC). MAC can then attach to the bacterium resulting in cell death by osmotic flux.

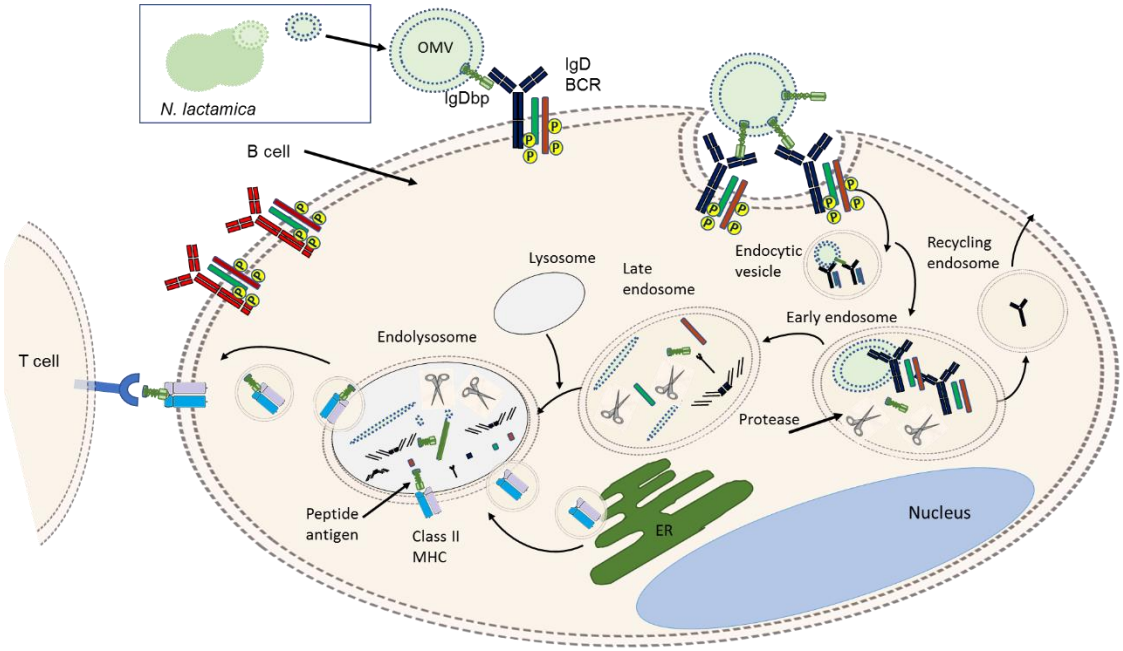

Figure 59 B cells prime naïve CD4 T cells by presenting antigen via class II MHC complex.

OMV from Nlac containing IgDbp binds to the IgDλ BCR. Antigen engagement with the BCR results in 2 simultaneous processes, signal induction and BCR-antigen complex endocytosis. Enzymes within the B cells degrade the antigens into smaller peptides and load it onto MHC class 2 molecule for presentation. These B cells can then perform the role of antigen presenting cells and activate CD4 T cells. Activated CD4 T cells will release interleukins which will activate the B cells resulting in proliferation, class switch recombination leading to production of memory B cells and plasma cells. The plasma cells will then secrete Abs which can bind to the bacterium tagging it for opsonisation and phagocytosis. Moreover, these secreted Abs will activate classical path of complement and prevent overgrowth of the bacterium (Chen and Jensen, 2008).

6.3 Future work

This investigation has generated several avenues of future work.

6.3.1 Perform complementation for knock-out strain/strains

Complementation involves the reinsertion of the knocked-out gene back into the mutant strain lacking that gene. This is done to prove that the phenotypic change is in fact due to the absence of the knocked-out gene and not due to a mutation (van Dam and Bos, 2012).

For future work, the knocked-out genes from the proliferation-inducing strains can be reinserted into the original loci in order to avoid interfering with the transcription at a different site on the chromosome. Additionally, reinsertion at the original site on the chromosome will provide a better comparison to the original WT strain.

Additionally, ΔNLY_37260 gene insertion into *N. polysaccharea* ΔNEIPOLOT_RS07545 can be attempted as throughout this project the genetic manipulation of *N. polysaccharea* was less challenging compared to *N. lactamica* (Figure 60). Furthermore, more DNA uptake sequences (DUS) can be incorporated into the insert as in literature a linear relationship between the number of DUS and the likelihood of transformation has been observed (Goodman and Scocca, 1991; Ambur *et al.*, 2012).

Following successful complementation, potentially interesting clones can be commercially sequenced to ensure that the insert has gone into the correct locus and the clone is free from mutations. Subsequently, to confirm whether the complemented strain has recovered its phenotype, a proliferation assay could be performed following the method described in chapter 2.16. If the proliferation assay shows that the dOMV from complemented strains to be mitogenic for CD19+IgDλ+ cells it would suggest that the gene encoding the putative IgDbp is involved in the induction of B cell proliferative response.

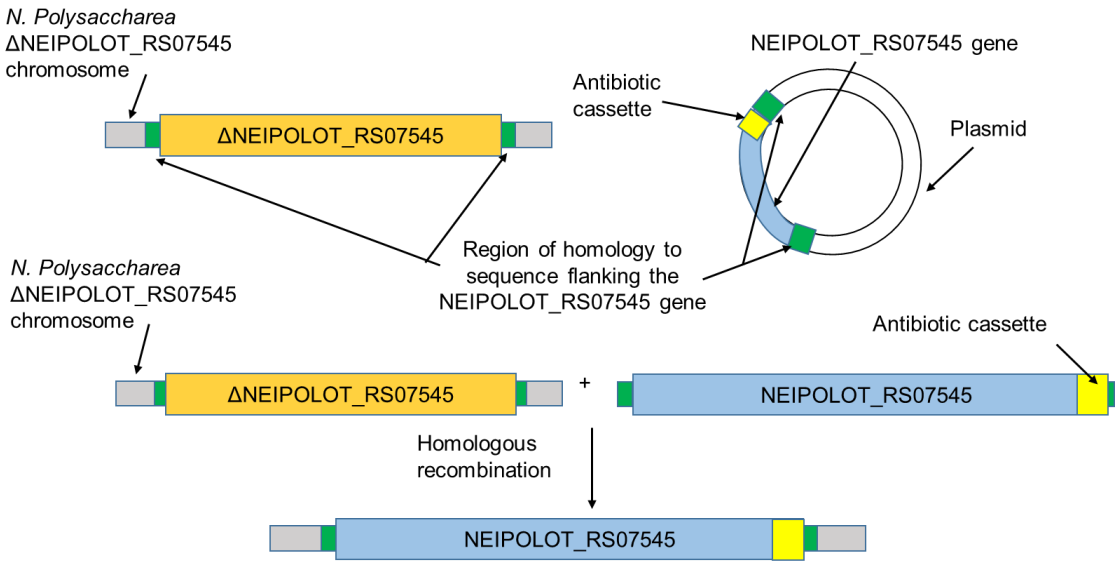

Figure 60 Overview of complementation strategy using *N. polysaccharea* as an example.

The gene of interest NEIPOLOT_RS07545 + antibiotic cassette incorporated within homologous sequence to the region flanking NEIPOLOT_RS07545 on the chromosome of WT *N. polysaccharea* is expressed in a plasmid. NEIPOLOT_RS07545 gene + antibiotic cassette is reintroduced into the *N. polysaccharea* ΔNEIPOLOT_RS07545 strain chromosome at its original locus. NEIPOLOT_RS07545 gene + antibiotic cassette replaces ΔNEIPOLOT_RS07545 by homologous recombination resulting in new strains with restored NEIPOLOT_RS07545 gene that is homologous to WT strains.

6.3.2 Identify the smallest functioning IgDbp fragment present in the mitogenic *Neisseria*

Based on homology to MID aa 962-1200 all putative IgDbp gene present in mitogenic *Neisseria* strains that colonize humans are approximately 3000 amino acid residues. In future, the smallest possible fragment of MID homologues with preserved IgDbp property could be identified. The putative IgDbp could be divided into small fragments covering the entire molecule and express the truncated IgDbp fragments into *E. coli* DH5α. All promising clones could then be commercially sequenced to avoid using a strain with a mutated gene of interest.
Subsequently, these strains can be tested for their mitogenic property towards IgDλ+ B cells in order to identify the smallest functioning IgDbp fragment. Identifying the exact region of IgDbp is important as it will ease the process of genetic insertion of IgDbp into a strain of choice due to the small sequence manipulation.

6.3.3 Investigate the molecular structure of NLY_37260

As part of future work, the molecular structure of NLY_37260 can be determined by X-ray crystallography. In order to do so, the protein will need to be cloned and expressed at sufficient levels for purification. Following purification, the purified protein can be crystallized using the appropriate crystallization solutions. Once the protein crystal has been generated the molecular structure of the crystallized protein can be determined by firing X-rays at the crystal and measure how they scatter (McPherson and Gavira, 2014). A similar procedure can be performed on other MID homologues in order to determine their molecular structures which will then allow the comparison of the differences between the 3D structure of these MID homologues.

6.3.4 Measuring expression levels of MID homologues

In this thesis, a semi-quantitative approach to gene expression was adopted and thus the results can only confirm the transcription of the target genes. Perhaps for future work, a quantitative method such as qPCR could be employed to investigate the levels of gene expression of target genes.

Ideally, the measurement of expression is done by detecting the final gene product i.e. protein using methods such as Western Blotting. However, a limitation of these

techniques is the need for an antibody specific to the protein of interest. As part of future work, the protein expression of MID homologues/putative TAA proteins could be investigated by Western blot. However, that would require detection antibodies specific for the protein of interest. Thus, to confirm the protein expression of these putative IgDbps, anti-IgDbp Ab will need to be generated. Another limitation is that reliance upon the new Abs makes this a lengthy process and an Ab that binds a naive protein may not be useful for detecting the denatured protein on a western blot.
Alternatively, a technique that does not require an antibody to a protein of interest e.g. Selected Reaction Monitoring (SRM) (Lange *et al.*, 2008) and Mass Western (Arnott *et al.*, 2002), which utilizes on mass spectrometry could be used to investigate the expression levels of MID homologues in future.

6.3.5 Investigate the natural ΔNLY_37260 *N. lactamica* Y92-1009 strains

Investigation of the *N. lactamica* Y92-1009 genome has shown mutations in the large hypothetical protein NLY_37260 in 27% of the human subjects who were colonised (Pandey *et al.*, 2018). As proposed in my thesis NLY_37260 is a putative IgDbp and includes regions homologous to MID binding protein. As part of future work, the strains isolated from the *N. lactamica* carriage study displaying NLY_37260 natural mutants could be characterised. The expression levels of NLY_37260 mutants could be measured and subsequently, the level of the mitogenic property could also be measured. Characterising the natural NLY_37260 mutants may provide insight into the region of NLY_37260 gene that is crucial for B cell mitogenicity.

6.3.6 Controlled human infection model

The knockout strains generated throughout this project may be used as tools to further explore the putative IgDλ binding protein present in commensal *Neisseria* spp and its effect on the immune response. In particular, the Nlac ΔNLY_36660 ΔNLY_37260 DM is of great importance as it can be used to investigate the different nature of WT Nlac compared to WT Nmen. As part of future work, a controlled human infection study could be carried out using a Control Human Infection Model (CHIM). Participants will need to be inoculated with WT Nlac and Nlac ΔNLY_36660 ΔNLY_37260 DM.

The colonization density can be measured for both strains to determine whether the IgDbp present in WT Nlac is helping the bacterium to remain colonised compared to DM lacking the putative IgDbp.

Samples of peripheral blood could be taken pre- and post-challenge to measure the plasma and memory cell responses of both test groups. If there is a high plasma cell response in DM colonised participants this would suggest that putative IgDbp of Nlac plays a key role in colonisation and prevention of clearance by the immune system.

The saliva and nasal washes of participants can be checked for anti-*lactamica* IgA, IgG, IgM and IgD Ig responses. Previously, carriers inoculated with WT Nlac strains have been shown to develop salivary IgA (Evans *et al.*, 2011); it would be interesting to find out whether this response will be present in the participants inoculated with DM strain. Lack of salivary IgA in response to Nlac would suggest an involvement of Nlac putative IgDbps in the generation of salivary IgA. Depending on the Ig class present in the salivary and nasal washes in response to the inoculum, various hypothesise can be generated to explain the mechanism of the commensal nature of Nlac. Moreover, the difference in the immune response to DM colonisation compared to WT Nlac would verify the importance of IgD BCR and IgDbp present in commensal *Neisseria* spp.

References

Agrawal, S. *et al.* (2013) 'Transitional B cell subsets in human bone marrow', *Clin Exp Immunol*, 174(1), pp. 53-9.

Ahmad-Nejad, P. *et al.* (2002) 'Bacterial CpG-DNA and lipopolysaccharides activate Toll-like receptors at distinct cellular compartments', *Eur J Immunol*, 32(7), pp. 1958-68.

al-Gahtani, Y.M. *et al.* (1995) 'Epidemiological investigation of an outbreak of meningococcal meningitis in Makkah (Mecca), Saudi Arabia, 1992', *Epidemiol Infect*, 115(3), pp. 399-409.

Allman, D. and Pillai, S. (2008) 'Peripheral B cell subsets', *Current opinion in immunology*, 20(2), pp. 149-157.

Ambur, O.H. *et al.* (2012) 'Restriction and sequence alterations affect DNA uptake sequence-dependent transformation in Neisseria meningitidis', *PLoS One*, 7(7), p. e39742.

Antiabong, J.F., Ngoepe, M.G. and Abechi, A.S. (2016) 'Semi-quantitative digital analysis of polymerase chain reaction-electrophoresis gel: Potential applications in low-income veterinary laboratories', *Veterinary world*, 9(9), pp. 935-939.

Armant, M.A. and Fenton, M.J. (2002) 'Toll-like receptors: a family of pattern-recognition receptors in mammals', *Genome Biology*, 3(8), pp. reviews3011.1-reviews3011.6.

Arnott, D. *et al.* (2002) 'Selective Detection of Membrane Proteins Without Antibodies', *Molecular & Cellular Proteomics*, 1(2), p. 148.

Aspholm, M. *et al.* (2010) 'Structural alterations in a component of cytochrome c oxidase and molecular evolution of pathogenic Neisseria in humans', *PLoS Pathog*, 6(8), p. e1001055.

Avalos, A.M. and Ploegh, H.L. (2014) 'Early BCR Events and Antigen Capture, Processing, and Loading on MHC Class II on B Cells', *Frontiers in Immunology*, 5, p. 92.

Balazs, M. *et al.* (2002) 'Blood dendritic cells interact with splenic marginal zone B cells to initiate T-independent immune responses', *Immunity*, 17(3), pp. 341-52.

Banck, G. and Forsgren, A. (1978) 'Many bacterial species are mitogenic for human blood B lymphocytes', *Scand J Immunol*, 8(4), pp. 347-54.

Baneyx, F. and Mujacic, M. (2004) 'Recombinant protein folding and misfolding in Escherichia coli', *Nat Biotechnol*, 22(11), pp. 1399-408.

Bassler, J. *et al.* (2015) 'A domain dictionary of trimeric autotransporter adhesins', *International Journal of Medical Microbiology*, 305(2), pp. 265-275.

Becker, M. *et al.* (2017) 'CXCR4 signaling and function require the expression of the IgD-class B-cell antigen receptor', *Proc Natl Acad Sci U S A*, 114(20), pp. 5231-5236.

Becker, S.C. *et al.* (2018) 'A comparative analysis of human bone marrow-resident and peripheral memory B cells', *J Allergy Clin Immunol*, 141(5), pp. 1911-1913.e7.

Behrouzi, A. *et al.* (2014) 'In Silico Studies of Outer Membrane of Neisseria Meningitidis Por A: Its Expression and Immunogenic Properties', *International Journal of Molecular and Cellular Medicine*, 3(3), pp. 166-175.

Bekeredjian-Ding, I. *et al.* (2012) 'Poke weed mitogen requires Toll-like receptor ligands for proliferative activity in human and murine B lymphocytes', *PLoS One*, 7(1), p. e29806.

Belkaid, Y. and Hand, T.W. (2014) 'Role of the microbiota in immunity and inflammation', *Cell*, 157(1), pp. 121-141.

Bennett, J.S. *et al.* (2010) 'Independent evolution of the core and accessory gene sets in the genus Neisseria: insights gained from the genome of Neisseria lactamica isolate 020-06', *BMC genomics*, 11, pp. 652-652.

Bennett, J.S. *et al.* (2012) 'A genomic approach to bacterial taxonomy: an examination and proposed reclassification of species within the genus Neisseria', *Microbiology*, 158(Pt 6), pp. 1570-80.
Bennett, J.S. *et al.* (2014) 'Identifying Neisseria species by use of the 50S ribosomal protein L6 (rplF) gene', *J Clin Microbiol*, 52(5), pp. 1375-81.
Bentancor, L.V. *et al.* (2012) 'Identification of Ata, a multifunctional trimeric autotransporter of Acinetobacter baumannii', *J Bacteriol*, 194(15), pp. 3950-60.
Bernardini, G. *et al.* (2004) 'Proteome analysis of Neisseria meningitidis serogroup A', *Proteomics*, 4(10), pp. 2893-926.
Bernasconi, N.L., Onai, N. and Lanzavecchia, A. (2003) 'A role for Toll-like receptors in acquired immunity: up-regulation of TLR9 by BCR triggering in naive B cells and constitutive expression in memory B cells', *Blood*, 101(11), pp. 4500-4.
Bernasconi, N.L., Traggiai, E. and Lanzavecchia, A. (2002) 'Maintenance of serological memory by polyclonal activation of human memory B cells', *Science*, 298(5601), pp. 2199-202.
Bingaman, A.W. *et al.* (2000) 'Vigorous allograft rejection in the absence of danger', *J Immunol*, 164(6), pp. 3065-71.
Bitto, N.J. *et al.* (2017) 'Bacterial membrane vesicles transport their DNA cargo into host cells', *Scientific Reports*, 7, p. 7072.
Blacher, E. *et al.* (2017) 'Microbiome-Modulated Metabolites at the Interface of Host Immunity', *J Immunol*, 198(2), pp. 572-580.
Bolin, I., Norlander, L. and Wolf-Watz, H. (1982) 'Temperature-inducible outer membrane protein of Yersinia pseudotuberculosis and Yersinia enterocolitica is associated with the virulence plasmid', *Infect Immun*, 37(2), pp. 506-12.
Bortnick, A. and Allman, D. (2013) 'What Is and What Should Always Have Been: Long-lived Plasma cells Induced by T-cell Independent Antigens', *Journal of immunology (Baltimore, Md. : 1950)*, 190(12), pp. 5913-5918.
Bosch, A.A. *et al.* (2016) 'Development of Upper Respiratory Tract Microbiota in Infancy is Affected by Mode of Delivery', *EBioMedicine*, 9, pp. 336-45.
Bouladoux, N. *et al.* (2012) 'Regulatory role of suppressive motifs from commensal DNA', *Mucosal Immunol*, 5(6), pp. 623-34.
Brandtzaeg, P. (2003) 'Immunology of tonsils and adenoids: everything the ENT surgeon needs to know', *Int J Pediatr Otorhinolaryngol*, 67 Suppl 1, pp. S69-76.
Brandtzaeg, P. (2011) 'Immune functions of nasopharyngeal lymphoid tissue', *Adv Otorhinolaryngol*, 72, pp. 20-4.
Brandtzaeg, P. *et al.* (1979) 'The human secretory immune system shows striking heterogeneity with regard to involvement of J chain-positive IgD immunocytes', *J Immunol*, 122(2), pp. 503-10.
Brink, R., Goodnow, C.C. and Basten, A. (1995) 'IgD expression on B cells is more efficient than IgM but both receptors are functionally equivalent in up-regulation CD80/CD86 co-stimulatory molecules', *Eur J Immunol*, 25(7), pp. 1980-4.
Brown, N.M., Ragge, N.K. and Speller, D.C. (1987) 'Septicaemia due to Neisseria lactamica--initial confusion with Neisseria meningitidis', *J Infect*, 15(3), pp. 243-5.
Busillo, J.M. and Benovic, J.L. (2007) 'Regulation of CXCR4 Signaling', *Biochimica et biophysica acta*, 1768(4), pp. 952-963.
Cariappa, A. *et al.* (2005) 'Perisinusoidal B cells in the bone marrow participate in T-independent responses to blood-borne microbes', *Immunity*, 23(4), pp. 397-407.
Cartwright, K.A. *et al.* (1987) 'The Stonehouse survey: nasopharyngeal carriage of meningococci and Neisseria lactamica', *Epidemiol Infect*, 99(3), pp. 591-601.
Casteleyn, C. *et al.* (2011) 'The tonsils revisited: review of the anatomical localization and histological characteristics of the tonsils of domestic and laboratory animals', *Clin Dev Immunol*, 2011, p. 472460.

Caugant, D.A. *et al.* (1992) 'Transmission of Neisseria meningitidis among asymptomatic military recruits and antibody analysis', *Epidemiol Infect*, 109(2), pp. 241-53.
Cesta, M.F. (2006) 'Normal structure, function, and histology of mucosa-associated lymphoid tissue', *Toxicol Pathol*, 34(5), pp. 599-608.
Chakravarti, B. *et al.* (2008) 'A highly uniform UV transillumination imaging system for quantitative analysis of nucleic acids and proteins', *PROTEOMICS*, 8(9), pp. 1789-1797.
Chamaillard, M. *et al.* (2003) 'An essential role for NOD1 in host recognition of bacterial peptidoglycan containing diaminopimelic acid', *Nat Immunol*, 4(7), pp. 702-7.
Chaturvedi, A., Dorward, D. and Pierce, S.K. (2008) 'The B cell receptor governs the subcellular location of Toll-like receptor 9 leading to hyperresponses to DNA-containing antigens', *Immunity*, 28(6), pp. 799-809.
Chen, J. and Alt, F.W. (1993) 'Gene rearrangement and B-cell development', *Curr Opin Immunol*, 5(2), pp. 194-200.
Chen, K. and Cerutti, A. (2010) 'New insights into the enigma of immunoglobulin D', *Immunol Rev*, 237(1), pp. 160-79.
Chen, K. and Cerutti, A. (2011) 'The function and regulation of immunoglobulin D', *Curr Opin Immunol*, 23(3), pp. 345-52.
Chen, K. *et al.* (2009) 'Immunoglobulin D enhances immune surveillance by activating antimicrobial, pro-inflammatory and B cell-stimulating programs in basophils', *Nature immunology*, 10(8), pp. 889-898.
Chen, X. and Jensen, P.E. (2008) 'The role of B lymphocytes as antigen-presenting cells', *Arch Immunol Ther Exp (Warsz)*, 56(2), pp. 77-83.
Chu, H. and Mazmanian, S.K. (2013) 'Innate immune recognition of the microbiota promotes host-microbial symbiosis', *Nature immunology*, 14(7), pp. 668-675.
Comanducci, M. *et al.* (2002) 'NadA, a novel vaccine candidate of Neisseria meningitidis', *J Exp Med*, 195(11), pp. 1445-54.
Corbeil, L.B., Bastida-Corcuera, F.D. and Beveridge, T.J. (1997) 'Haemophilus somnus immunoglobulin binding proteins and surface fibrils', *Infection and Immunity*, 65(10), pp. 4250-4257.
Corthesy, B. (2007) 'Roundtrip ticket for secretory IgA: role in mucosal homeostasis?', *J Immunol*, 178(1), pp. 27-32.
Corthésy, B. (2013) 'Role of secretory IgA in infection and maintenance of homeostasis', *Autoimmunity Reviews*, 12(6), pp. 661-665.
Coupat, B. *et al.* (2008) 'Natural transformation in the Ralstonia solanacearum species complex: number and size of DNA that can be transferred', *FEMS Microbiology Ecology*, 66(1), pp. 14-24.
Covens, K. *et al.* (2013) 'Characterization of proposed human B-1 cells reveals pre-plasmablast phenotype', *Blood*, 121(26), pp. 5176-83.
Cunningham, S.A., Mainella, J.M. and Patel, R. (2014) 'Misidentification of Neisseria polysaccharea as Neisseria meningitidis with the Use of Matrix-Assisted Laser Desorption Ionization–Time of Flight Mass Spectrometry', *Journal of Clinical Microbiology*, 52(6), pp. 2270-2271.
Daigneault, M.C. and Lo, R.Y. (2009) 'Analysis of a collagen-binding trimeric autotransporter adhesin from Mannheimia haemolytica A1', *FEMS Microbiol Lett*, 300(2), pp. 242-8.
Davenport, V. *et al.* (2003) 'Evidence for naturally acquired T cell-mediated mucosal immunity to Neisseria meningitidis', *J Immunol*, 171(8), pp. 4263-70.
Deasy, A.M. *et al.* (2015) 'Nasal Inoculation of the Commensal Neisseria lactamica Inhibits Carriage of Neisseria meningitidis by Young Adults: A Controlled Human Infection Study', *Clin Infect Dis*, 60(10), pp. 1512-20.
Deknuydt, F., Nordstrom, T. and Riesbeck, K. (2014) 'Diversion of the host humoral response: a novel virulence mechanism of Haemophilus influenzae mediated via outer membrane vesicles', *J Leukoc Biol*, 95(6), pp. 983-91.

Denning, D.W. and Gill, S.S. (1991) 'Neisseria lactamica meningitis following skull trauma', *Rev Infect Dis*, 13(2), pp. 216-8.
Desvaux, M. *et al.* (2006) 'The unusual extended signal peptide region of the type V secretion system is phylogenetically restricted', *FEMS Microbiol Lett*, 264(1), pp. 22-30.
Duchmann, R. *et al.* (1995) 'Tolerance exists towards resident intestinal flora but is broken in active inflammatory bowel disease (IBD)', *Clinical and Experimental Immunology*, 102(3), pp. 448-455.
Duffin, P.M. and Seifert, H.S. (2010) 'DNA Uptake Sequence-Mediated Enhancement of Transformation in Neisseria gonorrhoeae Is Strain Dependent', *Journal of Bacteriology*, 192(17), p. 4436.
Elkins, C., Morrow, K.J., Jr. and Olsen, B. (2000) 'Serum resistance in Haemophilus ducreyi requires outer membrane protein DsrA', *Infection and immunity*, 68(3), pp. 1608-1619.
Erntell, M. *et al.* (1988) 'Streptococcal protein G has affinity for both Fab- and Fc-fragments of human IgG', *Molecular Immunology*, 25(2), pp. 121-126.
Evans, C. *et al.* (2008) 'Pilot study of human experimental challenge with neisseria lactamica', *Journal of Infection*, 57(5), p. 424.
Evans, C.M. *et al.* (2011) 'Nasopharyngeal colonization by Neisseria lactamica and induction of protective immunity against Neisseria meningitidis', *Clin Infect Dis*, 52(1), pp. 70-7.
Everts, R.J. *et al.* (2010) 'Neisseria lactamica arthritis and septicemia complicating myeloma', *Journal of clinical microbiology*, 48(6), pp. 2318-2318.
Fagarasan, S. and Honjo, T. (2000) 'T-Independent immune response: new aspects of B cell biology', *Science*, 290(5489), pp. 89-92.
Fialho, A. and Mil-Homens, D. (2011) 'Trimeric Autotransporter Adhesins in Members of the Burkholderia Cepacia Complex: A Multifunctional Family of Proteins Implicated in Virulence', *Frontiers in Cellular and Infection Microbiology*, 1(13).
Finkelman, F.D. *et al.* (1976) 'Cell membrane IgD: demonstration of IgD on human lymphocytes by enzyme-catalyzed iodination and comparison with cell surface Ig of mouse, guinea pig, and rabbit', *J Immunol*, 116(4), pp. 1173-81.
Forsgren, A. *et al.* (2003) 'The Immunoglobulin D-Binding Protein MID from Moraxella catarrhalis Is Also an Adhesin', *Infection and Immunity*, 71(6), pp. 3302-3309.
Forsgren, A. *et al.* (2001) 'Isolation and characterization of a novel IgD-binding protein from Moraxella catarrhalis.', *The Journal of Immunology*, 167(4), p. 2112.
Forsgren, A. and Grubb, A.O. (1979) 'Many Bacterial Species Bind Human IgD', *The Journal of Immunology*, 122(4), pp. 1468-1472.
Forsgren, A. *et al.* (1988) 'Branhamella catarrhalis activates human B lymphocytes following interactions with surface IgD and class I major histocompatibility complex antigens', *Cell Immunol*, 112(1), pp. 78-88.
Forsgren, A., Riesbeck, K. and Janson, H. (2008) 'Protein D of Haemophilus influenzae: a protective nontypeable H. influenzae antigen and a carrier for pneumococcal conjugate vaccines', *Clin Infect Dis*, 46(5), pp. 726-31.
Forsgren, A. and Sjoquist, J. (1966) '"Protein A" from S. aureus. I. Pseudo-immune reaction with human gamma-globulin', *J Immunol*, 97(6), pp. 822-7.
Fowler, M.I. *et al.* (2006) 'Comparison of the inflammatory responses of human meningeal cells following challenge with Neisseria lactamica and with Neisseria meningitidis', *Infect Immun*, 74(11), pp. 6467-78.
Fredriksen, J.H. *et al.* (1991) 'Production, characterization and control of MenB-vaccine "Folkehelsa": an outer membrane vesicle vaccine against group B meningococcal disease', *NIPH Ann*, 14(2), pp. 67-79; discussion 79-80.
Frithz, E., Hedén, L.O. and Lindahl, G. (1989) 'Extensive sequence homology between IgA receptor and M proteins in Streptococcus pyogenes', *Molecular Microbiology*, 3(8), pp. 1111-1119.

Garraud, O. *et al.* (2012) 'Revisiting the B-cell compartment in mouse and humans: more than one B-cell subset exists in the marginal zone and beyond', *BMC Immunology*, 13(1), p. 63.
Gathings, W.E., Lawton, A.R. and Cooper, M.D. (1977) 'Immunofluorescent studies of the development of pre-B cells, B lymphocytes and immunoglobulin isotype diversity in humans', *Eur J Immunol*, 7(11), pp. 804-10.
Geisberger, R., Lamers, M. and Achatz, G. (2006) 'The riddle of the dual expression of IgM and IgD', *Immunology*, 118(4), pp. 429-437.
Gergely, L., Cook, L. and Agnello, V. (1997) 'A simplified method for Ca2+ flux measurement on isolated human B cells that uses flow cytometry', *Clinical and Diagnostic Laboratory Immunology*, 4(1), pp. 70-74.
Gibson, D.G. *et al.* (2008) 'Complete chemical synthesis, assembly, and cloning of a Mycoplasma genitalium genome', *Science*, 319(5867), pp. 1215-20.
Gjorloff Wingren, A. *et al.* (2002) 'The novel IgD binding protein from Moraxella catarrhalis induces human B lymphocyte activation and Ig secretion in the presence of Th2 cytokines', *J Immunol*, 168(11), pp. 5582-8.
Glowczyk, I. *et al.* (2017) 'Inactive Gingipains from P. gingivalis Selectively Skews T Cells toward a Th17 Phenotype in an IL-6 Dependent Manner', *Frontiers in cellular and infection microbiology*, 7, pp. 140-140.
Gold, R. *et al.* (1978) 'Carriage of Neisseria meningitidis and Neisseria lactamica in Infants and Children', *J. Infect. Dis*, 137(2), pp. 112-121.
Goldschneider, I., Gotschlich, E.C. and Artenstein, M.S. (1969a) 'Human immunity to the meningococcus. I. The role of humoral antibodies', *J Exp Med*, 129(6), pp. 1307-26.
Goldschneider, I., Gotschlich, E.C. and Artenstein, M.S. (1969b) 'Human immunity to the meningococcus. II. Development of natural immunity', *J Exp Med*, 129(6), pp. 1327-48.
Goodman, S.D. and Scocca, J.J. (1991) 'Factors influencing the specific interaction of Neisseria gonorrhoeae with transforming DNA', *Journal of bacteriology*, 173(18), pp. 5921-5923.
Goodyear, C.S. and Silverman, G.J. (2005) 'B cell superantigens: a microbe's answer to innate-like B cells and natural antibodies', *Springer Seminars in Immunopathology*, 26(4), pp. 463-484.
Gorringe, A. *et al.* (2005) 'The development of a meningococcal disease vaccine based on Neisseria lactamica outer membrane vesicles', *Vaccine*, 23(17–18), pp. 2210-2213.
Gorringe, A.R. (2005) 'Can Neisseria lactamica antigens provide an effective vaccine to prevent meningococcal disease?', *Expert Rev Vaccines*, 4(3), pp. 373-9.
Graille, M. *et al.* (2000) 'Crystal structure of a Staphylococcus aureus protein A domain complexed with the Fab fragment of a human IgM antibody: Structural basis for recognition of B-cell receptors and superantigen activity', *Proceedings of the National Academy of Sciences of the United States of America*, 97(10), pp. 5399-5404.
Griffin, D.O., Holodick, N.E. and Rothstein, T.L. (2011) 'Human B1 cells in umbilical cord and adult peripheral blood express the novel phenotype CD20(+)CD27(+)CD43(+)CD70(−)', *The Journal of Experimental Medicine*, 208(1), pp. 67-80.
Griffin, D.O. and Rothstein, T.L. (2012) 'Human B1 Cell Frequency: Isolation and Analysis of Human B1 Cells', *Frontiers in Immunology*, 3, p. 122.
Gutzeit, C., Chen, K. and Cerutti, A. (2018) 'The enigmatic function of IgD: some answers at last', *Eur J Immunol*, 48(7), pp. 1101-1113.
Hall, J.A. *et al.* (2008) 'Commensal DNA limits regulatory T cell conversion and is a natural adjuvant of intestinal immune responses', *Immunity*, 29(4), pp. 637-49.
Hallström, T. *et al.* (2008) 'The Moraxella IgD-binding protein MID/Hag is an oligomeric autotransporter', *Microbes and Infection*, 10(4), pp. 374-381.
Hallstrom, T. and Riesbeck, K. (2010) 'Haemophilus influenzae and the complement system', *Trends Microbiol*, 18(6), pp. 258-65.
Halperin, S.A. *et al.* (2012) 'The changing and dynamic epidemiology of meningococcal disease', *Vaccine*, 30 Suppl 2, pp. B26-36.

Hamilton, H.L. and Dillard, J.P. (2006) 'Natural transformation of Neisseria gonorrhoeae: from DNA donation to homologous recombination', *Mol Microbiol*, 59(2), pp. 376-85.
Hoffman, W., Lakkis, F.G. and Chalasani, G. (2016) 'B Cells, Antibodies, and More', *Clinical Journal of the American Society of Nephrology : CJASN*, 11(1), pp. 137-154.
Hoiczyk, E. *et al.* (2000) 'Structure and sequence analysis of Yersinia YadA and Moraxella UspAs reveal a novel class of adhesins', *The EMBO journal*, 19(22), pp. 5989-5999.
Hol, C. *et al.* (1996) 'Moraxella catarrhalis in acute laryngitis: infection or colonization?', *J Infect Dis*, 174(3), pp. 636-8.
Hooper, L.V. and Gordon, J.I. (2001) 'Commensal host-bacterial relationships in the gut', *Science*, 292(5519), pp. 1115-8.
Hyams, C. *et al.* (2010) 'The Streptococcus pneumoniae capsule inhibits complement activity and neutrophil phagocytosis by multiple mechanisms', *Infect Immun*, 78(2), pp. 704-15.
Inui, M. *et al.* (2015) 'Human CD43+ B cells are closely related not only to memory B cells phenotypically but also to plasmablasts developmentally in healthy individuals', *Int Immunol*, 27(7), pp. 345-55.
Janson, H. *et al.* (1991) 'Protein D, an immunoglobulin D-binding protein of Haemophilus influenzae: cloning, nucleotide sequence, and expression in Escherichia coli', *Infect Immun*, 59(1), pp. 119-25.
Jendholm, J. *et al.* (2008) 'Moraxella catarrhalis-dependent tonsillar B cell activation does not lead to apoptosis but to vigorous proliferation resulting in nonspecific IgM production', *J Leukoc Biol*, 83(6), pp. 1370-8.
Jesumirhewe, C. *et al.* (2016) 'Accuracy of conventional identification methods used for Enterobacteriaceae isolates in three Nigerian hospitals', *PeerJ*, 4, pp. e2511-e2511.
Jiang, F. *et al.* (2017) 'The symbiotic bacterial surface factor polysaccharide A on Bacteroides fragilis inhibits IL-1beta-induced inflammation in human fetal enterocytes via toll receptors 2 and 4', *PLoS One*, 12(3), p. e0172738.
Jiang, H.Q. *et al.* (2004) 'Interactions of commensal gut microbes with subsets of B- and T-cells in the murine host', *Vaccine*, 22(7), pp. 805-811.
Jiang, W. *et al.* (2007) 'TLR9 stimulation drives naive B cells to proliferate and to attain enhanced antigen presenting function', *Eur J Immunol*, 37(8), pp. 2205-13.
Johansen, F.-E. *et al.* (2005) 'Regional induction of adhesion molecules and chemokine receptors explains disparate homing of human B cells to systemic and mucosal effector sites: dispersion from tonsils', *Blood*, 106(2), pp. 593-600.
Johnson, A.P. (1983) 'The pathogenic potential of commensal species of Neisseria', *Journal of Clinical Pathology*, 36(2), pp. 213-223.
Kainz, P. (2000) 'The PCR plateau phase - towards an understanding of its limitations', *Biochim Biophys Acta*, 1494(1-2), pp. 23-7.
Kim, J.J., Mandrell, R.E. and Griffiss, J.M. (1989) 'Neisseria lactamica and Neisseria meningitidis share lipooligosaccharide epitopes but lack common capsular and class 1, 2, and 3 protein epitopes', *Infection and Immunity*, 57(2), pp. 602-608.
Kim, K.M. and Reth, M. (1995a) 'The B cell antigen receptor of class IgD induces a stronger and more prolonged protein tyrosine phosphorylation than that of class IgM', *J Exp Med*, 181(3), pp. 1005-14.
Kim, K.M. and Reth, M. (1995b) 'Signaling difference between class IgM and IgD antigen receptors', *Ann N Y Acad Sci*, 766, pp. 81-8.
Kirjavainen, V. *et al.* (2008) 'Yersinia enterocolitica serum resistance proteins YadA and ail bind the complement regulator C4b-binding protein', *PLoS Pathog*, 4(8), p. e1000140.
Knapp, J.S. and Hook, E.W. (1988) 'Prevalence and persistence of Neisseria cinerea and other Neisseria spp. in adults', *Journal of Clinical Microbiology*, 26(5), pp. 896-900.
Kobayashi, S.D. and DeLeo, F.R. (2013) 'Staphylococcus aureus protein A promotes immune suppression', *mBio*, 4(5), p. e00764.

Koretke, K.K. *et al.* (2006) 'Model structure of the prototypical non-fimbrial adhesin YadA of Yersinia enterocolitica', *J Struct Biol*, 155(2), pp. 154-61.
Kozera, B. and Rapacz, M. (2013) 'Reference genes in real-time PCR', *J Appl Genet*, 54(4), pp. 391-406.
Kremastinou, J. *et al.* (2003) 'Carriage of Neisseria meningitidis and Neisseria lactamica in northern Greece', *FEMS Immunology and Medical Microbiology*, 39(1), pp. 23-29.
Kremastinou, J. *et al.* (1999) 'Detection of IgG and IgM to meningococcal outer membrane proteins in relation to carriage of Neisseria meningitidis or Neisseria lactamica', *FEMS Immunology and Medical Microbiology*, 24(1), pp. 73-78.
Kung, S.H. *et al.* (2013) 'Effects of DNA size on transformation and recombination efficiencies in Xylella fastidiosa', *Applied and environmental microbiology*, 79(5), pp. 1712-1717.
Kuper, C.F. *et al.* (1992) 'The role of nasopharyngeal lymphoid tissue', *Immunol Today*, 13(6), pp. 219-24.
Ladunga, I. (2017) 'Finding Homologs in Amino Acid Sequences Using Network BLAST Searches', *Curr Protoc Bioinformatics*, 59, pp. 3.4.1-3.4.24.
Laemmli, U.K. (1970) 'Cleavage of structural proteins during the assembly of the head of bacteriophage T4', *Nature*, 227(5259), pp. 680-5.
Lafontaine, E.R. *et al.* (2000) 'The UspA1 protein and a second type of UspA2 protein mediate adherence of Moraxella catarrhalis to human epithelial cells in vitro', *J Bacteriol*, 182(5), pp. 1364-73.
Lange, V. *et al.* (2008) 'Selected reaction monitoring for quantitative proteomics: a tutorial', *Molecular systems biology*, 4, pp. 222-222.
Lee, J. *et al.* (2009) 'Identification and characterization of a human CD5+ pre-naive B cell population', *J Immunol*, 182(7), pp. 4116-26.
Lee, P.Y. *et al.* (2012) 'Agarose gel electrophoresis for the separation of DNA fragments', *Journal of visualized experiments : JoVE*, (62), p. 3923.
Leo, J.C. and Goldman, A. (2009) 'The immunoglobulin-binding Eib proteins from Escherichia coli are receptors for IgG Fc', *Mol Immunol*, 46(8-9), pp. 1860-6.
Leo, J.C., Grin, I. and Linke, D. (2012) 'Type V secretion: mechanism(s) of autotransport through the bacterial outer membrane', *Philosophical Transactions of the Royal Society B: Biological Sciences*, 367(1592), pp. 1088-1101.
Leo, J.C. *et al.* (2011) 'The structure of E. coli IgG-binding protein D suggests a general model for bending and binding in trimeric autotransporter adhesins', *Structure*, 19(7), pp. 1021-30.
Lewis, L.A., Carter, M. and Ram, S. (2012) 'The relative roles of factor H binding protein, neisserial surface protein A, and lipooligosaccharide sialylation in regulation of the alternative pathway of complement on meningococci', *J Immunol*, 188(10), pp. 5063-72.
Li, Y. *et al.* (2006) 'Immunization with Live Neisseria lactamica Protects Mice against Meningococcal Challenge and Can Elicit Serum Bactericidal Antibodies', *Infection and Immunity*, 74(11), pp. 6348-6355.
Linke, D. *et al.* (2006a) 'Trimeric autotransporter adhesins: variable structure, common function', *Trends Microbiol*, 14(6), pp. 264-70.
Linke, D. *et al.* (2006b) 'Trimeric autotransporter adhesins: variable structure, common function', *Trends in Microbiology*, 14(6), pp. 264-270.
Littman, D.R. and Pamer, E.G. (2011) 'Role of the commensal microbiota in normal and pathogenic host immune responses', *Cell host & microbe*, 10(4), pp. 311-323.
Litwin, S.D., Zehr, B.D. and Insel, R.A. (1990) 'Selective concentration of IgD class-specific antibodies in human milk', *Clin Exp Immunol*, 80(2), pp. 263-7.
Lo, H., Tang, C.M. and Exley, R.M. (2009) 'Mechanisms of avoidance of host immunity by Neisseria meningitidis and its effect on vaccine development', *Lancet Infect Dis*, 9(7), pp. 418-27.
Loh, R., Vale, S. and McLean-Tooke, A. (2013) 'Quantitative serum immunoglobulin tests', *Australian Family Physician*, 42, pp. 195-198.

Lu, S. *et al.* (2019) 'CDD/SPARCLE: the conserved domain database in 2020', *Nucleic Acids Research*, 48(D1), pp. D265-D268.
Lu, Y. *et al.* (2006) 'A new immunoglobulin-binding protein, EibG, is responsible for the chain-like adhesion phenotype of locus of enterocyte effacement-negative, shiga toxin-producing Escherichia coli', *Infect Immun*, 74(10), pp. 5747-55.
Lutz, C. *et al.* (1998) 'IgD can largely substitute for loss of IgM function in B cells', *Nature*, 393(6687), pp. 797-801.
Lyskowski, A., Leo, J.C. and Goldman, A. (2011) 'Structure and biology of trimeric autotransporter adhesins', *Adv Exp Med Biol*, 715, pp. 143-58.
Macpherson, A.J. *et al.* (2000) 'A primitive T cell-independent mechanism of intestinal mucosal IgA responses to commensal bacteria', *Science*, 288(5474), pp. 2222-6.
Macpherson, A.J., Geuking, M.B. and McCoy, K.D. (2005) 'Immune responses that adapt the intestinal mucosa to commensal intestinal bacteria', *Immunology*, 115(2), pp. 153-162.
Macpherson, A.J., Martinic, M.M. and Harris, N. (2002) 'The functions of mucosal T cells in containing the indigenous commensal flora of the intestine', *Cell Mol Life Sci*, 59(12), pp. 2088-96.
Maity, P.C. *et al.* (2015) 'B cell antigen receptors of the IgM and IgD classes are clustered in different protein islands that are altered during B cell activation', *Sci Signal*, 8(394), p. ra93.
Man, W.H., de Steenhuijsen Piters, W.A.A. and Bogaert, D. (2017) 'The microbiota of the respiratory tract: gatekeeper to respiratory health', *Nat Rev Micro*, 15(5), pp. 259-270.
Mantis, N.J., Rol, N. and Corthésy, B. (2011) 'Secretory IgA's Complex Roles in Immunity and Mucosal Homeostasis in the Gut', *Mucosal immunology*, 4(6), pp. 603-611.
Martin, F., Oliver, A.M. and Kearney, J.F. (2001) 'Marginal Zone and B1 B Cells Unite in the Early Response against T-Independent Blood-Borne Particulate Antigens', *Immunity*, 14(5), pp. 617-629.
Matsumoto, A. and Igo, M.M. (2010) 'Species-specific type II restriction-modification system of Xylella fastidiosa temecula1', *Applied and environmental microbiology*, 76(12), pp. 4092-4095.
Matzinger, P. (2002) 'The danger model: a renewed sense of self', *Science*, 296(5566), pp. 301-5.
Matzinger, P. (2007) 'Friendly and dangerous signals: is the tissue in control?', *Nat Immunol*, 8(1), pp. 11-3.
McBroom, A.J. and Kuehn, M.J. (2005) 'Outer Membrane Vesicles', *EcoSal Plus*, 1(2).
Meng, G. *et al.* (2006) 'Structure of the outer membrane translocator domain of the Haemophilus influenzae Hia trimeric autotransporter', *Embo j*, 25(11), pp. 2297-304.
Merkel, V. *et al.* (2010) 'Distribution and phylogeny of immunoglobulin-binding protein G in Shiga toxin-producing Escherichia coli and its association with adherence phenotypes', *Infect Immun*, 78(8), pp. 3625-36.
Mikula, K.M. *et al.* (2012) 'The translocation domain in trimeric autotransporter adhesins is necessary and sufficient for trimerization and autotransportation', *J Bacteriol*, 194(4), pp. 827-38.
Moens, L. *et al.* (2008) 'Human Memory B Lymphocyte Subsets Fulfill Distinct Roles in the Anti-Polysaccharide and Anti-Protein Immune Response', *The Journal of Immunology*, 181(8), p. 5306.
Mollenkvist, A. *et al.* (2003) 'The Moraxella catarrhalis immunoglobulin D-binding protein MID has conserved sequences and is regulated by a mechanism corresponding to phase variation', *J Bacteriol*, 185(7), pp. 2285-95.
Mond, J.J., Lees, A. and Snapper, C.M. (1995) 'T cell-independent antigens type 2', *Annu Rev Immunol*, 13, pp. 655-92.
Mond, J.J. *et al.* (1995) 'T cell independent antigens', *Curr Opin Immunol*, 7(3), pp. 349-54.
Mukhopadhyay, T.K. *et al.* (2005) 'Rapid characterization of outer-membrane proteins in Neisseria lactamica by SELDI-TOF-MS (surface-enhanced laser desorption ionization-time-of-flight MS) for use in a meningococcal vaccine', *Biotechnol Appl Biochem*, 41(Pt 2), pp. 175-82.
Murphy, B.S. *et al.* (2007) 'Yersinia pestis YadC: a novel vaccine candidate against plague', *Adv Exp Med Biol*, 603, pp. 400-14.
Murphy, K. *et al.* (2012) *Janeway's immunobiology*. 8th edn. New York: Garland Science.

Murphy, T.F. *et al.* (2005) 'Moraxella catarrhalis in chronic obstructive pulmonary disease: burden of disease and immune response', *Am J Respir Crit Care Med*, 172(2), pp. 195-9.
Myhre, E.B. and Erntell, M. (1985) 'A non-immune interaction between the light chain of human immunoglobulin and a surface component of a Peptococcus magnus strain', *Mol Immunol*, 22(8), pp. 879-85.
Neal, K.R. *et al.* (2000) 'Changing carriage rate of Neisseria meningitidis among university students during the first week of term: cross sectional study', *BMJ (Clinical research ed.)*, 320(7238), pp. 846-849.
Noelle, R.J. *et al.* (1983) 'Activation of antigen-specific B cells: role of T cells, cytokines, and antigen in induction of growth and differentiation', *Proceedings of the National Academy of Sciences of the United States of America*, 80(21), pp. 6628-6631.
Nordstrom, T., Forsgren, A. and Riesbeck, K. (2002) 'The immunoglobulin D-binding part of the outer membrane protein MID from Moraxella catarrhalis comprises 238 amino acids and a tetrameric structure', *J Biol Chem*, 277(38), pp. 34692-9.
Nummelin, H. *et al.* (2004) 'The Yersinia adhesin YadA collagen-binding domain structure is a novel left-handed parallel beta-roll', *Embo j*, 23(4), pp. 701-11.
Nygaard, T.K. *et al.* (2016) 'Interaction of Staphylococci with Human B cells', *PLoS One*, 11(10), p. e0164410.
O'Dwyer C, A. *et al.* (2004) 'Expression of heterologous antigens in commensal Neisseria spp.: preservation of conformational epitopes with vaccine potential', *Infect Immun*, 72(11), pp. 6511-8.
Ohta, Y. and Flajnik, M. (2006) 'IgD, like IgM, is a primordial immunoglobulin class perpetuated in most jawed vertebrates', *Proc Natl Acad Sci U S A*, 103(28), pp. 10723-8.
Oliver, K.J. *et al.* (2002) 'Neisseria lactamica Protects against Experimental Meningococcal Infection', *Infection and Immunity*, 70(7), pp. 3621-3626.
Olsen, S.F. *et al.* (1991) 'Pharyngeal carriage of Neisseria meningitidis and Neisseria lactamica in households with infants within areas with high and low incidences of meningococcal disease', *Epidemiology and Infection*, 106(3), pp. 445-457.
Owen, J.A. *et al.* (2013) *Kuby immunology*. New York: W.H. Freeman.
Pandey, A. *et al.* (2018) 'Microevolution of Neisseria lactamica during nasopharyngeal colonisation induced by controlled human infection', *Nat Commun*, 9(1), p. 4753.
Paramithiotis, E. and Cooper, M.D. (1997) 'Memory B lymphocytes migrate to bone marrow in humans', *Proceedings of the National Academy of Sciences of the United States of America*, 94(1), pp. 208-212.
Parija, S.C. (2014) *Textbook of Microbiology & Immunology*. Elsevier Health Sciences APAC.
Parra, D. *et al.* (2012) 'Pivotal advance: peritoneal cavity B-1 B cells have phagocytic and microbicidal capacities and present phagocytosed antigen to CD4+ T cells', *J Leukoc Biol*, 91(4), pp. 525-36.
Pearson, W.R. (2013) 'An Introduction to Sequence Similarity ("Homology") Searching', *Current protocols in bioinformatics / editoral board, Andreas D. Baxevanis ... [et al.]*, 0 3, p. 10.1002/0471250953.bi0301s42.
Perez-Cruz, C. *et al.* (2015) 'Outer-inner membrane vesicles naturally secreted by gram-negative pathogenic bacteria', *PLoS One*, 10(1), p. e0116896.
Perez Vidakovics, M.L.A. *et al.* (2010) 'B Cell Activation by Outer Membrane Vesicles—A Novel Virulence Mechanism', *PLoS Pathogens*, 6(1), p. e1000724.
Perry, M. and Whyte, A. (1998) 'Immunology of the tonsils', *Immunol Today*, 19(9), pp. 414-21.
Pertsemlidis, A. and Fondon, J.W., 3rd (2001) 'Having a BLAST with bioinformatics (and avoiding BLASTphemy)', *Genome Biol*, 2(10), p. Reviews2002.
Piet, J.R. *et al.* (2011) 'Genome Sequence of Neisseria meningitidis Serogroup B Strain H44/76', *Journal of Bacteriology*, 193(9), pp. 2371-2372.

Pillai, S. and Cariappa, A. (2009) 'The follicular versus marginal zone B lymphocyte cell fate decision', *Nat Rev Immunol*, 9(11), pp. 767-777.
Pollard, M. and Sharon, N. (1970) 'Responses of the Peyer's Patches in Germ-Free Mice to Antigenic Stimulation', *Infect Immun*, 2(1), pp. 96-100.
Pradeu, T. and Cooper, E.L. (2012) 'The danger theory: 20 years later', *Frontiers in Immunology*, 3, p. 287.
Raghunathan, D. *et al.* (2011) 'SadA, a trimeric autotransporter from Salmonella enterica serovar Typhimurium, can promote biofilm formation and provides limited protection against infection', *Infect Immun*, 79(11), pp. 4342-52.
Renelli, M. *et al.* (2004) 'DNA-containing membrane vesicles of Pseudomonas aeruginosa PAO1 and their genetic transformation potential', *Microbiology*, 150(Pt 7), pp. 2161-9.
Reth, M. (1992) 'Antigen receptors on B lymphocytes', *Annu Rev Immunol*, 10, pp. 97-121.
Riesbeck, K. and Nordstrom, T. (2006) 'Structure and immunological action of the human pathogen Moraxella catarrhalis IgD-binding protein', *Crit Rev Immunol*, 26(4), pp. 353-76.
Riess, T. *et al.* (2004) 'Bartonella adhesin a mediates a proangiogenic host cell response', *The Journal of experimental medicine*, 200(10), pp. 1267-1278.
Rio, D.C. (2014) 'Reverse transcription-polymerase chain reaction', *Cold Spring Harb Protoc*, 2014(11), pp. 1207-16.
Roben, P.W., Salem, A.N. and Silverman, G.J. (1995) 'VH3 family antibodies bind domain D of staphylococcal protein A', *J Immunol*, 154(12), pp. 6437-45.
Robinson, J. (2004) 'Colonization and infection of the respiratory tract: What do we know?', *Paediatrics & Child Health*, 9(1), pp. 21-24.
Rocha, D.J., Santos, C.S. and Pacheco, L.G. (2015) 'Bacterial reference genes for gene expression studies by RT-qPCR: survey and analysis', *Antonie Van Leeuwenhoek*, 108(3), pp. 685-93.
Roes, J. and Rajewsky, K. (1993) 'Immunoglobulin D (IgD)-deficient mice reveal an auxiliary receptor function for IgD in antigen-mediated recruitment of B cells', *J Exp Med*, 177(1), pp. 45-55.
Roos, A. *et al.* (2001) 'Human IgA Activates the Complement System Via the Mannan-Binding Lectin Pathway', *The Journal of Immunology*, 167(5), p. 2861.
Rosales-Reyes, R. *et al.* (2005) 'Survival of Salmonella enterica serovar Typhimurium within late endosomal-lysosomal compartments of B lymphocytes is associated with the inability to use the vacuolar alternative major histocompatibility complex class I antigen-processing pathway', *Infect Immun*, 73(7), pp. 3937-44.
Rosenstein, N.E. *et al.* (2001) 'Meningococcal disease', *N Engl J Med*, 344(18), pp. 1378-88.
Rothstein, T.L. *et al.* (2013) 'Human B-1 cells take the stage', *Annals of the New York Academy of Sciences*, 1285, pp. 97-114.
Round, J.L. *et al.* (2011) 'The Toll-like receptor 2 pathway establishes colonization by a commensal of the human microbiota', *Science*, 332(6032), pp. 974-7.
Rowe, D. and Fahey, J. (1965) 'A NEW CLASS OF HUMAN IMMUNOGLOBULINS: II. NORMAL SERUM IGD', *Journal of Experimental Medicine*, 121(1), pp. 185-189.
Ruan, M.R. *et al.* (1990) 'Protein D of Haemophilus influenzae. A novel bacterial surface protein with affinity for human IgD', *J Immunol*, 145(10), pp. 3379-84.
Ruddick, J.H. and Leslie, G.A. (1977) 'Structure and biologic functions of human IgD. XI. Identification and ontogeny of a rat lymphocyte immunoglobulin having antigenic cross-reactivity with human IgD', *J Immunol*, 118(3), pp. 1025-31.
Sabate, R., de Groot, N.S. and Ventura, S. (2010) 'Protein folding and aggregation in bacteria', *Cell Mol Life Sci*, 67(16), pp. 2695-715.
Sandt, C.H. and Hill, C.W. (2000) 'Four Different Genes Responsible for Nonimmune Immunoglobulin-Binding Activities within a Single Strain ofEscherichia coli', *Infection and Immunity*, 68(4), p. 2205.
Sandt, C.H. *et al.* (1997) 'Escherichia coli strains with nonimmune immunoglobulin-binding activity', *Infection and Immunity*, 65(11), pp. 4572-4579.

Santos, S. *et al.* (2012) 'Outer membrane vesicles (OMV) production of Neisseria meningitidis serogroup B in batch process', *Vaccine*, 30(42), pp. 6064-6069.
Sardinas, G. *et al.* (2006) 'Outer membrane vesicles of Neisseria lactamica as a potential mucosal adjuvant', *Vaccine*, 24(2), pp. 206-14.
Sasaki, K. and Munson, R.S., Jr. (1993) 'Protein D of Haemophilus influenzae is not a universal immunoglobulin D-binding protein', *Infection and immunity*, 61(7), pp. 3026-3031.
Scarselli, M. *et al.* (2006) 'Neisseria meningitidis NhhA is a multifunctional trimeric autotransporter adhesin', *Mol Microbiol*, 61(3), pp. 631-44.
Schaar, V. *et al.* (2011) 'Multicomponent Moraxella catarrhalis outer membrane vesicles induce an inflammatory response and are internalized by human epithelial cells', *Cell Microbiol*, 13(3), pp. 432-49.
Schelonka, R.L. and Maheshwari, A. (2013) 'The Many Faces of B Cells', *NeoReviews*, 14(9), p. e438.
Schifman, R.B. and Ryan, K.J. (1983) 'Neisseria lactamica septicemia in an immunocompromised patient', *J Clin Microbiol*, 17(5), pp. 934-5.
Schneider, P. and Tschopp, J. (2003) 'BAFF and the regulation of B cell survival', *Immunol Lett*, 88(1), pp. 57-62.
Schroeder, H.W. and Cavacini, L. (2010) 'Structure and Function of Immunoglobulins', *The Journal of allergy and clinical immunology*, 125(2 0 2), pp. S41-S52.
Schwechheimer, C. and Kuehn, M.J. (2015) 'Outer-membrane vesicles from Gram-negative bacteria: biogenesis and functions', *Nat Rev Micro*, 13(10), pp. 605-619.
Sechet, B. *et al.* (2003) 'Immunoglobulin D enhances interleukin-6 release from the KU812 human prebasophil cell line', *Gen Physiol Biophys*, 22(2), pp. 255-63.
Serruto, D. *et al.* (2009) 'HadA is an atypical new multifunctional trimeric coiled-coil adhesin of Haemophilus influenzae biogroup aegyptius, which promotes entry into host cells', *Cellular Microbiology*, 11(7), pp. 1044-1063.
Sheets, A.J. *et al.* (2008) 'Identification of a novel trimeric autotransporter adhesin in the cryptic genospecies of Haemophilus', *J Bacteriol*, 190(12), pp. 4313-20.
Sheikhi, R. *et al.* (2015) 'Oropharyngeal Colonization With Neisseria lactamica, Other Nonpathogenic Neisseria Species and Moraxella catarrhalis Among Young Healthy Children in Ahvaz, Iran', *Jundishapur J Microbiol*, 8(3), p. e14813.
Shinnakasu, R. and Kurosaki, T. (2017) 'Regulation of memory B and plasma cell differentiation', *Curr Opin Immunol*, 45, pp. 126-131.
Shroff, K.E., Meslin, K. and Cebra, J.J. (1995) 'Commensal enteric bacteria engender a self-limiting humoral mucosal immune response while permanently colonizing the gut', *Infect Immun*, 63(10), pp. 3904-13.
Sillanpää, S. *et al.* (2016) 'Moraxella catarrhalis Might Be More Common than Expected in Acute Otitis Media in Young Finnish Children', *Journal of Clinical Microbiology*, 54(9), pp. 2373-2379.
Slobodin, B. *et al.* (2017) 'Transcription Impacts the Efficiency of mRNA Translation via Co-transcriptional N6-adenosine Methylation', *Cell*, 169(2), pp. 326-337.e12.
Smith, K., McCoy, K.D. and Macpherson, A.J. (2007) 'Use of axenic animals in studying the adaptation of mammals to their commensal intestinal microbiota', *Semin Immunol*, 19(2), pp. 59-69.
Smith, N.H. *et al.* (1999) 'Networks and groups within the genus Neisseria: analysis of argF, recA, rho, and 16S rRNA sequences from human Neisseria species', *Mol Biol Evol*, 16(6), pp. 773-83.
Solomon, A. and Weiss, D.T. (1995) 'Structural and functional properties of human lambda-light-chain variable-region subgroups', *Clinical and Diagnostic Laboratory Immunology*, 2(4), pp. 387-394.
Sorensen, C.H. and Larsen, P.L. (1988) 'IgD in nasopharyngeal secretions and tonsils from otitis-prone children', *Clin Exp Immunol*, 73(1), pp. 149-54.

Souwer, Y. *et al.* (2009) 'B cell receptor-mediated internalization of salmonella: a novel pathway for autonomous B cell activation and antibody production', *J Immunol*, 182(12), pp. 7473-81.
Spencer-Smith, R. *et al.* (2016) 'DNA uptake sequences in Neisseria gonorrhoeae as intrinsic transcriptional terminators and markers of horizontal gene transfer', *Microbial genomics*, 2(8), pp. e000069-e000069.
St Geme, J.W., 3rd and Cutter, D. (2000) 'The Haemophilus influenzae Hia adhesin is an autotransporter protein that remains uncleaved at the C terminus and fully cell associated', *J Bacteriol*, 182(21), pp. 6005-13.
St Geme, J.W., 3rd, Cutter, D. and Barenkamp, S.J. (1996) 'Characterization of the genetic locus encoding Haemophilus influenzae type b surface fibrils', *J Bacteriol*, 178(21), pp. 6281-7.
Stavnezer, J. and Amemiya, C.T. (2004) 'Evolution of isotype switching', *Semin Immunol*, 16(4), pp. 257-75.
Stearns, J.C. *et al.* (2015) 'Culture and molecular-based profiles show shifts in bacterial communities of the upper respiratory tract that occur with age', *ISME J*, 9(5), pp. 1246-1259.
Stevens, M.P. *et al.* (2005) 'Identification of a bacterial factor required for actin-based motility of Burkholderia pseudomallei', *Mol Microbiol*, 56(1), pp. 40-53.
Sun, Z. *et al.* (2005) 'Semi-extended solution structure of human myeloma immunoglobulin D determined by constrained X-ray scattering', *J Mol Biol*, 353(1), pp. 155-73.
Surjan, L., Jr., Brandtzaeg, P. and Berdal, P. (1978) 'Immunoglobulin systems of human tonsils. II. Patients with chronic tonsillitis or tonsillar hyperplasia: quantification of Ig-producing cells, tonsillar morphometry and serum Ig concentrations', *Clin Exp Immunol*, 31(3), pp. 382-90.
Suzuki, K. *et al.* (2004) 'Aberrant expansion of segmented filamentous bacteria in IgA-deficient gut', *Proc Natl Acad Sci U S A*, 101(7), pp. 1981-6.
Swidsinski, A. *et al.* (2005) 'Spatial organization and composition of the mucosal flora in patients with inflammatory bowel disease', *J Clin Microbiol*, 43(7), pp. 3380-9.
Szczesny, P. and Lupas, A. (2008) 'Domain annotation of trimeric autotransporter adhesins--daTAA', *Bioinformatics (Oxford, England)*, 24(10), pp. 1251-1256.
Tak Mak, M.S., Bradley Jett. (2014) *Primer to The Immune Response. 2nd Edition*. 2nd edn. 6.
Tan, T.T. *et al.* (2007) 'Haemophilus influenzae survival during complement-mediated attacks is promoted by Moraxella catarrhalis outer membrane vesicles', *J Infect Dis*, 195(11), pp. 1661-70.
Tang, G. *et al.* (2008) 'EmaA, a potential virulence determinant of Aggregatibacter actinomycetemcomitans in infective endocarditis', *Infect Immun*, 76(6), pp. 2316-24.
Tlaskalova-Hogenova, H. *et al.* (2004) 'Commensal bacteria (normal microflora), mucosal immunity and chronic inflammatory and autoimmune diseases', *Immunol Lett*, 93(2-3), pp. 97-108.
Tlaskalova-Hogenova, H. *et al.* (2002) 'Mucosal immunity: its role in defense and allergy', *Int Arch Allergy Immunol*, 128(2), pp. 77-89.
Tlaskalova-Hogenova, H. *et al.* (2005) 'Interaction of mucosal microbiota with the innate immune system', *Scand J Immunol*, 62 Suppl 1, pp. 106-13.
Toussi, D.N. *et al.* (2012) 'The amino acid sequence of Neisseria lactamica PorB surface-exposed loops influences Toll-like receptor 2-dependent cell activation', *Infect Immun*, 80(10), pp. 3417-28.
Townsend, C.L. *et al.* (2016) 'Significant Differences in Physicochemical Properties of Human Immunoglobulin Kappa and Lambda CDR3 Regions', *Front Immunol*, 7, p. 388.
Troncoso, G. *et al.* (2002) 'Analysis of Neisseria lactamica antigens putatively implicated in acquisition of natural immunity to Neisseria meningitidis', *FEMS Immunology and Medical Microbiology*, 34(1), pp. 9-15.
Tung, J.W. *et al.* (2004) 'Identification of B-Cell Subsets', in Gu, H. and Rajewsky, K. (eds.) *B Cell Protocols*. Totowa, NJ: Humana Press, pp. 37-58.
Tuominen-Gustafsson, H. *et al.* (2006) 'Use of CFSE staining of borreliae in studies on the interaction between borreliae and human neutrophils', *BMC Microbiology*, 6, pp. 92-92.
Turnbaugh, P.J. *et al.* (2007) 'The human microbiome project', *Nature*, 449.

Tutt, A.L. *et al.* (2015) 'Development and Characterization of Monoclonal Antibodies Specific for Mouse and Human Fcgamma Receptors', *J Immunol*, 195(11), pp. 5503-16.
Uren, T.K. *et al.* (2005) 'Vaccine-induced protection against gastrointestinal bacterial infections in the absence of secretory antibodies', *Eur J Immunol*, 35(1), pp. 180-8.
Uria, M.J. *et al.* (2008) 'A generic mechanism in Neisseria meningitidis for enhanced resistance against bactericidal antibodies', *J Exp Med*, 205(6), pp. 1423-34.
Vale, A.M. *et al.* (2015) *Molecular Biology of B Cells*. Second Edition edn. London: Academic Press. Molecular Biology of B Cells (Second Edition).
Valle, J. *et al.* (2008) 'UpaG, a new member of the trimeric autotransporter family of adhesins in uropathogenic Escherichia coli', *J Bacteriol*, 190(12), pp. 4147-61.
van Dam, V. and Bos, M.P. (2012) 'Generating knock-out and complementation strains of Neisseria meningitidis', *Methods Mol Biol*, 799, pp. 55-72.
Vaughan, A.T. *et al.* (2010) 'Neisseria lactamica selectively induces mitogenic proliferation of the naive B cell pool via cell surface Ig', *J Immunol*, 185(6), pp. 3652-60.
Vaughan, A.T. *et al.* (2009) 'Absence of mucosal immunity in the human upper respiratory tract to the commensal bacteria Neisseria lactamica but not pathogenic Neisseria meningitidis during the peak age of nasopharyngeal carriage', *J Immunol*, 182(4), pp. 2231-40.
Vaughan, A.T. *et al.* (2014) 'Inhibitory FcgammaRIIb (CD32b) becomes activated by therapeutic mAb in both cis and trans and drives internalization according to antibody specificity', *Blood*, 123(5), pp. 669-77.
Vaughan, A.T., Roghanian, A. and Cragg, M.S. (2011) 'B cells--masters of the immunoverse', *Int J Biochem Cell Biol*, 43(3), pp. 280-5.
Vazquez, M.I., Catalan-Dibene, J. and Zlotnik, A. (2015) 'B cells responses and cytokine production are regulated by their immune microenvironment', *Cytokine*, 74(2), pp. 318-326.
Verduin, C.M. *et al.* (2002) 'Moraxella catarrhalis: from Emerging to Established Pathogen', *Clinical Microbiology Reviews*, 15(1), p. 125.
Verjans, G.M. *et al.* (1994) 'Entrance and survival of Salmonella typhimurium and Yersinia enterocolitica within human B- and T-cell lines', *Infection and immunity*, 62(6), pp. 2229-2235.
Vidarsson, G., Dekkers, G. and Rispens, T. (2014) 'IgG Subclasses and Allotypes: From Structure to Effector Functions', *Frontiers in Immunology*, 5, p. 520.
Vladutiu, A.O. (2000) 'Immunoglobulin D: Properties, Measurement, and Clinical Relevance', *Clinical and Diagnostic Laboratory Immunology*, 7(2), pp. 131-140.
Vos, Q. *et al.* (2000) 'B-cell activation by T-cell-independent type 2 antigens as an integral part of the humoral immune response to pathogenic microorganisms', *Immunol Rev*, 176, pp. 154-70.
Wang, C.Y. *et al.* (2006) 'Bacteraemic pneumonia caused by Neisseria lactamica with reduced susceptibility to penicillin and ciprofloxacin in an adult with liver cirrhosis', *J Med Microbiol*, 55(Pt 8), pp. 1151-2.
Wang, H. *et al.* (2016) 'Effect of growth media on gene expression levels in Salmonella Typhimurium biofilm formed on stainless steel surface', *Food Control*, 59, pp. 546-552.
Weill, J.C., Weller, S. and Reynaud, C.A. (2009) 'Human marginal zone B cells', *Annu Rev Immunol*, 27, pp. 267-85.
Wertlake, P.T. and Williams, T.W. (1968) 'Septicaemia caused by Neisseria flavescens', *Journal of Clinical Pathology*, 21(4), pp. 437-439.
Wilson, M., McNab, R. and Henderson, B. (2002) *Bacterial Disease Mechanisms.. An introduction to cellular microbiology*.
Wissinger, E., Goulding, J. and Hussell, T. (2009) 'Immune homeostasis in the respiratory tract and its impact on heterologous infection', *Semin Immunol*, 21(3), pp. 147-55.
Wong, H.E.E. *et al.* (2011) 'Genome wide expression profiling reveals suppression of host defence responses during colonisation by Neisseria meningitides but not N. lactamica', *PloS one*, 6(10), pp. e26130-e26130.

Yazdankhah, S.P. and Caugant, D.A. (2004) 'Neisseria meningitidis: an overview of the carriage state', *Journal of Medical Microbiology*, 53(9), pp. 821-832.
Yeo, H.-J. *et al.* (2004) 'Structural basis for host recognition by the Haemophilus influenzae Hia autotransporter', *The EMBO journal*, 23(6), pp. 1245-1256.
Zavascki, A.P. *et al.* (2006) 'First case report of Neisseria lactamica causing cavitary lung disease in an adult organ transplant recipient', *Journal of clinical microbiology*, 44(7), pp. 2666-2668.
Zhang, N. and He, Q.S. (2015) 'Commensal Microbiome Promotes Resistance to Local and Systemic Infections', *Chin Med J (Engl)*, 128(16), pp. 2250-5.
Zhang, P. *et al.* (2004) 'A family of variably expressed outer-membrane proteins (Vomp) mediates adhesion and autoaggregation in Bartonella quintana', *Proc Natl Acad Sci U S A*, 101(37), pp. 13630-5.

Appendix A: Supplementary data for protein domains of MID homologues

Table 52 Conserved domains hits on NLY_36660 (*N. lactamica*) ORF

Name	Accession	Description	Interval	E-value
Hia	COG5295	Autotransporter adhesin	3503-3733	1.67e-31
LbR_YadA-like	cd12820	YadA-like, left-handed beta-roll	87-213	6.18e-30
YadA_anchor	pfam03895	YadA-like membrane anchor domain	3674-3733	7.39e-16
LbR_YadA-like	cd12820	YadA-like, left-handed beta-roll	499-605	5.42e-13
ESPR	pfam13018	Extended Signal Peptide of Type V secretion system	1-23	2.88e-07
Smc	COG1196	Chromosome segregation ATPase	966-1274	3.37e-05
YadA_stalk	pfam05662	Coiled stalk of trimeric autotransporter adhesin	1366-1406	3.52e-04
DUF3584	pfam12128	Protein of unknown function (DUF3584)	954-1119	6.13e-04
SMC_prok_B	TIGR02168	chromosome segregation protein SMC	966-1281	6.15e-04
PRK08026	PRK08026	flagellin	2421-2652	1.29e-03
YadA_stalk	pfam05662	Coiled stalk of trimeric autotransporter adhesin	791-834	2.55e-03
LbR_YadA-like	cd12820	YadA-like, left-handed beta-roll	683-735	5.66e-03

Table 53 Conserved domains hits on NLY_37260 (*N. lactamica*) ORF

Name	Accession	Description	Interval	E-value
Hia	COG5295	Autotransporter adhesin	2088-2626	7.04e-16
YadA_anchor	pfam03895	YadA-like membrane anchor domain	3338-3398	2.61e-14
LbR_YadA-like	cd12820	YadA-like, left-handed beta-roll	3095-3186	4.60e-13
Hia	COG5295	Autotransporter adhesin	704-1050	9.30e-12
ESPR	pfam13018	Extended Signal Peptide of Type V secretion system	1-23	2.02e-09
Hia	COG5295	Autotransporter adhesin	1177-1780	1.68e-05
TAA-Trp-ring	pfam15401	Tryptophan-ring motif of head of Trimeric autotransporter adhesin	2727-2793	6.68e-04
YadA_stalk	pfam05662	Coiled stalk of trimeric autotransporter adhesin	2363-2405	1.16e-03
HiaBD2	pfam15403	HiaBD2_N domain of Trimeric autotransporter adhesin (GIN)	1883-1938	1.27e-03
TAA-Trp-ring	pfam15401	Tryptophan-ring motif of head of Trimeric autotransporter adhesin	1578-1640	6.23e-03
YadA_stalk	pfam05662	Coiled stalk of trimeric autotransporter adhesin	3280-3310	7.34e-03
PHA03255	PHA03255	BDLF3	1116-1242	9.16e-03

Table 54 Conserved domains hits on NEICINOT_03770_346 (*N. cinerea*) ORF

Name	Accession	Description	Interval	E-value
LbR_YadA-like	cd12820	YadA-like, left-handed beta-roll	121-243	6.50e-32
YadA_anchor	pfam03895	YadA-like membrane anchor domain	3655-3715	1.21e-15
LbR_YadA-like	cd12820	YadA-like, left-handed beta-roll	188-300	7.60e-14
LbR_YadA-like	cd12820	YadA-like, left-handed beta-roll	501-628	2.59e-12
Hia	COG5295	Autotransporter adhesin	3292-3715	5.42e-12
ESPR	pfam13018	Extended Signal Peptide of Type V secretion system	1-23	6.61e-08
LbR_YadA-like	cd12820	YadA-like, left-handed beta-roll	572-752	1.57e-07
LbR-like	cd12813	Left-handed beta-roll	73-165	9.65e-07
YadA_stalk	pfam05662	Coiled stalk of trimeric autotransporter adhesin	3611-3652	1.92e-04
TAA-Trp-ring	pfam15401	Tryptophan-ring motif of head of Trimeric autotransporter adhesin	3130-3194	2.63e-04
DUF1542	pfam07564	Domain of Unknown Function (DUF1542)	2780-2837	3.33e-03
YadA_stalk	pfam05662	Coiled stalk of trimeric autotransporter adhesin	806-851	3.83e-03

Table 55 Conserved domains hits on NEICINOT_04577_346 (*N. cinerea*) ORF

Name	Accession	Description	Interval	E-value
Hia	COG5295	Autotransporter adhesin	1526-1780	2.80e-19
YadA_anchor	pfam03895	YadA-like membrane anchor domain	1721-1780	4.07e-14
LbR_YadA-like	cd12820	YadA-like, left-handed beta-roll	248-446	1.01e-13
LbR_YadA-like	cd12820	YadA-like, left-handed beta-roll	143-303	3.57e-09
ESPR	pfam13018	Extended Signal Peptide of Type V secretion system	1-23	9.15e-08
YadA_stalk	pfam05662	Coiled stalk of trimeric autotransporter adhesin	1659-1700	7.65e-05
YadA_stalk	pfam05662	Coiled stalk of trimeric autotransporter adhesin	517-562	1.70e-03

Table 56 Conserved domains hits on DYC64_RS10620_17913 (*N. flavescens*) ORF

Name	Accession	Description	Interval	E-value
LbR_YadA-like	cd12820	YadA-like, left-handed beta-roll	79-196	8.83e-31
YadA_anchor	pfam03895	YadA-like membrane anchor domain	4265-4325	1.83e-15
LbR_YadA-like	cd12820	YadA-like, left-handed beta-roll	155-264	1.01e-11
Hia	COG5295	Autotransporter adhesin	4187-4325	2.36e-10
ESPR	pfam13018	Extended Signal Peptide of Type V secretion system	1-23	1.22e-07
YadA_stalk	pfam05662	Coiled stalk of trimeric autotransporter adhesin	1436-1477	2.04e-05
LbR_YadA-like	cd12820	YadA-like, left-handed beta-roll	466-665	2.13e-05
PRK05035	PRK05035	electron transport complex protein RnfC	3360-3486	3.67e-05
YadA_stalk	pfam05662	Coiled stalk of trimeric autotransporter adhesin	4221-4262	5.27e-04
TAA-Trp-ring	pfam15401	Tryptophan-ring motif of head of Trimeric autotransporter adhesin	3760-3824	9.12e-04
DUF4398	pfam14346	Domain of unknown function (DUF4398)	3408-3469	4.09e-03
YadA_head	pfam05658	Head domain of trimeric autotransporter adhesin	111-135	5.70e-03

Table 57 Conserved domains hits on NEIFLAOT_01884_17913 (*N. flavescens*) ORF

Name	Accession	Description	Interval	E-value
Hia	COG5295	Autotransporter adhesin	2035-2250	4.34e-29
YadA_anchor	pfam03895	YadA-like membrane anchor domain	2191-2250	2.10e-16
ESPR	pfam13018	Extended Signal Peptide of Type V secretion system	1-23	2.32e-09
Hia	COG5295	Autotransporter adhesin	521-879	2.73e-06
YadA_stalk	pfam05662	Coiled stalk of trimeric autotransporter adhesin	2139-2181	5.10e-04
Hia	COG5295	Autotransporter adhesin	1061-1495	5.30e-04
TAA-Trp-ring	pfam15401	Tryptophan-ring motif of head of Trimeric autotransporter adhesin	769-834	5.37e-04
HiaBD2	pfam15403	HiaBD2_N domain of Trimeric autotransporter adhesin (GIN)	1066-1122	1.15e-03
TAA-Trp-ring	pfam15401	Tryptophan-ring motif of head of Trimeric autotransporter adhesin	1743-1803	5.86e-03

Table 58 Conserved domains hits on DBY97_RS02575_23930 (*N. subflava*) ORF

Name	Accession	Description	Interval	E-value
LbR_YadA-like	cd12820	YadA-like, left-handed beta-roll	193-314	1.98e-16
Hia	COG5295	Autotransporter adhesin	2657-3168	5.89e-11
YadA_anchor	pfam03895	YadA-like membrane anchor domain	3108-3168	1.19e-10
ESPR	pfam13018	Extended Signal Peptide of Type V secretion system	1-23	2.79e-06
YadA_stalk	pfam05662	Coiled stalk of trimeric autotransporter adhesin	954-996	2.08e-03
YadA_stalk	pfam05662	Coiled stalk of trimeric autotransporter adhesin	1637-1679	2.08e-03

Table 59 Conserved domains hits on NEIPOLOT_RS07545_18031 (*N. polysaccharea*) ORF

Name	Accession	Description	Interval	E-value
Hia	COG5295	Autotransporter adhesin	3481-3711	4.21e-31
LbR_YadA-like	cd12820	YadA-like, left-handed beta-roll	87-227	2.06e-26
YadA_anchor	pfam03895	YadA-like membrane anchor domain	3652-3711	1.91e-15
LbR_YadA-like	cd12820	YadA-like, left-handed beta-roll	521-645	5.70e-15
LbR_YadA-like	cd12820	YadA-like, left-handed beta-roll	200-311	2.70e-11
ESPR	pfam13018	Extended Signal Peptide of Type V secretion system	1-23	3.18e-07
SMC_prok_B	TIGR02168	chromosome segregation protein SMC	1009-1324	1.85e-05
mukB	PRK04863	cell division protein MukB; Provisional	1029-1171	2.88e-04
YadA_stalk	pfam05662	Coiled stalk of trimeric autotransporter adhesin	1409-1449	3.37e-04
LbR_YadA-like	cd12820	YadA-like, left-handed beta-roll	722-777	4.15e-04
PRK08026	PRK08026	flagellin	2002-2269	4.38e-04
YadA_stalk	pfam05662	Coiled stalk of trimeric autotransporter adhesin	833-876	2.43e-03

Table 60 Conserved domains hits on DYA92_RS09215_2043 (*N. elongata*) ORF

Name	Accession	Description	Interval	E-value
LbR_YadA-like	cd12820	YadA-like, left-handed beta-roll	498-621	1.04e-20
LbR_YadA-like	cd12820	YadA-like, left-handed beta-roll	863-1014	3.08e-16
LbR_YadA-like	cd12820	YadA-like, left-handed beta-roll	399-538	3.91e-15
Hia	COG5295	Autotransporter adhesin	2072-2765	6.61e-13
LbR_YadA-like	cd12820	YadA-like, left-handed beta-roll	78-197	5.51e-12
LbR_YadA-like	cd12820	YadA-like, left-handed beta-roll	1122-1241	1.42e-10
LbR_YadA-like	cd12820	YadA-like, left-handed beta-roll	566-737	1.79e-10
YadA_anchor	pfam03895	YadA-like membrane anchor domain	2705-2765	2.66e-10
Hia	COG5295	Autotransporter adhesin	410-912	4.01e-06
Hia	COG5295	Autotransporter adhesin	882-1485	1.63e-04
YadA_stalk	pfam05662	Coiled stalk of trimeric autotransporter adhesin	793-834	3.08e-04
YadA_stalk	pfam05662	Coiled stalk of trimeric autotransporter adhesin	2643-2685	1.49e-04

Table 61 Conserved domains hits on nhhA DV147_RS09460 (*N. meningitidis*) ORF

Name	Accession	Description	Interval	E-value
Hia	COG5295	Autotransporter adhesin	1-591	2.89e-90
YadA_anchor	pfam03895	YadA-like membrane anchor domain	532-591	4.85e-17
ESPR	pfam13018	Extended Signal Peptide of Type V secretion system	1-23	2.86e-09
TAA-Trp-ring	pfam15401	Tryptophan-ring motif of head of Trimeric autotransporter adhesin	259-317	7.99e-06
YadA_stalk	pfam05662	Coiled stalk of trimeric autotransporter adhesin	480-522	2.35e-05

Appendix B: Growth curves of Neisseria strains used in chapter 4.4.5-6

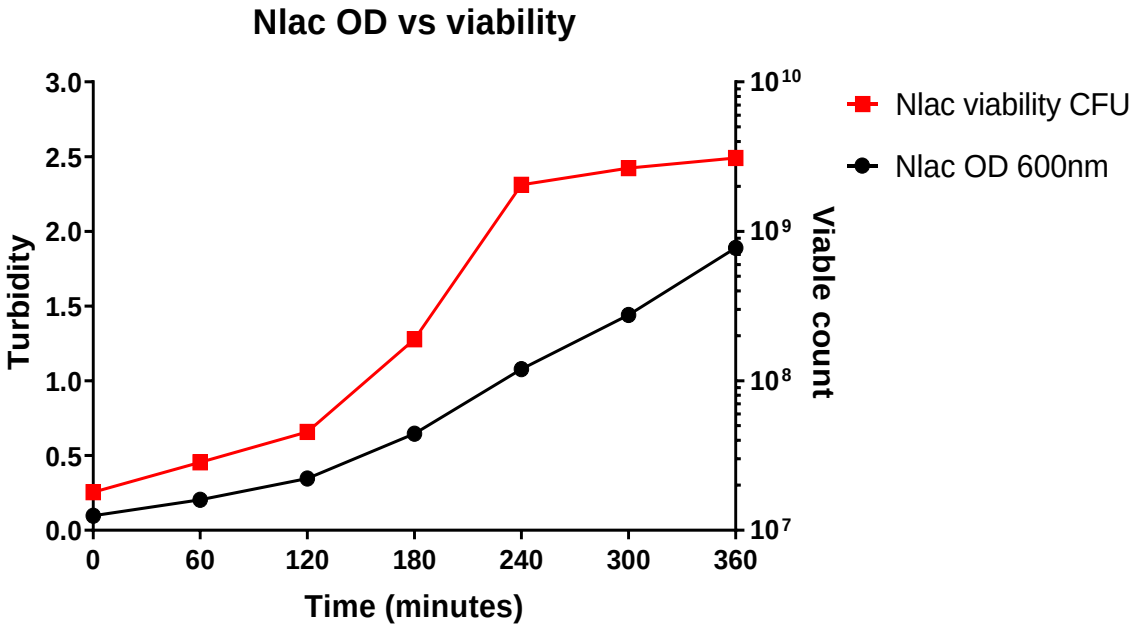

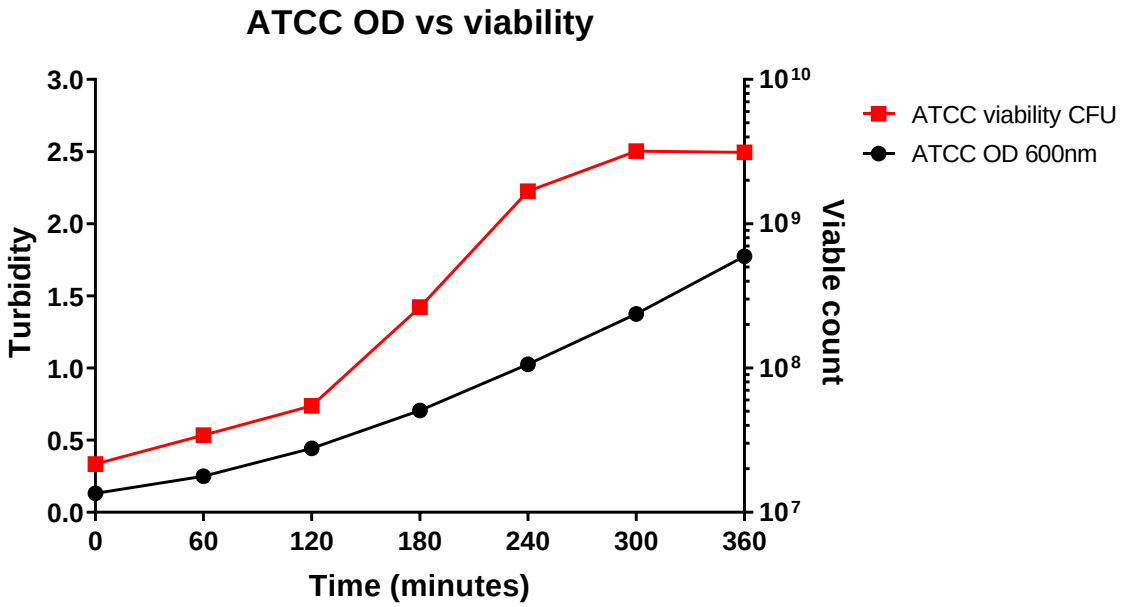

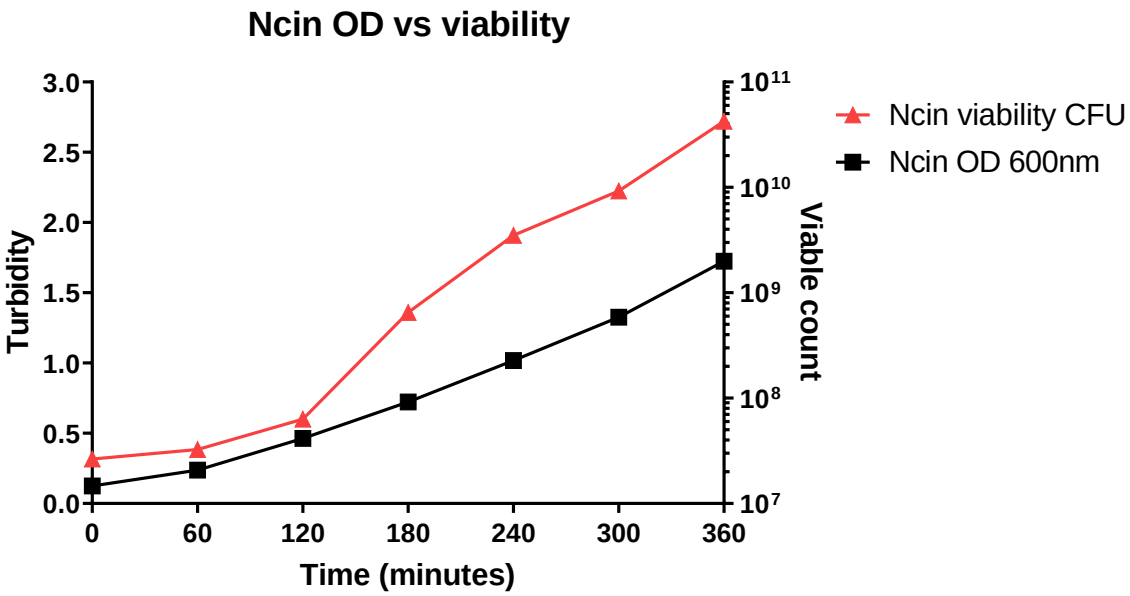
Ncin OD vs viability
Turbidity
Viable count
Time (minutes)
Ncin viability CFU
Ncin OD 600nm

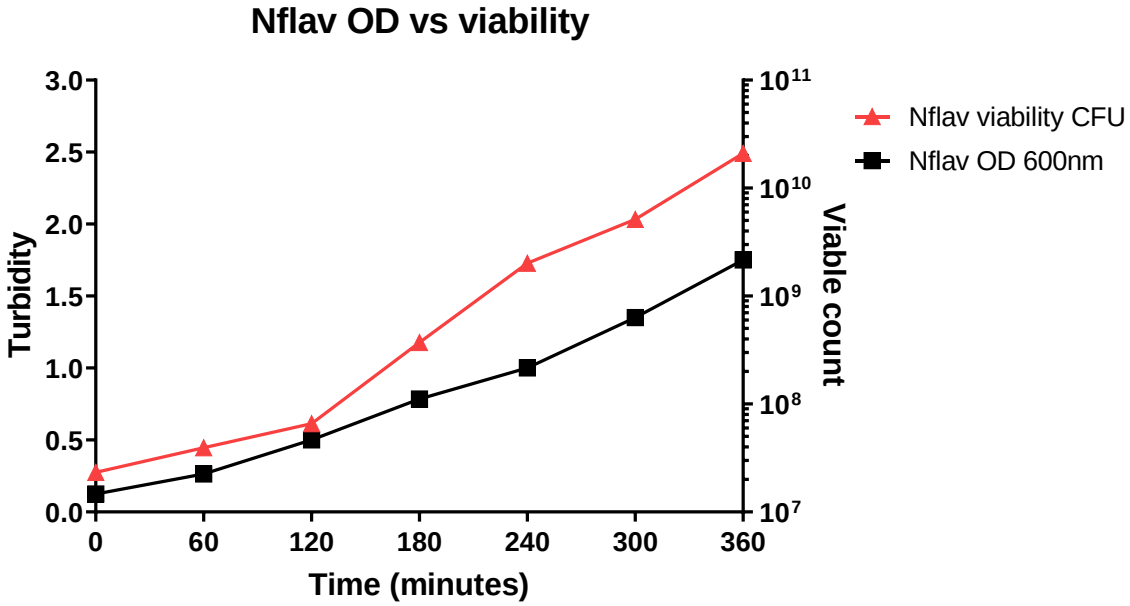
Nflav OD vs viability
Turbidity
Viable count
Time (minutes)
Nflav viability CFU
Nflav OD 600nm

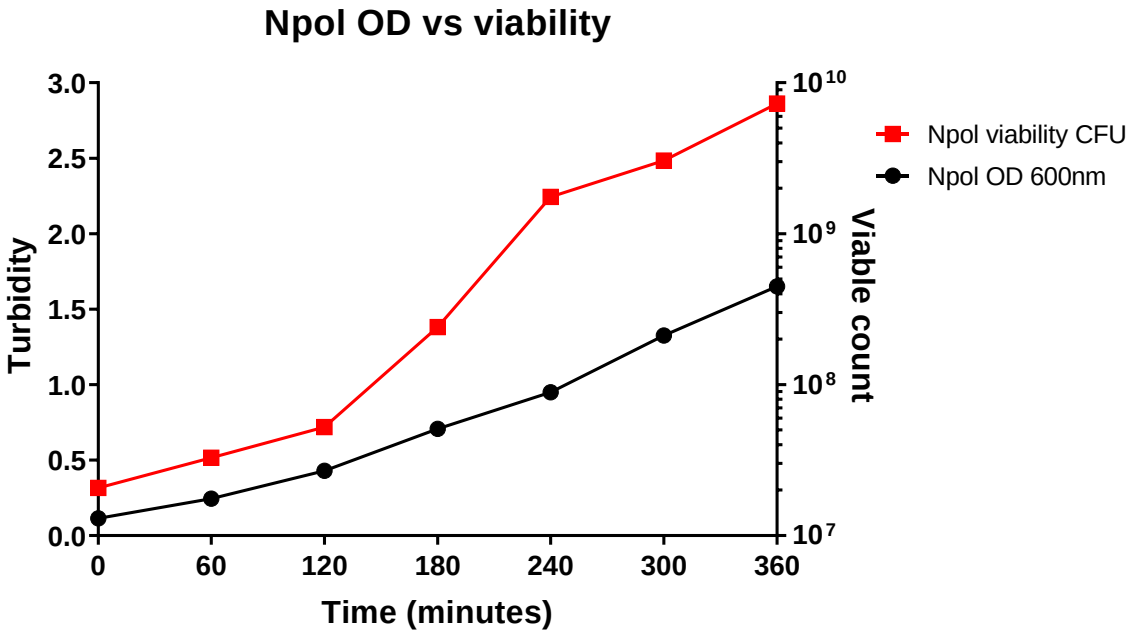
Npol OD vs viability
Turbidity
Viable count
Time (minutes)
Npol viability CFU
Npol OD 600nm
3.0
2.5
2.0
1.5
1.0
0.5
0.0
0
60
120
180
240
300
360
10^10
10^9
10^8
10^7

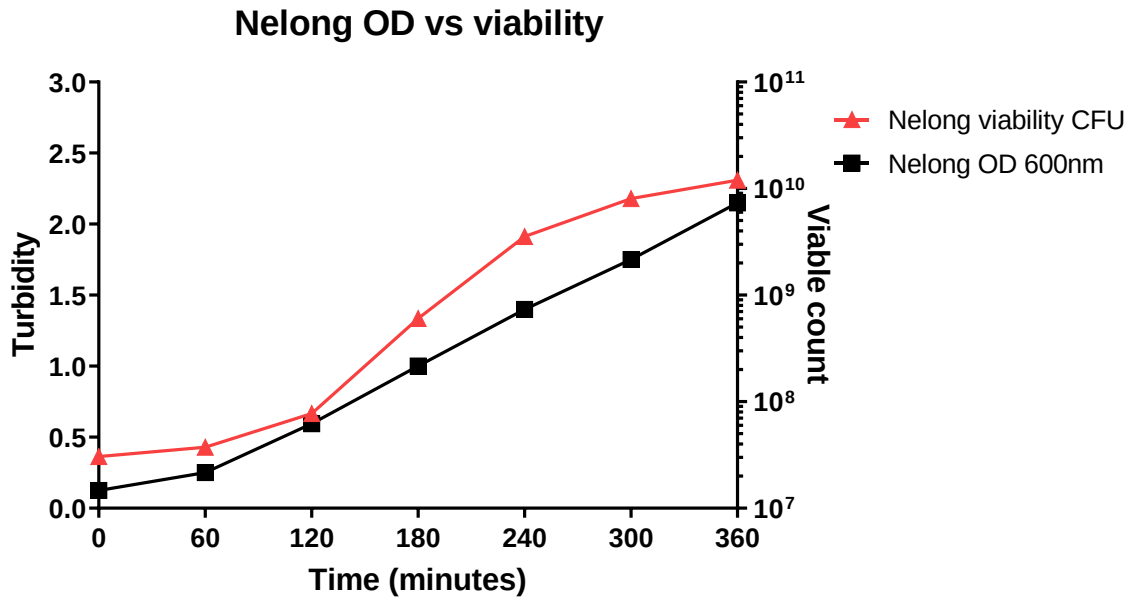
Nelong OD vs viability
Turbidity
Viable count
Time (minutes)
Nelong viability CFU
Nelong OD 600nm
3.0
2.5
2.0
1.5
1.0
0.5
0.0
0
60
120
180
240
300
360
10^11
10^10
10^9
10^8
10^7

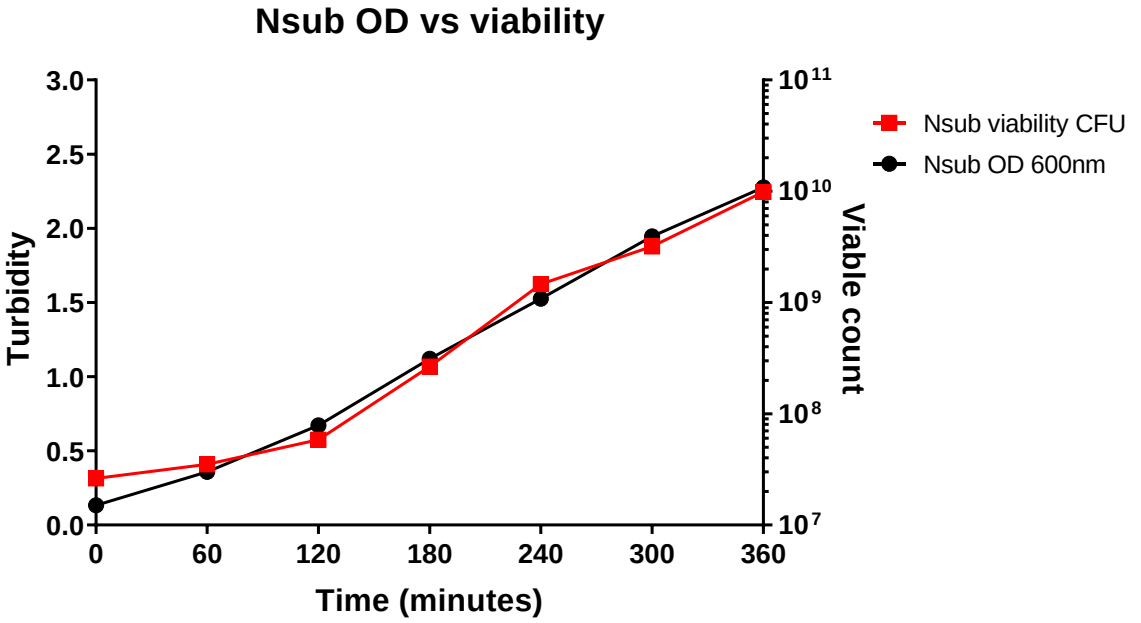
Nsub OD vs viability
Turbidity
Viable count
Time (minutes)
Nsub viability CFU
Nsub OD 600nm
3.0
2.5
2.0
1.5
1.0
0.5
0.0
0
60
120
180
240
300
360
10^{11}
10^{10}
10^{9}
10^{8}
10^{7}

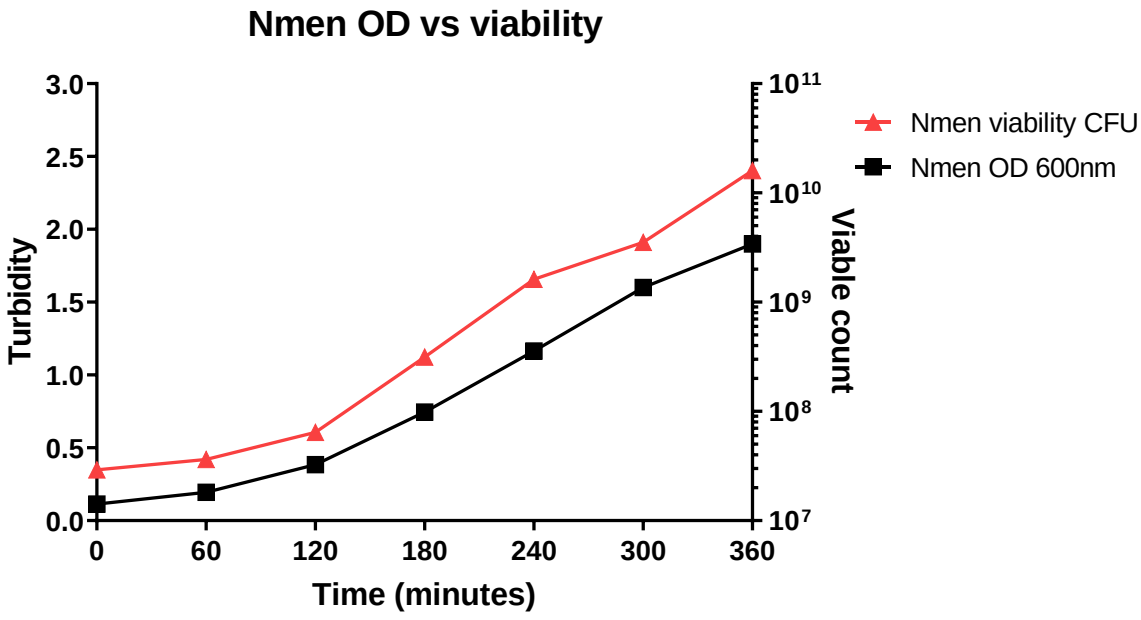
Nmen OD vs viability
Turbidity
Viable count
Time (minutes)
Nmen viability CFU
Nmen OD 600nm
3.0
2.5
2.0
1.5
1.0
0.5
0.0
0
60
120
180
240
300
360
10^{11}
10^{10}
10^{9}
10^{8}
10^{7}